

The role of the human glycine receptor
transmembrane domains for the function,
assembly and allosteric modulation by the general
anesthetic propofol and closely related derivatives

Vom Fachbereich Biologie
der Technischen Universität Darmstadt

zur Erlangung des Grades
eines Doktors der Naturwissenschaften
(Dr. rer. nat.)

genehmigte Dissertation
von Dipl.-Biol. Michael Peter Kilb
aus Worms

1. Prüfer: Prof. Dr. Bodo Laube

2. Prüfer: Prof. Dr. Ralf Galuske

Tag der Einreichung: 25.07.2016

Tag der mündlichen Prüfung: 12.09.2016

Darmstadt 2016

(D17)

Keine Schuld ist dringender als die, Danke zu sagen

Marcus Tullius Cicero (106-43), römischer Redner und Schriftsteller

Danke euch allen

Table of contents

1. General introduction	- 1-
2. Chapter 1 - An intramembrane aromatic network determines pentameric assembly of Cys- loop receptors	- 19-
3. Chapter 2 - 4-chlorination endows propofol with subtype-specific effects on inhibitory glycine receptors via a unique high-affinity transmembrane-domain binding-site	- 34-
4. Chapter 3 - Characterization of propofol binding sites and site specific effects at $\alpha 1$ glycine receptors	- 59-
5. Chapter 4 - Characterization of thymol and 4-chlorothymol effects on the function of human glycine receptors	- 94-
6. General discussion	-124-
7. Summary	-134-
8. Appendix	-140-
8.1. Author contributions	-140-
8.2. Primer sequences	-141-
8.3. Glycine activation of wt and mutated glycine receptors	-141-
8.4. Biochemical and pharmacological characterization of heteromeric $\alpha 1\beta$ GlyR expression and formation	-142-
8.5. Protein alignment	-144-
8.6. Common used abbreviations	-145-
9. Danksagungen	-147-
10. Ehrenwörtliche Erklärung	-148-
11. Curriculum vitae	-149-

1. General introduction

Communication makes the difference

Fossil records showed that the first multicellular organism appeared 2.5 billion years after the development of unicellular organisms. One aspect why multicellularity enforced so slowly was the need to develop various forms of communication mechanisms by which cell to cell communication is achieved. Indeed this long time development was necessary because cell to cell communication balanced the lost of the generalization and enhanced the specification of different cell types to specialized tissues which is a characteristic feature of higher evolved organism like the mammalians.

For these highly variable and differentiate communication mechanisms a wide variety of distinct extracellular signal molecules, like neurotransmitters, are produced by cells to signal neighboring and far away localized cells. Examples are shown in figure 1.

Signaling molecules and ion channels

In highly specialized tissues like the brain, the mayor part of the cell to cell communication between 15–33 billion neurons is achieved by the use of extracellular signal molecules and specific cell surface proteins, like ion channels. Ion channels are in general integral membrane proteins with three important features. First, they conduct ions through the cell membrane which acts as a barrier for them. The ion transport is achieved by an ion selective pore and starts after the second important feature, the recognition of a specific signaling molecule like a neurotransmitter.

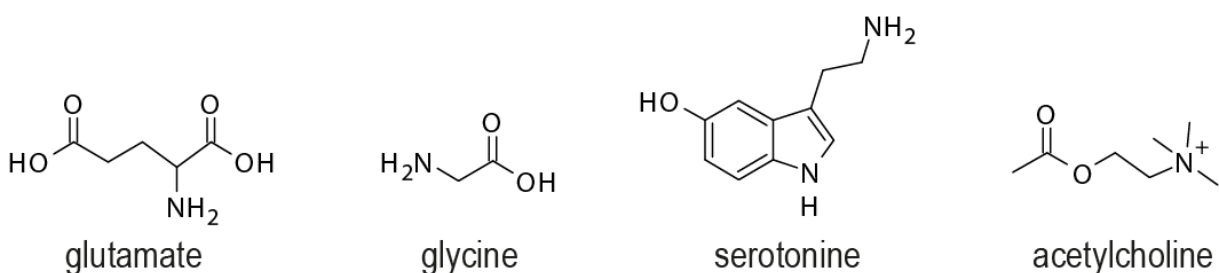


Figure 1: Chemical structures of neurotransmitters known to activate ligand gated ion channels (LGICs).

The binding of a neurotransmitter leads to a global change in the protein structure resulting in the exposure of a central located, ion conducting pore. These specific ion channels are classified as ligand gated ion channels (LGICs). The following figure 2

illustrates the three major types of LGICs in the mammalian central nervous system (cns).

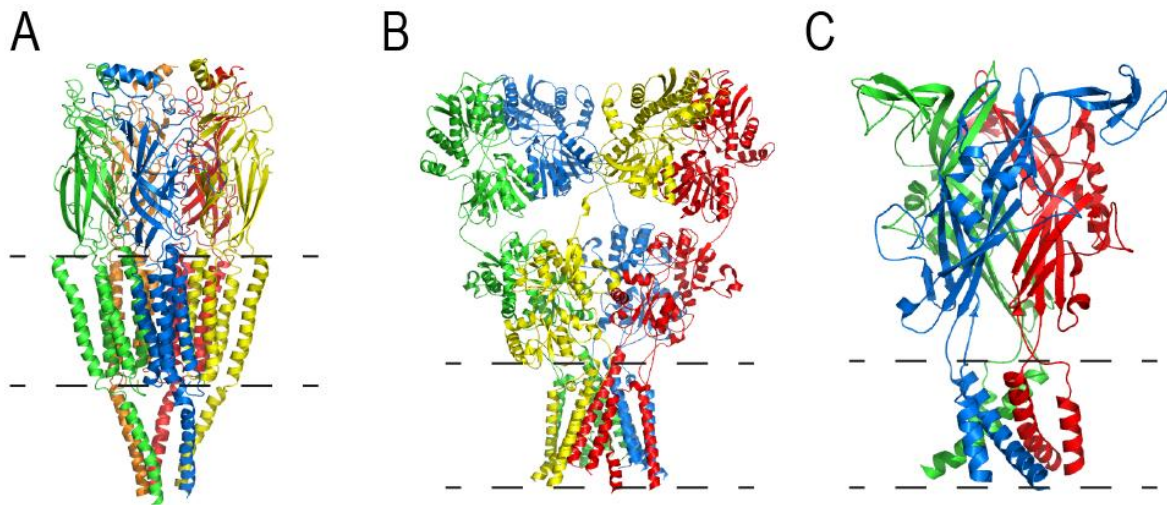


Figure 2: Side views of ion channel crystal structures. **A.** Pentameric cys-loop receptor (PDB:2BG9). **B.** Tetrameric GluA2-type AMPA-receptor (PDB ID:3KG2). **C.** Trimeric P2X4 ATP-gated receptor (PDB:3I5D). To highlight the different amount of subunits, single subunits were colored. Receptor structures between the dashed lines are the lipid embedded transmembrane domains.

After the channel pore is accessible, ions can pass the membrane following their ion concentration gradient resulting in a local change of the natural membrane potential. Nearby, as well as distant located potential controlled ion channels, detect these changes in the membrane potential and respond with additional, voltage dependent ion transfers, reproducing the signal.

The selective transport of a specific ion type is the third feature of these proteins and a key determinant for the existence of a dualistic neuronal signal transmission system: The cation driven excitatory and anion mediated inhibitory neurotransmission.

Signal transmissions generated and controlled by these two strong connected systems are important for several physiological relevant processes like the processing of sensory information.

Glycine receptors

The amino acid glycine (Gly) was identified as an inhibitory neurotransmitter about 40 years ago (Aprison and Werman, 1965). In the late seventies Gly was characterized as a molecule which affects an inhibitory chloride (Cl^-) conductance in the spinal cord. Dissection of the Gly mediated currents unmasked a strychnine (stry) sensitive Cl^- channel as the responsible structure for the inhibitory transmission in the spinal cord. Stry affinity chromatography of rat spinal cord tissue by Pfeiffer and colleagues led to the purification of three distinct polypeptides with molecular masses of 48-, 58- and 98 kDA (Pfeiffer et al., 1982). In-depth analysis of the purified peptides revealed an irreversible incorporation of stry to the 48 kDA peptide indicating the presence of the high affinity binding site (Graham et al., 1983). Following studies including cloning and genomic analyses identified the 48 kDA peptide as the $\alpha 1$ GlyR subtype, the 58 kDA peptide as the β GlyR subtype and the 93 kDA peptide as the β associated cytoplasmatic gephyrin molecule (Lynch, 2004).

The GlyR belongs to the superfamily of pentameric LGICs. Functional GlyRs are formed either from four α subtypes alone (homomeric) or from both α and β subtypes (heteromeric) (Langosch et al., 1988). Each subtype comprised of a large N-terminal extracellular domain (ECD), four transmembranedomains (M1–M4), a long intracellular loop (IL) connecting M3 and M4, and a short extracellular C-terminus (Fig. 3). Amino acid homologies are particularly high within the transmembranedomains (TMDs) and a cysteine-bonded loop in the ECD compared to the γ -aminobutyricacid type A receptor (GABA(A)R). The channel pore is build by the M2 of each subunit in the final pentameric protein and displays a strict selectivity for the anions $\text{I}^- > \text{Br}^- > \text{Cl}^-$. The ligand binding site is located in the ECD formed by amino acid residues of the (+) and (-) interfaces of neighboring subunits. Binding of gly initiated an iris like conformational change of the ECD that results in a structural reorientation of the channel forming M2 amino acids resulting in an increased accessibility of the Cl^- conducting pore.

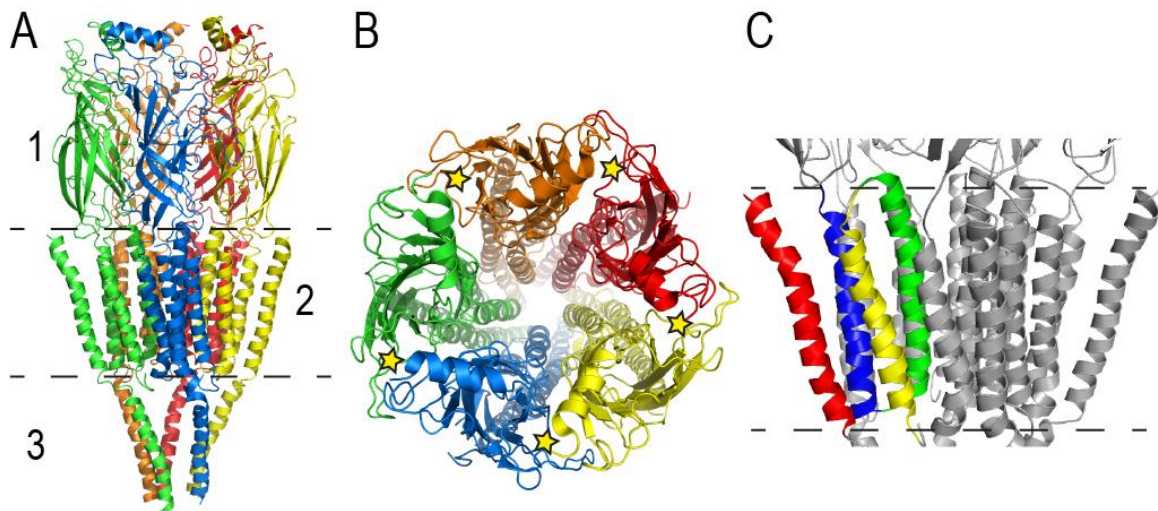


Figure 3: Crystal structure of the nicotinic acetylcholine receptor and overview of the ion channels modulatory regions. **A.** Side view showing three prominent regions: **1.** Extracellular domain with the ligand binding domain. **2.** The lipid embedded transmembrane domains. **3.** The intracellular loop between the M3 and M4 which interacts with cellular components. **B.** Top view showing the central ion conducting pore. Yellow stars indicate the agonist binding pocket. **C.** Side view of the transmembrane domains M1 (blue), M2 (green), M3 (yellow) and M4 (red).

In the past, glycinergic synapses were thought to be restricted to the spinal cord and brain stem, where they control motor rhythm generation, coordination of spinal reflex responses, and processing of sensory signals (Legendre et al., 2002). The role of GlyRs in these physiological functions was obtained by the use of the potent GlyR specific antagonist stry. Intoxication with low μM concentrations, results in convulsions and death (Young and Snyder, 1973).

Interestingly, the blockade of GlyR actions by non lethal stry concentrations causes motor disturbance by an increased muscle tone, hyperactivity of visual and acoustic perceptions. These effects perfectly mirrored the loss of the fast glycinergic regulation of both motor and sensory functions in the spinal cord and brainstem by the GlyR related channelopathy named hereditary neuromotor disorder hyperekplexia (HKPX; startle disease).

In the case of HKPX, mutations in the *GLRA1* gene result in amino acid substitutions at the highly conserved residue Arg271 in the M2, resulting in a decreased GlyR sensitivity towards Gly and single-channel ion conductance of recombinant $\alpha 1$ GlyRs (Langosch et al., 1994; Rajendra et al., 1994).

Following molecular studies, GlyR distribution is not only limited to the spinal cord and brainstem. In adult mammals, GlyR activity was identified in the cochlear nuclei, superior olivary complex, medial nuclei of trapezoid body, the cerebellar

cortex, deep cerebellar nuclei, and the area postrema by immunoreactivity (IR) indicating receptor distribution in higher mammalian CNS areas (Danglot et al., 2004; Legendre et al., 2002). In-depth electrophysiological and in-situ hybridization studies unmasked GlyR activity in important mammalian brain areas like the prefrontal cortex, hippocampus, amygdala, hypothalamus, cerebellum, nucleus accumbens, ventral tegmental area and substantia nigra (Chattipakorn and McMahon, 2002; Flint et al., 1998; Gaiarsa et al., 2002; Laube et al., 2002; Mangin et al., 2003; McCool and Farroni, 2001; Ren et al., 1998; Tapia et al., 2000; Ye et al., 1999; Zhou, 2001).

The α GlyR subtypes, roles and distribution

Today, four different genes (*GLRA1–4*) encoding $\alpha 1$ - $\alpha 4$ GlyR subunits and one gene (*GLRB*) encoding the β subunit, have been identified in vertebrates (Matzenbach et al. 1994; Laube et al. 2002). Functional GlyRs are formed either from the four α subtypes alone (homomeric) or from both α and β subtypes (heteromeric) (Langosch et al., 1988). The heteromer consists of two α and three β subtypes and can be found primarily in synaptic membranes (Grudzinska et al., 2005; Laube et al., 2002). Distinct β subtype interactions with gephyrin provide clustering of GlyRs in synaptic areas (Kneussel et al., 1999; Meyer et al., 1995). In contrast, the non clustered homomeric variant is thought to be localized in extrasynaptic areas (Laube et al., 2002; Rajendra et al., 1997).

Comparison of the α subunits amino acid sequences display a more than 80 % overall identity.

Whereas GlyRs consisting of $\alpha 1$ subunits are the predominant version, expressed during all developmental stages in the spinal cord, in retinal neurons and a host of brainstem nuclei, high $\alpha 2$ GlyR subunit expression is found only during the embryonic and neonatal stages. In neonatal developmental stages, extrasynaptic homomeric $\alpha 2$ GlyRs induce excitation by a stimulation of a calcium influx (Flint et al., 1998). During these stages, the activity of the K^+/Cl^- co-transporter (KCC2) leads to a highly intracellular concentration of Cl^- in neurons (Rivera et al., 1999).

Postnatal however, the $\alpha 2$ subtype is widely replaced by the $\alpha 1$ GlyR subunit. IR staining indicates a synaptic localization in different adult CNS regions like the spinal cord, brainstem, midbrain, olfactory bulb, retina and corresponds to heteromeric $\alpha 2\beta$ GlyRs (Weltzien et al., 2012).

The exact physiological role of the $\alpha 2$ subtype is still enigmatic because *Glr2*^{-/-} mice are phenotypically normal. Recent findings although have displayed that hyperalgesia induced by injection of zymosan is prolonged compared to wild-type animals (Kallenborn-Gerhardt et al., 2012).

IR staining of $\alpha 3$ GlyRs indicated a high expression pattern in the spinal cord (laminae I and II of the dorsal horn). In these areas, glycinergic activity inhibits the propagation of nociceptive signals to higher brain regions. $\alpha 3$ subunits containing heteromeric GlyRs serve in these regions as molecular substrates of pain sensitization by the prostaglandin E₂ (PGE₂), the mediator for inflammatory processes. PGE₂ binds to prostaglandin EP2 receptors and thereby activates protein kinase A (PKA). PKA activation leads to the phosphorylation of a $\alpha 3$ GlyR serine in the intracellular domain which results in a down-regulation of Gly currents in dorsal horn neurons. In *Glr3*^{-/-} mice, the PGE₂ regulation of GlyR activity is abolished resulting in a strong reduced pain response and the analgesic effects by cannabinoids are although absent indicating the relevance of the $\alpha 3$ subtype as a target for the treatment of chronic inflammatory and neuropathic pain (Harvey et al., 2004; Harvey et al., 2009; Xiong et al., 2012; Zeilhofer, 2005; Zeilhofer et al., 2012).

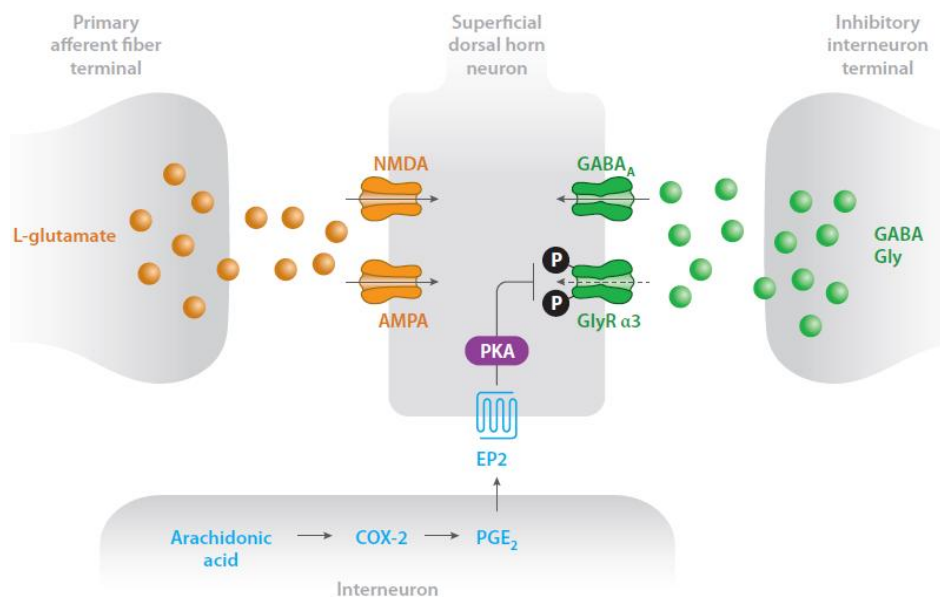


Figure 4: $\alpha 3$ GlyR related mechanisms involved in inflammatory pain. Enzymatic produced prostaglandin E₂ (PEG2) lead to an activation of G protein_s and adenylyl cyclases resulting in an increase of intracellular cyclic adenosine monophosphate (cAMP). cAMP activates protein kinase A (PKA) that phosphorylates $\alpha 3$ GlyRs subtypes resulting in an inhibition of the receptor function (Zeilhofer et al., 2012).

The GLRA4 gene encoding the $\alpha 4$ GlyR subunit is a pseudo gene in humans (Simon et al., 2004). However, it is strongly expressed in the neuronal tissue of chicks (Harvey et al., 2000).

The GlyR TMDs and their role for the receptor function and allosteric modulation

Theoretically, every amino acid of a protein could be a putative target for an allosteric modulator. But specific chemical and structural properties of an allosteric modulator limit the area of possible binding sites in a membrane protein. Important target structures for allosteric modulators are the GlyR TMDs. At the first sight, one would suppose that the primary task of the TMDs is only to anchor the protein in the cell membrane. However, TMDs are essential structures which are important for the correct function and assembly of membrane bound proteins. This has been recently shown for $\alpha 1$ GlyR (Haeger et al., 2010). In addition, the GlyR function is also directly linked to amino acid interactions organized in form of a dynamical subunit connecting network of mutual amino acid contacts. These conjunctions build the molecular base for the correct signal transduction process in the protein leading to structural reorganizations resulting in the receptor activation.

The idea that allosteric modulators of membrane embedded ion channels can act via buried and lipid exposed parts of a protein based on the Meyer-Overton correlation. Meyer and Overton discovered simultaneously that highly potent anesthetics also are high soluble in lipids. Their findings lead to the definition of the so called Meyer-Overton rule (Franks, 2006).

The first exact identifications of an allosteric modulator binding site in the TMDs of GlyRs were the ivermectin and endocannabinoids site (Lynagh et al., 2011; Xiong et al., 2011). In the case of ivermectin, the binding site was verified by a crystallographic study showing ivermectin bound to the structural GlyR homologue glutamate gated chloride channel (GluCl) from the nematode *Caenorhabditis elegans* (*C.elegans*) (Hibbs and Gouaux, 2011). The following figure illustrates the ivermectin binding site in GluCls.

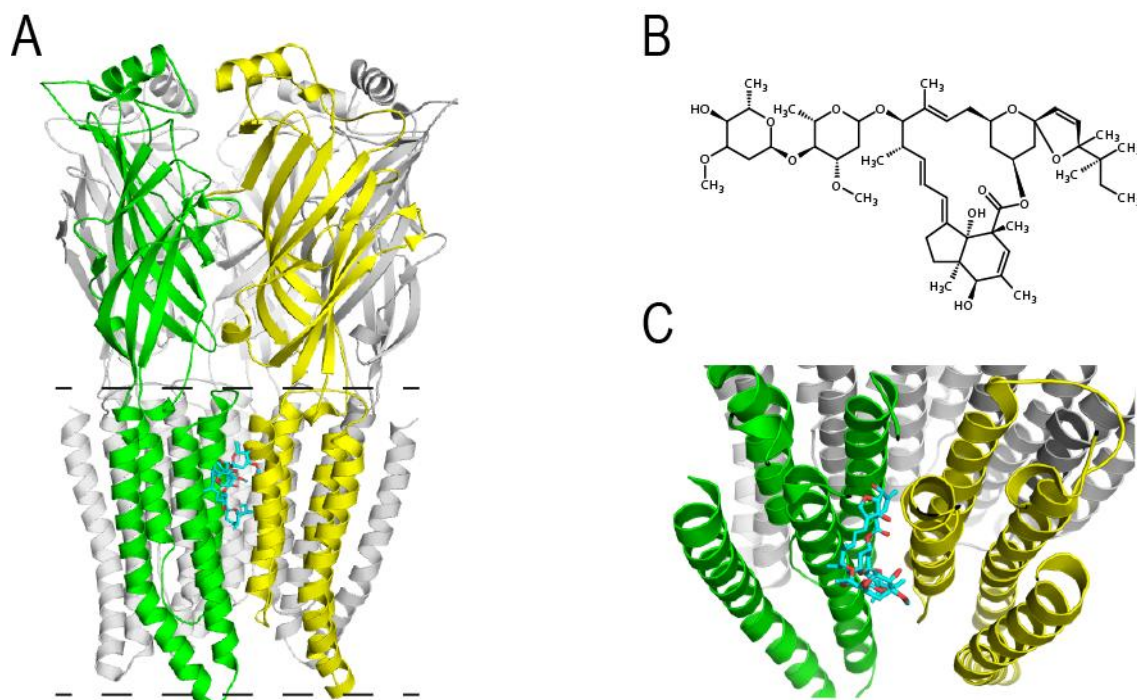


Figure 5: Ivermectin structure and TMD binding site in glutamate gated chloride channels (GluCl). **A.** Side view showing the IVM (cyan molecule) binding site in the TMD interface of adjacent GluCl subunits (PDB: 3RHW). **B.** Chemical structure of Ivermectin **C.** Ivermectin binding site in the interface of adjacent subunits (Hibbs and Gouaux, 2011).

For several other GlyR modulators like alcohols, neurosteroids and the general anesthetic propofol (pro) indications for a putative binding site in the TMDs are given but the exact binding site determinants in form of amino acid residues are still unknown (Ahrens et al., 2008; Belelli et al., 1999; Duret et al., 2011; Haeseler et al., 2005; Lobo et al., 2004; Yevenes and Zeilhofer, 2011)

Pro binding sites in pLGICs

High resolution crystal structures showing a direct binding of pro to a mammalian protein were first shown for the human serum albumin (HSA) and apoferritin (Bhattacharya et al., 2000; Vedula et al., 2009). In the case of the HSA, pro-protein interactions are of high interest because nearly 98% of pro during an anesthesia is bound to blood proteins (Mazoit and Samii, 1999). The crystal structure of pro bound to these two molecules revealed a direct binding to helical organized amino acids. Interestingly, the α -helical organization of the apoferritin reflects nearly perfectly the TMDs of pLGICs. Remarkably, the affinity of pro binding to apoferritin correlate with the EC₅₀ values of the pro potentiation of GABA evoked chloride currents at GABA(A)Rs (Vedula et al., 2009). In depth analysis targeting the mode of binding

identified a hydrogen bond, van-der-Waals forces and hydrophobic interactions between pro and the protein (Vedula et al., 2009). The first high resolution crystal structure of pro binding to a pLGIC was published in 2011 by Nury and colleagues. They showed at a pH sensitive chloride conducting ion channel in *Gloeobacter violaceus* (GLIC), pro binding between the TMDs of one subunit (Nury et al., 2011). The following figure 6 illustrates the pro binding site in GLIC.

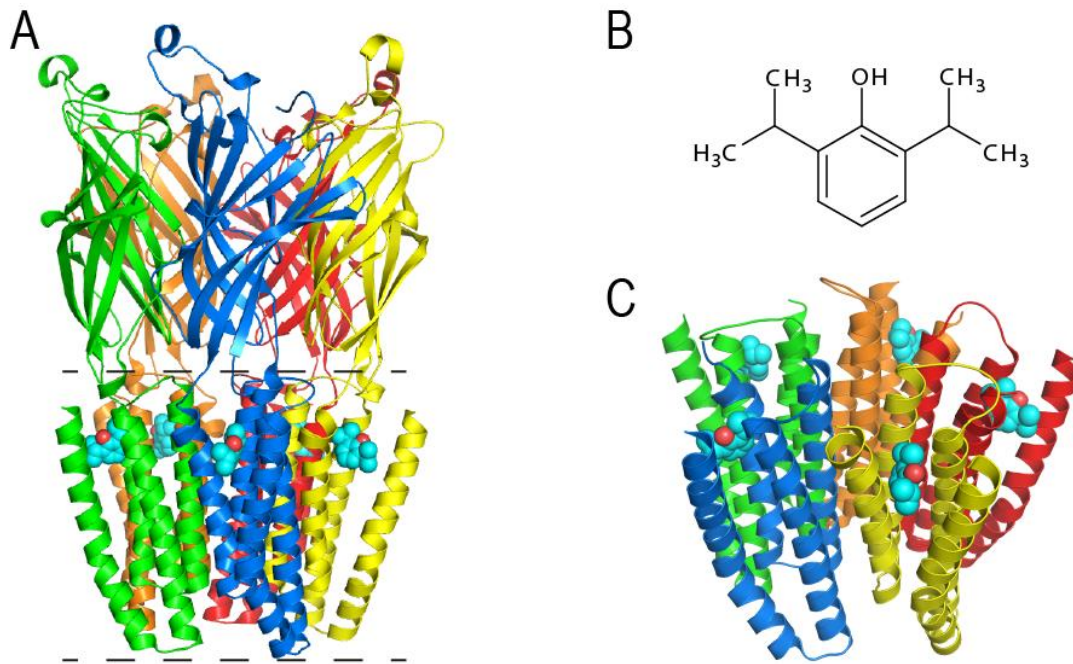


Figure 6: Pro structure and TMD binding sites in GLIC. **A.** Side view showing pro binding sites in the TMDs of GLIC (PDB:3P50). **B.** Chemical structure of pro (2,6 diisopropylphenol). **C.** Intrasubunit binding site of pro in GLIC (Nury et al., 2011).

However, a comparison of the native unbound with the pro bound GLIC structure, revealed a clear mismatch according to the inhibitory action of pro at GLIC. There are no obvious structural differences in the pro bound and unbound GLIC structure which could explain the action of pro on the protein function (Ghosh et al., 2013; Nury et al., 2011). Moreover, a recently published study showed that in the resting state pro binding to GLIC did not protect the modification of the pro binding site by a cysteine attaching molecule (Ghosh et al., 2013).

Although this discrepancy exists, it seems clear that pro modulates GLIC and GlyR function via a binding site in the TMDs like shown by Duret and colleagues (Duret et al., 2011).

Another step forward concerning the localization of pro binding sites in pLGICs was done by the development of photo reactive pro derivatives with regulatory effects on the receptor function (Hall et al., 2010; Stewart et al., 2011). With the use of these molecules, a TMD interface binding site for pro was identified in a mammalian GABA(A)Rs (Yip et al., 2013). Interestingly, a study targeting the binding of a structural close related reactive pro derivative in nAChRs unmasked the presence of multiple distinct binding sites. Binding sites were found in the channel pore, the interface between adjacent subunits within the TMDs of one subunit (Jayakar et al., 2013). Indeed, pro binding to more than one site is supported by its multiple effects at pLGICs (Adodra and Hales, 1995; Pistis et al., 1997).

Pro enhances the actions of GABA and Gly evoked currents. The potentiation is reversible and dose-dependent (Hales and Lambert, 1991; Pistis et al., 1997). Pro also increases the apparent affinity of the receptor towards its agonist without altering the maximum response (O'Shea et al., 2004; Orser et al., 1994). At higher concentrations, pro acts as a partial agonist at GABA(A)- and GlyRs (Pistis et al., 1997).

That pro enhancement of GABAergic activity contributes to a great part to the induction of anesthesia is demonstrated by “knock-in” mice's bearing a single substitution at position 15 in the M2 of the $\beta 3$ subunit ($\beta 3M2-15'$). This was supported by in vitro experiments, showing that the TMD substitution reduce the sensitivity of the GABA(A)Rs towards the general anesthetics etomidate, pro and pentobarbital (Chiara et al., 2013; Jurd et al., 2003). However, GlyRs may although play an important role for the pro mediated general anesthesia. Hales and Lambert demonstrated sensitivity of GlyRs to pro, as pro dose-dependently potentiated stry-sensitive currents evoked by Gly in spinal neurons (Hales and Lambert, 1991). Similar effects of pro on recombinant GlyRs expressed in *Xenopus laevis* oocytes were found by Pistis and colleagues (Pistis et al., 1997). Interestingly, in vivo GlyR malfunction in mice can be restored by the administration of sub anesthetic concentrations of pro. In addition, small structural changes at the pro scaffold in forms of halogenations increases the modulatory potency exclusively at GlyRs, indicating a therapeutic relevance of the molecule for the treatment of GlyR related diseases (de la Roche et al., 2012; O'Shea et al., 2004).

Surprisingly, the exact mechanisms by which pro and other potent general anesthetics act are not completely understood, but clear indications are given that

the allosteric modulation of ion channels contribute to a great part to the molecule's effects (Franks, 2006).

Allosteric modulators of GlyRs

Why is there a general interest in the identification and characterization of allosteric modulators? Firstly, they can help collecting more information about the physiological role of the target protein. Secondly, in contrary to an agonistic molecule, allosteric modulators bind to a distinct protein site that is able to modulate the function. The identification and characterization of a binding site can build the base for the design of novel drugs. Thirdly, in the case of the GlyR only a few agents are known which are able to modulate the receptor function. Moreover, none of them is able to distinguish between the physiological relevant subtypes (Yevenes and Zeilhofer, 2011). Today, the exact location of only four allosteric modulator binding sites (ivermectin, tropeines, cannabinoids and zinc) at GlyRs are known (Laube et al., 2000; Lynagh et al., 2011; Maksay et al., 2009; Xiong et al., 2011).

As mentioned above, glycinergic synapses are found in higher brain regions of mammals and a decreased $\alpha 1$ and $\alpha 3$ GlyR activity is evident in chronic inflammatory and neuropathic pain as well as in the hyperekplexia disease. Therefore a widespread knowledge about GlyR subtype specific modulators is important for the development of GlyR malfunction related diseases like spasticity, motor disturbance and chronic inflammatory pain or to gain more information about the role and distribution of a specific GlyR subtype in neuronal tissues (Laube et al., 2002; Yevenes and Zeilhofer, 2011).

Aim of this work

The aim of this work is to increase the knowledge about the glycine receptor (GlyR) transmembrane domains (TMDs) concerning their role for the function, assembly and allosteric modulation by the general anesthetic propofol (pro) and derivatives. GlyRs are pentameric ligand-gated ion channels (pLGICs) that mediate fast synaptic transmission. A GlyR subunit comprised of a large N-terminal extracellular domain (ECD), four transmembranedomains (TMD1–4), a long intracellular loop (IL) connecting the M3 and M4, and a short extracellular C-terminus.

In this complex structure, the TMDs have several important functions: They interact with components of the membrane and build a central located ion conducting channel. They also interact with allosteric modulators and mutations of TMD amino acids can result in massive functional disorders. Moreover, structural rearrangements between the TMDs are key processes for the opening and closing of the channel.

Therefore, it is of great interest to increase the knowledge about the GlyR TMDs. Especially since a change in the GlyR activity is evident in chronic inflammatory and neuropathic pain as well as in the hyperekplexia disease.

References

- Adodra S and Hales TG (1995) Potentiation, activation and blockade of GABAA receptors of clonal murine hypothalamic GT1-7 neurones by propofol. *Br J Pharmacol* **115**(6): 953-960.
- Ahrens J, Leuwer M, Stachura S, Krampfl K, Belelli D, Lambert JJ and Haeseler G (2008) A transmembrane residue influences the interaction of propofol with the strychnine-sensitive glycine alpha1 and alpha1beta receptor. *Anesth Analg* **107**(6): 1875-1883.
- Aprison MH and Werman R (1965) The distribution of glycine in cat spinal cord and roots. *Life Sci* **4**(21): 2075-2083.
- Belelli D, Pistis M, Peters JA and Lambert JJ (1999) The interaction of general anaesthetics and neurosteroids with GABA(A) and glycine receptors. *Neurochem Int* **34**(5): 447-452.
- Bhattacharya AA, Curry S and Franks NP (2000) Binding of the general anesthetics propofol and halothane to human serum albumin. High resolution crystal structures. *J Biol Chem* **275**(49): 38731-38738.
- Chattipakorn SC and McMahon LL (2002) Pharmacological characterization of glycine-gated chloride currents recorded in rat hippocampal slices. *J Neurophysiol* **87**(3): 1515-1525.
- Chiara DC, Jayakar SS, Zhou X, Zhang X, Savechenkov PY, Bruzik KS, Miller KW and Cohen JB (2013) Specificity of intersubunit general anesthetic-binding sites in the transmembrane domain of the human alpha1beta3gamma2 gamma-aminobutyric acid type A (GABAA) receptor. *J Biol Chem* **288**(27): 19343-19357.
- Danglot L, Rostaing P, Triller A and Bessis A (2004) Morphologically identified glycinergic synapses in the hippocampus. *Mol Cell Neurosci* **27**(4): 394-403.
- de la Roche J, Leuwer M, Krampfl K, Haeseler G, Dengler R, Buchholz V and Ahrens J (2012) 4-Chloropropofol enhances chloride currents in human hyperekplexic and artificial mutated glycine receptors. *BMC Neurol* **12**: 104.
- Duret G, Van Renterghem C, Weng Y, Prevost M, Moraga-Cid G, Huon C, Sonner JM and Corringer PJ (2011) Functional prokaryotic-eukaryotic chimera from the pentameric ligand-gated ion channel family. *Proc Natl Acad Sci U S A* **108**(29): 12143-12148.
- Flint AC, Liu X and Kriegstein AR (1998) Nonsynaptic glycine receptor activation during early neocortical development. *Neuron* **20**(1): 43-53.
- Franks NP (2006) Molecular targets underlying general anaesthesia. *Br J Pharmacol* **147 Suppl 1**: S72-81.

- Gaiarsa JL, Caillard O and Ben-Ari Y (2002) Long-term plasticity at GABAergic and glycinergic synapses: mechanisms and functional significance. *Trends Neurosci* **25**(11): 564-570.
- Ghosh B, Satyshur KA and Czajkowski C (2013) Propofol binding to the resting state of the gloeobacter violaceus ligand-gated ion channel (GLIC) induces structural changes in the inter- and intrasubunit transmembrane domain (TMD) cavities. *J Biol Chem* **288**(24): 17420-17431.
- Graham D, Pfeiffer F and Betz H (1983) Photoaffinity-labelling of the glycine receptor of rat spinal cord. *Eur J Biochem* **131**(3): 519-525.
- Grudzinska J, Schemm R, Haeger S, Nicke A, Schmalzing G, Betz H and Laube B (2005) The beta subunit determines the ligand binding properties of synaptic glycine receptors. *Neuron* **45**(5): 727-739.
- Haeger S, Kuzmin D, Detro-Dassen S, Lang N, Kilb M, Tsetlin V, Betz H, Laube B and Schmalzing G (2010) An intramembrane aromatic network determines pentameric assembly of Cys-loop receptors. *Nat Struct Mol Biol* **17**(1): 90-98.
- Haeseler G, Ahrens J, Krampfl K, Bufler J, Dengler R, Hecker H, Aronson JK and Leuwer M (2005) Structural features of phenol derivatives determining potency for activation of chloride currents via alpha(1) homomeric and alpha(1)beta heteromeric glycine receptors. *Br J Pharmacol* **145**(7): 916-925.
- Hales TG and Lambert JJ (1991) The actions of propofol on inhibitory amino acid receptors of bovine adrenomedullary chromaffin cells and rodent central neurones. *Br J Pharmacol* **104**(3): 619-628.
- Hall MA, Xi J, Lor C, Dai S, Pearce R, Dailey WP and Eckenhoff RG (2010) m-Azipropofol (AziPm) a photoactive analogue of the intravenous general anesthetic propofol. *J Med Chem* **53**(15): 5667-5675.
- Harvey RJ, Depner UB, Wassle H, Ahmadi S, Heindl C, Reinold H, Smart TG, Harvey K, Schutz B, Abo-Salem OM, Zimmer A, Poisbeau P, Welzl H, Wolfer DP, Betz H, Zeilhofer HU and Muller U (2004) GlyR alpha3: an essential target for spinal PGE2-mediated inflammatory pain sensitization. *Science* **304**(5672): 884-887.
- Harvey RJ, Schmieden V, Von Holst A, Laube B, Rohrer H and Betz H (2000) Glycine receptors containing the alpha4 subunit in the embryonic sympathetic nervous system, spinal cord and male genital ridge. *Eur J Neurosci* **12**(3): 994-1001.
- Harvey VL, Caley A, Muller UC, Harvey RJ and Dickenson AH (2009) A Selective Role for alpha3 Subunit Glycine Receptors in Inflammatory Pain. *Front Mol Neurosci* **2**: 14.
- Hibbs RE and Gouaux E (2011) Principles of activation and permeation in an anion-selective Cys-loop receptor. *Nature* **474**(7349): 54-60.

- Jayakar SS, Dailey WP, Eckenhoff RG and Cohen JB (2013) Identification of propofol binding sites in a nicotinic acetylcholine receptor with a photoreactive propofol analog. *J Biol Chem* **288**(9): 6178-6189.
- Jurd R, Arras M, Lambert S, Drexler B, Siegwart R, Crestani F, Zaugg M, Vogt KE, Ledermann B, Antkowiak B and Rudolph U (2003) General anesthetic actions in vivo strongly attenuated by a point mutation in the GABA(A) receptor beta3 subunit. *FASEB J* **17**(2): 250-252.
- Kallenborn-Gerhardt W, Lu R, Lorenz J, Gao W, Weiland J, Del Turco D, Deller T, Laube B, Betz H, Geisslinger G and Schmidtko A (2012) Prolonged zymosan-induced inflammatory pain hypersensitivity in mice lacking glycine receptor alpha2. *Behav Brain Res* **226**(1): 106-111.
- Kneussel M, Hermann A, Kirsch J and Betz H (1999) Hydrophobic interactions mediate binding of the glycine receptor beta-subunit to gephyrin. *J Neurochem* **72**(3): 1323-1326.
- Langosch D, Laube B, Rundstrom N, Schmieden V, Bormann J and Betz H (1994) Decreased agonist affinity and chloride conductance of mutant glycine receptors associated with human hereditary hyperekplexia. *EMBO J* **13**(18): 4223-4228.
- Langosch D, Thomas L and Betz H (1988) Conserved quaternary structure of ligand-gated ion channels: the postsynaptic glycine receptor is a pentamer. *Proc Natl Acad Sci U S A* **85**(19): 7394-7398.
- Laube B, Kuhse J and Betz H (2000) Kinetic and mutational analysis of Zn²⁺ modulation of recombinant human inhibitory glycine receptors. *J Physiol* **522 Pt 2**: 215-230.
- Laube B, Maksay G, Schemm R and Betz H (2002) Modulation of glycine receptor function: a novel approach for therapeutic intervention at inhibitory synapses? *Trends Pharmacol Sci* **23**(11): 519-527.
- Legendre P, Muller E, Badiu CI, Meier J, Vannier C and Triller A (2002) Desensitization of homomeric alpha1 glycine receptor increases with receptor density. *Mol Pharmacol* **62**(4): 817-827.
- Lobo IA, Mascia MP, Trudell JR and Harris RA (2004) Channel gating of the glycine receptor changes accessibility to residues implicated in receptor potentiation by alcohols and anesthetics. *J Biol Chem* **279**(32): 33919-33927.
- Lynagh T, Webb TI, Dixon CL, Cromer BA and Lynch JW (2011) Molecular determinants of ivermectin sensitivity at the glycine receptor chloride channel. *J Biol Chem* **286**(51): 43913-43924.
- Lynch JW (2004) Molecular structure and function of the glycine receptor chloride channel. *Physiol Rev* **84**(4): 1051-1095.

- Maksay G, Laube B, Schemm R, Grudzinska J, Drwal M and Betz H (2009) Different binding modes of tropeines mediating inhibition and potentiation of alpha1 glycine receptors. *J Neurochem* **109**(6): 1725-1732.
- Mangin JM, Baloul M, Prado De Carvalho L, Rogister B, Rigo JM and Legendre P (2003) Kinetic properties of the alpha2 homo-oligomeric glycine receptor impairs a proper synaptic functioning. *J Physiol* **553**(Pt 2): 369-386.
- Mazoit JX and Samii K (1999) Binding of propofol to blood components: implications for pharmacokinetics and for pharmacodynamics. *Br J Clin Pharmacol* **47**(1): 35-42.
- McCool BA and Farroni JS (2001) Subunit composition of strychnine-sensitive glycine receptors expressed by adult rat basolateral amygdala neurons. *Eur J Neurosci* **14**(7): 1082-1090.
- Meyer G, Kirsch J, Betz H and Langosch D (1995) Identification of a gephyrin binding motif on the glycine receptor beta subunit. *Neuron* **15**(3): 563-572.
- Nury H, Van Renterghem C, Weng Y, Tran A, Baaden M, Dufresne V, Changeux JP, Sonner JM, Delarue M and Corringer PJ (2011) X-ray structures of general anaesthetics bound to a pentameric ligand-gated ion channel. *Nature* **469**(7330): 428-431.
- O'Shea SM, Becker L, Weiher H, Betz H and Laube B (2004) Propofol restores the function of "hyperekplexic" mutant glycine receptors in *Xenopus* oocytes and mice. *J Neurosci* **24**(9): 2322-2327.
- Orser BA, Wang LY, Pennefather PS and MacDonald JF (1994) Propofol modulates activation and desensitization of GABAA receptors in cultured murine hippocampal neurons. *J Neurosci* **14**(12): 7747-7760.
- Pfeiffer F, Graham D and Betz H (1982) Purification by affinity chromatography of the glycine receptor of rat spinal cord. *J Biol Chem* **257**(16): 9389-9393.
- Pistis M, Belelli D, Peters JA and Lambert JJ (1997) The interaction of general anaesthetics with recombinant GABAA and glycine receptors expressed in *Xenopus laevis* oocytes: a comparative study. *Br J Pharmacol* **122**(8): 1707-1719.
- Rajendra S, Lynch JW, Pierce KD, French CR, Barry PH and Schofield PR (1994) Startle disease mutations reduce the agonist sensitivity of the human inhibitory glycine receptor. *J Biol Chem* **269**(29): 18739-18742.
- Rajendra S, Lynch JW and Schofield PR (1997) The glycine receptor. *Pharmacol Ther* **73**(2): 121-146.
- Ren J, Ye JH and McArdle JJ (1998) cAMP-dependent protein kinase modulation of glycine-activated chloride current in neurons freshly isolated from rat ventral tegmental area. *Brain Res* **811**(1-2): 71-78.

- Rivera C, Voipio J, Payne JA, Ruusuvuori E, Lahtinen H, Lamsa K, Pirvola U, Saarma M and Kaila K (1999) The K⁺/Cl⁻ co-transporter KCC2 renders GABA hyperpolarizing during neuronal maturation. *Nature* **397**(6716): 251-255.
- Simon J, Wakimoto H, Fujita N, Lalande M and Barnard EA (2004) Analysis of the set of GABA(A) receptor genes in the human genome. *J Biol Chem* **279**(40): 41422-41435.
- Stewart DS, Savechenkov PY, Dostalova Z, Chiara DC, Ge R, Raines DE, Cohen JB, Forman SA, Bruzik KS and Miller KW (2011) p-(4-Azipentyl)propofol: a potent photoreactive general anesthetic derivative of propofol. *J Med Chem* **54**(23): 8124-8135.
- Tapia JC, Cardenas AM, Nualart F, Mentis GZ, Navarrete R and Aguayo LG (2000) Neurite outgrowth in developing mouse spinal cord neurons is modulated by glycine receptors. *Neuroreport* **11**(13): 3007-3010.
- Vedula LS, Brannigan G, Economou NJ, Xi J, Hall MA, Liu R, Rossi MJ, Dailey WP, Grasty KC, Klein ML, Eckenhoff RG and Loll PJ (2009) A unitary anesthetic binding site at high resolution. *J Biol Chem* **284**(36): 24176-24184.
- Weltzien F, Puller C, O'Sullivan GA, Paarmann I and Betz H (2012) Distribution of the glycine receptor beta-subunit in the mouse CNS as revealed by a novel monoclonal antibody. *J Comp Neurol* **520**(17): 3962-3981.
- Xiong W, Cheng K, Cui T, Godlewski G, Rice KC, Xu Y and Zhang L (2011) Cannabinoid potentiation of glycine receptors contributes to cannabis-induced analgesia. *Nat Chem Biol* **7**(5): 296-303.
- Xiong W, Cui T, Cheng K, Yang F, Chen SR, Willenbring D, Guan Y, Pan HL, Ren K, Xu Y and Zhang L (2012) Cannabinoids suppress inflammatory and neuropathic pain by targeting alpha3 glycine receptors. *J Exp Med* **209**(6): 1121-1134.
- Ye JH, Schaefer R, Wu WH, Liu PL, Zbuzek VK and McArdle JJ (1999) Inhibitory effect of ondansetron on glycine response of dissociated rat hippocampal neurons. *J Pharmacol Exp Ther* **290**(1): 104-111.
- Yevenes GE and Zeilhofer HU (2011) Allosteric modulation of glycine receptors. *Br J Pharmacol* **164**(2): 224-236.
- Yip GM, Chen ZW, Edge CJ, Smith EH, Dickinson R, Hohenester E, Townsend RR, Fuchs K, Sieghart W, Evers AS and Franks NP (2013) A propofol binding site on mammalian GABAA receptors identified by photolabeling. *Nat Chem Biol* **9**(11): 715-720.
- Young AB and Snyder SH (1973) Strychnine binding associated with glycine receptors of the central nervous system. *Proc Natl Acad Sci U S A* **70**(10): 2832-2836.
- Zeilhofer HU (2005) The glycinergic control of spinal pain processing. *Cell Mol Life Sci* **62**(18): 2027-2035.

Zeilhofer HU, Benke D and Yevenes GE (2012) Chronic pain states: pharmacological strategies to restore diminished inhibitory spinal pain control. *Annu Rev Pharmacol Toxicol* **52**: 111-133.

Zhou ZJ (2001) A critical role of the strychnine-sensitive glycinergic system in spontaneous retinal waves of the developing rabbit. *J Neurosci* **21**(14): 5158-5168.

An intramembrane aromatic network determines pentameric assembly of Cys-loop receptors

Svenja Haeger¹, Dmitry Kuzmin^{2,3}, Silvia Detro-Dassen¹, Niklas Lang¹, Michael Kilb⁴, Victor Tsetlin³, Heinrich Betz², Bodo Laube^{2,4} & Günther Schmalzing¹

Cys-loop receptors are pentameric ligand-gated ion channels (pLGICs) that mediate fast synaptic transmission. Here functional pentameric assembly of truncated fragments comprising the ligand-binding N-terminal ectodomains and the first three transmembrane helices, M1–M3, of both the inhibitory glycine receptor (GlyR) α 1 and the 5HT₃A receptor subunits was found to be rescued by coexpressing the complementary fourth transmembrane helix, M4. Alanine scanning identified multiple aromatic residues in M1, M3 and M4 as key determinants of GlyR assembly. Homology modeling and molecular dynamics simulations revealed that these residues define an interhelical aromatic network, which we propose determines the geometry of M1–M4 tetrahelical packing such that nascent pLGIC subunits must adopt a closed fivefold symmetry. Because pLGIC ectodomains form random nonstoichiometric oligomers, proper pentameric assembly apparently depends on intersubunit interactions between extracellular domains and intrasubunit interactions between transmembrane segments.

Early evidence for a crucial role of transmembrane domains in membrane-protein tertiary structure came from the observation that bacteriorhodopsin, an integral membrane protein containing seven transmembrane helices, could be functionally reconstituted from non-overlapping proteolytic fragments comprising two and five transmembrane helices^{1,2}. These and related data on other membrane proteins (reviewed in ref. 3) showed that significant insight into protein folding can be achieved by analyzing split-membrane proteins, and provided the conceptual basis for the two-stage model of membrane-protein folding^{4,5}. According to this model, first, stretches of ~20 residues of sufficient net hydrophobicity are inserted into the membrane bilayer. These stretches then spontaneously fold into stable α -helices as a result of the thermodynamically favored formation of backbone hydrogen bonds within the lipid environment. Aromatic (tryptophan and tyrosine, but not phenylalanine) and basic (lysine and arginine) residues near the ends of the transmembrane segments contribute to their precise interfacial positioning in biological membranes (reviewed in ref. 6). In the second stage of the folding process, membrane-imbedded α -helices associate with each other to form helix bundles, resulting for most polytopic membrane proteins in a compact packing of their respective hydrophobic cores⁷. In addition to tertiary structure formation, helix-helix interactions within the bilayer can direct homo-oligomeric and hetero-oligomeric subunit assemblies, which are widespread among polytopic membrane proteins⁸. How exactly the association of transmembrane α -helices is accomplished remains an open question^{9,10}, because with the advent of higher-resolution structures it has become clear that helical membrane proteins are not more tightly packed than water-soluble proteins^{11,12}.

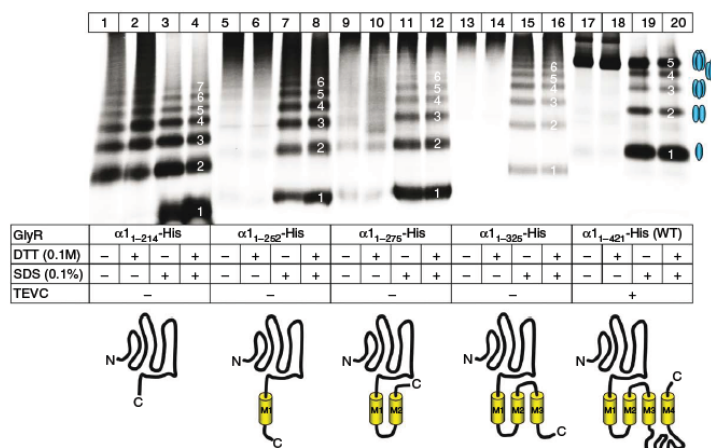
pLGICs are polytopic membrane proteins, which, at neuron-muscle and neuron-neuron synapses, convert chemical signals within milliseconds into membrane-potential changes by opening an intrinsic transmembrane ion pore in response to neurotransmitter binding. Individual subfamilies of the pLGIC superfamily include nicotinic acetylcholine receptors (nAChRs), serotonin type 3 receptors (5HT₃Rs), γ -amino butyric acid type A receptors (GABA_ARs) and glycine receptors (GlyRs). pLGICs function as obligate pentamers of identical or homologous subunits, which comprise an extracellular neurotransmitter-binding domain followed by a transmembrane region characterized by four membrane-spanning helical segments, M1–M4. The assembly of pLGICs is thought to be driven by interactions between the N-terminal extracellular domains of the subunits^{13,14}. Mutational analysis of nAChR subunits has identified sequence elements and residues in the extracellular domain that control the specificity of subunit oligomerization and receptor stoichiometry^{15,16}. Also, using chimeric GlyR α and β subunits and dominant negative mutants, we have found that hetero-oligomerization of the GlyR α 1 and β subunits requires interactions between their N-terminal extracellular regions^{17,18}. Here, we address the role of transmembrane domains in human GlyR and mouse 5HT₃A receptor assembly and function by subunit truncations, site-directed mutagenesis and homology modeling. Our results indicate that a network of aromatic residues between transmembrane helices M1, M3 and M4 provides for precise intramembrane α -helical packing and thereby determines pLGIC subunit stoichiometry.

¹Molecular Pharmacology, RWTH Aachen University of Aachen, Aachen, Germany. ²Department of Neurochemistry, Max Planck Institute for Brain Research, Frankfurt am Main, Germany. ³Shemyakin-Ovchinnikov Institute of Bioorganic Chemistry, Russian Academy of Sciences, Moscow, Russia. ⁴Department Molekulare und zelluläre Neurophysiologie, Technische Universität Darmstadt, Darmstadt, Germany. Correspondence should be addressed to G.S. (gschmalzing@ukaachen.de).

Received 25 January; accepted 19 October; published online 20 December 2009; doi:10.1038/nsmb.1721



Figure 1 Oligomeric structures of $\alpha 1$ GlyR truncation mutants. The indicated [^{35}S]methionine-labeled GlyR $\alpha 1$ -His constructs were purified by nondenaturing nickel nitriloacetic acid (Ni-NTA) chromatography from digitonin extracts of *X. laevis* oocytes, resolved by BN-PAGE and visualized by phosphorimaging. Protein migration is shown both under native conditions and after partial denaturation produced by a 1-h incubation with SDS and/or DTT as indicated. Blue ovals schematically illustrate oligomeric states. Bottom cartoons depict the topology and size of the truncation mutants used.



RESULTS

We used *Xenopus laevis* oocytes to express the various receptor subunit constructs, which all carried a C-terminal hexahistidyl tag for protein purification. After metabolic and cell-surface labeling with [^{35}S]methionine and fluorescent cyanine 5 (Cy5) dye, respectively, we extracted the proteins with the mild nonionic detergent digitonin, affinity-purified them on a metal affinity resin and released them in nondenaturing buffer. We analyzed the oligomeric state of the purified proteins by blue native PAGE (BN-PAGE), which has been shown to reliably display the quaternary structures of various membrane proteins^{18–26}. We also expressed the same constructs for two-electrode voltage clamp (TEVC) recordings.

Truncated GlyR subunits oligomerize but not into pentamers

We have previously shown that the 48-kDa $\alpha 1$ subunits of homopentameric GlyRs are proteolytically cleaved within the cytoplasmic M3-M4 loop into fragments of ~35 kDa and ~13 kDa in *X. laevis* oocytes²¹. The split homopentamer maintains the same mass as the uncleaved $\alpha 1$ GlyR²¹. This indicates that the 13-kDa fragments remain tightly associated with the core of the nicked $\alpha 1$ GlyR and suggests that sequence motifs C-terminal to the ectodomain may play a role in GlyR assembly. To address this issue, we generated four C-terminally truncated constructs of the mature GlyR $\alpha 1$ subunit (see schemes in Fig. 1). All four proteins migrated on SDS-PAGE gels as anticipated for their expected respective molecular masses (results not shown).

BN-PAGE of the N-terminal fragment comprising the GlyR $\alpha 1$ ectodomain showed a strong propensity to self-associate randomly into dimers or higher-order oligomers (Fig. 1, lane 1). Notably, there was no preferential formation of any individual oligomer. Truncation at a position to include M1 (Fig. 1, lane 5), M2 (Fig. 1, lane 9) or M3

(Fig. 1, lane 13) led to complete aggregation, as judged from the undefined high-mass protein migrating at the top of the gel. The random oligomers and the aggregates were resistant to DTT (Fig. 1, lanes 2, 6, 10 and 14) but sensitive to SDS (Fig. 1, lanes 3, 4, 7, 8, 11, 12, 15 and 16), indicating that they were held together by noncovalent bonds. The wild-type (WT) $\alpha 1$ GlyR migrated under identical conditions as a defined homopentamer (Fig. 1, lane 17) that disassembled into tetramers, trimers, dimers and monomers in the presence of SDS but not DTT¹⁸ (Fig. 1, lanes 18–20).

Coexpression of M4 with GlyR $\alpha 1_{1-325}$ rescues assembly

To examine the role of the C-terminal region in GlyR assembly, we generated GlyR $\alpha 1_{376-421}$ -His, comprising a small portion of the M3-M4 loop, the M4 domain and the extracellular C-terminal tail. The $\alpha 1_{376-421}$ -His fragment should behave like a type II membrane protein, with the genuine M4 acting as a signal anchor, resulting in an $N_{\text{Cyt}}\text{-}C_{\text{out}}$ orientation relative to the membrane which would be identical to that within the full-length $\alpha 1$ subunit.

The singly expressed $\alpha 1_{376-421}$ -His fragment formed predominantly aggregates (Fig. 2, lane 1). Coexpression with the $\alpha 1_{1-252}$ -His truncation mutant failed to prevent aggregate formation (Fig. 2, lane 4). However, coexpression of $\alpha 1_{376-421}$ -His with the longest truncation mutant, $\alpha 1_{1-325}$ -His, resulted in a defined protein complex (Fig. 2, lanes 7 and 10) that migrated at the same position upon BN-PAGE as the homopentameric WT $\alpha 1$ GlyR (Fig. 2, lane 16). Partial denaturation generated five bands, each spaced by the 35-kDa mass of the $\alpha 1_{1-325}$ -His truncation mutant (Fig. 2, lanes 8, 9, 11 and 12). This band pattern resembles that formed upon partial dissociation of the WT $\alpha 1$ GlyR (Fig. 1) and is consistent with a pentameric stoichiometry. A defined protein complex was also formed when we coexpressed the $\alpha 1_{1-325}$ -His truncation mutant with the $\alpha 1_{341-421}$ -His fragment (Fig. 2, lane 13), which included a larger part of the cytosolic

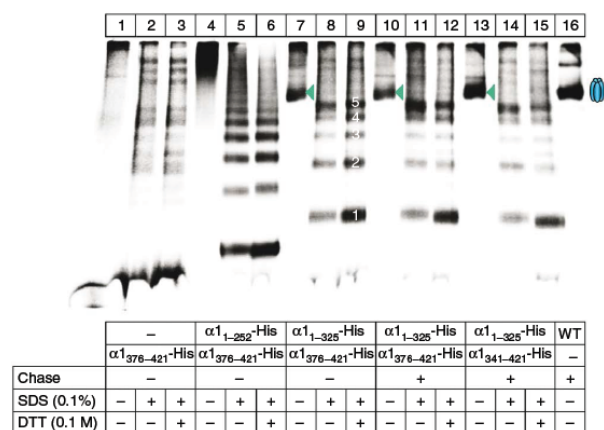
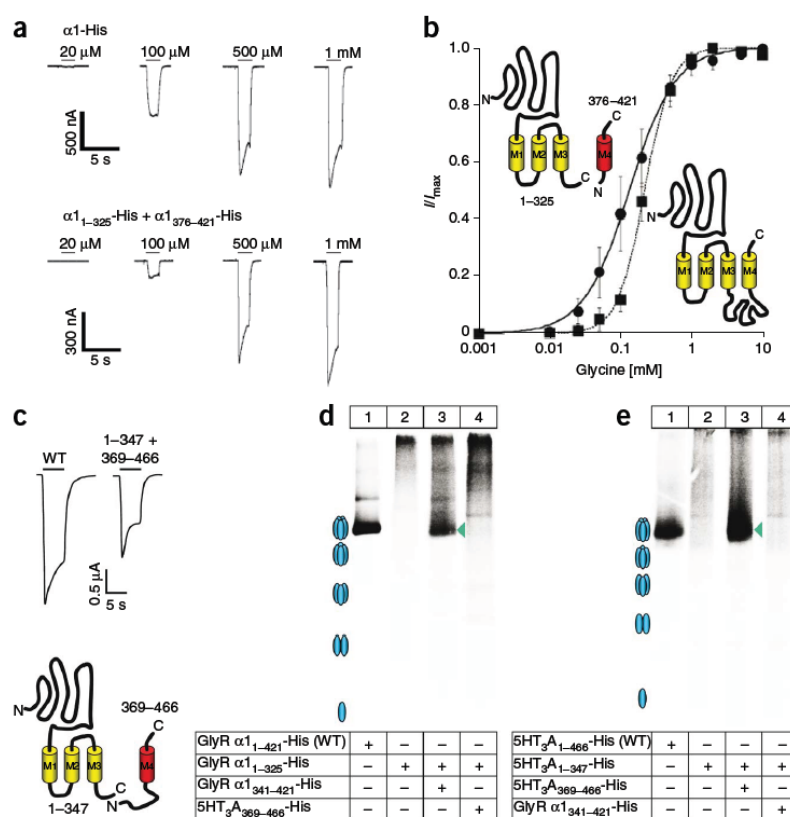


Figure 2 Reconstitution of pentamer formation upon coexpression of N- and C-terminally truncated GlyR $\alpha 1$ subunit fragments. We coexpressed C-terminally truncated GlyR $\alpha 1$ -His constructs with C-terminal $\alpha 1$ fragments as indicated. The affinity-purified proteins were resolved by BN-PAGE either under native conditions or after partial denaturation with 0.1% (w/v) SDS for 1 h at 37 °C in the absence or presence of 100 mM DTT as indicated and visualized by phosphorimaging. Note that coexpression of the $\alpha 1_{1-325}$ -His N-domain with a short C-terminal fragment encompassing M4 resulted in the formation of pentameric protein complexes (green arrowheads) that migrated at the same position as the WT $\alpha 1$ -His GlyR (blue ovals). White numbers indicate oligomerization states of respective bands produced upon partial denaturation.

Figure 3 Reconstitution of $\alpha 1$ GlyR and 5HT₃A receptor function from complementary homotypic fragments. (a) Typical whole-oocyte current traces elicited by various glycine concentrations in oocytes expressing the WT $\alpha 1$ GlyR or the split $\alpha 1_{376-421}$ -His/ $\alpha 1_{1-325}$ -His GlyR. (b) Glycine concentration-response curves for the WT $\alpha 1$ GlyR ($EC_{50} = 218 \pm 50 \mu M$; Hill coefficient $n_H = 2.3 \pm 0.3$) and the split $\alpha 1_{376-421}$ -His/ $\alpha 1_{1-325}$ -His GlyR ($EC_{50} = 170 \pm 112 \mu M$; $n_H = 1.7 \pm 0.3$) were not significantly different ($P > 0.05$, $n = 6$ each); data are mean \pm s.d. (c) Coexpression of 5HT₃A₃₆₉₋₄₆₆-His and 5HT₃A₁₋₃₄₇-His fragments generates serotonin-gated ion channels. Shown are typical whole-cell current traces elicited by a saturating (100 μM) concentration of serotonin in oocytes expressing the indicated constructs for 2 d. (d,e) Complementary $\alpha 1$ GlyR and 5HT₃A fragments do not coassemble. Oligomeric state of the indicated Ni-NTA-purified proteins as visualized by BN-PAGE and phosphorimaging. No defined receptor complexes were formed when the GlyR $\alpha 1$ -His N-terminal fragment was combined with the 5HT₃A-His C-terminal fragment (d) or when the 5HT₃A-His N-terminal fragment was combined with the GlyR $\alpha 1$ -His C-terminal fragment (e). Assembly of N- and C-terminal fragments into pentameric receptor complexes (green arrowheads) occurred only with fragments originating from the same receptor species. We adjusted the contrast of individual lanes using ImageQuant software to avoid overexposure of protein bands representing assembled receptor complexes. Blue ovals schematically indicate oligomeric states as produced by partial denaturation of the respective WT receptor.



M3-M4 loop than $\alpha 1_{376-421}$ -His. The mass shift to a smaller oligomer produced by low SDS treatment of the split GlyR complexes (Fig. 2, lanes 8, 9, 11, 12, 14 and 15) can be readily attributed to the SDS-induced dissociation of the coassembled C-terminal fragments. The remaining oligomers seem to consist exclusively of $\alpha 1_{1-325}$ -His fragments that associate more strongly among themselves than with the $\alpha 1_{376-421}$ -His or the $\alpha 1_{341-421}$ -His fragments. Other split $\alpha 1$ subunit fragments did not result in the formation of a defined oligomer when combined in a manner to supplement the four transmembrane domains of the full-length $\alpha 1$ subunit (Supplementary Fig. 1). Thus, the interaction of M4-containing peptides with $\alpha 1_{1-325}$ polypeptides may require preformed M1-M3 trihelical structures.

Coexpression of M4 with GlyR $\alpha 1_{1-325}$ restores function

To examine whether restoration of assembly coincides with the acquisition of function, we screened for glycine-activated currents. In oocytes expressing either N- or C-terminal GlyR $\alpha 1$ fragments, no currents could be elicited by glycine (data not shown). However, the same GlyR $\alpha 1_{1-325}$ -His/ $\alpha 1_{376-421}$ -His combination that rescued pentameric assembly also rescued function (Fig. 3a). The mean maximal glycine-induced current ($I_{max} \pm$ s.d.) of $3.4 \pm 1.4 \mu A$ ($n = 6$) corresponded to about half that of the WT $\alpha 1$ GlyR ($I_{max} = 6.4 \pm 1.9 \mu A$; $n = 12$). Glycine concentration-response curves yielded similar half maximal effective concentration (EC_{50}) values for the WT $\alpha 1$ GlyR and the split $\alpha 1_{1-325}$ -His/ $\alpha 1_{376-421}$ -His GlyR, respectively (Fig. 3b). Consistent with our BN-PAGE data (Fig. 2), coexpression of the split $\alpha 1_{1-325}$ -His/ $\alpha 1_{341-421}$ -His GlyR also resulted in functional

glycine-gated channels, whereas coexpression of $\alpha 1_{1-214}$ -His, $\alpha 1_{1-252}$ -His or $\alpha 1_{1-275}$ -His with either $\alpha 1_{341-421}$ -His or $\alpha 1_{376-421}$ -His failed to generate functional GlyRs (data not shown). The ability of the $\alpha 1_{376-421}$ -His C-terminal fragment to rescue channel function of the truncated $\alpha 1_{1-325}$ -His subunit is consistent with a highly specific interaction between M4 and the M1-M3 segments of the GlyR $\alpha 1$ subunit.

5HT₃ receptor formed of M1-M3- and M4-containing fragments

To examine whether interactions similar to those of the $\alpha 1$ GlyR exist in other pLGICs, we investigated the 5HT₃A receptor. Like the $\alpha 1$ GlyR, the 5HT₃A receptor was efficiently targeted to the plasma membrane (Supplementary Fig. 2a, lane 1) and migrated as a distinct band upon BN-PAGE (Supplementary Fig. 2c, lane 2). Consistent with a pentameric structure^{23,27}, partial denaturation with SDS generated five bands, each separated by the mass of a 5HT₃A monomer (Supplementary Fig. 2c, lane 1).

The mature 5HT₃A subunit encompasses 466 residues. An N-terminal fragment comprising the entire ectodomain and M1-M3, but lacking most of the cytoplasmic M3-M4 loop and M4 (5HT₃A₁₋₃₄₇-His; see cartoon in Fig. 3c), did not migrate at a defined assembly state (Supplementary Fig. 2c, lane 3), was degraded more rapidly (Supplementary Fig. 2b, lane 2) and did not appear at the cell surface (Supplementary Fig. 2a, lane 2). Coexpression with a complementary M4-containing fragment, 5HT₃A₃₆₉₋₄₆₆-His, rescued assembly, as evidenced by the appearance of a defined oligomer in the BN-PAGE gel (Supplementary Fig. 2c, lanes 4-6) at almost the same position as the full-length 5HT₃A-His homopentamer (Supplementary

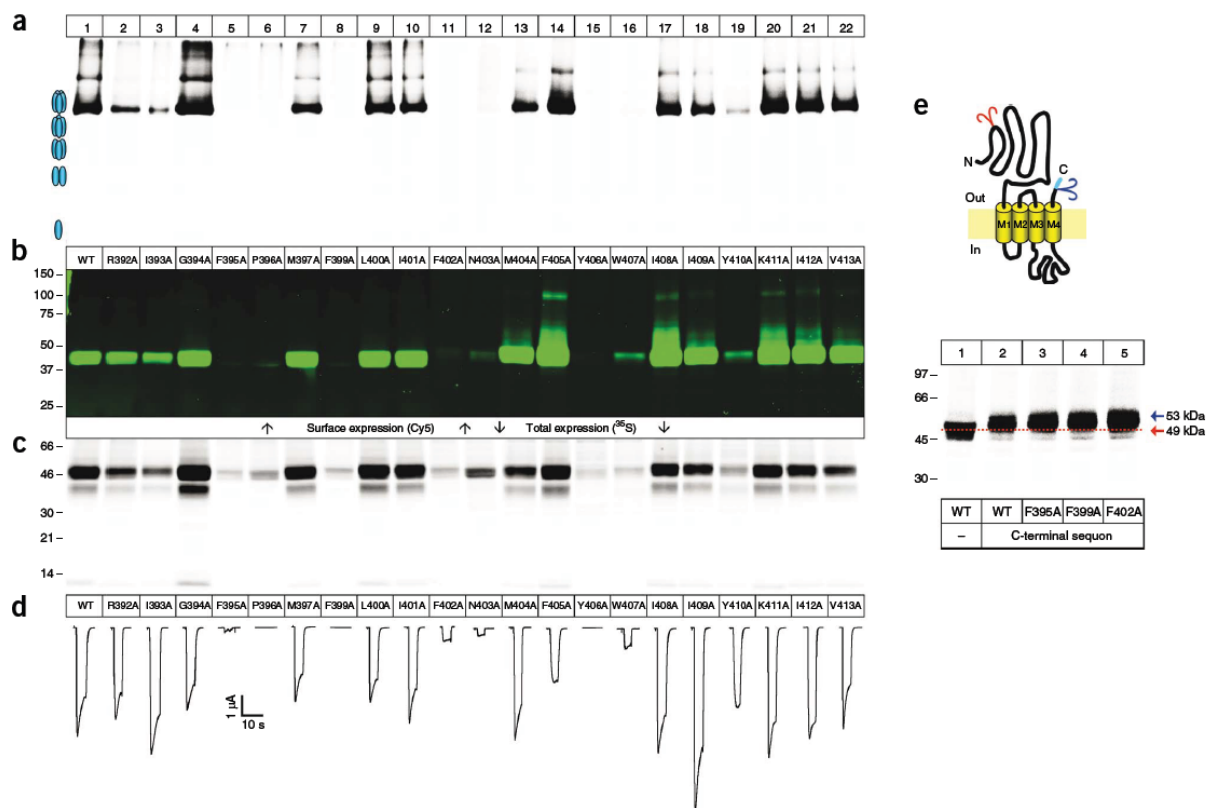


Figure 4 Effect of single alanine substitutions in M4 on assembly, surface expression and function of the $\alpha 1$ GlyR. WT residues were singly replaced by alanines as indicated. (a–c) Proteins labeled with [35 S]methionine and Cy5 were purified and resolved by BN-PAGE and their oligomeric states were displayed by phosphorimaging (a), or resolved by reducing SDS-urea-PAGE to display Cy5-labeled surface GlyR polypeptides (b) and [35 S]methionine-labeled GlyR subunits (c). Ovals schematically illustrate the oligomeric states of the non-denatured and partially denatured WT $\alpha 1$ GlyR. Panels shown are from two separate experiments with mutants R392A to I401A and F402A to V413A, respectively. Each mutant was analyzed at least twice with identical results. Note that residue 398 is already an alanine in the WT GlyR $\alpha 1$ subunit. (d) Typical whole-oocyte current traces elicited by a saturating (10 mM) concentration of glycine in oocytes expressing the indicated $\alpha 1$ GlyR constructs for 2 d. (e) The indicated WT GlyR polypeptides and M4 mutants were purified by Ni-NTA chromatography after a 4-h [35 S]methionine pulse and resolved by reducing SDS-PAGE. The *N*-glycan acceptor site (428 NWS) introduced as part of the StrepII tag (marked sky blue) after the C-terminal hexahistidine sequence was efficiently used by both the WT and the M4 mutant GlyR $\alpha 1$ -His-StrepII subunits, as indicated by the 4-kDa mass increase. The cartoon depicts the topology of the WT GlyR $\alpha 1$ -His-StrepII subunit including the position of the two *N*-glycans (γ -like symbols), one in the single native position (orange, 38 NVS) and the second in the artificially introduced C-terminal position (dark blue, 428 NWS).

Fig. 2c, lane 2). Partial denaturation with SDS produced five bands, each spaced by the ~40-kDa mass of the 5HT₃A_{1–347}-His (Supplementary Fig. 2c, lane 7). Proper assembly of the split 5HT₃A_{1–347}-His protein at the plasma membrane (Supplementary Fig. 2a, lanes 3–5).

No serotonin-induced currents could be elicited from oocytes singly expressing the 5HT₃A_{1–347}-His N-terminal domain or the 5HT₃A_{369–466}-His C-terminal domain (data not shown). If, however, we coexpressed both domains, serotonin elicited inward currents that were almost as large as those generated by the WT 5HT₃A_{1–347}-His receptor (Fig. 3c). Taken together, these data suggest that the M4-containing C-terminal domain has a general role in the assembly of Cys-loop receptors.

To reveal whether the interactions between the M1–M3- and M4-containing fragments are receptor-specific, we coexpressed the truncated GlyR $\alpha 1_{1–325}$ -His polypeptide with the 5HT₃A_{369–466}-His fragment (Fig. 3d) and vice versa (5HT₃A_{1–347}-His with GlyR $\alpha 1_{341–421}$ -His) (Fig. 3e). None of these combinations resulted in productive assembly of defined receptor complexes (lane 4 in Fig. 3d,e).

Consistent with biochemical analysis, we could not detect glycine- or serotonin-gated inward currents in oocytes coexpressing the above-mentioned fragment combinations for up to 4 d (data not shown). These findings highlight the specificity of transmembrane segment interactions.

GlyR M4 assembly interface mapped by scanning mutagenesis

To identify residues critical for M4 interaction, we analyzed single alanine substitutions of all predicted 21 residues (Ile393–Val413) in M4. Most of the mutants assembled well into pentamers (Fig. 4a) and were abundantly expressed at the plasma membrane (Fig. 4b). Eight mutants, F395A, P396A, F399A, F402A, N403A, Y406A, W407A and Y410A, showed strongly reduced or no pentameric assembly (Fig. 4a) and diminished or absent cell-surface expression (Fig. 4b). In addition, total expression of these assembly-impaired alanine mutants was strongly reduced (Fig. 4c). Pulse-chase experiments showed, for example, that the assembly-incompetent M4 mutants F395A, P396A and F399A were well synthesized during a 4 h pulse, but were largely degraded during a subsequent chase

(Supplementary Fig. 3). In contrast, the assembly-competent M4 mutants M397A, L400A and I401A were metabolically stable throughout the chase. Assembly-dependent stabilization of Cys-loop receptor subunits has been observed previously with muscle-type $\alpha\beta\gamma\delta$ nAChRs^{28,29}. This can readily be explained by the existence of an active 'endoplasmic reticulum quality control' mechanism that degrades incompletely assembled proteins.

In TEVC recordings, three of the alanine mutants gave no response to up to 100 mM glycine and were hence rated as nonfunctional (P396A, F399A, Y406A; $n = 10$, each). Five mutations (F395A, F402A, N403A, W407A and Y410A) resulted in a highly significant reduction of glycine I_{\max} values ($P < 0.01$, $n = 5-9$; Fig. 4d; Table 1). Thus, all assembly-impaired mutants also had impaired GlyR function. All other mutants (13) produced maximal glycine-evoked currents comparable to that of the WT $\alpha 1$ GlyR (I_{\max} in the range of 4.9–7.9 μA , Table 1).

To exclude the possibility that the mutations affected transmembrane topology (as observed for aquaporin³⁰), we performed reporter glycosylation experiments. To monitor the orientation of M4, we added an N-glycan acceptor site as part of a StrepII affinity tag (NWSHPQFEK)³¹ to the C-terminal end of the WT $\alpha 1$ -His GlyR (cartoon in Fig. 4e) and three representative assembly-impaired M4 mutants. SDS-PAGE directly after a [³⁵S]methionine pulse revealed a 4-kDa mass increase of the WT $\alpha 1$ -His-StrepII (Fig. 4e, lane 2) and the $\alpha 1$ -His-StrepII M4 mutants (Fig. 4e, lanes 2–5) as compared to the parental $\alpha 1$ -His subunit lacking a C-terminal N-glycan acceptor site (Fig. 4e, lane 1). The efficient hyperglycosylation is consistent with a luminal localization of the engineered glycan acceptor site in both WT and mutant polypeptides. These results demonstrate that the M4 segment of assembly-impaired M4 mutants adopts the correct N_{cyt}-C_{out} orientation, with the C-terminal tail being located lumenally as in the WT $\alpha 1$ GlyR.

Interaction delineated by *in silico* and mutational screening

The eight M4 residues identified by alanine replacement to be critical for homopentamer formation cluster on one face of the M4 α -helix (Fig. 5a). Given, in addition, the peripheral position of M4 (Fig. 5b), it is plausible to suggest that the assembly-relevant aromatic face of the M4 helix interacts side to side with M1 and M3, thus explaining the physically stable association of M4-incorporating fragments with the truncated $\alpha 1_{1-325}$ GlyR. To verify this, we constructed a set of homology models for mutant M4 analogs (residues Lys389–Val413) and tested them *in silico* for docking to the $\alpha 1_{1-325}$ homopentameric GlyR modeled using as templates the atomic structures of the prokaryotic pLGIC ELIC³² and the *Torpedo californica* nAChR³³. The calculated energies of interaction and the relative rotational freedom of the M4-mimetic peptides are presented in Table 1. In the case of P396A, we did not observe any distinct interaction between the ligand and peptide and the truncated receptor owing to a highly distorted conformation of the peptide. For mutants F395A, F399A, F402A, N403A, Y406A, W407A and Y410A, the predicted binding energies

Table 1 Pharmacological effects and energy calculations of alanine mutations in $\alpha 1$ GlyR M4

	EC ₅₀ [μM]	n_H	I_{\max} [μA]	Surface labeling	Binding energy [kJ mol ⁻¹]	Rotational freedom
WT	218 ± 50	2.3 ± 0.3	6.4 ± 1.6	+	-2.8 ± 0.01	1.0
R392A	228 ± 114	2.7 ± 0.3	5.5 ± 1.7	+	-2.0 ± 0.04	0.7
I393A	105 ± 19	1.7 ± 0.6	7.3 ± 1.5	+	-2.3 ± 0.03	1.1
G394A	110 ± 37	3.0 ± 0.4	6.5 ± 2.6	+	-2.0 ± 0.04	1.4
F395A	475 ± 159 ^a	1.6 ± 0.5	0.3 ± 0.2 ^b	-	-0.10 ± 0.04 ^a	1.8
P396A	nf	-	-	-	No cluster	-
M397A	323 ± 71	2.2 ± 0.4	4.9 ± 1.3	+	-1.1 ± 0.05 ^a	1.0
F399A	nf	-	-	-	-0.11 ± 0.01 ^b	4.1 ^b
L400A	195 ± 47	2.0 ± 0.3	5.2 ± 0.5	+	-2.1 ± 0.05	1.0
I401A	234 ± 61	1.9 ± 0.4	5.8 ± 1.2	+	-2.3 ± 0.04	1.1
F402A	217 ± 29	1.8 ± 0.2	0.9 ± 0.2 ^a	(+)	-0.12 ± 0.01 ^b	1.4
N403A	318 ± 87	1.7 ± 0.2	1.1 ± 0.2 ^a	(+)	-0.97 ± 0.04 ^a	1.0
M404A	276 ± 54	2.1 ± 0.3	6.2 ± 1.4	+	-2.1 ± 0.05	1.1
F405A	440 ± 76 ^a	2.0 ± 0.3	5.1 ± 0.9	+	-1.0 ± 0.06 ^a	1.8
Y406A	nf	-	-	-	-0.31 ± 0.03 ^b	3.8 ^b
W407A	1056 ± 358 ^b	1.4 ± 0.2 ^a	0.5 ± 0.1 ^b	(+)	-0.22 ± 0.02 ^b	2.6 ^a
I408A	273 ± 29	1.9 ± 0.4	6.3 ± 0.7	+	-1.8 ± 0.04	1.2
I409A	167 ± 45	2.1 ± 0.1	4.9 ± 1.0	+	-1.7 ± 0.02	1.0
Y410A	3521 ± 442 ^b	2.0 ± 0.4	0.7 ± 0.2 ^a	(+)	-0.31 ± 0.04 ^b	2.1 ^a
K411A	345 ± 91	2.2 ± 0.3	5.1 ± 1.3	+	-0.9 ± 0.05 ^a	0.9
I412A	298 ± 87	2.4 ± 0.2	7.9 ± 0.9	+	-2.1 ± 0.03	1.0
V413A	310 ± 105	2.2 ± 0.3	7.1 ± 0.4	+	-2.7 ± 0.02	1.0

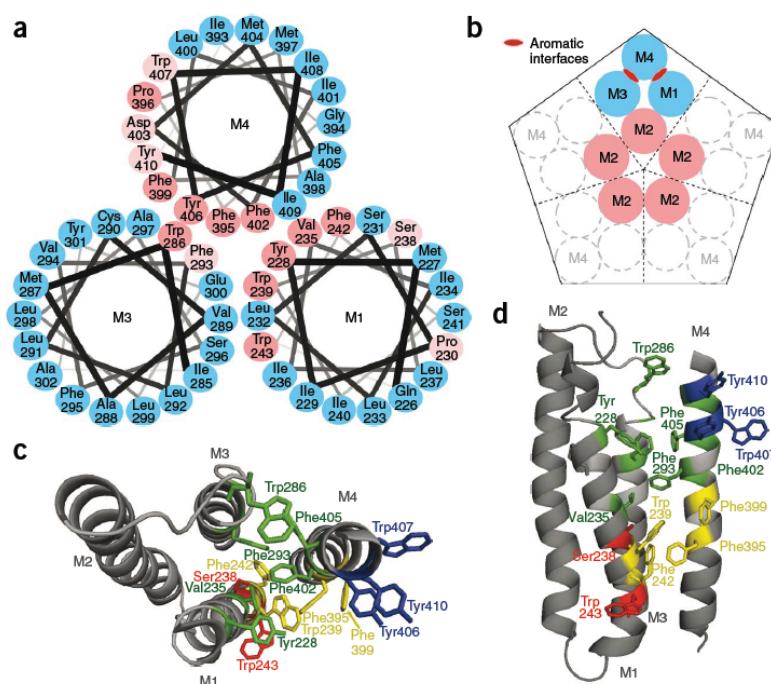
Glycine responses of the WT and mutant GlyRs were recorded by TEVC; data represent means ± s.d. from 6–12 experiments. n_H , Hill coefficient; nf, nonfunctional; I_{\max} , maximal inducible current. Surface labeling data are from Figure 4d; +, like WT; (+), weak; -, not detectable. The binding energies of C-terminal GlyR fragment docking to the mutant $\alpha 1_{1-325}$ GlyRs were determined *in silico* as described in Online Methods; data represent means ± s.d. from 20 experiments. Values significantly different from WT $\alpha 1$ GlyR (^a $P < 0.01$; ^b $P < 0.001$) are indicated.

were rather low as compared to that of the WT Lys389–Val413 M4 peptide (Table 1). Homology modeling suggests that three of these residues, Tyr406, Trp407 and Tyr410, are not directly involved in interhelical interactions but are lipid-facing (Fig. 5c,d). Thus, the respective side chains may stabilize the M4 helix in the bilayer through interactions with lipid molecules. These *in silico* data are fully consistent with the view that the residues shown to be assembly-relevant by BN-PAGE and TEVC are crucial for keeping the split GlyR fragments assembled.

To identify residues in M1 and M3 that contact M4, we generated models of the homopentameric $\alpha 1_{1-325}$ GlyR carrying alanine substitutions of single M1 and M3 residues and docked them to the WT M4 Lys389–Val413 peptide. For M1 mutants Y228A, V235A, W239A, F242A and W243A and M3 mutants W286A and F293A, docking simulations predicted significantly reduced binding energies ($P < 0.001$) as compared to the WT or the other $\alpha 1_{1-325}$ single alanine substitutions except P230A, which was unstable in energy minimization (Table 2). Notably, our docking results indicated only impaired binding energies for the alanine mutants, indicative of less stable contacts between the transmembrane segments but not of misfolding. Even during extended molecular dynamics simulation periods, none of the assembly-impaired mutants underwent unfolding of the membrane-embedded core tetrahelical bundle.

To verify the interaction sites predicted by modeling, we alanine-scanned M1 and M3 biochemically and functionally. Block mutagenesis showed that only the N-terminal half of M3 contained assembly-relevant residues (Supplementary Fig. 4d–f). Accordingly, alanine single mutants were generated only for this part of M3. Fully consistent with our homology modeling, single alanine replacement of each of the M1 and M3 residues predicted to be assembly-relevant drastically decreased I_{\max} (Phe293 in M3) or abolished channel

Figure 5 Location of membrane-embedded aromatic residues crucial for homopentameric assembly of the $\alpha 1$ GlyR. (a) Helical wheel projections of M1, M3 and M4 are arranged relative to each other according to the structural data obtained by computational docking and viewed from the synaptic cleft. Results obtained from alanine scanning are color coded. Alanine substitutions that impair (light pink) or abolish (pink) pentamer formation are located on the same sides of the α -helices (except Pro230 in M1) and consist predominantly of aromatic residues. Alanine substitutions that were well tolerated in terms of pentameric assembly, surface expression and function are blue. (b) Arrangement of transmembrane helices in a pentameric pLGIC based on the 4-Å electron microscopy structure of the *Torpedo* nAChR³⁶ as viewed from the synaptic cleft. Individual subunits are delineated by dashed symmetry axes. The aromatic intrasubunit interfaces crucial for pentamer formation are indicated for one subunit. (c,d) Homology-modeled structure showing aromatic residues involved in interactions between transmembrane helices M1–M3 as viewed from the synaptic cleft (c) and from the side (d). The color code indicates residues important for pentamer formation by being involved in interactions between upper and lower tiers of helices of the same subunit (green and yellow, respectively) or supposedly different subunits (red); residues supposed to interact with lipids are colored blue.



function (Tyr228, Trp239, Phe242 in M1 or Trp286 in M3; Table 2) and impaired assembly (Supplementary Fig. 4a–c,g–i). There was only one mutant, S238A in M1, for which the data were not entirely concordant. From the otherwise excellent agreement of the interaction sites predicted by modeling with the impaired assembly and channel function, the following intramembrane interactions can be deduced (Fig. 5c,d): Tyr228 in M1 interacts with Phe293 in M3 and with Phe402 and Phe405 in M4; Trp239 and Phe242 in M1 interact with Phe395 and Phe399 in M4, respectively; and Trp286 in M3 covers the aromatic stack like a cap.

We also docked the 5HT₃A_{369–466} M4 fragment to the truncated 5HT₃A_{1–347} receptor and observed a high interaction energy of 3.3 ± 0.05 kJ mol⁻¹, indicative of a strong association. In contrast, cross-docking of the 5HT₃A_{369–466} M4 fragment to the truncated $\alpha 1_{1–325}$ homopentameric GlyR resulted in a very low binding energy (-0.13 ± 0.03 kJ mol⁻¹). This corroborates our biochemical data showing that M4 interactions are receptor specific (compare Fig. 3d,e).

DISCUSSION

pLGIC subunits pentamerize cotranslationally in the endoplasmic reticulum and reside in intracellular compartments and in the plasma membrane as obligate pentamers^{14,18,21–23}. Here we show that expression of GlyR $\alpha 1$ or 5HT₃A subunits as two separate polypeptides (one containing the ectodomain and M1–M3 and the other containing M4) results in the assembly of functional pLGICs indistinguishable in their electrophysiological properties from WT pLGICs consisting of contiguous subunits. None of the pLGIC subunit fragments gave rise to channel activity upon single expression, nor did coexpressed complementary fragments split between M1 and M2 or M2 and M3. A high-affinity, stable interaction of M4 with the neighboring M1 and M3 helices can be inferred from the retention of the recombinant GlyR and 5-HT₃A receptor M4 domains in a BN-PAGE-resistant complex formed with the respective C-terminally truncated pLGIC fragments comprising the ectodomain and M1–M3. Retrospectively, tight intramembrane binding of M4 also explains the retention of

the C-terminal fragment in the proteolytically nicked GlyR²¹. Strong interactions between M4 and M1 and M3 would have not been expected from the crystal structures of prokaryotic pLGICs, which show M4 to be peripheral to the other transmembrane segments as a result of intercalating lipid molecules^{32,34,35}. Together our results unveil an as-yet-undefined requirement for M1, M3 and M4 in pLGIC assembly in addition to the well-known role of the ectodomain in this process.

An aromatic net between M1, M3 and M4 is key for GlyR assembly

One important role of aromatic residues is to stabilize the transmembrane topology of proteins by anchoring interactions in the membrane-water interfacial region⁶. Indeed, Tyr406, Trp407 and Tyr410 are predicted by homology modeling to be lipid-facing and to strongly stabilize the M4 structure by interacting with bilayer lipids, thus supporting assembly by interfacial anchoring of M4. The remaining four aromatic residues are located toward the center of the M4 helix (Fig. 5d) and form a stacking interface for intramembrane helix-helix interactions. Although Phe405 is assigned as lipid-facing by helical wheel projection of M4 (Fig. 5a), homology modeling predicts with high probability that even Phe405 is part of the aromatic network and interacts by π - π stacking with Phe293 (Fig. 5c,d).

The 4-Å electron microscopy structure of the *Torpedo* nAChR³³ places the M4 helix to the periphery of the barrel-like pentamer in contact with M1 and M3, and it is thus consistent the existence of two interhelical interfaces, M1–M4 and M3–M4 (Fig. 5b). Here, homology modeling based on the crystal structure of a bacterial pLGIC predicted that the aromatic face of the M4 helix would contact three of the six aromatic residues located in the M1 helix (Tyr228, Trp239 and Phe242) and two of the four aromatic residues in the M3 helix (Trp286, Phe293) via π - π interactions³⁶. The loss of homopentamer formation and function seen upon alanine replacement of any of these predicted aromatic M1 and M3 contact residues strongly supports the existence of a membrane-embedded network of pairwise-interacting aromatic side chains that compacts and stabilizes the membrane core

Table 2 Effects of single alanine substitutions in M1 and M3 of the $\alpha 1$ GlyR on glycine-gated maximal currents, pentameric assembly and calculated docking parameters

	I_{\max} [μ A]	Surface labeling	Binding energy [kJ mol ⁻¹]	Rotational freedom
WT	6.4 ± 1.6	+	-2.8 ± 0.01	1.0
M220A	8.2 ± 1.8	+	-2.2 ± 0.3	1.1
G221A	6.0 ± 1.2	+	-2.7 ± 0.2	1.0
Y222A	5.6 ± 1.1	+	-2.0 ± 0.3	1.0
Y223A	0.9 ± 0.5 ^a	+	-1.9 ± 0.2	2.4 ^b
L224A	5.8 ± 0.7	+	-3.8 ± 0.2	1.0
I225A	7.1 ± 2.1	+	-3.1 ± 0.2	1.0
Q226A	2.0 ± 0.8	+	-2.4 ± 0.2	1.0
M227A	4.3 ± 0.9	+	-2.6 ± 0.2	1.0
Y228A	nf	-	-0.2 ± 0.05 ^b	1.1
I229A	4.0 ± 1.7	+	-1.6 ± 0.4	1.0
P230A	0.6 ± 0.3 ^b	(+)	No cluster	-
S231A	6.5 ± 0.9	+	-2.6 ± 0.1	1.0
L232A	7.5 ± 0.6	+	-3.0 ± 0.2	1.0
L233A	7.5 ± 1.4	+	-2.9 ± 0.2	0.8
I234A	7.6 ± 1.2	+	-2.5 ± 0.3	1.1
V235A	0.3 ± 0.1 ^b	-	-0.5 ± 0.2 ^b	1.0
I236A	8.0 ± 1.9	+	-2.6 ± 0.2	1.0
L237A	5.8 ± 0.4	+	-2.2 ± 0.3	0.9
S238A	4.4 ± 0.4	(+)	-2.5 ± 0.3	1.0
W239A	nf	-	-0.3 ± 0.05 ^b	1.0
I240A	7.6 ± 1.7	+	-3.0 ± 0.2	1.0
S241A	9.2 ± 1.2	+	-3.1 ± 0.3	1.0
F242A	0.1 ± 0.05 ^b	-	-0.15 ± 0.05 ^b	1.0
W243A	0.5 ± 0.03 ^b	-	-0.4 ± 0.1 ^b	0.9
I244A	3.4 ± 0.7	+	-1.5 ± 0.2 ^a	1.5
I285A	4.7 ± 0.8	+	-3.2 ± 0.2	1.0
W286A	nf	-	-0.1 ± 0.05 ^b	1.2
M287A	9.7 ± 1.7	+	-2.5 ± 0.3	1.0
A288W	2.8 ± 1.1	+	-3.3 ± 0.1	1.0
V289A	6.0 ± 0.7	+	-2.8 ± 0.2	1.0
C290A	5.1 ± 1.3	+	-2.8 ± 0.3	1.0
L291A	6.1 ± 2.6	+	-2.6 ± 0.3	1.1
L292A	2.1 ± 1.3	+	-0.8 ± 0.3	1.1
F293A	0.8 ± 0.6 ^b	(+)	-0.3 ± 0.1 ^b	1.7
V294A	8.8 ± 1.0	+	-2.9 ± 0.3	1.0

Glycine responses of the WT and mutant GlyRs were recorded by TEVC and are given as means ± s.d. from 6–12 experiments; nf, nonfunctional; I_{\max} , maximal glycine-inducible current. Surface labeling data are from **Supplementary Figure 4b,h**; +, like WT; (+), weak; -, not detectable. The binding energies of C-terminal GlyR fragment docking to the $\alpha 1_{-325}$ subunit were determined *in silico*; data represent means ± s.d. from 5 experiments. Values significantly different from WT $\alpha 1$ GlyR (* $P < 0.01$; ^b $P < 0.001$) are indicated.

region of the GlyR. Aromatic residues not engaged in contacts (Tyr222 and Tyr223 in M1 as well as Tyr301 and Phe306 in M3) were dispensable for assembly. The sole exemption is Phe405, which is predicted to participate in the aromatic network by interacting with Tyr228, but could be substituted by alanine without affecting assembly. It appears that the multiple contacts formed by Tyr228, with Phe293 and Phe402 in M3 and M4, respectively, compensate for the loss of the interaction with Phe405. An important role of the aromatic residues in M1, M3, and M4 is further supported by their strict conservation among the GlyR $\alpha 1$, $\alpha 2$, $\alpha 3$, $\alpha 4$ and β isoforms of both human and mouse.

Motifs driving association of transmembrane helices

Major driving forces for the association of α helices in membrane proteins are (i) van der Waals interactions, such as those mediated by the artificial membrane-spanning leucine-zipper domain³⁷ or the abundant GXXXG (small-XXX-small) motif^{38,39}, and (ii) hydrogen bonding between polar residues^{40,41}. The transmembrane segments of the GlyR $\alpha 1$ subunit do not contain a leucine zipper-like motif,

and only a few residues with small side chains (glycine, alanine and serine) are present in M1, M3 and M4. Of these, only the sequence ³⁹⁴GFPMA³⁹⁸ (GXXXA) in M4 is reminiscent of the small-XXX-small pattern. However, replacement of Gly394 by a bulky tryptophan residue did not impair homopentamerization (G.S. and S.D.-D., unpublished results), arguing against a role of complementary 'knobs into holes' packing in helix-helix interactions of the GlyR $\alpha 1$ subunit.

Attractive nonbonded interactions important in general molecular recognition and self-assembly involve in addition aromatic residues. Interactions between either pairs of aromatic residues (π - π) or a basic and an aromatic residue (cation- π) have long been recognized as key elements in the stabilization of the tertiary structure of soluble proteins⁴² (see also ref. 43 and references therein). Evidence that aromatic residues also support the association of membrane helices was provided by the identification of tryptophan enriched at randomized heptad repeat distance in strongly self-interacting artificial transmembrane segments⁴⁴. Similarly, the strength of self-assembly of designed transmembrane segments composed of largely alternating small (alanine) and large (isoleucine) residues was significantly enhanced by introducing aromatic residues⁴⁵. That aromatic motifs can also be important for self-assembly of natural transmembrane segments was recently shown for the cholera secretion protein EpsM, which contains a WXXW motif that is overrepresented in a bacterial database of transmembrane segments⁴⁶. Our data provide the first evidence to our knowledge that a dense intramembrane network of aromatic residues may be of key structural importance for membrane protein assembly. Aromatic residues also occur frequently in M1, M3 and M4 of the 5HT_{3A} subunit and are well conserved between the transmembrane domains of the GABA_AR $\alpha 1$ and GlyR subunits. Preliminary alanine scanning of M4 of the 5HT_{3A} subunit identified two assembly-relevant aromatic residues, Phe442 and Tyr445 (B.L. and G.S., unpublished data), consistent with aromatic residues being of general importance for the assembly of pLGICs.

Intramembrane trihelical interactions and pLGICs assembly

pLGICs are circularly arranged proteins that, at the level of the lipid bilayer, consist of two concentric rings of helices, an outer ring formed by five M1, M3 and M4 helices each, and an inner ring composed of five pore-lining M2 helices (Fig. 5b). In view of the strong helical propensity of alanine⁴⁷, a significant change in the helical content of the transmembrane segments by single alanine replacements seems highly unlikely. Topological misfolding as a cause of subunit aggregation³⁰ could be excluded by the efficient use of an *N*-glycan acceptor site added to the C-terminal end of assembly-impaired GlyR M4 mutants. Also, our extensive molecular dynamics calculations provided absolutely no evidence for misfolding of or aberrant intersubunit contacts between the membrane-embedded tetrahelical bundles of assembly-impaired alanine mutants that might cause nonspecific aggregation. Altogether, our results provide firm evidence for the view that aromatic interhelical interactions must play a direct role in homopentamer formation.

The most reasonable interpretation of the data presented here is that it is the precise geometry of M1-M4 tetrahelical packing which crucially defines transmembrane segment packing and thereby pentameric assembly. One possible scenario is that a perfectly folded compact M1-M4 tetrahelical bundle is a prerequisite to allow the circular arrangement of the subunits that is stabilized essentially by earlier occurring subunit interactions between the ectodomains. Accordingly, the trihelical aromatic network would serve to fix the transmembrane domains of individual subunits in a pentamer-compatible conformation by determining the geometry of subunit

interfaces (Fig. 5b) and/or preventing aggregative interactions in the membrane through unpaired aromatic residues.

An alternative scenario is that the extensive interactions between the transmembrane helices serve to lock sticky residues in an exact spatial position, allowing them to form intersubunit contacts at the membrane level. The atomic structures of the prokaryotic pLGICs show only loose intramembrane interactions between the transmembrane helices, with intrasubunit interfaces being mainly populated with small hydrophobic residues, such as alanine and valine. In the $\alpha 1$ GlyR, however, two M1 residues, Ser238 and Trp243, that were found to be crucial for efficient pentameric assembly are located in positions (Fig. 5) that make them candidates for docking to M3 of an adjacent subunit. Hence, intersubunit contacts mediated by these residues and complementary side chains on M3 may, in concert with the aromatic network-defined geometric arrangement of M1-M3 helices in the membrane (Fig. 5b), force the subunits into a circular symmetry⁴⁸ that defines the final pentameric stoichiometry in concert with the linear head-to-tail interactions between the ectodomains. This view receives indirect support from our observation that the soluble ectodomain of the GlyR $\alpha 1$ subunit has a strong propensity for random nonstoichiometric aggregation, consistent with head-to-tail oligomerization occurring in the absence of constraints required for pentamer formation⁴⁸.

Although important for pentameric assembly, intramembrane helical interactions are unlikely to determine the subunit stoichiometry of heteromeric pLGICs. In case of the GlyR, nonconserved 'assembly cassettes' localized within the N-terminal extracellular domain of the GlyR β subunit^{17,18} have been shown to govern the fixed $2\alpha:3\beta$ stoichiometry of heteropentameric GlyRs⁴⁹. In conclusion, proper pLGIC assembly requires both tight intersubunit interactions between extracellular domains and intrasubunit interactions between transmembrane segments.

METHODS

Methods and any associated references are available in the online version of the paper at <http://www.nature.com/nsmb/>.

Note: Supplementary information is available on the Nature Structural & Molecular Biology website.

ACKNOWLEDGMENTS

We thank U. Braam for expert help in generating cDNA constructs, G. Drwal for electrophysiological recording and F. Pult for sharing with us the data of her M.D. work on C-terminal N-glycosylation. Supported by Deutsche Forschungsgemeinschaft (La1086/5-3; Schm536/4-3), Fonds der Chemischen Industrie (H.B.), the Hertie Foundation (B.L.), the Alexander von Humboldt Foundation (H.B., V.T.), Deutscher Akademischer Austauschdienst (D.K.) and the Russian Academy of Sciences grant "Molecular and Cell Biology" (V.T., D.K.).

AUTHOR CONTRIBUTIONS

S.H. designed and generated DNA constructs and performed biochemical experiments; D.K. performed homology modeling and molecular dynamics simulations and analyzed the data; S.D.-D. synthesized cRNAs, generated DNA constructs and performed biochemical experiments; N.L. generated mutants and performed biochemical experiments; M.K. performed electrophysiological recordings; V.T. supervised homology modeling and analyzed data; H.B. designed experiments and wrote the paper; B.L. designed experiments, performed electrophysiological recordings, analyzed data and wrote the paper; G.S. designed constructs and biochemical experiments, analyzed the data and wrote the paper.

Published online at <http://www.nature.com/nsmb/>.

Reprints and permissions information is available online at <http://npg.nature.com/reprintsandpermissions/>.

- Liao, M.J., Huang, K.S. & Khorana, H.G. Regeneration of native bacteriorhodopsin structure from fragments. *J. Biol. Chem.* **259**, 4200–4204 (1984).
- Popot, J.L., Gerchman, S.E. & Engelman, D.M. Refolding of bacteriorhodopsin in lipid bilayers. A thermodynamically controlled two-stage process. *J. Mol. Biol.* **198**, 655–676 (1987).

- Mackenzie, K.R. Folding and stability of α -helical integral membrane proteins. *Chem. Rev.* **106**, 1931–1977 (2006).
- Popot, J.L. & Engelman, D.M. Membrane protein folding and oligomerization: the two-stage model. *Biochemistry* **29**, 4031–4037 (1990).
- Popot, J.L. & Engelman, D.M. Helical membrane protein folding, stability, and evolution. *Annu. Rev. Biochem.* **69**, 881–922 (2000).
- de Planque, M.R. & Killian, J.A. Protein-lipid interactions studied with designed transmembrane peptides: role of hydrophobic matching and interfacial anchoring. *Mol. Membr. Biol.* **20**, 271–284 (2003).
- Eilers, M., Shekar, S.C., Shieh, T., Smith, S.O. & Fleming, P.J. Internal packing of helical membrane proteins. *Proc. Natl. Acad. Sci. USA* **97**, 5796–5801 (2000).
- Liu, Y., Gerstein, M. & Engelman, D.M. Transmembrane protein domains rarely use covalent domain recombination as an evolutionary mechanism. *Proc. Natl. Acad. Sci. USA* **101**, 3495–3497 (2004).
- Bowie, J.U. Solving the membrane protein folding problem. *Nature* **438**, 581–589 (2005).
- Hildebrand, P.W. *et al.* Hydrogen-bonding and packing features of membrane proteins: functional implications. *Biophys. J.* **94**, 1945–1953 (2008).
- Gimpelev, M., Forrest, L.R., Murray, D. & Honig, B. Helical packing patterns in membrane and soluble proteins. *Biophys. J.* **87**, 4075–4086 (2004).
- Hildebrand, P.W., Rother, K., Goede, A., Preissner, R. & Frommel, C. Molecular packing and packing defects in helical membrane proteins. *Biophys. J.* **88**, 1970–1977 (2005).
- Hall, Z.W. Recognition domains in assembly of oligomeric membrane proteins. *Trends Cell Biol.* **2**, 66–68 (1992).
- Green, W.N. & Millar, N.S. Ion-channel assembly. *Trends Neurosci.* **18**, 280–287 (1995).
- Gu, Y., Camacho, P., Gardner, P. & Hall, Z.W. Identification of two amino acid residues in the epsilon subunit that promote mammalian muscle acetylcholine receptor assembly in COS cells. *Neuron* **6**, 879–887 (1991).
- Chavez, R.A., Maloof, J., Beeson, D., Newsom-Davis, J. & Hall, Z.W. Subunit folding and $\alpha\delta$ heterodimer formation in the assembly of the nicotinic acetylcholine receptor. Comparison of the mouse and human α subunits. *J. Biol. Chem.* **267**, 23028–23034 (1992).
- Kuhse, J., Laube, B., Magalei, D. & Betz, H. Assembly of the inhibitory glycine receptor: identification of amino acid sequence motifs governing subunit stoichiometry. *Neuron* **11**, 1049–1056 (1993).
- Griffon, N. *et al.* Molecular determinants of glycine receptor subunit assembly. *EMBO J.* **18**, 4711–4721 (1999).
- Nicke, A. *et al.* P2X₁ and P2X₃ receptors form stable trimers: a novel structural motif of ligand-gated ion channels. *EMBO J.* **17**, 3016–3028 (1998).
- Nicke, A., Rettinger, J., Mutschler, E. & Schmalzing, G. Blue native PAGE as a useful method for the analysis of the assembly of distinct combinations of nicotinic acetylcholine receptor subunits. *J. Recept. Signal Transduct. Res.* **19**, 493–507 (1999).
- Büttner, C. *et al.* Ubiquitination precedes internalization and proteolytic cleavage of plasma membrane-bound glycine receptors. *J. Biol. Chem.* **276**, 42978–42985 (2001).
- Sadtler, S. *et al.* A basic cluster determines topology of the cytoplasmic M3–M4 loop of the glycine receptor $\alpha 1$ subunit. *J. Biol. Chem.* **278**, 16782–16790 (2003).
- Nicke, A., Thureau, H., Sadtler, S., Rettinger, J. & Schmalzing, G. Assembly of nicotinic $\alpha 7$ subunits in *Xenopus* oocytes is partially blocked at the tetramer level. *FEBS Lett.* **575**, 52–58 (2004).
- Gendreau, S. *et al.* A trimeric quaternary structure is conserved in bacterial and human glutamate transporters. *J. Biol. Chem.* **279**, 39505–39512 (2004).
- Detro-Dassen, S. *et al.* Conserved dimeric subunit stoichiometry of SLC26 multifunctional anion exchangers. *J. Biol. Chem.* **283**, 4177–4188 (2008).
- Duckwitz, W., Hausmann, R., Aschrafi, A. & Schmalzing, G. P2X₅ subunit assembly requires scaffolding by the second transmembrane domain and a conserved aspartate. *J. Biol. Chem.* **281**, 39561–39572 (2006).
- Green, T., Stauffer, K.A. & Lummis, S.C. Expression of recombinant homo-oligomeric 5-hydroxytryptamine₃ receptors provides new insights into their maturation and structure. *J. Biol. Chem.* **270**, 6056–6061 (1995).
- Claudio, T. *et al.* Fibroblasts transfected with Torpedo acetylcholine receptor β -, γ -, and δ -subunit cDNAs express functional receptors when infected with a retroviral α recombinant. *J. Cell Biol.* **108**, 2277–2290 (1989).
- Blount, P. & Merlie, J.P. Mutational analysis of muscle nicotinic acetylcholine receptor subunit assembly. *J. Cell Biol.* **111**, 2613–2622 (1990).
- Buck, T.M., Wagner, J., Grund, S. & Skach, W.R. A novel tripartite motif involved in aquaporin topogenesis, monomer folding and tetramerization. *Nat. Struct. Mol. Biol.* **14**, 762–769 (2007).
- Schmidt, T.G., Koepke, J., Frank, R. & Skerra, A. Molecular interaction between the Strep-tag affinity peptide and its cognate target, streptavidin. *J. Mol. Biol.* **255**, 753–766 (1996).
- Hilf, R.J. & Dutzler, R. X-ray structure of a prokaryotic pentameric ligand-gated ion channel. *Nature* **452**, 375–379 (2008).
- Unwin, N. Refined structure of the nicotinic acetylcholine receptor at 4 Å resolution. *J. Mol. Biol.* **346**, 967–989 (2005).
- Hilf, R.J. & Dutzler, R. Structure of a potentially open state of a proton-activated pentameric ligand-gated ion channel. *Nature* **457**, 115–118 (2009).
- Bocquet, N. *et al.* X-ray structure of a pentameric ligand-gated ion channel in an apparently open conformation. *Nature* **457**, 111–114 (2009).
- McGaughey, G.B., Gagne, M. & Rappe, A.K. π -Stacking interactions. Alive and well in proteins. *J. Biol. Chem.* **273**, 15458–15463 (1998).

ARTICLES

37. Gurezka, R., Laage, R., Brosig, B. & Langosch, D. A heptad motif of leucine residues found in membrane proteins can drive self-assembly of artificial transmembrane segments. *J. Biol. Chem.* **274**, 9265–9270 (1999).
38. Lemmon, M.A., Treutlein, H.R., Adams, P.D., Brunger, A.T. & Engelman, D.M. A dimerization motif for transmembrane α -helices. *Nat. Struct. Biol.* **1**, 157–163 (1994).
39. Rath, A. & Deber, C.M. Surface recognition elements of membrane protein oligomerization. *Proteins* **70**, 786–793 (2008).
40. Choma, C., Gratkowski, H., Lear, J.D. & Degrado, W.F. Asparagine-mediated self-association of a model transmembrane helix. *Nat. Struct. Biol.* **7**, 161–166 (2000).
41. Zhou, F.X., Cocco, M.J., Russ, W.P., Brunger, A.T. & Engelman, D.M. Interhelical hydrogen bonding drives strong interactions in membrane proteins. *Nat. Struct. Biol.* **7**, 154–160 (2000).
42. Burley, S.K. & Petsko, G.A. Aromatic-aromatic interaction: a mechanism of protein structure stabilization. *Science* **229**, 23–28 (1985).
43. Gervasio, F.L., Chelli, R., Procacci, P. & Schettino, V. The nature of intermolecular interactions between aromatic amino acid residues. *Proteins* **48**, 117–125 (2002).
44. Ridder, A., Skupjen, P., Unterreitmeier, S. & Langosch, D. Tryptophan supports interaction of transmembrane helices. *J. Mol. Biol.* **354**, 894–902 (2005).
45. Johnson, R.M., Hecht, K. & Deber, C.M. Aromatic and cation- π interactions enhance helix-helix association in a membrane environment. *Biochemistry* **46**, 9208–9214 (2007).
46. Sal-Man, N., Gerber, D., Bloch, I. & Shai, Y. Specificity in transmembrane helix-helix interactions mediated by aromatic residues. *J. Biol. Chem.* **282**, 19753–19761 (2007).
47. Li, S.C. & Deber, C.M. A measure of helical propensity for amino acids in membrane environments. *Nat. Struct. Biol.* **1**, 368–373 (1994).
48. Nooren, I.M. & Thornton, J.M. Diversity of protein-protein interactions. *EMBO J.* **22**, 3486–3492 (2003).
49. Grudzinska, J. *et al.* The β subunit determines the ligand binding properties of synaptic glycine receptors. *Neuron* **45**, 727–739 (2005).

ONLINE METHODS

cDNA constructs. The cDNA constructs encoding C-terminally hexahistidine-tagged versions of the human GlyR $\alpha 1$ subunit ($\alpha 1$ -His) or the mouse 5HT₃A receptor subunit (5HT₃A-His) have been described previously^{18,23}. We introduced mutations and insertions with the QuikChange site-directed mutagenesis kit (Stratagene) using mutagenesis primers that incorporated or removed a silent restriction site. We identified positive clones by restriction enzyme analysis and confirmed by DNA sequencing. We generated a double-tagged version of the GlyR $\alpha 1$ -His designated $\alpha 1$ -His-StrepII by adding the sequence for the StrepII-affinity tag (NWSHPQFEK)³¹ to the C terminus of the C-terminal hexahistidine sequence. To generate C-terminally truncated versions of the full-length GlyR $\alpha 1$ subunit of different length, we inserted nucleotide sequences encoding a hexahistidine tag followed by a stop codon and an XbaI restriction site at codon positions Phe214, Arg252, Pro275 and Lys325, to yield $\alpha 1_{1-214}$ -His, $\alpha 1_{1-252}$ -His, $\alpha 1_{1-275}$ -His and $\alpha 1_{1-325}$ -His, respectively. In all of these constructs, the DNA sequence for the genuine signal peptide was preserved to ensure correct membrane insertion and orientation of the corresponding fragments; residue numbers refer to the sequence of the mature GlyR $\alpha 1_{1-421}$ subunit. We excised the 3' noncoding region of each construct with SnaBI—which cuts twice, 3' to the stop codon and immediately 5' to the polyA tail of ~100 A of the vector pNKS2 (ref. 50)—and religated the plasmid. To generate an N-terminally truncated GlyR $\alpha 1$ polypeptide, we amplified a DNA fragment encoding residues Met341–Gln421–HHHHHH by PCR and cloned it into pNKS2 between its BamHI and XbaI sites to yield $\alpha 1_{341-421}$ -His.

Using essentially the same strategy, C- or N-terminally truncated fragments of the 5HT₃A subunit encoding residues Ser1–Arg347 (with the genuine signal sequence) and Met369–Ser466 were generated and designated 5HT₃A₁₋₃₄₇-His and 5HT₃A₃₆₉₋₄₆₆-His, respectively; residue numbering refers to the sequence of the mature 5HT₃A₁₋₄₆₆ subunit.

Oocyte expression and TEVC electrophysiology. We obtained and injected collagenase-defolliculated *X. laevis* oocytes (stages V or VI) with capped cRNAs as described previously¹⁹. We kept oocytes at 19 °C in sterile frog Ringer's solution (ORi: 90 mM NaCl, 1 mM KCl, 1 mM CaCl₂, 1 mM MgCl₂ and 10 mM HEPES, pH 7.4) supplemented with 50 mg l⁻¹ gentamycin. At 1–3 d after cRNA injection, we measured glycine responses by TEVC at a holding potential of –70 mV as described previously⁴⁹. Concentration–response curves and current traces shown in the figures were drawn using KaleidaGraph (Synergy Software).

Protein labeling, purification, and PAGE. We metabolically labeled cRNA-injected oocytes by overnight incubation with L-[³⁵S]methionine, and, if indicated, additionally surface-labeled by Cy5 NHS ester, an amine-reactive, membrane-impermeant fluorescent dye, just before protein extraction exactly as described previously⁵¹. We purified His-tagged proteins by Ni-NTA agarose (Qiagen) chromatography from digitonin (1%, w/v) extracts of oocytes as detailed previously^{19,22}. We performed BN-PAGE⁵² immediately after protein purification as described¹⁹ in the presence of 0.02% (w/v) Coomassie blue G250. Where indicated, we treated samples before BN-PAGE for 1 h at 37 °C with 100 mM DTT or 0.1% (w/v) SDS, or a combination of both, to induce partial dissociation of receptor complexes. We exposed the dried gels to a phosphor

screen, followed by scanning on a PhosphorImager (Storm 820, GE Healthcare) and displayed images by the ImageQuant software.

For SDS-PAGE, we supplemented proteins with SDS sample buffer containing 20 mM DTT and electrophoresed in parallel with ¹⁴C-labeled molecular mass markers (Rainbow, Amersham) on discontinuous tricine SDS-PAGE gels (4%, 10% and 16.5% acrylamide)⁵³ or SDS-urea-PAGE gradient gels. SDS-PAGE gels were scanned wet in a fluorescence scanner (Typhoon, GE Healthcare) for visualization of fluorescently labeled plasma membrane-bound proteins, and then dried for subsequent PhosphorImager detection of ³⁵S incorporation. Figures were prepared by using ImageQuant TL v2005 (Amersham) for contrast adjustments, Adobe Photoshop CS 8.0 for level adjustment and cropping, and Microsoft PowerPoint 2000 for lettering.

Computational methods. We performed sequence alignments using ClustalW⁵⁴. We built all structural models with Modeller 9v4 (ref. 55) using as template structures the Brookhaven Protein Data Bank entries 2BG9 (nAChR³³), 119b (AChBP⁵⁶) and 2VL0 (ELIC³²). We performed energy minimization for all models with CHARMM27⁵⁷. After docking preparation with Chimera⁵⁸ (University of California, San Francisco), we performed final dockings with AutoDock 4 (ref. 59) using internal energy evaluation and scoring functions. We repeated the docking procedure five times for each receptor–ligand pair and considered docking prediction successful when at least five occurrences with r.m.s. deviation < 0.5 Å were obtained in every computation round. We calculated s.d. for the binding energies of all mutants. We determined the degree of ligand rotational freedom as a flat angle between the ligand central axis and the receptor five-fold symmetry plane, followed by normalization to the value obtained for the WT peptide. For simulated annealing of complexes resulting from docking, we used GROMACS4 (ref. 60). We prepared the figures using Chimera⁵⁸ and PyMol (DeLano Scientific LLC; <http://www.pymol.org>).

50. Gloor, S., Pongs, O. & Schmalzing, G. A vector for the synthesis of cRNAs encoding Myc epitope-tagged proteins in *Xenopus laevis* oocytes. *Gene* **160**, 213–217 (1995).
51. Becker, D. *et al.* The P2X₇ carboxyl tail is a regulatory module of P2X₇ receptor channel activity. *J. Biol. Chem.* **283**, 25725–25734 (2008).
52. Schägger, H., Cramer, W.A. & von Jagow, G. Analysis of molecular masses and oligomeric states of protein complexes by blue native electrophoresis and isolation of membrane protein complexes by two-dimensional native electrophoresis. *Anal. Biochem.* **217**, 220–230 (1994).
53. Schägger, H. & von Jagow, G. Tricine-sodium dodecyl sulfate-polyacrylamide gel electrophoresis for the separation of proteins in the range from 1 to 100 kDa. *Anal. Biochem.* **166**, 368–379 (1987).
54. Larkin, M.A. *et al.* Clustal W and Clustal X version 2.0. *Bioinformatics* **23**, 2947–2948 (2007).
55. Eswar, N., Eramian, D., Webb, B., Shen, M.Y. & Sali, A. Protein structure modeling with MODELLER. *Methods Mol. Biol.* **426**, 145–159 (2008).
56. Brejc, K. *et al.* Crystal structure of an ACh-binding protein reveals the ligand-binding domain of nicotinic receptors. *Nature* **411**, 269–276 (2001).
57. Brooks, B.R. *et al.* CHARMM: A program for macromolecular energy, minimization, and dynamics calculations. *J. Comput. Chem.* **4**, 187–217 (1983).
58. Pettersen, E.F. *et al.* UCSF Chimera—a visualization system for exploratory research and analysis. *J. Comput. Chem.* **25**, 1605–1612 (2004).
59. Morris, G.M. & Lim-Wilby, M. Molecular docking. *Methods Mol. Biol.* **443**, 365–382 (2008).
60. Hess, B. P-LINCS: A parallel linear constraint solver for molecular simulation. *J. Chem. Theory Comput.* **4**, 116–122 (2008).

Supplementary Information

An intramembrane aromatic network determines pentameric assembly of Cys-loop receptors

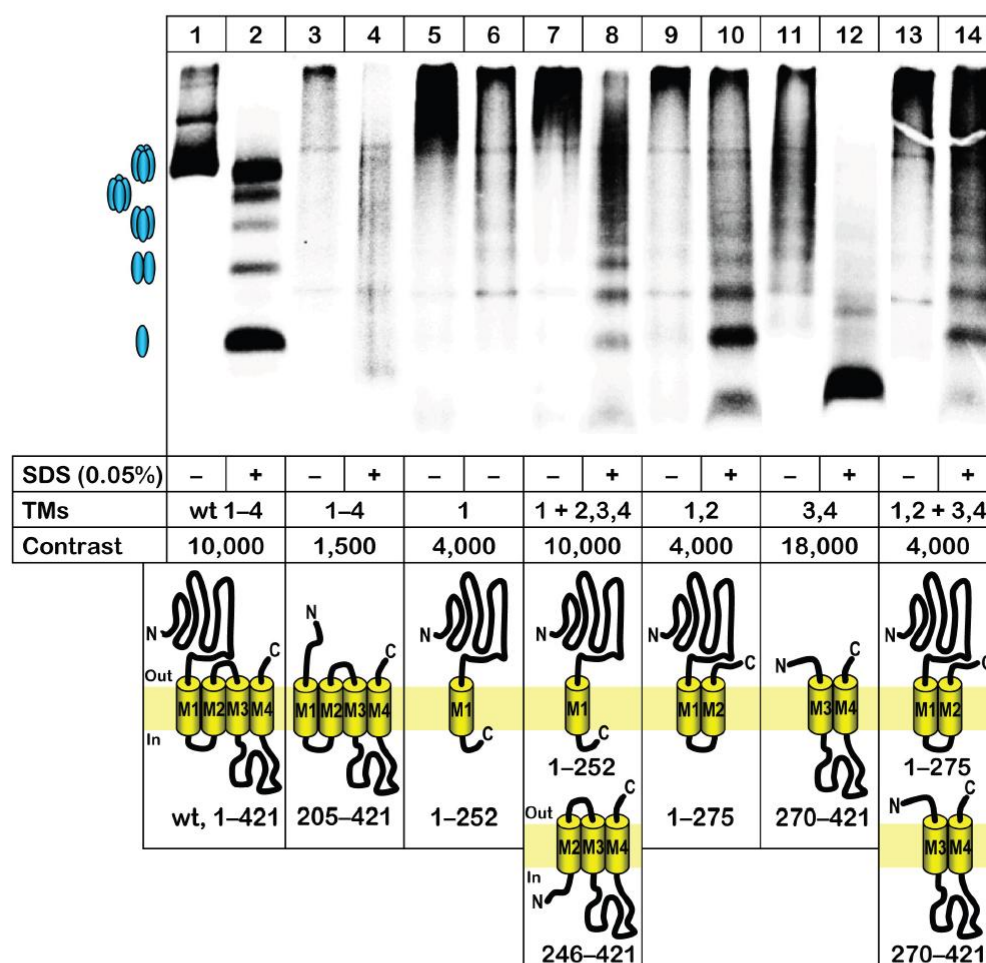
Svenja Haeger¹, Dmitry Kuzmin^{2,3}, Silvia Detro-Dassen¹, Niklas Lang¹, Michael Kilb⁴, Victor Tsetlin³, Heinrich Betz², Bodo Laube^{2,4}, and Günther Schmalzing¹

¹Molecular Pharmacology, RWTH Aachen University of Aachen, Wendlingweg 2, D-52074 Aachen, Germany

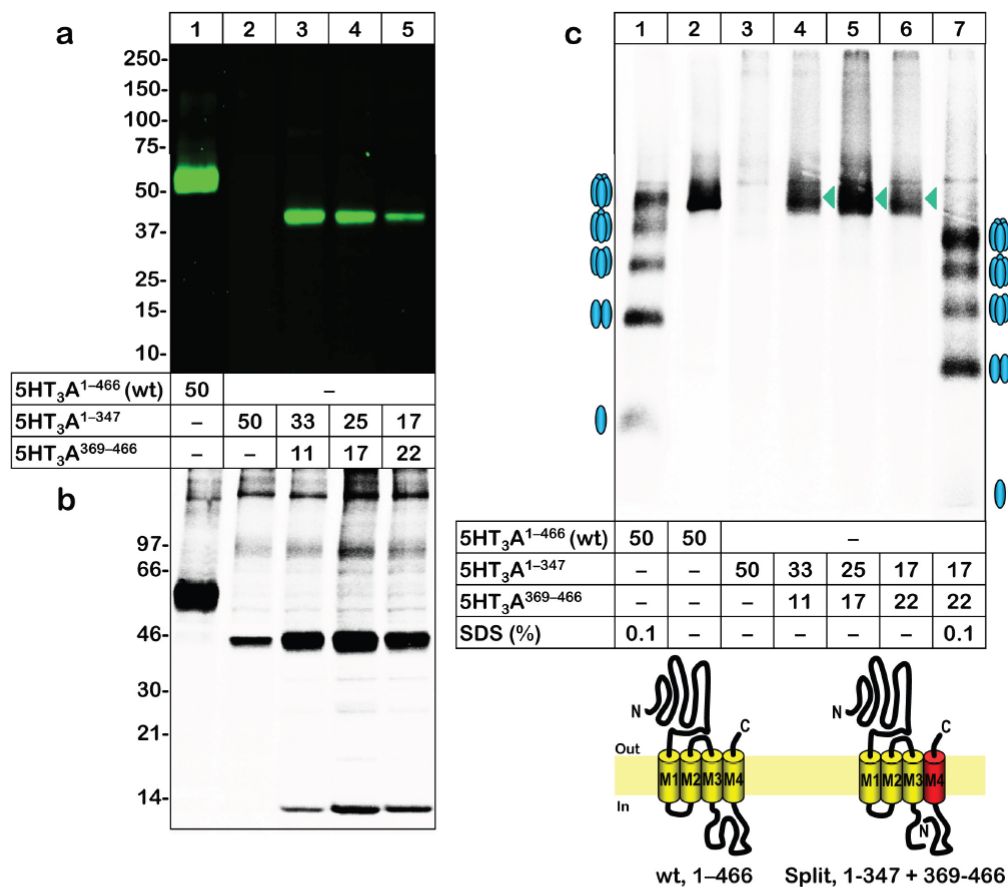
²Department of Neurochemistry, Max-Planck-Institute for Brain Research, Deutschordenstrasse 46, D-60528

Frankfurt am Main, Germany; ³Shemyakin-Ovchinnikov Institute of Bioorganic Chemistry, Russian Academy of

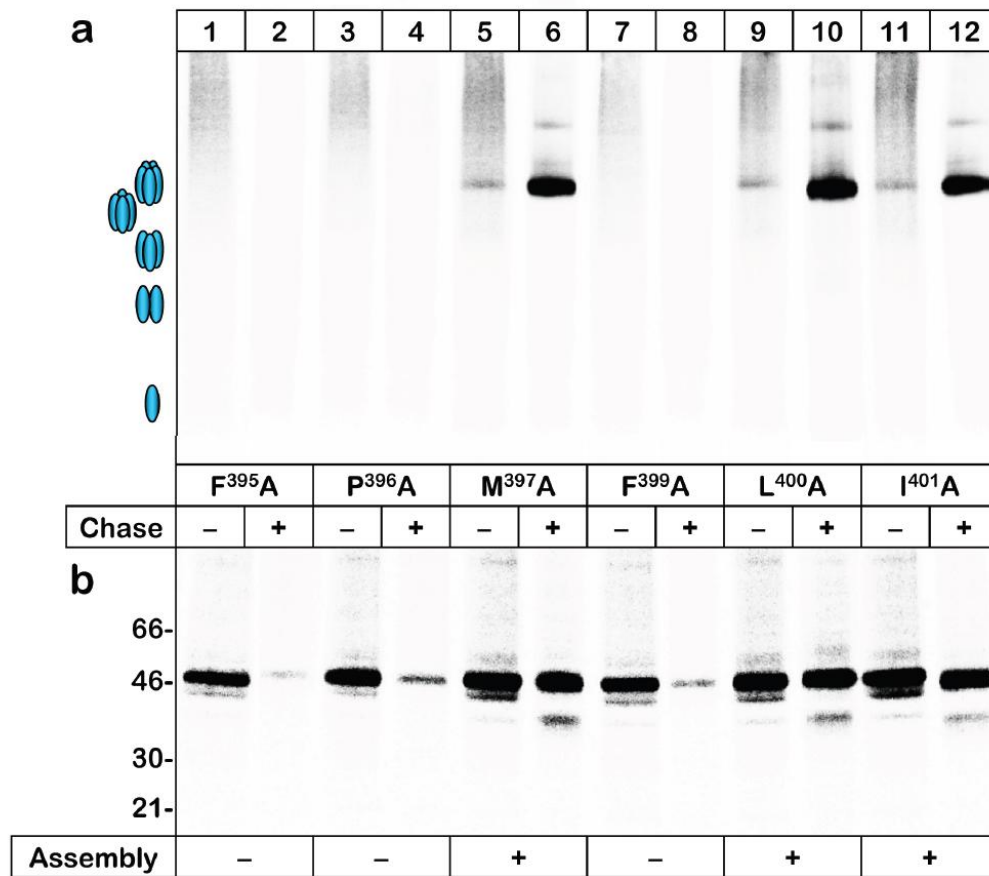
Sciences, 16/10 Miklukho-Maklaya Str., Moscow 117977, Russia; ⁴Department Molekulare und zelluläre Neurophysiologie, Technische Universität Darmstadt, Schnittspahnstr. 3, D-64287 Darmstadt, Germany



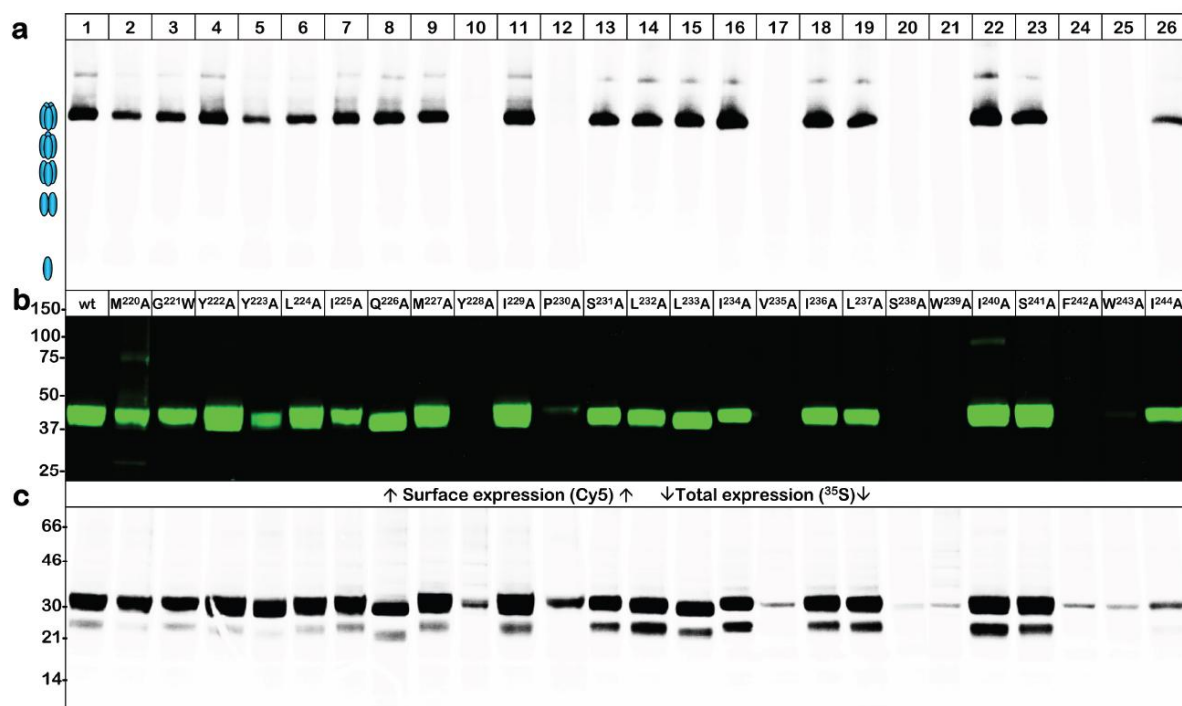
Supplementary Figure 1. Complementary GlyR $\alpha 1$ fragments split between M1 and M2, or M2 and M3, do not form defined oligomers. The indicated GlyR $\alpha 1$ fragments were expressed singly or in combination in oocytes, labeled with [³⁵S]methionine, and then purified by non-denaturing Ni-NTA chromatography. Protein migration is shown under native conditions and after partial denaturation by a 1 h incubation at 37°C with 0.05% SDS (w/v) as indicated. After BN-PAGE and phosphorimaging, we visualized the proteins by ImageQuant using the indicated high-contrast settings to simultaneously display both weakly and strongly expressed proteins. Blue ovals schematically illustrate oligomeric states. Bottom cartoons depict topology and positions of truncations as compared to the wt GlyR $\alpha 1$ subunit. Numbers refer to amino acid positions of the mature $\alpha 1$ subunit; fragments with a N_{out} membrane topology included in addition the genuine signal peptide.



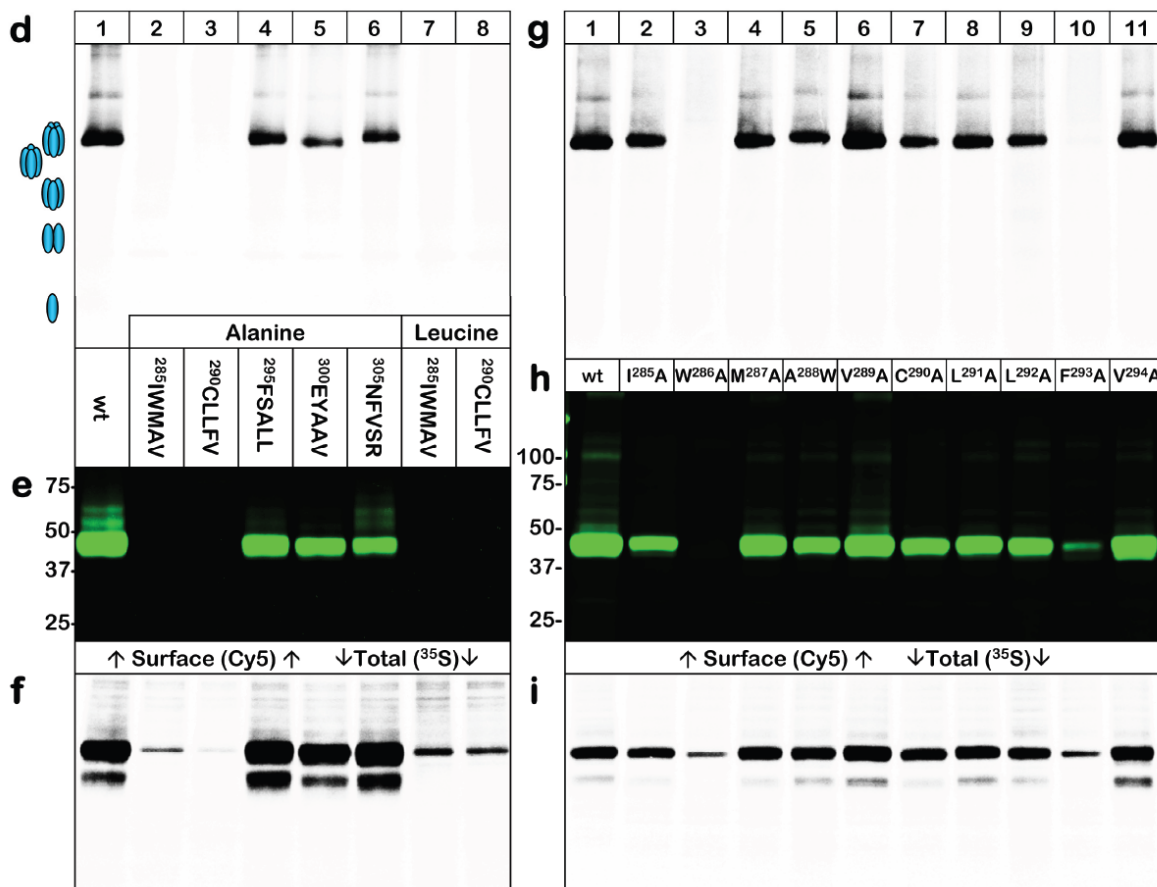
Supplementary Figure 2. Reconstitution of 5HT₃A receptor assembly from complementary fragments. **(a,b)** [³⁵S]Methionine-labeled oocytes were chased for 24 h and surface-labeled with the membrane-impermeant fluorescent Cy5 dye prior to protein purification by non-denaturing Ni-NTA chromatography. The purified proteins were then resolved by reducing SDS-urea-PAGE and visualized by Typhoon fluorescence scanning **(a)**, surface-bound receptors in green) and phosphorimaging **(b)**, ³⁵S-labeled receptor pool). Numbers indicate the amount of the respective cRNA (in ng) injected per oocyte. **(c)** We resolved aliquots of the samples analyzed in **a**, **b** by BN-PAGE and visualized the proteins by phosphorimaging. Receptor migration is shown in both the non-denatured and the partially denatured state produced upon SDS treatment. The ovals schematically illustrate oligomeric states. Note that co-expression of the 5HT₃A¹⁻³⁴⁷-His N-domain with a short C-terminal fragment encompassing M4 resulted in the formation of pentameric protein complexes (green arrowhead) that migrated at the same position as the wt 5HT₃A-His pentamer (blue ovals).



Supplementary Figure 3. Assembly-incompetent M4 mutants of the $\alpha 1$ GlyR are efficiently synthesized but rapidly degraded. We purified the indicated M4 alanine single mutants from oocytes both after a 4 h [³⁵S]methionine pulse and an additional 36 h chase interval. Mutants M397A, L400A and I401A identified as assembly-competent by BN-PAGE (**a**) were metabolically stable as inferred from reducing SDS-PAGE showing unchanged band intensities after the chase (**b**). Mutants F395A, P396A and F399A identified as assembly-incompetent by BN-PAGE in **a** were similarly abundant after the 4 h pulse in **b**, as indicated by the band intensities detected by SDS-PAGE, but largely degraded during the chase period.



Supplementary Figure 4a-c. Effect of alanine substitutions in M1 on the assembly and surface expression of the $\alpha 1$ GlyR. We singly replaced wt residues of the entire M1 by alanines as indicated, with the exception of Gly221 that we replaced by a bulky tryptophan. Proteins labeled with [³⁵S]methionine and Cy5 were purified and resolved by BN-PAGE followed by phosphorimaging to display their oligomeric state (**a**), or by reducing SDS-urea-PAGE to display Cy5-labeled surface GlyR polypeptides (**b**) and [³⁵S]methionine-labeled GlyR subunits (**c**). Ovals schematically illustrate the oligomeric states of the non-denatured and partial denatured wt $\alpha 1$ GlyR. The panels shown are from two separate experiments with mutants M220A to P230A and S231A to I244A, respectively. Each mutant was analyzed at least twice with identical results.



Supplementary Figure 4d-i. Effect of alanine substitutions in M3 on the assembly and surface expression of the $\alpha 1$ GlyR. We singly replaced wt residues of the N-terminal half of M3 (**g-i**) by alanines as indicated, with the exception of Ala288 that we replaced by a bulky tryptophan. The C-terminal half of M3 tolerated block replacements of five contiguous wt residues by alanines (**d-f**), was therefore judged assembly-irrelevant and not subjected to single alanine scanning. Proteins labeled with [³⁵S]methionine and Cy5 were purified and resolved by BN-PAGE followed by phosphorimaging to display their oligomeric state (**d,g**), or by reducing SDS-urea-PAGE to display Cy5-labeled surface GlyR polypeptides (**e,h**) and [³⁵S]methionine-labeled GlyR subunits (**f,i**). Ovals schematically illustrate the oligomeric states of the non-denatured and partial denatured wt $\alpha 1$ GlyR. Each mutant was analyzed at least twice with identical results.

4-chlorination endows propofol with subtype-specific effects on inhibitory glycine receptors via a unique high-affinity transmembrane-domain binding-site

Michael Kilb¹, Timothy Lynagh^{1*}, Jaclyn Bibby³, Neil G. Berry³, Paul M. O'Neill³, Martin Leuwer² and Bodo Laube¹

¹Neurophysiology and Neurosensory Systems, Department of Biology, Technical University of Darmstadt. Schnittspahnstraße 3, 64287 Darmstadt, Germany.

²Critical Care Research Unit, University of Liverpool, Liverpool, U.K.

³Robert Robinson Laboratories, Department of Chemistry, University of Liverpool, Liverpool, U.K. L69 7ZD

*Present address: Center for Biopharmaceuticals, Department of Drug Design and Pharmacology, University of Copenhagen, Jagtvej 160, 2100 Copenhagen, Denmark

Corresponding Author: Bodo Laube, Department of Neurophysiology and Neurosensory Systems, TU-Darmstadt, Schnittspahnstrasse 3, 64287 Darmstadt, Germany, Tel.: (+49) 6151 16 20970; Fax: (+49) 6151 16 5105; E-mail: laube@bio.tu-darmstadt.de

Conflict of interest: The authors declare no competing financial interests.

Acknowledgements: The work was funded by a MRC DPFS grant to Martin Leuwer (MR/J014826/1). Martin Leuwer is a named inventor in WO2007/071967. Bodo Laube acknowledges funding by the LOEWE project iNAPO of the Hessen State Ministry of Higher Education, Research and the Arts.

Abstract

The differential roles of inhibitory glycine receptors (GlyRs) in neuronal signaling call for specific positive allosteric modulators as a new therapeutic principle. Here, we present a comprehensive pharmacological assessment of human GlyRs revealing that the anesthetic propofol (pro) exhibits three distinct effects on GlyRs: low nanomolar concentrations moderately potentiate glycine-induced activation; high micromolar concentrations strongly potentiate; and millimolar concentrations activate in the absence of Gly. Remarkably, this was unveiled by the halogenated derivative, 4-chloropropofol (4-cpro), whose nanomolar effect, specifically, is (1) much more potent than that of pro, (2) manifests as inhibition uniquely at $\alpha 3$ GlyRs and (3) is not present at $\alpha 1\beta$ heteromeric GlyRs. Based on homology modeling and site-directed mutagenesis we provide evidence for a so far unrecognized intra-subunit transmembrane-domain (TMD) binding site determining high-affinity (HA) subtype-specificity to the GlyR. Thus, pro derivatives hold promise as novel drugs for inhibitory glycinergic pathways due to an enhanced potency at a unique, structurally divergent HA modulatory binding site in the GlyR.

Methods

Reagents

Glycine (Gly), propofol (2,6-diisopropylphenol, pro), lindane (Li), anadamide (AEA), NaCl, KCl, CaCl₂, MgCl₂, HEPES, dimethyl sulphoxide (DMSO), tricaine, gentamycin, type IIA collagenase were purchased from Sigma-Aldrich. NaOH from AppliChem GmbH; 4-cpro (4-chloro-2,6-diisopropylphenol, 4-cpro) was synthesized by Dr. Paul M. O'Neill (UK, Liverpool). 1 M stocks of Gly were prepared in bath solution (components under *Oocyte preparation and electrophysiology*). Stocks of pro (1 M), 4-cpro (100 mM), AEA (1 mM) and Li (10 mM) were prepared in DMSO. Stocks were stored at -20 °C, and dilutions were prepared directly before experiments. NotI was purchased from New England Biolabs GmbH; the Quikchange II XL Site-Directed Mutagenesis kit from Agilent Technologies; and mMESSAGING mMACHINE transcription kits from Life Technologies GmbH.

Site-directed mutagenesis and cRNA synthesis

cDNAs encoding human α 1, α 2, α 3K (short version) and β GlyR subtypes in pNKS2 were linearized and translated into cRNA as described previously (Kondratskaya et al., 2005). Mutant cDNAs were generated with the Quikchange II XL Site-Directed Mutagenesis kit. Sequences of entire GlyR inserts were confirmed (Eurofins MWG Operon) and cDNAs were linearized with NotI and transcribed with SP6 transcription kits.

Oocyte preparation and electrophysiology

Oocytes were surgically removed from adult female *Xenopus laevis* clawfrogs anaesthetized by immersion in 0.3% tricaine in water (w/v). All protocols were approved by the local animal care and use committee (II25.3-19c20/15; RP Darmstadt, Germany). Stage V and VI Oocytes were dissected and stored in sterile-filtered ND96 medium (composition in mM: 96 NaCl, 2 KCl, 1 CaCl, 1 MgCl, 5 HEPES, pH 7.4) containing gentamycin (50 μ g/ mL). The oocytes were isolated and enzymatically and maintained as described previously (Grudzinska et al., 2005). Oocytes were injected with 5 ng of cRNA using a Drummond microinjector (Drummond Scientific, Broomall, USA) and incubated in ND96 for 24 h at 18 °C

before electrophysiological recording. Two-electrode voltage-clamp (TEVC) with microelectrodes containing 3 M KCl was performed in bath solution at a holding potential of -70 mV as described previously (Laube et al., 2000). Currents were acquired at 200 Hz with a Geneclamp 500B amplifier, a Digidata 1322A digitizer and Clampex 9.2 software (Molecular Devices). Gly, dissolved in bath solution, was applied alone or after 30 s pre-application of pro, also dissolved in bath solution. Formation of heteromeric $\alpha 1\beta$ GlyRs was verified by Li as described previously (Islam and Lynch, 2012). For direct activation, pro or 4-cpro were applied in the absence of Gly. All experiments were performed at room temperature.

Data analysis

Currents were measured with Clampfit 9.2 software (Molecular Devices), Results were analyzed using the KaleidaGraph program (Synergy Software, Reading, PA) and GraphPad Prism version 5.0 (GraphPad Software Inc., San Diego, CA). Peak current responses to Gly were plotted against agonist concentration and fit with variable slope non-linear regression to establish agonist EC_{20} and EC_{50} parameters. For pro and 4-cpro modulation, responses to EC_{20} Gly after application were analyzed as described previously (Lynagh and Laube, 2014); mean \pm standard error of the mean (S.E.M.) are reported. Drug-induced fold enhancement or remaining fractional current were fit with variable slope non-linear regression (Prism 4), giving EC_{50} or IC_{50} parameters for each individual experiment. For stry inhibition, responses to pro after stry application were divided by the response without strychnine, giving the remaining fractional current indicated. Biphasic pro- and 4-cpro-induced current changes were fit with a biphasic Hill equation as described previously (Laube et al., 1998). In calculating increases in current for the low affinity phase, the maximal increase in current of the high affinity phase was subtracted from each data point. In all experiments, each construct was tested in at least two batches of oocytes. Means for mutants were compared with means for wild-type GlyRs by unpaired Student's t test. Differences with a P value less than 0.05 were considered significant.

Sequence alignment, homology modeling, molecular dynamics simulations and ligand optimization by GOLD 5.2

Sequence alignments including that in figure 4 were performed with ClustalW (Goujon et al., 2010). Docking calculations were carried out into the crystal structure of α 1 GlyR transmembrane structure (4X5T), residues missing from the crystal were modelled using SCWRL4 (Krivov et al., 2009). Small molecules structures were generated and energy minimized using molecular mechanics in Spartan'14 (Wavefunction Inc., Irvine, California, USA; 1991–2009). Calculations were carried out with GOLD 5.2 (CCDC Software Limited, Cambridge, UK), Hydrogen atoms were added to the protein, and all crystallographic water molecules were removed. Default settings were used throughout with the exception that 50 docking poses were generated, search efficiency was set to 200% and the early termination option was disabled. The docking cavity defined as a 15 Å radius around the c-alpha of S296. CHEMPLP fitness function was used to perform the docking. CHEMPLP is used to model the steric complementarity between the protein and the ligand together with the distance- and angle- dependent hydrogen bonding terms (Korb et al., 2009). The docking posed displayed in figure 4B and discussed in the text was the only docking pose revealed from the 50 docking calculations.

Figures were generated in PyMol v1.4.1 (Schrödinger, LLC) or VMD v.1.9.1 (Humphrey et al., 1996), respectively.

Introduction

Pentameric ligand-gated ion channels (pLGICs) that are selective for chloride mediate rapid inhibitory signaling in the nervous system in response to binding the neurotransmitters glycine (Gly) or γ -aminobutyric acid (GABA). GABA type A receptors (GABA(A)Rs) dominate inhibitory signaling in the brain (Sigel and Steinmann, 2012), whereas strychnine-sensitive glycine receptors (GlyRs) are more common in the spinal cord and selected circuits in the brain, where specific GlyR subtypes play specific roles in physiology or disease (Lynch, 2009) (Lynagh Laube Betz rev dazu). For example, underactivity of $\alpha 1\beta$ GlyRs leads to hypertonia in response to touch or sound (Chung et al., 2013), underactivity of $\alpha 3$ GlyRs in dorsal root ganglia of the spinal cord leads to chronic pain (Harvey et al., 2004), and overactivity of $\alpha 3$ GlyRs in the hippocampus is associated with epileptic seizures (Eichler et al., 2009; Eichler et al., 2008). This tissue- and disease-specific expression makes GlyRs a pharmacotherapeutic target of unique specificity (Betz and Laube, 2006), but pharmacological modulators that are specific for GlyRs (over other receptors) or for individual GlyR subtypes ($\alpha 1$, $\alpha 2$, and $\alpha 3$ homomers and $\alpha 1\beta$ heteromers) are unfortunately scarce (Yevenes and Zeilhofer, 2011).

GlyR-specific modulators have recently been identified in certain halogenated derivatives of propofol (pro). Pro is a widely used intravenous general anesthetic that depresses neuronal activity by potentiating inhibitory pLGIC, primarily GABA(A)R, function (Franks, 2008; Jurd et al., 2003). At GlyRs, subsaturating Gly-induced currents are potentiated by pro, although pro EC_{50} values are generally greater (apparent affinity is less) than at GABA(A)Rs (Pistis et al., 1997). However, halogenation of the C4 position of pro (*para* to the hydroxyl) has recently emerged as a strategy to enhance selectivity for GlyRs. A study with 4-cpro reported a sub-nanomolar EC_{50} value for potentiation of GlyRs (de la Roche et al., 2012), much lower than the micromolar EC_{50} value of the parent compound. Similarly, low nanomolar concentrations of 4-bromopropofol increase GlyR activity in spinal cord preparations (Eckle et al., 2014). GABA(A)Rs, on the other hand, are potentiated with substantially *less* or unaltered potency by C4 halogenated derivatives of pro (Krasowski et al., 2001; Lingamaneni et al., 2001; Sanna et al., 1999), suggesting that C4 halogenation specifically enhances activity at GlyRs. Thus, the GlyR binding

site for these compounds holds great promise as a target for new drugs for pain, epilepsy and hypertonia.

GlyR modulation by pro is influenced by residues in the transmembrane domain (TMD), at the interface of adjacent subunits (Lynagh and Laube, 2014), suggesting that the binding site in the GlyR overlaps with the intersubunit cavity in GABA(A)Rs identified as the key pro binding site (Bali and Akabas, 2004; Li et al., 2010; Yip et al., 2013). Recently, however, pro was shown to bind to multiple sites in the TMD of pLGICs (Jayakar et al., 2013). Thus, and especially in light of the wide range of pro EC_{50} values reported at GlyRs (5 μ M, Ahrens et al., 2008; 16 μ M, Pistis et al., 1997; ~100 μ M, Daniels and Roberts, 1998; 690 μ M, Lynagh and Laube, 2014), our knowledge of the GlyR/pro interaction is very murky, which hinders the development of promising therapeutics.

In the present study, we sought to establish a molecular basis for the enhanced effects of 4-cpro at GlyRs. A detailed pharmacology of both 4-cpro and pro at GlyR subtypes and a subsequent mutagenesis analysis based on the docking of 4-cpro into a transmembrane inter-subunit binding-site of our homology-model together show that these drugs exert a high-affinity effect on the GlyR via a unique binding site. This site is located in a region containing several non-conserved amino acids that determine the subtype specificity of 4-cpro.

Results

A chlorinated pro derivative reveals three distinct effects at GlyRs

To investigate GlyR modulation by 4-cpro, human homomeric $\alpha 1$ GlyRs were expressed in *Xenopus laevis* oocytes, and EC_{20} Gly induced currents were measured alone or after the pre-application of increasing concentrations of 4-cpro. Current responses were measured by two-electrode voltage clamp. As shown in Fig. 1A, nanomolar concentrations of 4-cpro dose-dependently potentiated EC_{20} Gly-induced currents at $\alpha 1$ GlyRs up to 1.5 ± 0.2 -fold, saturating at $10 \mu\text{M}$ and with an EC_{50} of $21 \pm 6 \text{ nM}$ ($n = 10$). Remarkably, increasing 4-cpro concentrations above $100 \mu\text{M}$ resulted in an additional, pronounced potentiation of the Gly-induced current, saturating between 1 and 5 mM (Fig. 1A, lower panel). Dose-response analysis of this effect yielded an EC_{50} value of $617 \pm 160 \mu\text{M}$ with maximal potentiation of 2.6 ± 0.4 -fold ($n = 10$). Thus, the full range of data obtained for 4-cpro from nanomolar to millimolar concentrations for homomeric $\alpha 1$ GlyRs could not adequately described by a simple monophasic fit. In contrast, fitting the data with a biphasic dose–response curve (see Material and Methods) resulted in two clearly distinct high-affinity and low-affinity components with a combined maximal potentiation of 4.2-fold with fractional contributions from the first and second phases of about 35 % and 65 %, respectively (Fig. 1B). Finally, higher concentrations of 4-cpro ($\geq 1 \text{ mM}$) directly activated currents at $\alpha 1$ GlyRs (Fig. 1A, lower panel) with a maximal current (I_{max}) of $8 \pm 0.5 \%$ of the Gly-induced I_{max} ($n = 10$). Thus, homomeric $\alpha 1$ GlyRs are potentiated by 4-cpro in two phases, with three orders of magnitude separating EC_{50} values for the two effects, and are activated by yet higher concentrations.

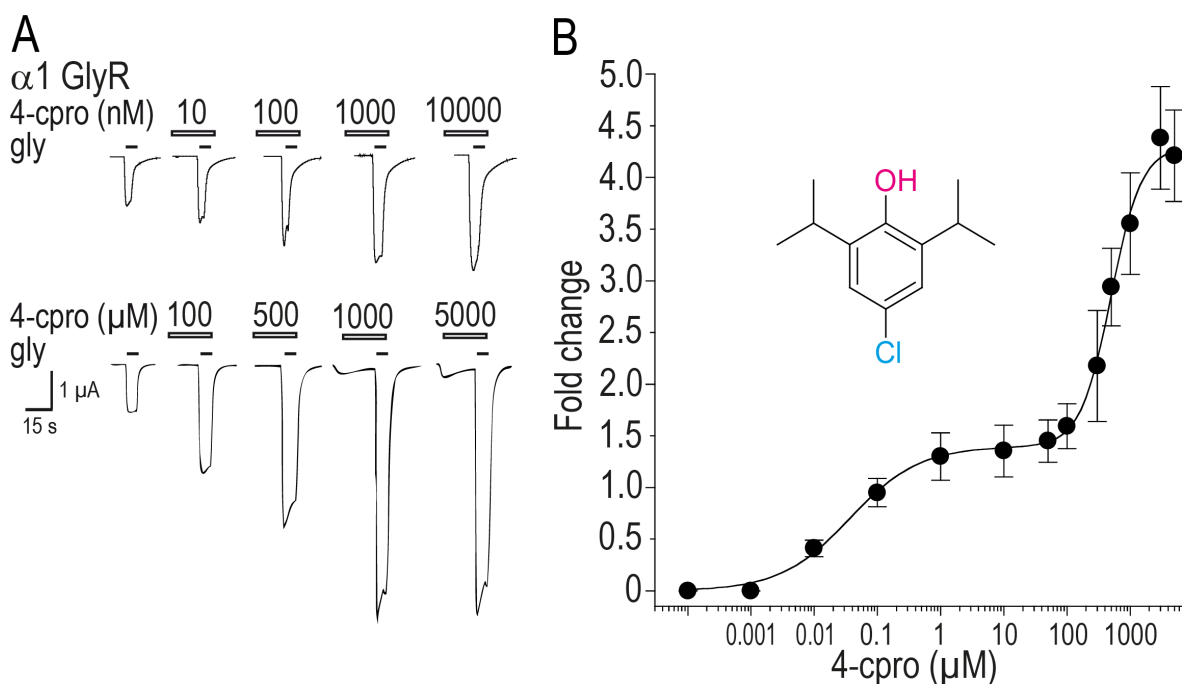


Figure 1: Biphasic effect of 4-cpro at homomeric $\alpha 1$ GlyRs. **A.** Current traces illustrating the effects of increasing concentrations of 4-cpro on Gly-induced currents at human $\alpha 1$ GlyRs expressed in *Xenopus* oocytes. Saturation of the first effect is seen between 1 and 10 μ M (upper panel) and of the second effect between 1 and 5 m M (lower panel) 4-cpro. Note also the direct activation of $\alpha 1$ GlyRs by 1 and 5 m M 4-cpro in the absence of Gly. In this and all subsequent figures, small filled bars indicate application of EC_{20} Gly concentrations and unfilled bars application of 4-cpro. **B.** Averaged potentiation of EC_{20} Gly-induced currents by increasing 4-cpro concentrations. The biphasic dose–response of $\alpha 1$ GlyRs is composed of high-affinity and low-affinity components with corresponding EC_{50} values of 21 ± 6 nM and 617 ± 160 μ M. Each point represents the mean \pm S.E.M. of 10 experiments. Inset: Chemical structure of 4-cpro.

To establish if the distinct high-affinity phase of potentiation extends to other GlyR subtypes, the effect of low concentrations of 4-cpro on human homomeric $\alpha 2$ and $\alpha 3$ and heteromeric $\alpha 1\beta$ GlyRs was tested. Indeed, nanomolar concentrations potentiated EC_{20} Gly-induced currents at $\alpha 2$ GlyRs similarly to $\alpha 1$ GlyRs, although to a slightly lesser extent (Table 1). Dose-response analysis of this effect yielded an EC_{50} value of 230 ± 20 nM for $\alpha 2$ GlyRs, 10-fold higher than the corresponding EC_{50} value at $\alpha 1$ GlyRs (Table 1). Curiously, at $\alpha 3$ GlyRs, currents were actually inhibited to 0.5 ± 0.05 -fold their initial amplitude by 4-cpro at these concentrations (Fig. 2A, upper panel), with an IC_{50} value of 50 ± 8 nM, quite similar to the EC_{50} value at $\alpha 1$ GlyRs (Table 1). At heteromeric $\alpha 1\beta$ GlyRs, however, such nanomolar and low micromolar concentrations of 4-cpro exerted no effect, even up to 100 μ M ($n = 6$; Fig. 2A, lower panel). Taken together, these data reveal that high-affinity sensitivity to 4-cpro is conserved among α GlyR subtypes, although the effects are of

decreased potency at $\alpha 2$ and of opposing direction at $\alpha 3$ GlyRs (Fig. 2B). In contrast, heteromeric $\alpha 1\beta$ GlyRs are not affected by low concentrations of 4-cpro.

We next probed for the low-affinity phase of potentiation in homomeric $\alpha 2$ and $\alpha 3$ and heteromeric $\alpha 1\beta$ GlyRs in the presence of high concentrations of 4-cpro ($>100 \mu\text{M}$). Indeed, high micromolar concentrations of 4-cpro induced an additional, stronger phase of modulation at all homomeric α subunits tested (Fig. 2A,B). Remarkably, also at heteromeric $\alpha 1\beta$ GlyRs, increasing 4-cpro concentrations above $100 \mu\text{M}$ resulted in a pronounced potentiation of the Gly-induced current, saturating between 1 and 5 mM (Fig. 2A,B). Dose-response analysis of this low-affinity effect yielded similar EC_{50} values of $617 \pm 34 \mu\text{M}$ for $\alpha 1$, $406 \pm 50 \mu\text{M}$ for $\alpha 2$, $350 \pm 52 \mu\text{M}$ for $\alpha 3$ and $757 \pm 111 \mu\text{M}$ for $\alpha 1\beta$ GlyRs (Table 1), although maximal potentiation was lower at homomeric $\alpha 3$ and heteromeric $\alpha 1\beta$ receptors ($\alpha 1$, 2.6 ± 0.4 -fold *additional* potentiation; $\alpha 3$, 1.5 ± 0.12 -fold potentiation; $\alpha 1\beta$, 0.9 ± 0.06 -fold potentiation; $P < 0.001$). In contrast to the effects of nanomolar concentrations, where efficacy (at $\alpha 1\beta$), potency (at $\alpha 2$) or direction of modulation (at $\alpha 3$) differed from $\alpha 1$ GlyRs, low-affinity potentiation was ostensibly similar at each subtype tested (Fig. 2B). Similar to its effects at $\alpha 1$ GlyRs, 4-cpro also directly activated $\alpha 2$ and $\alpha 3$ GlyRs (Fig. 2A middle panel), with I_{max} values $27 \pm 3\%$ and $20 \pm 0.9\%$ of the Gly I_{max} ($n = 6$), respectively. These results clearly describe two phases of modulation, of which only the high-affinity effect differs significantly across $\alpha 1$, $\alpha 2$, $\alpha 3$ homomers and $\alpha 1\beta$ heteromers and also an additional phase of agonist activity in the millimolar range at each homomeric subtype. Henceforth, high-affinity and low-affinity modulation will be referred to as “HA” and “LA” modulation.

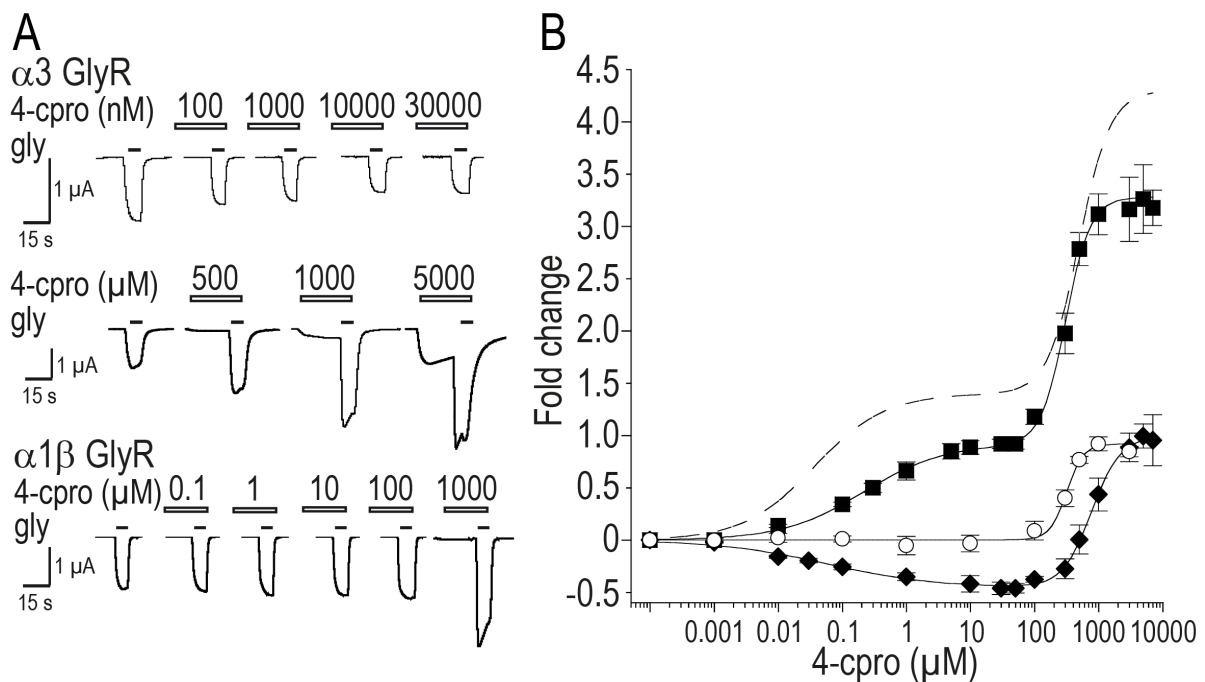


Figure 2: Subtype specific high-affinity modulation by 4-cpro. **A.** Current traces illustrating the differential effects of 4-cpro on EC_{20} Gly-induced currents at $\alpha 3$ (upper and middle panel) and $\alpha 1\beta$ (lower panel) GlyRs. **B.** Averaged potentiation by 4-cpro of EC_{20} Gly-induced currents at $\alpha 1$ (dashed line), $\alpha 2$ (filled squares), $\alpha 3$ (filled diamonds) and $\alpha 1\beta$ (open circles) GlyRs. $\alpha 1$ GlyR data in B are taken from Fig. 1B. Each point represents the mean \pm S.E.M. of 6-7 experiments.

The anesthetic pro exerts similar biphasic effects on all GlyR subunits

Several studies have shown that the anesthetic pro exerts both modulatory and agonist effects on $\alpha 1$ GlyRs over a wide concentration range (Ahrens et al., 2008; Daniels and Roberts, 1998). Prompted by our findings with 4-cpro, which extended this notion to three distinct effects, we revisited the parent compound, questioning if pro itself might also exhibit effects at lower concentrations than previously tested. We therefore analyzed the effects of nanomolar up to millimolar pro concentrations on homomeric $\alpha 1$, $\alpha 2$ and $\alpha 3$ and heteromeric $\alpha 1\beta$ GlyRs. Indeed, nanomolar concentrations of pro induced a small but significant potentiation of EC_{20} Gly responses, but in contrast to 4-cpro, at *both* $\alpha 1$ homomers and $\alpha 1\beta$ heteromers (Fig. 3A). This HA effect saturated between 1 and 10 μM , with 0.56 ± 0.05 -fold ($\alpha 1$, $n = 10$) and 0.44 ± 0.07 -fold ($\alpha 1\beta$, $n = 5$) potentiation. Similar to our findings with 4-cpro, pro at concentrations of 100 μM and greater induced an additional 3.1 ± 0.3 -fold ($\alpha 1$, $n = 10$) and 2.4 ± 0.2 -fold ($\alpha 1\beta$, $n = 5$) level of potentiation, saturating between 1 and 5 mM (Fig. 3B). Again, when data for the complete concentration ranges were

plotted, biphasic equations fit the data with higher fidelity than monophasic, confirming the distinction between the two effects (Fig. 3B). HA EC_{50} values ($\alpha 1$, 176 ± 29 nM; $\alpha 1\beta$, 386 ± 104 nM) differed slightly between homomers and heteromers, whereas LA EC_{50} values ($\alpha 1$, 685 ± 34 μ M; $\alpha 1\beta$, 597 ± 70 μ M) were not significantly different (Table 1). Pro differed from 4-cpro in that the contribution of the HA component to total potentiation was much less pronounced (less than 20%, *cf* to 35% for 4-cpro at $\alpha 1$ GlyRs), and the HA EC_{50} values for pro were generally some 5-fold higher than for 4-cpro (Table 1). Finally, we also observed that millimolar concentrations of pro directly activated both $\alpha 1$ homomeric and $\alpha 1\beta$ heteromeric GlyRs (Fig. 3A, lower panel), with I_{max} values equivalent to $32 \pm 3\%$ and $7 \pm 2\%$ of the Gly I_{max} , respectively. Thus, evidence for an additional HA effect extends to the anesthetic pro, although the potency in comparison to 4-cpro is less biased towards homomeric GlyRs.

We next questioned if the HA effect of pro differs across homomeric GlyR subtypes, as was the case with 4-cpro. In contrast to 4-cpro, where HA effects included inhibition of $\alpha 3$ GlyRs, nanomolar concentrations of pro weakly potentiated both $\alpha 2$ and $\alpha 3$ GlyRs, saturating at concentrations of approximately 10 μ M (Fig. 3B). EC_{50} values for this effect were 970 ± 48 nM at $\alpha 2$ and 194 ± 10 nM at $\alpha 3$ homomers ($n = 8$ for both), and thus, a higher EC_{50} value at $\alpha 2$ receptors is common to both pro and 4-cpro. LA modulation by pro appeared similar across homomeric subtypes (Fig. 3B): high micromolar concentrations potentiated $\alpha 2$ GlyRs up to 2.2 ± 0.3 -fold (EC_{50} 865 ± 32 μ M, $n = 8$) and $\alpha 3$ GlyRs up to 1.5 ± 0.2 -fold (EC_{50} 1152 ± 55 μ M, $n = 8$). Thus, LA EC_{50} values for pro differ no more than 2-fold between any two GlyRs tested, whereas HA EC_{50} values for pro differ up to 6-fold among subunits (Table 1). Finally, we also measured small direct activation of $\alpha 2$ and $\alpha 3$ GlyRs in response to pro at concentrations above 1 mM (Table 1).

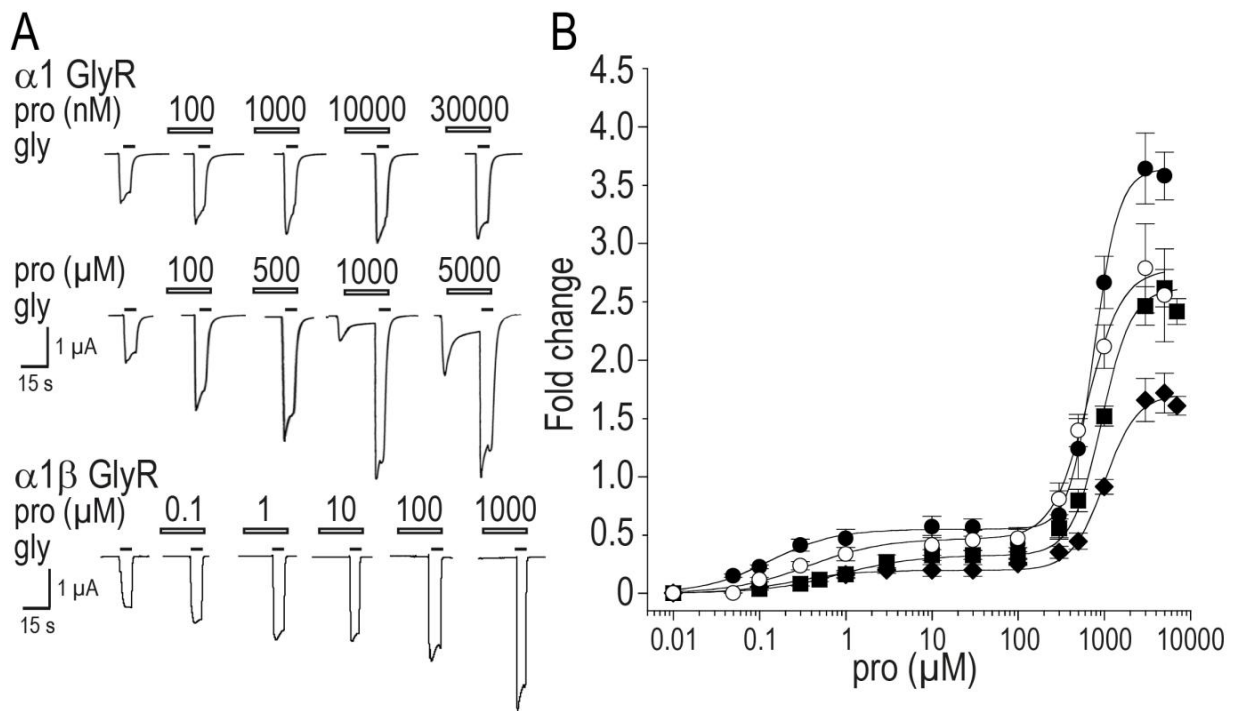


Figure 3: Biphasic modulation of homomeric $\alpha 1$, $\alpha 2$, $\alpha 3$ and heteromeric $\alpha 1\beta$ GlyRs by pro. **A.** Current traces illustrating the effects of low and high concentrations of pro on Gly-induced currents at $\alpha 1$ and $\alpha 1\beta$ GlyRs. **B.** Pro dose-response curves obtained in the presence of Gly concentrations corresponding to the respective EC_{20} value of $\alpha 1$ (filled circles), $\alpha 2$ (filled squares), $\alpha 3$ (filled diamonds), $\alpha 1\beta$ (open circles) GlyRs. Note HA and LA potentiation is evident at all tested GlyRs subunits. Each point represents the mean \pm S.E.M. of 6-7 experiments.

Table 1: Modulatory effects of low and high concentrations of 4-cpro and pro at wt GlyRs.

GlyR	High-affinity EC_{50} (nM)	fold change	Low-affinity EC_{50} (μ M)	fold change	n
	<i>4-cpro</i>				
α 1	21 \pm 6	1.5 \pm 0.2	617 \pm 160	2.6 \pm 0.4	10
α 1 β	<i>NE</i>	<i>NE</i>	406 \pm 50	0.9 \pm 0.06***	6
α 2	230 \pm 20***	0.9 \pm 0.05*	350 \pm 52	2.4 \pm 0.3	8
α 3	50 \pm 8 ^a	-0.5 \pm 0.05***	757 \pm 111	1.5 \pm 0.12***	9
	<i>pro</i>				
α 1	176 \pm 29	0.56 \pm 0.05	685 \pm 44	3.1 \pm 0.3	10
α 1 β	386 \pm 104*	0.44 \pm 0.07	597 \pm 70	2.2 \pm 0.2	5
α 2	970 \pm 48***	0.34 \pm 0.02	865 \pm 32	2.2 \pm 0.2	8
α 3	194 \pm 10	0.2 \pm 0.03	1152 \pm 55*	1.5 \pm 0.2*	8

Parameters for high-affinity (HA) and low-affinity (LA) modulation by 4-cpro and pro at homo- and heteromeric GlyRs. Modulation was determined at EC_{20} concentrations of Gly. Data are means \pm S.E.M.. The respective Hill coefficients (nH) were between 0.7 and 1 for the HA site and between 1.3 and 2.2 for the LA site, respectively. *NE* no effect; **a** value represents IC_{50} ; * $P < 0.05$, ** $P < 0.01$, *** $P < 0.001$ compared to α 1 GlyR, unpaired t-test.

In summary, these data illustrate that pro exerts a so far unrecognized HA potentiating effect at homomeric and heteromeric GlyRs. Strikingly, 4C-chlorination of pro selectively alters the differential pharmacology of this HA site at the GlyR: 4-cpro showed no HA modulation of α 1 β heteromers, caused unique HA inhibition of α 3 homomers and was approximately fivefold more potent than pro at all homomers, whereas 4-cpro differed little from the parent compound in LA modulation of each receptor. The large differences in the EC_{50} value of each effect at each receptor, together with the differential manifestation only of the high-affinity effect in certain receptors, suggests that homomeric GlyRs possess multiple and distinct sites for these drugs: a HA (nanomolar) site that is substantially different in each subtype and a third site, via which direct activation occurs with millimolar concentrations. These points lead us to conclude that the HA effects of pro and 4-cpro at the GlyR are mediated by a uniquely divergent binding site, different from those described so far for these compounds.

4-cpro docking to the cannabinoid binding site in $\alpha 1$ GlyRs

So far, our results reveal that GlyRs possess multiple sites for modulation and activation by pro and 4-chloropropofol and hint that the increased potency of 4-cpro is likely due to increased activity at specifically the HA site, via which 4-cpro can uniquely inhibit $\alpha 3$ GlyRs. In a final set of experiments, we therefore sought to identify the molecular determinants of the HA site. Due to the subtype-specific HA modulation by 4-cpro, we assume that divergent TMD residues might be involved in this allosteric modulation of channel function (Fig. 4A). Interestingly, the subtype specific residue Ser296 in the M3 of $\alpha 1$ GlyRs was recently identified as a determinant of the subtype specific modulation of GlyRs by cannabinoids (Xiong et al., 2011). Inspection of the amino acids in the vicinity Ser296, including M4 residues, reveals the presence of multiple α GlyR subtype specific residues (Fig. 4A). Therefore, we asked us if 4-cpro and AEA have the same binding site in GlyRs. First, we investigated AEA effects on the function of homomeric $\alpha 3$ GlyRs. Concerning the agonist concentration depend type of AEA modulation, we choosed a Gly concentration equating to the EC_5 Gly for observing a current enhancement. Nanomolar to μM pre- and coapplications of AEA concentrations increased the Gly evoked currents dose dependently 0.2 ± 0.05 fold, with an EC_{50} of 3.2 ± 1.4 nM and an hill coefficient of 1.2 ± 0.15 (Fig 4B, inset; $n = 4$). Next, we analyzed the effects 5 nM AEA on the HA site inhibition of homomeric $\alpha 3$ GlyRs by 4-cpro (Fig. 4B). 4-cpro inhibited again the $\alpha 3$ GlyR currents, reaching in the presence of AEA an IC_{50} of 118 ± 9 nM, compared to the inhibition of $\alpha 3$ by 4-cpro alone this equates to a 2.4-fold significant increase ($P < 0.001$, $n = 4$). The currents were inhibited 0.38 ± 0.02 -fold ($n = 4$).

Based on the AEA dependent right shift in the IC_{50} value of the 4-cpro HA site inhibition of $\alpha 3$ GyRs, we docked 4-cpro in the vicinity of Ser296 in our homology model and ran free MD simulations as an initial probe for 4-cpro binding at this position. The binding pose of 4-cpro is shown as an inset in figure 4D (yellow molecule) and indicates several cooperative non-covalent interactions which drive the binding process. There is a notable hydrogen bond bewteen Ser296 and the hydroxy moeity of 4-cpro. We propose that the chlorine atom significantly enhances this hydrogen bonding interaction due ot the increased acidity of the hydroxy functionality compared with propofol (4-cpro $pK_a = 10.6$, pro $pK_a = 11.1$). In addition,

there is an edge-to-face π - π stacking interaction between the aromatic ring of Phe402 and 4-cpro, a hydrophobic contact between Leu292 and an isopropyl group of 4-cpro whilst the other isopropyl group makes a hydrophobic contact with Phe293.

Molecular determinants of the 4-cpro HA modulation at α 1 GlyRs

The prominent hydroxyl-hydroxyl interaction would not be available to α 2 GlyRs with an Ala at this position, providing a tentative explanation for the reduced affinity and efficacy of the HA phase of 4-cpro modulation at α 2 GlyRs. We tested this idea by measuring 4-cpro modulation of mutant α 1Ser296Ala GlyRs. Strikingly, HA (concentrations up to 100 μ M) modulation was abolished in Ser296Ala α 1 GlyRs, despite what is ostensibly the typical LA phase of modulation by higher μ M concentrations remaining indistinguishable from WT (Fig. 4D; Table 2). Thus, the specific disruption of the HA phase by mutating Ser296 establishes functional evidence for two distinct modulatory sites in the α 1 GlyR and that an interaction between 4-cpro and receptor hydroxyls at position Ser296 may indeed contribute selectively to HA 4-cpro potentiation.

Remarkably, when we tested 4-cpro modulation of Gly responses at the α 1Phe293Ala mutant, we observed that HA modulation was abolished (Fig. 4D). LA potentiation was intact at α 1Phe293Ala receptors and EC_{50} value and maximum potentiation was not significantly different from WT (Table 2). In contrast, biphasic modulation by 4-cpro was evident at the Phe402Ala mutant but we observed a significant increase in EC_{50} from 21 to 55 nM and a decrease in maximum potentiation from 1.5 ± 0.3 to 0.3 ± 0.04 fold ($P < 0.01$) without an effect on LA potentiation (Table 2). Regarding the dockings, the side chains of the M3 residues Val289 and Leu292 may form putative hydrophobic contacts and ionic backbone interactions with one of the diisopropyl groups (Leu292) and the chloride atom (Val289) of 4-cpro (Fig. 4D). When we tested 4-cpro modulation of Gly responses at Val289Ala mutant α 1 GlyRs, we observed a significant increase in EC_{50} from 21 to 134 nM and a decrease in maximum potentiation from 1.0 ± 0.3 to 0.5 ± 0.06 fold for the HA site ($P < 0.01$) without affecting LA potentiation (Fig. 4D; Table 2). In contrast, HA modulation of Gly-induced currents by 4-cpro was absent at the Leu292Ala mutant and the potency of the LA potentiation significantly reduced compared to WT (Table 2).

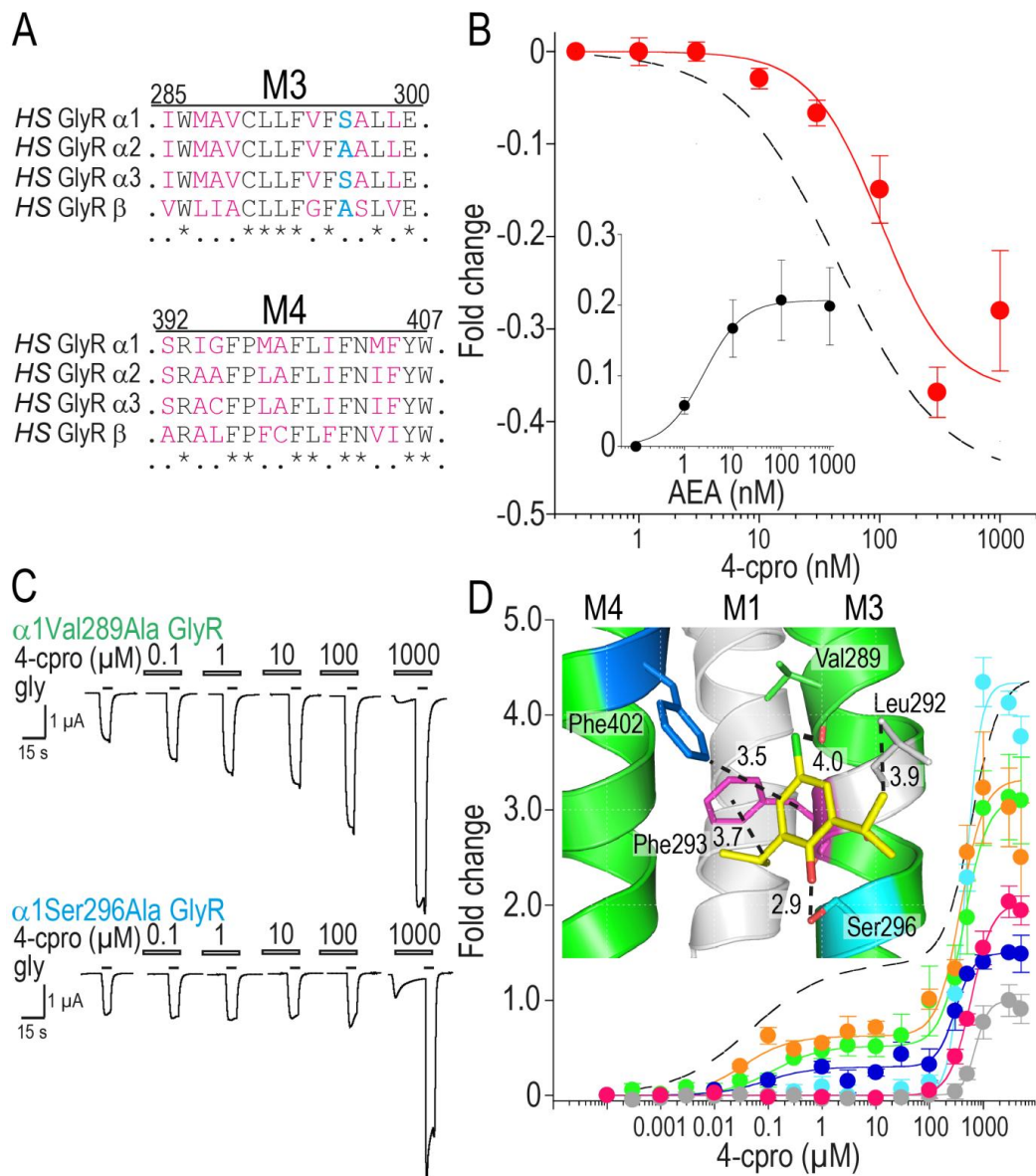


Figure 4: Model and mutational analyses of the high-affinity 4-cpro-binding site at the α 1 GlyR. **A.** Partial sequence alignment of the M3 and M4 transmembrane regions of the GlyR subunits. Conserved amino acid positions are indicated by stars. Sequence divergences are colored in magenta. Numbers above the sequences indicate the position of the first amino acid in the respective transmembrane domain of the mature α 1 subunit. **B.** AEA induced right shift (red filled circles) in the HA inhibition by 4-cpro of α 3 GlyRs. **Inset** represents the AEA potentiation of the ECs Gly evoked currents at α 3 GlyRs. Each data point represents mean \pm S.E.M. of 4 cells, respectively. **C.** Current traces illustrating the 4-cpro effect on Gly evoked currents of mutated α 1GlyRs. **D.** 4-cpro dose–response curves of the mutant respective EC_{20} value of wt α 1 (dashed line), α 1Val289Ala (green filled circles), α 1Leu292Ala (grey filled circles), α 1Phe293Ala (magenta filled circles), α 1Ser296Ala (cyan filled circles), α 1Met397Ala (orange filled circles) and α 1Phe402Ala (blue filled circles) GlyRs. Remarkably, a biphasic modulation by 4-cpro is only seen for α 1Val289Ala, α 1Met397Ala and α 1Phe402Ala GlyRs. Each data point represents mean \pm S.E.M. of 3 to 10 cells. **Inset** represents the homology model of the α 1 GlyR illustrating the docking result (see Material and Methods). A subunit (shown in green) viewed from lateral indicating the HA binding site of 4-cpro (in yellow) in the TMD. Residues indicated by our docking results are highlighted and colored following the code explained in **D**.

Table 2: High- and low-affinity 4-cpro modulation at wt and mutant $\alpha 1$ GlyRs

GlyR	High-affinity EC_{50} (nM)	fold change	Low-affinity EC_{50} (μ M)	fold change	n
$\alpha 1$	21 ± 6	1.5 ± 0.2	617 ± 160	2.6 ± 0.4	10
$\alpha 1$ Val289Ala	$134 \pm 18^{***}$	$0.55 \pm 0.06^*$	462 ± 21	2.7 ± 0.4	5
$\alpha 1$ Leu292Ala	<i>NE</i> ^{***}	<i>NE</i> ^{***}	730 ± 88	$1.0 \pm 0.2^*$	5
$\alpha 1$ Phe293Ala	<i>NE</i> ^{***}	<i>NE</i> ^{***}	920 ± 212	1.9 ± 0.3	7
$\alpha 1$ Ser296Ala	<i>NE</i> ^{***}	<i>NE</i> ^{***}	464 ± 13	3.9 ± 0.4	6
$\alpha 1$ Met397Ala	33 ± 2	0.62 ± 0.08	385 ± 47	2.6 ± 0.6	3
$\alpha 1$ Phe402Ala	$55 \pm 11^{**}$	$0.3 \pm 0.04^{**}$	597 ± 101	$1.3 \pm 0.5^*$	5

Parameters for high-affinity (HA) and low-affinity (LA) modulation by 4-cpro at homomeric wt and mutant $\alpha 1$ GlyRs. Modulation was determined at EC_{20} concentrations of Gly. Data are means \pm S.E.M.. The respective Hill coefficients (η H) were between 0.7 and 1 for the HA site and between 1.3 and 2.2 for the LA site, respectively. *NE* no effect; a value represents IC_{50} ; * $P < 0.05$, ** $P < 0.01$, *** $P < 0.001$ compared to wt $\alpha 1$ GlyR, unpaired t-test.

Discussion

This study used a detailed pharmacological and mutational analysis to show that pro and its halogenated derivative, 4-cpro, exert multiple effects at homo- and heteromeric GlyRs: (i) HA modulation in the nanomolar range, which is subtype-specific, of opposing effects for pro and 4-cpro at $\alpha 3$ GlyRs, and altered by single mutations of non-conserved residues in M3 and M4; (ii) LA potentiation in the micromolar range, which is similar for pro and 4-cpro at all homo- and heteromeric GlyRs tested and altered by mutation of conserved TMD residues; and iii) direct activation in the millimolar range, which is competitively inhibited by strychnine and of varying potency at homo- and heteromeric GlyRs. From these data we conclude that GlyRs possess two distinct binding sites for allosteric modulation by these compounds and a third site for the agonist effect. Finally, the results suggest that C4-halogenation confers increased potency and altered subtype-specificity by specifically altering interactions with the HA site in the GlyR.

One striking finding of this study is that pro exerts both HA and LA modulation on Gly-gated currents. Previously, it was known that micromolar pro concentrations strongly potentiate Gly-gated currents and high micromolar/low millimolar concentrations activate small currents at $\alpha 1$ homomeric and $\alpha 1\beta$ heteromeric GlyRs (Pistis et al., 1997); biphasic *potentiation* was so far not reported. However, relative to the strong potentiation of the LA effect, it is easy to imagine that the weak potentiation of the HA effect was previously overlooked. Indeed, it was the enhanced HA modulation by 4-cpro that alerted us to the HA effect. Thus, the relative weakness of the HA effect of pro seems a plausible explanation for its absence in previous, similar experiments (Daniels and Roberts, 1998; Lynagh and Laube, 2014; Pistis et al., 1997), although we note that small potentiation of GlyR currents with low pro concentrations ($<1 \mu\text{M}$) has been described (Hales and Lambert, 1991; O'Shea et al., 2004). It is difficult, however, to explain why the stronger, LA potentiation seems to occur over such a wide range of concentrations in various studies, from the low micromolar range in HEK cells (Ahrens et al., 2008) or oocytes (Pistis et al., 1997) to the high μM range in oocytes (Daniels and Roberts, 1998; Lynagh and Laube, 2014). We speculate that this is related to the ability of pro to bind to membrane-embedded sites, which probably depends on expression system (Bass

and Spencer, 2006) and the length of time over which pro is pre-applied and thus partition into the membrane (Lee and MacKinnon, 2004).

By alerting us to two distinct phases of modulation, 4-cpro in turn led us to question if these effects were mediated by an identical site (of which five occur in a homopentamer) or by discrete binding sites. On one hand, identical sites could mediate different effects based on incremental occupancy of one to five of the same sites, as is the case with ivermectin, which modulates GlyRs *via* one or two and activates GlyRs *via* two or more sites (Lynagh and Lynch, 2010). A related idea was recently proposed for pro at a cation-selective pLGIC, where occupancy of zero or five sites facilitates channel opening and occupancy of two to four sites facilitates channel closure (Mowrey et al., 2013). However, several experiments of ours argue that pro and 4-cpro mediate three effects via three discrete sites. Firstly, the three effects differ across GlyR subtypes. HA modulation (by both pro and 4-cpro) is markedly less potent at $\alpha 2$ GlyRs whereas LA modulation is very similar at each subtype. Secondly, C4-chlorination alters the HA and LA effects differently: 4-cpro is much more potent than pro regarding only the HA effect; LA modulation is remarkably similar for the two drugs. Finally, we identified TMD residues whose mutation selectively alters one of the two effects. HA modulation was altered by mutating M3 and M4 residues deep in the TMD.

Although evidence for multiple pro binding sites in pLGICs has been emerging over the last four years, this study provides the first definitive evidence for distinct modulatory effects corresponding to pro binding to distinct sites. The previously identified sites include two sites in the GABA(A)R TMD (Jayakar et al., 2014) and three sites in the nicotinic acetylcholine receptor TMD (Jayakar et al., 2013). In both of those cases, none of the sites identified overlaps with the HA site we have characterized in the GlyR. The unique presence of this site in the GlyR makes it a promising target for drugs that distinguish GlyRs from other structurally related pLGICs. Equally exciting is the fact that this site is subtly divergent in different GlyR subtypes, as demonstrated by the selective inhibition by 4-cpro of $\alpha 3$ GlyRs due to a divergent residue on one side of the HA binding site. Whereas pro affects several ion channel families (Franks and Lieb, 1994) and can potentiate or inhibit certain pLGICs *via* the same LA site (Lynagh and Laube, 2014), the 4-chlorinated derivative selectively targets GlyRs in the *nM* range and exerts different effects on GlyR

subtypes *via* a divergent HA site. C4-halogenated pro derivatives thus hold great promise as GlyR-specific, subtype-selective modulators.

References

- Ahrens J, Leuwer M, Stachura S, Krampfl K, Belelli D, Lambert JJ and Haeseler G (2008) A transmembrane residue influences the interaction of propofol with the strychnine-sensitive glycine alpha1 and alpha1beta receptor. *Anesth Analg* **107**(6): 1875-1883.
- Bali M and Akabas MH (2004) Defining the propofol binding site location on the GABAA receptor. *Mol Pharmacol* **65**(1): 68-76.
- Bass RB and Spencer RH (2006) Approaches for Ion Channel Structural Studies, in *Expression and Analysis of Recombinant Ion Channels* pp 213-239, Wiley-VCH Verlag GmbH & Co. KGaA.
- Betz H and Laube B (2006) Glycine receptors: recent insights into their structural organization and functional diversity. *J Neurochem* **97**(6): 1600-1610.
- Chung SK, Bode A, Cushion TD, Thomas RH, Hunt C, Wood SE, Pickrell WO, Drew CJ, Yamashita S, Shiang R, Leiz S, Longardt AC, Raile V, Weschke B, Puri RD, Verma IC, Harvey RJ, Ratnasinghe DD, Parker M, Rittey C, Masri A, Lingappa L, Howell OW, Vanbellinghen JF, Mullins JG, Lynch JW and Rees MI (2013) GLRB is the third major gene of effect in hyperekplexia. *Hum Mol Genet* **22**(5): 927-940.
- Daniels S and Roberts RJ (1998) Post-synaptic inhibitory mechanisms of anaesthesia; glycine receptors. *Toxicol Lett* **100-101**: 71-76.
- de la Roche J, Leuwer M, Krampfl K, Haeseler G, Dengler R, Buchholz V and Ahrens J (2012) 4-Chloropropofol enhances chloride currents in human hyperekplexic and artificial mutated glycine receptors. *BMC Neurol* **12**: 104.
- Eckle VS, Grasshoff C, Mirakaj V, O'Neill PM, Berry NG, Leuwer M and Antkowiak B (2014) 4-bromopropofol decreases action potential generation in spinal neurons by inducing a glycine receptor-mediated tonic conductance. *Br J Pharmacol* **171**(24): 5790-5801.
- Eichler SA, Forstera B, Smolinsky B, Juttner R, Lehmann TN, Fahling M, Schwarz G, Legendre P and Meier JC (2009) Splice-specific roles of glycine receptor alpha3 in the hippocampus. *Eur J Neurosci* **30**(6): 1077-1091.
- Eichler SA, Kirischuk S, Juttner R, Schaefermeier PK, Legendre P, Lehmann TN, Gloveli T, Grantyn R and Meier JC (2008) Glycinergic tonic inhibition of hippocampal neurons with depolarizing GABAergic transmission elicits histopathological signs of temporal lobe epilepsy. *J Cell Mol Med* **12**(6B): 2848-2866.

- Franks NP (2008) General anaesthesia: from molecular targets to neuronal pathways of sleep and arousal. *Nat Rev Neurosci* **9**(5): 370-386.
- Franks NP and Lieb WR (1994) Molecular and cellular mechanisms of general anaesthesia. *Nature* **367**(6464): 607-614.
- Goujon M, McWilliam H, Li W, Valentin F, Squizzato S, Paern J and Lopez R (2010) A new bioinformatics analysis tools framework at EMBL-EBI. *Nucleic Acids Res* **38**(Web Server issue): W695-699.
- Grudzinska J, Schemm R, Haeger S, Nicke A, Schmalzing G, Betz H and Laube B (2005) The beta subunit determines the ligand binding properties of synaptic glycine receptors. *Neuron* **45**(5): 727-739.
- Hales TG and Lambert JJ (1991) The actions of propofol on inhibitory amino acid receptors of bovine adrenomedullary chromaffin cells and rodent central neurones. *Br J Pharmacol* **104**(3): 619-628.
- Harvey RJ, Depner UB, Wassle H, Ahmadi S, Heindl C, Reinold H, Smart TG, Harvey K, Schutz B, Abo-Salem OM, Zimmer A, Poisbeau P, Welzl H, Wolfer DP, Betz H, Zeilhofer HU and Muller U (2004) GlyR alpha3: an essential target for spinal PGE2-mediated inflammatory pain sensitization. *Science* **304**(5672): 884-887.
- Humphrey W, Dalke A and Schulten K (1996) VMD: visual molecular dynamics. *J Mol Graph* **14**(1): 33-38, 27-38.
- Islam R and Lynch JW (2012) Mechanism of action of the insecticides, lindane and fipronil, on glycine receptor chloride channels. *Br J Pharmacol* **165**(8): 2707-2720.
- Jayakar SS, Dailey WP, Eckenhoff RG and Cohen JB (2013) Identification of propofol binding sites in a nicotinic acetylcholine receptor with a photoreactive propofol analog. *J Biol Chem* **288**(9): 6178-6189.
- Jayakar SS, Zhou X, Chiara DC, Dostalova Z, Savechenkov PY, Bruzik KS, Dailey WP, Miller KW, Eckenhoff RG and Cohen JB (2014) Multiple propofol-binding sites in a gamma-aminobutyric acid type A receptor (GABAAR) identified using a photoreactive propofol analog. *J Biol Chem* **289**(40): 27456-27468.
- Jurd R, Arras M, Lambert S, Drexler B, Siegwart R, Crestani F, Zaugg M, Vogt KE, Ledermann B, Antkowiak B and Rudolph U (2003) General anesthetic actions in vivo strongly attenuated by a point mutation in the GABA(A) receptor beta3 subunit. *FASEB J* **17**(2): 250-252.

- Kondratskaya EL, Betz H, Krishtal OA and Laube B (2005) The beta subunit increases the ginkgolide B sensitivity of inhibitory glycine receptors. *Neuropharmacology* **49**(6): 945-951.
- Korb O, Stutzle T and Exner TE (2009) Empirical scoring functions for advanced protein-ligand docking with PLANTS. *J Chem Inf Model* **49**(1): 84-96.
- Krasowski MD, Jenkins A, Flood P, Kung AY, Hopfinger AJ and Harrison NL (2001) General anesthetic potencies of a series of propofol analogs correlate with potency for potentiation of gamma-aminobutyric acid (GABA) current at the GABA(A) receptor but not with lipid solubility. *J Pharmacol Exp Ther* **297**(1): 338-351.
- Krivov GG, Shapovalov MV and Dunbrack RL, Jr. (2009) Improved prediction of protein side-chain conformations with SCWRL4. *Proteins* **77**(4): 778-795.
- Laube B, Kuhse J and Betz H (1998) Evidence for a tetrameric structure of recombinant NMDA receptors. *J Neurosci* **18**(8): 2954-2961.
- Laube B, Kuhse J and Betz H (2000) Kinetic and mutational analysis of Zn²⁺ modulation of recombinant human inhibitory glycine receptors. *J Physiol* **522 Pt 2**: 215-230.
- Lee SY and MacKinnon R (2004) A membrane-access mechanism of ion channel inhibition by voltage sensor toxins from spider venom. *Nature* **430**(6996): 232-235.
- Li GD, Chiara DC, Cohen JB and Olsen RW (2010) Numerous classes of general anesthetics inhibit etomidate binding to gamma-aminobutyric acid type A (GABAA) receptors. *J Biol Chem* **285**(12): 8615-8620.
- Lingamaneni R, Krasowski MD, Jenkins A, Truong T, Giunta AL, Blackbeer J, MacIver MB, Harrison NL and Hemmings HC, Jr. (2001) Anesthetic properties of 4-iodopropofol: implications for mechanisms of anesthesia. *Anesthesiology* **94**(6): 1050-1057.
- Lynagh T and Laube B (2014) Opposing effects of the anesthetic propofol at pentameric ligand-gated ion channels mediated by a common site. *J Neurosci* **34**(6): 2155-2159.
- Lynagh T and Lynch JW (2010) A glycine residue essential for high ivermectin sensitivity in Cys-loop ion channel receptors. *Int J Parasitol* **40**(13): 1477-1481.
- Lynch JW (2009) Native glycine receptor subtypes and their physiological roles. *Neuropharmacology* **56**(1): 303-309.

- Mowrey DD, Cui T, Jia Y, Ma D, Makhov AM, Zhang P, Tang P and Xu Y (2013) Open-channel structures of the human glycine receptor alpha1 full-length transmembrane domain. *Structure* **21**(10): 1897-1904.
- O'Shea SM, Becker L, Weiher H, Betz H and Laube B (2004) Propofol restores the function of "hyperekplexic" mutant glycine receptors in *Xenopus* oocytes and mice. *J Neurosci* **24**(9): 2322-2327.
- Pistis M, Belelli D, Peters JA and Lambert JJ (1997) The interaction of general anaesthetics with recombinant GABAA and glycine receptors expressed in *Xenopus laevis* oocytes: a comparative study. *Br J Pharmacol* **122**(8): 1707-1719.
- Sanna E, Motzo C, Usala M, Serra M, Dazzi L, Maciocco E, Trapani G, Latrofa A, Liso G and Biggio G (1999) Characterization of the electrophysiological and pharmacological effects of 4-iodo-2,6-diisopropylphenol, a propofol analogue devoid of sedative-anaesthetic properties. *Br J Pharmacol* **126**(6): 1444-1454.
- Sigel E and Steinmann ME (2012) Structure, function, and modulation of GABA(A) receptors. *J Biol Chem* **287**(48): 40224-40231.
- Xiong W, Cheng K, Cui T, Godlewski G, Rice KC, Xu Y and Zhang L (2011) Cannabinoid potentiation of glycine receptors contributes to cannabis-induced analgesia. *Nat Chem Biol* **7**(5): 296-303.
- Yevenes GE and Zeilhofer HU (2011) Allosteric modulation of glycine receptors. *Br J Pharmacol* **164**(2): 224-236.
- Yip GM, Chen ZW, Edge CJ, Smith EH, Dickinson R, Hohenester E, Townsend RR, Fuchs K, Sieghart W, Evers AS and Franks NP (2013) A propofol binding site on mammalian GABAA receptors identified by photolabeling. *Nat Chem Biol* **9**(11): 715-720.

Characterization of propofol binding sites and site specific effects at $\alpha 1$ GlyRs

Michael Kilb¹, Neil G. Berry², Rudolf Schemm³ and Bodo Laube¹

¹Neurophysiology and Neurosensory Systems, Department of Biology, Technical University of Darmstadt, Darmstadt, Germany

²Robert Robinson Laboratories, Department of Chemistry, University of Liverpool, Liverpool, U.K.

³Department of Theoretical and Computational Biophysics, Max-Planck-Institute for Biophysical Chemistry Göttingen, Germany

Abstract

Former analysis unmasked that the general anesthetic propofol (pro) and its chlorinated version 4-chloropropofol (4-cpro) modulate the function of recombinant expressed $\alpha 1$ glycine receptors (GlyRs) via a high-affinity (HA) and low-affinity (LA) potentiation. Concerning the 4-cpro HA potentiation, we recently identified an intrasubunit binding site formed by non- and conserved α GlyR subtype specific amino acids located in the transmembrane domains (TMDs) M3 and M4 (chapter 2). In this study, we estimate the location of three functional pro binding sites at the $\alpha 1$ GlyR by using the two-electrode-voltage clamp technique (TEVC) combined with site-directed mutagenesis, in silico dockings of pro to $\alpha 1$ GlyR homology models and the use of the GlyR modulating reagents ivermectin (IVM), anandamide (AEA) and strychnine (stry). We obtained data suggesting that the pro HA potentiation is the result of a pro binding to the 4-cpro HA site, whereas the pro LA potentiation is mediated by a site located in the TMD interface which overlaps with the IVM site. Concerning the partial agonism by pro, we unmasked that pro evoked chloride currents can be inhibited competitive by the antagonist stry underlining the presence of a pro binding site in the ligand binding domain (LBD) in the extracellular domain (ECD). By using a mutation (Phe293Ala) which abolishes pro and 4-cpro HA site potentiation in $\alpha 1$ GlyRs, we were able to estimate site specific mechanisms by which the pro modulation affect the agonist activation of $\alpha 1$ GlyRs. Whereas the pro HA site

potentiation increases the cooperativity, the pro LA site potentiation increases the apparent affinity towards Gly at $\alpha 1$ GlyRs. Moreover, we observed that the formation of a HA potentiation by pro, depends on the strength of the $\alpha 1$ GlyR activation. Finally, we investigated the pro insensitive M3 amino acid substitution Ala288Ile in a greater detail and unmasked that the substitution is not modulated by AEA and affects the gating in $\alpha 1$ GlyRs.

Introduction

The GlyR belong to the superfamily of pentameric ligand gated ion channels (pLGICs). Functional GlyRs are formed either from four α subtypes alone (homomeric) or from both α and β subtypes (heteromeric) (Langosch et al., 1988). Each subtype comprised of a large N-terminal ECD, four TMDs, a long intracellular loop (IL) connecting M3 and M4, and a short extracellular C-terminus.

In the case of the GlyR a few allosteric modulators are known which modulate the receptor function (Yevenes and Zeilhofer, 2011). However, the exact location of only four allosteric modulator binding sites (IVM, tropeines, cannabinoids and zinc) are known at GlyRs. Two of them, the IVM and cannabinoid site, are located in the TMDs whereas tropeines and zinc bind to sites located in the ECD (Laube et al., 2000; Lynagh et al., 2011; Maksay et al., 2009; Xiong et al., 2011). In the case of IVM, extensive electrophysiological studies at the GlyR point out the presence of a TMD binding site in the interface of adjacent subunits (Lynagh et al., 2011). This was verified by a crystallographic study showing IVM bound to the structural GlyR homologue glutamate gated chloride channel (GluCl) from the nematode *Caenorhabditis elegans* (*C.elegans*) (Hibbs and Gouaux, 2011). In the case of the cannabinoid binding site, Xiong and colleagues characterized recently a subtype specific amino acid in the α GlyR subtypes M3 as a binding determinant (Xiong et al., 2011).

One prominent allosteric modulator of the inhibitory Gly- and γ -aminobutyric acid type A receptors (GABA_ARs) is the general anesthetic pro. Pro enhances the function of GABA and Gly evoked chloride currents reversible and dose-dependent (Hales and Lambert, 1991; Pistis et al., 1997). Pro also increases the apparent affinities of the Gly- and GABA_ARs towards their agonists without altering the maximum responses (O'Shea et al., 2004; Orser et al., 1994). At higher concentrations, pro acts as a partial agonist at GABA_A- and GlyRs (Pistis et al., 1997).

That pro enhancement of GABAergic activity contributes to a great part to the induction of anesthesia is demonstrated by “knock-in” mice's bearing a single substitution at position 15 in the M2 of the β 3 subunit (β 3M2–15'). In vitro and vivo experiments showed that this TMD substitution reduces the sensitivity of GABA_ARs towards the general anesthetics etomidate, pro and pentobarbital (Chiara et al., 2013; Jurd et al., 2003). However, GlyRs may although play an important role for the pro induced general anesthesia. Hales and Lambert demonstrated sensitivity of

GlyRs to pro, as pro dose-dependently potentiated stry-sensitive currents evoked by Gly in spinal neurons (Hales and Lambert, 1991).

Low micromolar concentrations ($\geq 10 \mu\text{M}$) of pro also attenuate the symptoms of the GlyR related disease hyperekplexia in mice by restoring the function of the mutated homomeric $\alpha 1$ GlyRs and induces general anesthesia via the attenuation of the GABA(A)R function (Franks and Lieb, 1994; O'Shea et al., 2004; Pistis et al., 1997).

Till today, the location of the allosteric and partial agonistic pro binding site at GlyRs is still unknown but experiments by Duret and colleagues at chimeras of GlyRs and *Gloeobacter violaceus* (GLIC) receptors unmasked the TMDs as areas responsible for the allosteric modulation by pro (Duret et al., 2011). Recent investigations also showed that pro binds between all four TMDs of a single subunit in the bacterial cys-loop receptor homologue GLIC (Nury et al., 2011) and mutagenesis studies in the GlyR M3-M4 linker and TMD interface decreases and abolished the potentiation by pro (Lynagh and Laube, 2014; Moraga-Cid et al., 2011). By the use of photoreactive pro derivatives, binding to several sites in the TMDs of nACh- and mammalian GABA(A)Rs have been shown (Cui et al., 2011; Yip et al., 2013).

Recently published studies unmasked that chlorination of pro in the 4'position increases the allosteric potency only at homomeric $\alpha 1$ GlyRs (de la Roche et al., 2012; Trapani et al., 1998). We expanded the pharmacological characterization of 4-cpro effects on the function of homo- $\alpha 1$ -3 and heteromeric $\alpha 1\beta$ GlyRs and observed a novel, biphasic allosteric modulation of the GlyR function. Remarkably, this biphasic modulation was also evident for pro. By using TEVC combined with site-directed mutagenesis and computational dockings, we obtained data proofing that the high- (HA) and low affinity (LA) allosteric modulation based on the action of distinct binding sites, named HA and LA by us (chapter 2). Remarkably, in the case of 4-cpro, HA site modulation was subtype specific and at $\alpha 3$ GlyRs, sensitive towards the presence of the cannabinoid AEA.

Computational docking of 4-cpro into the AEA binding site in a $\alpha 1$ GlyR homology model based on the crystal structure of the GluCl and subsequent TEVC analysis of 4-cpro effects at mutant $\alpha 1$ GlyRs carrying amino acid substitutions in their M3 and M4, proofed the presence of an intrasubunit HA site for 4-cpro in $\alpha 1$ GlyRs (chapter 2).

In this study, we used the TEVC technique in combination with site-directed mutagenesis, molecular dynamic simulations (MDS) and pharmacological active

reagents to estimate the location of functional pro binding sites responsible for the previously identified biphasic allosteric modulation and partial agonism in $\alpha 1$ GlyRs (chapter 2). In addition, we obtained basic mechanistic data unmasking site specific effects on parameters of the Gly activation. Moreover, we observed that the formation of a HA potentiation by pro depends on the used Gly concentration. We also investigated in a greater detail the impact of the Ala288Ile substitution on the pro, AEA effects and partial agonist's activation to gain more information about the Ala288Ile substitution in $\alpha 1$ GlyRs.

Materials & Methods

cRNA synthesis

cRNAs of wildtype (wt) and mutated $\alpha 1$ GlyR subtypes were synthesized by in vitro transcription from linearised plasmid cDNAs using the Ambion SP6 mMESSAGE mMACHINE® SP6 Kit (Life-technologies, Carlsbad, USA) and injected in stage IV-V *Xenopus laevis* oocytes as described previously (Haeger et al., 2010).

Materials

All chemicals were purchased from Sigma-Aldrich (München, Germany) and from AppliChem (Darmstadt, Germany). The Ambion SP6 mMESSAGE mMACHINE®-Kit from Life-technologies (Carlsbad, USA).

Chemicals

2.6-diisopropylphenol (pro), IVM and AEA were diluted into glass vessels with a final stock concentration of 1 M pro, 10 mM IVM and 1mM AEA in DMSO. Stocks were frozen at -20°C and concentrations were manufactured at the day of the experiment in recording solution. The highest diluted pro concentration was 30 mM, for IVM 100 nM and for AEA 10 μ M.

Oocytes expression

Ovarian lobes were surgically removed from adult female *Xenopus laevis* claw frogs anaesthetized by immersion in 0.3% (w/v) tricaine methane sulfonate (Sigma). All protocols were approved by the local animal care and use committee (II25.3-19c20/15; RP Darmstadt, Germany). Oocytes were carefully dissected, stored and prepared as described in chapter 2.

Electrophysiological recordings and data analyzes

TEVC recordings of whole cell currents were performed in Ringer's solution at a holding potential of -70 mV as described previously (Laube et al., 2000). Modulation of Gly currents by pro, IVM and AEA were measured and analyzed following previously described procedures (Lynagh et al., 2011; (Lynagh and Laube, 2014; Xiong et al., 2012; Zhang and Xiong, 2009). Pro displacement by stry was calculated

by using the Schild-Gaddum and pA₂ estimation were done by plotting log (dose-ratio-1) and agonist (log B) as described (Lazareno and Birdsall, 1993).

Experimental values are presented as means ± S.E.M. of peak current responses. The statistical significance of differences between mean values was assessed by paired and unpaired student's t-test and considered to be significant at **P* < 0.05. All experiments were performed at room temperature.

Homology modeling and MDS

The docking of pro to the 4-cpro HA- and IVM site was done by using a α₁ GlyR homology model based on the Lilly structure (pdb code 4X5T) (Moraga-Cid et al., 2015). The dockings and GOLD optimizations were done as described in chapter 2. Concerning the docking of pro to the α₁ GlyR LBD, a homology model of the human α₁ GlyR based on the X-ray structure of the GluCl (pdb code 3RIF) was generated with Modeller9v8 (Hibbs and Gouaux, 2011; Sali and Blundell, 1993). The resulting model was then embedded in a DOPC membrane (Wolf et al., 2010) and the simulation box filled with tip3p water and NaCl (0.15 molar). For MDS we used the Gromacs software package (v. 4.5, 4.6) and the amber99sb*ildn force field (Hess et al., 2008; Hornak et al., 2006). The system was equilibrated for 10 ns by putting position restraints only on the protein ($fc = 1000 \text{ kJ}/(\text{mol}\cdot\text{nm}^2)$). A topology for pro was generated by using gaff (generalized amber force field), integrated in the antechamber software package and afterwards converted to a Gromacs applicable form using ACPYPE (Sousa da Silva and Vranken, 2012; Wang et al., 2006; Wang et al., 2004). Pro was then placed manually in the respective binding pockets with each of the five ligands adopting a different binding pose. Before starting the production runs, 5 ns simulations were performed applying position restraints to all ligands ($fc = 100 \text{ kJ}/(\text{mol}\cdot\text{nm}^2)$) to allow the protein to adapt to the respective ligand pose. Then 50 ns/250 ns unconstrained simulations for protein/pro combinations, were done. From these, the first 10-15 ns (pro) were discarded. The remaining trajectories were used to calculate the average binding enthalpies (sum of short range Coulomb and Lennard-Jones energies) and furthermore the minimized average structures (lowest energy dockings are shown).

Results

A pharmacological assessment of homo- and heteromeric GlyRs revealed that the anesthetic pro and its derivative 4-cpro exert complex biphasic modulating effects at Gly-evoked currents (chapter 2). Mutational analyses of residues within the transmembrane domains M3 and M4 of the $\alpha 1$ GlyR identified positions specifically affecting HA modulation by 4-cpro, indicating that the modulatory biphasic effects are mediated by distinct HA and LA binding sites. In addition, at very high concentrations, a substantial activation of the GlyRs independent from the modulatory effects of the compounds was obtained in the absence of the agonist Gly (chapter 2). Here, we intended to expand the analysis of the modulatory and agonistic action of pro to get insides in determinants and mechanisms of pro binding at the GlyR.

TEVC and MDS unmasked binding of pro to the 4-cpro HA site

We analyzed the effects of pro at mutant homomeric $\alpha 1$ GlyRs showing effects on the 4-cpro HA site modulation. Increasing pro concentrations were pre-applied to EC₂₀ concentrations of Gly. Pro effects on the current responses were measured by TEVC.

We started the investigation by measuring of pro effects on the function of $\alpha 1$ GlyRs carrying a Ser296Ala amino acid substitution in the M3. This mutation abolished HA potentiation by 4-cpro likely due to a missing hydrogen bond between the Ser296 side chain and the OH-group of 4-cpro (chapter 2). Interestingly, the OH-group is also an important molecular determinant for the subtype specific endocannabinoids modulation in GlyRs (Xiong et al. 2011). As shown in figure 1B, a pro HA and LA potentiation is evident at $\alpha 1$ Ser296Ala GlyRs indicating that a hydrogen bond between the Ser296 side chain and the OH-group of pro might not contribute significantly to pro binding. Maximum fold change in current was significantly reduced down to 0.39 ± 0.03 fold (compared to 0.56 fold at wt; $n = 5$, $P < 0.05$) whereas the EC₅₀ value of 195 ± 18 nM reflected perfectly the wt template value (176 nM). Concerning the LA site, affinity and efficacy of the potentiation reflected the wt $\alpha 1$ GlyR values perfectly (Fig. 1B). No direct activation was observable.

Next we analyzed pro effects on $\alpha 1$ GlyRs carrying the M3 Phe293Ala and M4 Phe402Ala substitution. Strikingly, HA potentiation by pro was abolished at $\alpha 1$ Phe293Ala GlyRs whereas the LA potentiation was evident (Fig.1A, B). Pro LA site potentiation was significantly different compared to wt $\alpha 1$ GlyRs. A right shift in the

EC₅₀ up to $1454 \pm 180 \mu\text{M}$ ($n = 4-8$; $P < 0.001$) and a decrease in the maximum fold change down to 1.9 ± 0.1 ($n = 4-8$; $P < 0.01$; Fig. 1B) is present at these mutated $\alpha 1$ GlyRs. Again, no direct activation by pro was observable.

At the $\alpha 1$ Phe402Ala substitution a pro HA inhibition was evident (Fig. 1A, B). The IC₅₀ was $610 \pm 91 \text{ nM}$ and the maximum current inhibition was 0.3 ± 0.07 fold. In contrast, LA potentiation was evident with an EC₅₀ of $752 \pm 43 \mu\text{M}$ reflecting the wt $\alpha 1$ GlyR value. The efficacy was significantly reduced down to 2.1 ± 0.5 ($n = 5$; $P < 0.05$). Again, no direct activation by pro was observable.

At the $\alpha 1$ Val289Ala substitution we observed a weak but significant reduction in the maximum fold change in current of the HA site potentiation. The value was reduced down to 0.39 ± 0.05 ($n = 5$; $P < 0.05$; Fig. 1B). Concerning the LA potentiation, we observed a slight but significant left shift in the EC₅₀ value down to $440 \pm 28 \mu\text{M}$ ($n = 5$; $P < 0.01$) and an maximum fold change in the current of 2.5 ± 0.7 (Fig. 1B).

Pro HA potentiation was not affected by the Leu292Ala substitution but a massive significant right shift in the LA EC₅₀ up to $2724 \pm 450 \mu\text{M}$ ($n = 7$; $P < 0.001$) and a significant decrease in the maximum fold change in current down to 1.9 ± 0.2 compared to wt $\alpha 1$ GlyR values was observable ($n = 7$; $P < 0.01$; Fig. 1B). Again no direct activation was observable. All values are summarized in table 1.

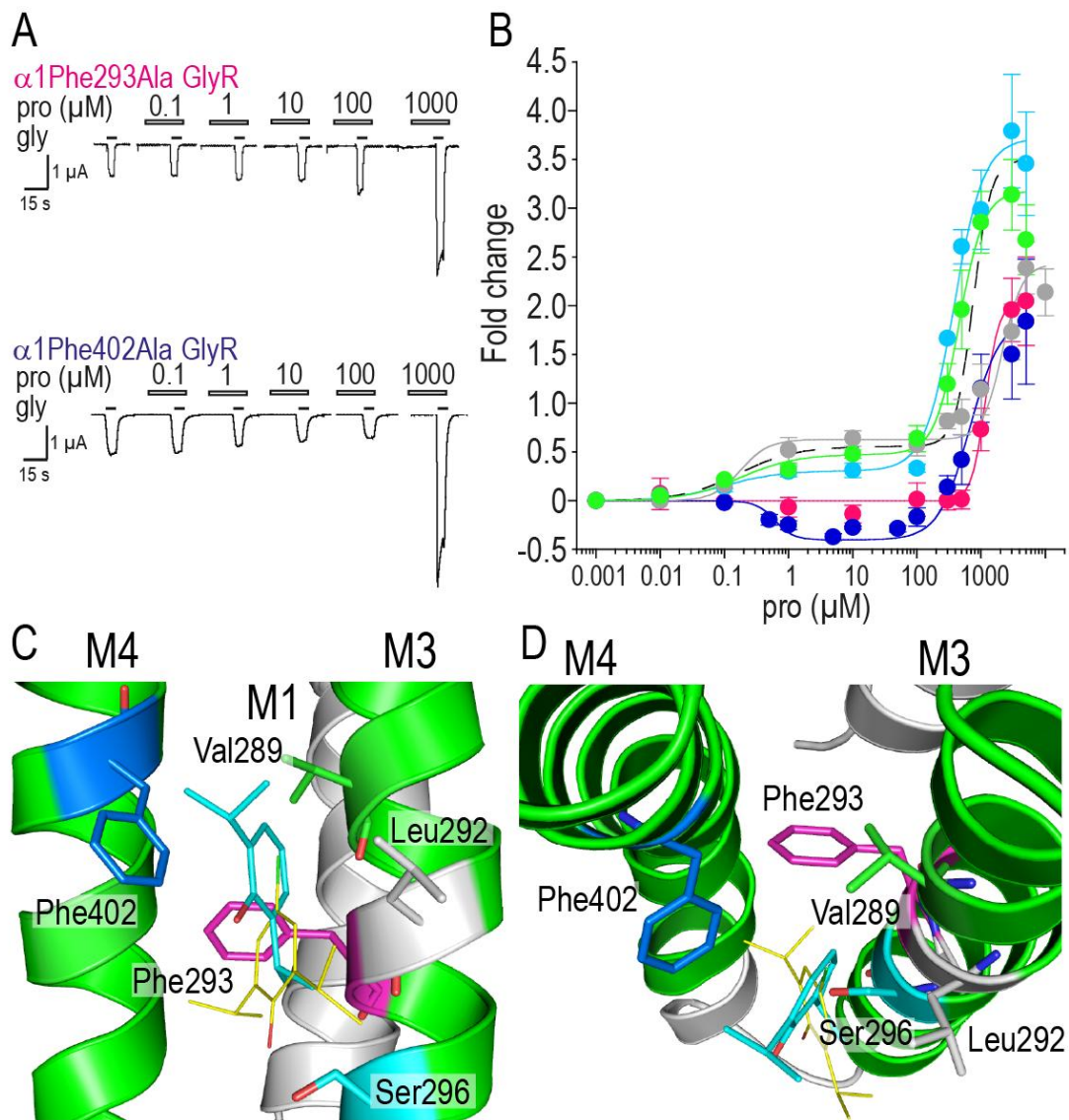


Figure 1: Analyses of pro effects at 4-cpro sensitive $\alpha 1$ GlyR mutants and docking of pro to the 4-cpro intrasubunit HA site. **A.** Recordings from oocytes showing a dose dependent LA potentiation by pro of the EC₂₀ Gly-evoked currents at $\alpha 1$ Phe293Ala (top panel) GlyRs and a dose-dependent HA inhibition and LA potentiation at Phe402Ala (bottom panel) GlyRs. **B.** Averaged fold change in current (mean \pm S.E.M. of 4 oocytes, respectively) caused by pM to mM molecule concentrations of pro (colored with the following code: green filled circles Val289Ala, grey filled circles Leu292Ala, magenta filled circles Phe293Ala, cyan filled circles Ser296Ala and blue filled circles Phe402Ala, dashed line indicates pro modulation obtained from chapter 2). **C.** Side view from the membrane showing pro (cyan) and 4-cpro (yellow) location and orientation in the HA site. Investigated M3 and M4 residues are named and colored following the code explained in the legend of figure 1. **D.** View from the extracellular space showing pro's OH-group orientation towards the membrane.

Concerning these results, we docked pro into the 4-cpro HA site identified by us (chapter 2). We used the GOLD program for optimizing the orientation of the molecule. Pro, stably integrates between the aromatic residues M4 Phe402, M3

Phe293 and the M3 Ser296 (Fig.1C, cyan molecule). Remarkably, this pro specific orientation prevents a hydrogen bonding with the Ser296 side chain which is an essential interaction for the presence of the 4-cpro HA site modulation (Fig. 1C and D, cyan vs. yellow molecule).

In summary, pro HA site modulation is affected at $\alpha 1$ GlyRs carrying amino acid substitutions in their 4-cpro HA binding site. Massive changes in the pro HA modulation were observable at the Phe293Ala (no modulation) and Phe402Ala (inhibition) substitution. In contrast, LA site potentiation was present at all investigated substitutions. Subsequent docking to and optimization of pro orientation in the 4-cpro HA site by GOLD, unmasked hydrophobic contacts between pro and the investigated amino acids.

Pro LA potentiation suppresses IVM potentiation; indication for overlapping binding sites

As shown previously, amino acids located in the Gly- and GABA_(A)Rs TMD interface of adjacent subunits mediate pro effects at pLGICs (Bali and Akabas, 2004; Li et al., 2010; Lynagh and Laube, 2014; Yip et al., 2013). Previously published studies characterized the M3 Ala288 residue as an important molecular determinant for the allosteric modulation of $\alpha 1$ GlyRs. Substitution to an isoleucine (Ile) eliminate the chloride current potentiation by volatile anesthetics and pro concentrations whereas the substitution to an phenylalanine (Phe) eliminated IVM effects (Lynagh and Laube, 2014; Lynagh et al., 2011). The fact that amino acid substitutions at this position abolished IVM and pro modulation suggests that the IVM and pro binding sites overlap (Fig. 2A). Thus, we sought to analyze if the presence of HA and LA modulation characteristic pro affect the IVM potentiation of the $\alpha 1$ GlyR function.

First, we measured modulation of the EC₂₀ Gly-evoked currents by a low, potentiating concentration of IVM (100 nM). After a 30s pre-application of IVM, EC₂₀ Gly-evoked currents were potentiated up to 0.21 ± 0.01 fold ($n = 4$, Fig. 2B). Co-application of 100 nM IVM and 1 μ M pro increased the EC₂₀ Gly-evoked currents nearly additive significantly up to 0.37 ± 0.01 ($n = 4$; $P < 0.01$; Fig. 2B). In contrast, 100 nM IVM suppressed significantly ($n = 4$; $P < 0.01$; Fig. 2B) the EC₂₀ Gly-evoked current potentiation by 1 mM pro down to 1.05 ± 0.015 fold.

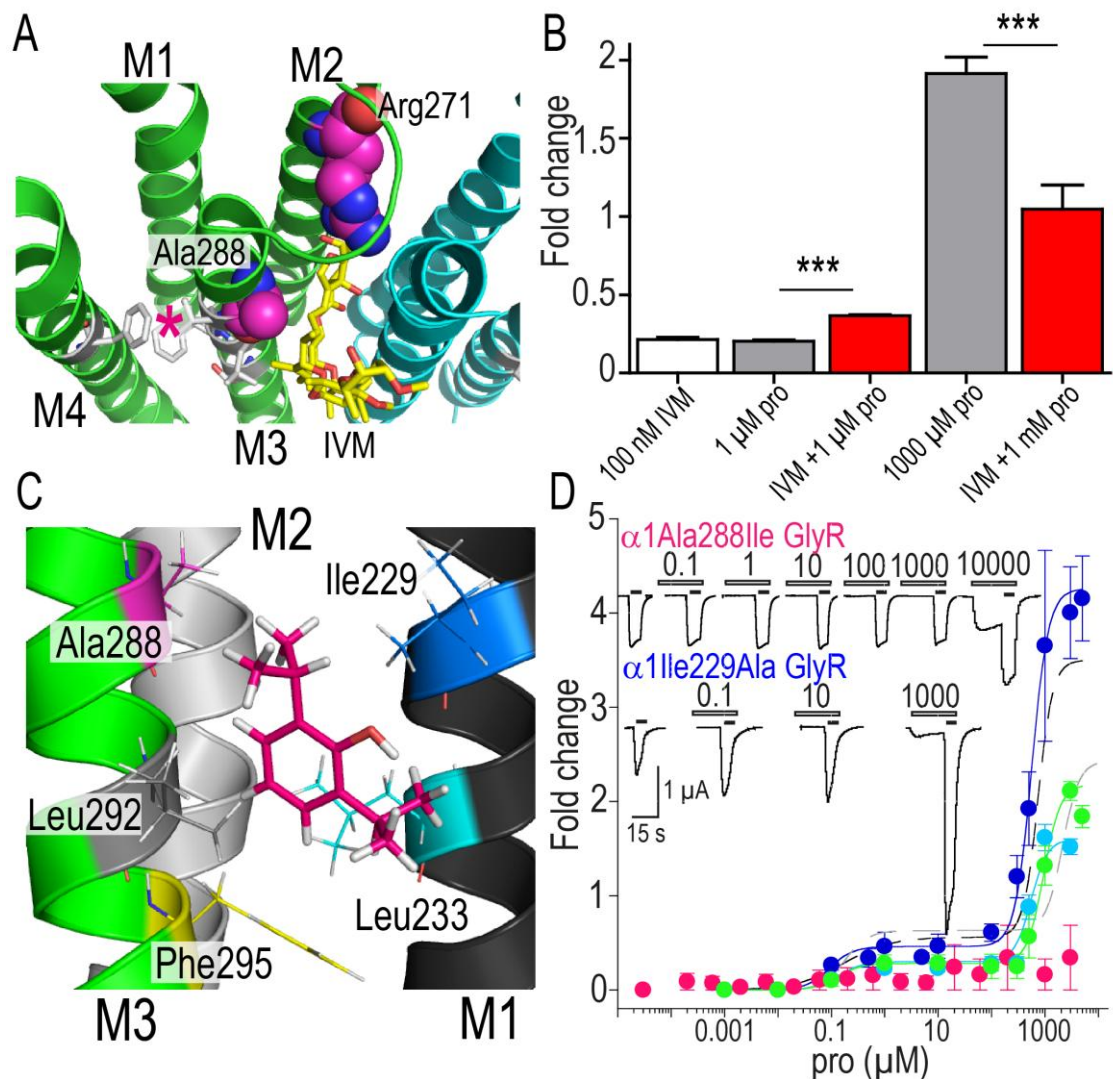


Figure 2: Analyses of IVM effects on the pro HA and LA modulation and docking of pro to the $\alpha 1$ GlyR TMD interface of adjacent subunits. **A.** Location of the IVM binding site in the $\alpha 1$ GlyR TMD interface. IVM is colored in yellow, the pro and 4-cpro HA site is indicated by a magenta colored star. M3 and M4 HA site residues are shown as sticks and colored in grey. Prominent interface residues Arg271 and Ala288 are shown as spheres and colored in magenta. **B.** Averaged fold change in current caused by 100 nM IVM (white filled bar) and pro alone (grey filled bars) as well as in co-application (red filled bars). Data are means \pm S.E.M. * $P < 0.05$, ** $P < 0.01$, *** $P < 0.001$ compared to the respective Gly potentiation by pro alone; paired t-test. **C.** Side view of the computational docking of pro to the TMD interface. Two subunits were colored in green (M3) and black (M1). Amino acids identified by the docking are colored with the following code: blue Ile229, cyan Leu233, magenta Ala288, grey Leu292, yellow Phe295. **D.** Averaged fold change in current (mean \pm S.E.M.) caused by pM to mM concentrations of pro (colored by the code from **C**, black dashed line shows wt $\alpha 1$ modulation from figure 1). Insets represent traces of the pro modulation.

Based on the suppression of the IVM potentiation by the pro LA potentiation, we speculate that these two sites overlap. Following this idea, we computationally docked pro to the IVM binding site in our $\alpha 1$ GlyR homology model. The molecule

stably integrated into four of the five interfaces (purple molecule in Fig. 2C). In this pose, pro's hydroxyl group contacts the backbone carbonyl of Ile229 and is in close proximity to Leu233, Ala288, Leu292 and Phe295 (Fig. 2C).

This prompted us to unravel the role of the amino acids for pro's effects at $\alpha 1$ GlyRs. Except for Ala288, where we created the pro insensitive Ile substitution, Ala substitutions were investigated.

Firstly, substitutions related effects on the agonist activation were analyzed. Interestingly, only the $\alpha 1$ Ala288Ile substitution showed significant changes in the Gly activation properties compared to wt values. As shown in figure 3C, we observed a massive increase in the apparent affinity towards Gly (37 ± 4 vs. 139 ± 11 μ M (wt); $n = 8$, $P < 0.001$) and a decrease in the Hill coefficient (1.7 ± 0.17 vs. 2.3 ± 0.2 (wt); $n = 8$, $P < 0.001$). All values are summarized in the appendix.

Next, pro effects at the mentioned mutant $\alpha 1$ GlyRs was investigated. Consistent with a backbone interaction between pro and Ile229 (Fig. 2C), the Ala substitution has no effect on pro modulation. In contrast, the Leu233Ala substitution show an decrease in the maximum fold change in current by the LA potentiation from 3.1 ± 0.3 down to 1.2 ± 0.1 fold ($P < 0.001$). HA potentiation is not affected.

Reflecting and expanding the observations obtained by Lynagh and colleagues, pro did not induce any allosteric modulation of the Ala288Ile substitutions function. However, the presence of pro concentrations ≥ 5 mM evoked chloride currents during incubation phase indicating that the partial agonism is not affected by the substitution (Fig. 2C).

At the below Ala288 located Leu292Ala mutation, an increase in the LA EC₅₀ value from 685 ± 34 μ M up to 2.7 ± 0.5 mM ($n = 6$; $P < 0.001$) and a decrease in the maximum fold change in current of the LA potentiation from 3.1 ± 0.3 down to 1.8 ± 0.3 fold ($n = 6$; $P < 0.01$) was observable. Again, HA site potentiation is unaffected (Fig. 2C).

The phenyl side chain of Phe295 is also in close proximity to the pro molecule in this binding pose (Fig. 2C). When we tested pro modulation and partial agonism, we observed that HA potentiation is not affected, whereas the maximum fold change in current of the LA potentiation significantly reduced from 3.1 ± 0.3 down to 1.3 ± 0.2 fold ($n = 4$; $P < 0.01$; Fig. 2C). No direct activation was observable. All values are summarized in table 1.

Table 1: Pro modulation of $\alpha 1$ GlyR TMD mutants. Parameters for HA and LA modulation of mutant homomeric $\alpha 1$ GlyRs by pro (mutants are listed in left column). EC₅₀ and hill values were calculated for each of n oocytes with the monophasic Hill equation, mean \pm S.E.M. are given. For HA and LA modulation fold change represents the maximum effect on the EC₂₀ Gly-evoked current elicited by saturating concentrations, respectively.

Type	HA EC ₅₀ (nM)	Fold change	LA EC ₅₀ (μ M)	Fold change	n
wt	176 \pm 29	0.56 \pm 0.05	685 \pm 44	3.1 \pm 0.1	10
Ile229Ala	113 \pm 10	0.58 \pm 0.2	730 \pm 24	3.6 \pm 0.2	4
Leu233Ala	106 \pm 12	0.2 \pm 0.02***	510 \pm 22	1.2 \pm 0.1***	3
Ala288Ile	<i>nm</i>	<i>nm</i>	<i>nm</i>	<i>nm</i>	4
Val289Ala	101 \pm 34	0.38 \pm 0.05*	440 \pm 28*	2.5 \pm 0.4	4-5
Leu292Ala	175 \pm 55	0.64 \pm 0.08	2724 \pm 454***	1.9 \pm 0.2*	7
Phe293Ala	<i>nm</i>	<i>nm</i>	1454 \pm 118***	1.9 \pm 0.1**	4-8
Phe295Ala	96 \pm 6	0.6 \pm 0.1	670 \pm 10	1.3 \pm 0.2***	4
Ser296Ala	195 \pm 30	0.39 \pm 0.05*	608 \pm 44	3.1 \pm 0.3	4-6
Phe402Ala	610 \pm 91 ^{a***}	-0.3 \pm 0.07 ^{b***}	752 \pm 43	2.1 \pm 0.5*	6-8

Data are means \pm S.E.M. The respective Hill coefficients (nH) were between 0.7 and 1 for the HA modulation and between 1.3 and 2.8 for the LA modulation, respectively. ^a IC₅₀, ^b current inhibition, *nm* no modulation; **P* < 0.05, ***P* < 0.01, ****P* < 0.001 compared to EC₂₀ Gly concentrations, unpaired t-test.

In summary, the additive increase of the IVM potentiated Gly evoked currents by the pro HA potentiation suggests that the molecules exert their effects via distinct binding sites. However, the suppression of the IVM potentiated Gly evoked currents by the pro LA potentiation indicate that the molecules use similar molecular determinants. In line with this assumption are the results obtained by the computational docking of pro to the IVM site and the subsequent TEVC characterization. Except for the Ala288Ile substitution which showed only a partial agonism by pro, all mutants unravel primary changes in the pro LA site potentiation and partial agonism (Fig. 2C). Taken together, we consider that the pro LA site is located in the interface and overlaps with the IVM binding site. Notably all residues are conserved in each α GlyR subunit and therefore in a good accord with the identical LA potentiation of each GlyR subtype by pro.

The Ala288Ile substitution affects the gating of $\alpha 1$ GlyRs

As shown above, pharmacological indications are given which support the existence of a pro LA site in the TMD interface. However, the fact that $\alpha 1$ GlyRs carrying the Ala288Ile substitution showed also no pro HA site modulation is hard to understand if

two distinct binding sites exist. Concerning investigations by Yamakura and colleagues, we assume that the Ile substitution affects the allosteric modulation of $\alpha 1$ GlyRs in general (Yamakura et al., 1999).

To proof this assumption, we investigated if the function of $\alpha 1$ Ala288Ile GlyRs is modulated by the endocannabinoid AEA. As shown by us, AEA binds to the 4-cpro and pro HA site and interacts there directly with the Ser296 side chain which is located 8 amino acids below Ala288 (chapter 2)

For measuring AEA modulation, we used agonist concentrations equating to the EC₅ Gly following the procedures described by Xiong and colleagues (Xiong et al. 2011). Visual inspection revealed the presence of a dose dependent AEA potentiation of the EC₅ Gly-evoked chloride currents at wt $\alpha 1$ GlyRs (Fig. 3A, top traces). The AEA EC₅₀ value reached 7.8 ± 1.5 nM and a maximum fold change in current of 0.91 ± 0.2 is observable ($n = 7$; Fig. 3B). Saturation occurs in the presence of low μ M AEA concentrations. Next, we investigated AEA effects on $\alpha 1$ Ala288Ile GlyRs, but observed no AEA dependent changes to the EC₅ Gly ($n = 6$; Fig. 3A, B).

Based on the above shown increase in the apparent affinity of $\alpha 1$ Ala288Ile GlyRs towards Gly, we ask us if the substitution has additional effects on the activation of the GlyR. We therefore investigated the gating of the mutant by the low efficient partial agonist GABA (Fig. 3D).

At wt $\alpha 1$ GlyRs, we observed that 10 and 100 mM GABA evoked chloride currents with a strength of 1.5 ± 1 % (10 mM) and 12 ± 6 % (100 mM) compared to the I_{MAX} Gly induced by saturating concentrations (3 mM Gly). In the case of $\alpha 1$ Ala288Ile GlyRs, chloride currents evoked by 10 mM GABA reached 57 ± 10 % and by 100 mM GABA 87 ± 5 % compared to the I_{MAX} Gly induced by saturating concentrations (3 mM Gly; Fig. 3D). Statistical comparison with the respective wt values revealed that each activation of $\alpha 1$ Ala288Ile GlyRs by GABA is significantly increased ($n = 5$; $P < 0.001$; Fig. 3D).

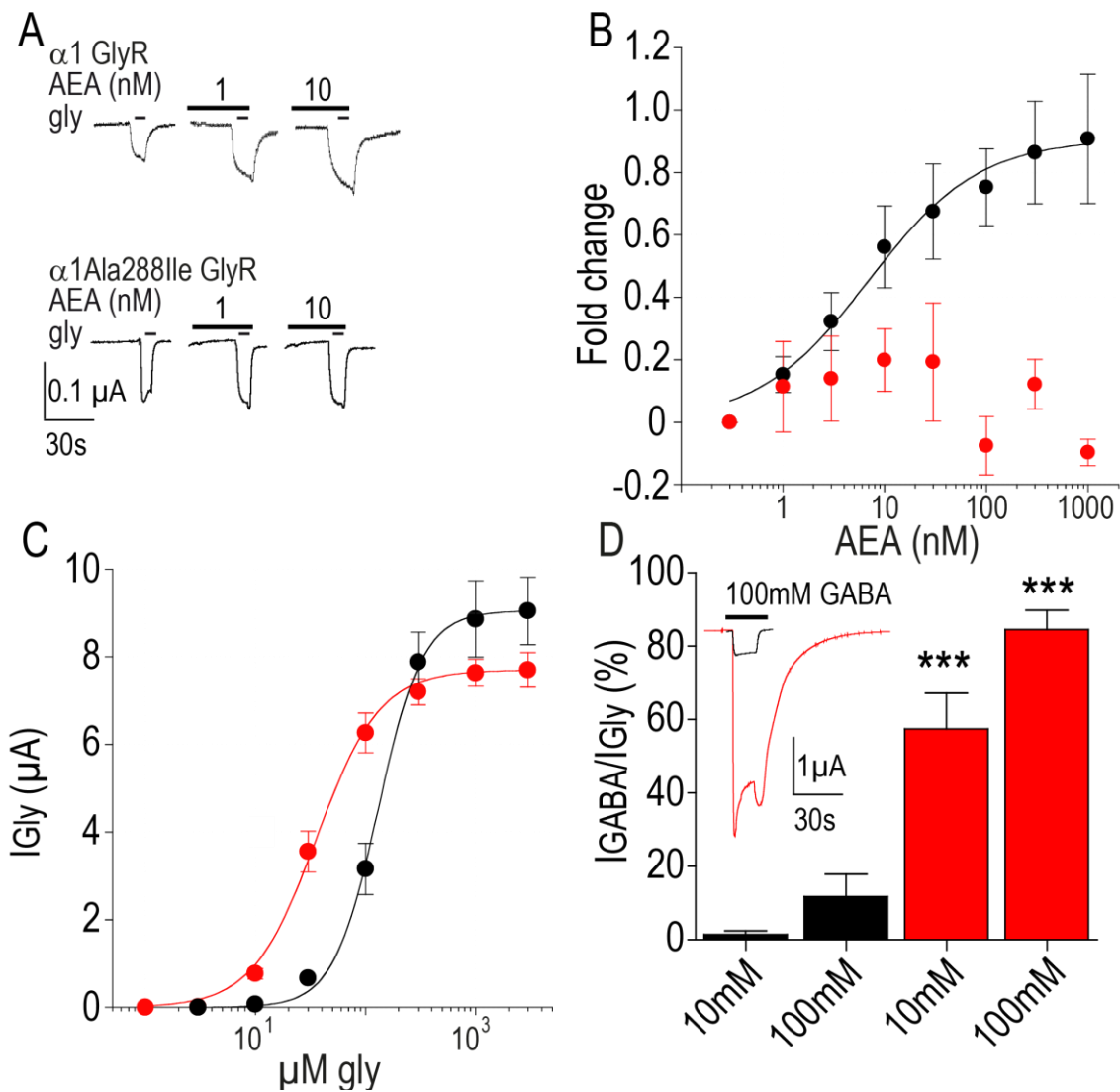


Figure 3: Analyses of AEA and GABA effects at $\alpha 1$ Ala288Ile GlyRs. **A.** Recordings from oocytes expressing wt (top) and $\alpha 1$ Ala288Ile (bottom) GlyR cRNA showing a different potentiation by AEA. **B.** Averaged fold changes (data mean \pm S.E.M.) in the Gly evoked currents caused by AEA (colored with the following code: black filled circles wt and red filled circles Ala288Ile GlyRs). **C.** Averaged changes in μ A (mean \pm S.E.M.) caused by Gly (colored with the following code: black filled circles wt, red filled circles Ala288Ile GlyRs). **D.** Averaged percentage activation by GABA compared to the IMAX Gly represented as a bar diagram (mean \pm S.E.M.) colored with the following code: black bars indicate wt, red bars Ala288Ile GlyRs. Inset show GABA (100 mM) evoked chloride currents from oocytes expressing wt (black) and $\alpha 1$ Ala288Ile (red) GlyR cRNA.

In summary, the endocannabinoid AEA did not affect the function of $\alpha 1$ Ala288Ile GlyRs. In addition, the efficacy of the partial agonist GABA at $\alpha 1$ Ala288Ile GlyRs is massively increased compared to wt $\alpha 1$ GlyRs. This phenomenon is characteristically for substitutions which affect the gating of an ion channel and can change the allosteric modulation by a molecule.

Competitive inhibition of pro's partial agonism by stry

As reported by Pistis and colleagues, stry abolish the partial agonism by pro at recombinant expressed $\alpha 1$ GlyRs (Pistis et al., 1997). However, no information exists about the exact type of inhibition. If a competitive inhibition of pro's partial agonism by stry exists, this would speak for the presence of a pro binding site in the ECD (Wyllie and Chen, 2007). Stry is the classical competitive antagonist of the GlyR and binds with high affinity in the same pocket as the agonist Gly (Grudzinska et al., 2005a).

First, we analyzed stry inhibition of the Gly activation at wt $\alpha 1$ GlyRs. The results are shown and summarized in the appendix. Next, direct activation by pro in the presence of 5 nM stry was analyzed. As shown in figure 4A the presence of stry induced a significant concentration dependent right shift of the pro DA EC₅₀ from 1.5 ± 0.1 mM up to 2.2 ± 0.2 mM (+1 nM stry; $P < 0.01$; paired t-test; $n = 7$), up to 4.4 ± 0.1 mM (+5 nM stry; $P < 0.001$; paired t-test; $n = 7$) and up to 10 ± 0.3 mM (+15 nM stry, $P < 0.001$; paired t-test; $n = 7$) without affecting significantly the I_{MAX} pro and Hill coefficients (Fig. 4A, B).

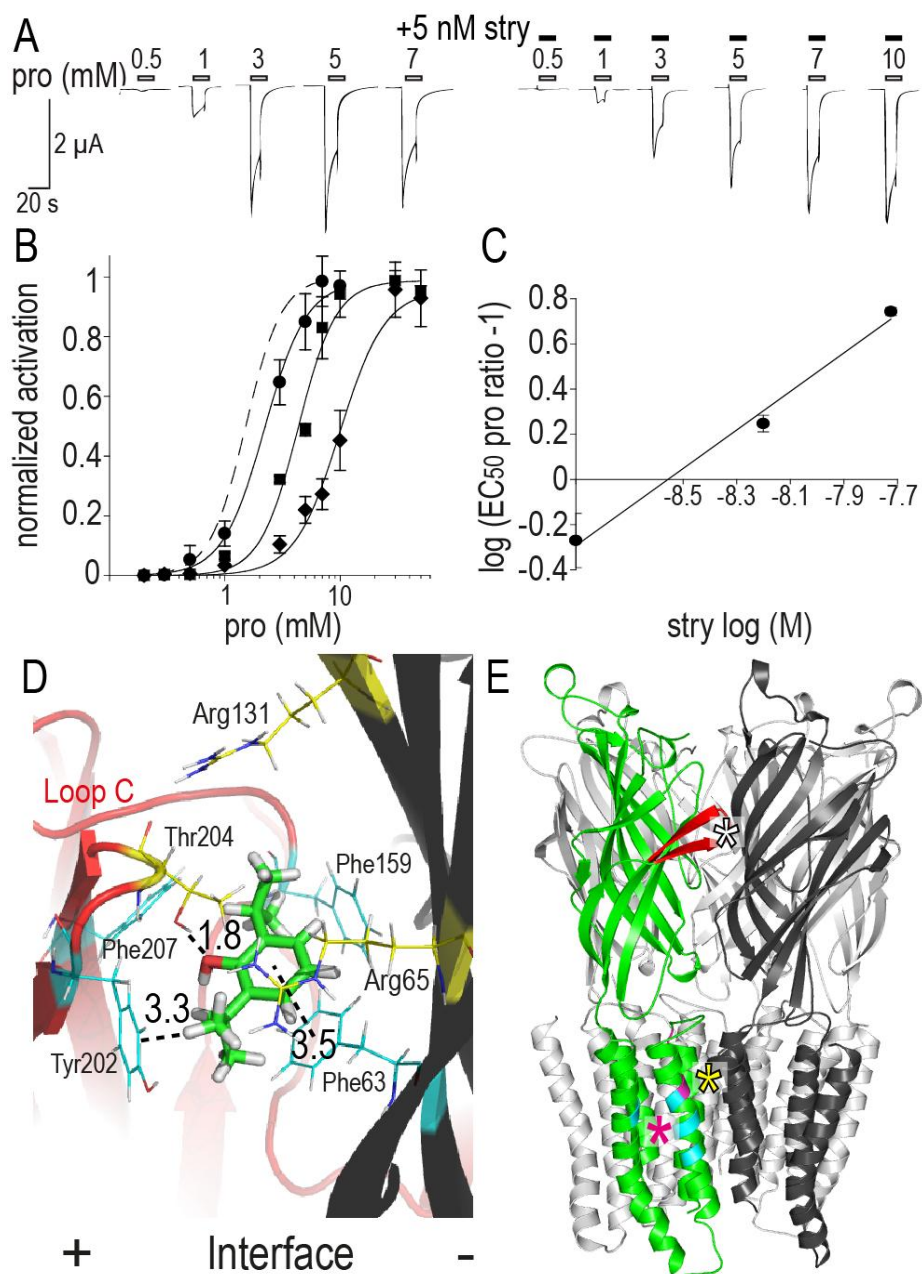


Figure 4: Competitive inhibition of the pro partial agonism by stry and subsequent docking of pro to the LBD. **A.** Example traces of pro partial agonism (right panel) and effects of the co-application of 5 nM stry (left panel). **B.** Averaged effect of stry co-applications to the partial agonism of homomeric $\alpha 1$ GlyRs by pro. Antagonist free activation is presented by a dashed line. Effects of 1- (filled circles), 5- (filled squares) and 15 nM stry (filled diamonds) on the direct activation are shown as dose response curves. Responses in the presence of stry were normalized to the respective I_{MAX} by pro. Each point represents mean \pm S.E.M. of 4 oocytes. **C.** Schild-plot analysis of the stry effects on the pro direct activation. Values were averaged and represent mean \pm S.E.M. of 5 oocytes, respectively. **D.** Side view from the - interface showing pro (green) location between loop C and the β -strand of the - interface. Molecule and residue distances between Phe63, Tyr202 and Thr204 were highlighted by dashed lines and presented in \AA . **E.** Overview of unmasked pro binding sites. Two subunits were colored in green and black. Pro HA site is marked with a magenta colored star; the LA site is marked with a yellow star and the DA site with a white star. Loop C is colored in red.

Based on the observed direct competition between stry and pro, we suggest that pro binds to a site located in the LBD. For a more precise localization of this site, we used in-silico docking of pro to the LBD of a $\alpha 1$ GlyR homology model based on the GluCl structure. We positioned five pro molecules outside of the LBD and ran free MD simulations. The most stable docking position of pro predicted from 50 ns MD simulation resulted in a ligand-receptor complex (Fig. 4D).

As illustrated in figure 4D, pro is bound in the interface of two adjacent subunits in close contact with amino acid side chains of Phe63, Arg65, Arg131, Phe159, Tyr202, Thr204 and Phe207 whose mutations have been shown to affect activation by Gly and inhibition by stry (Grudzinska et al., 2005b; Pless et al., 2011; Pless et al., 2008). Pro forms multiple π - π and cation- π stackings with the mentioned residues with binding length's between 1.8 to 3.5 Å.

In summary, stry induces a concentration dependent decrease of the pro DA EC₅₀ value without changing the maximum efficacy of the pro activation. By using the Schild-Gaddum equation, we quantified this effect as a direct competition between stry and pro. In silico docking of pro to the LBD, support this finding. Therefore, we assume that the partial agonism by pro is mediated by a pro binding site in the LBD.

HA and LA potentiation enhances distinct parameters of the $\alpha 1$ GlyR activation

As shown by O`Shea and colleagues 500 μ M of pro increases the apparent affinity of homomeric $\alpha 1$ GlyRs towards Gly (O'Shea et al., 2004). We asked us if comparable effects on the Gly activation by the HA site potentiation exist and repeated the experiment by using 10 μ M pro. As a control we determined the effects by 500 μ M pro on the Gly activation and observed a similar change on the apparent affinity towards Gly like O'Shea (Fig. 5A inset). The initial EC₅₀ for Gly ($148 \pm 6 \mu$ M, black squares) significantly increased up to $39 \pm 2 \mu$ M in the presence of 500 μ M pro ($n = 5$; $P < 0.001$, paired t-test; Fig. 5A inset). 10 μ M pro also increased the apparent affinity towards Gly from $148 \pm 6 \mu$ M to $138 \pm 9 \mu$ M but not significantly. Each situation significantly increased the cooperativity from 2.0 ± 0.1 up to 2.4 ± 0.1 ($n = 6$, respectively; $P < 0.001$, paired t-test; Fig. 5A inset) but did not affect the efficacy of the agonist (Fig. 5A).

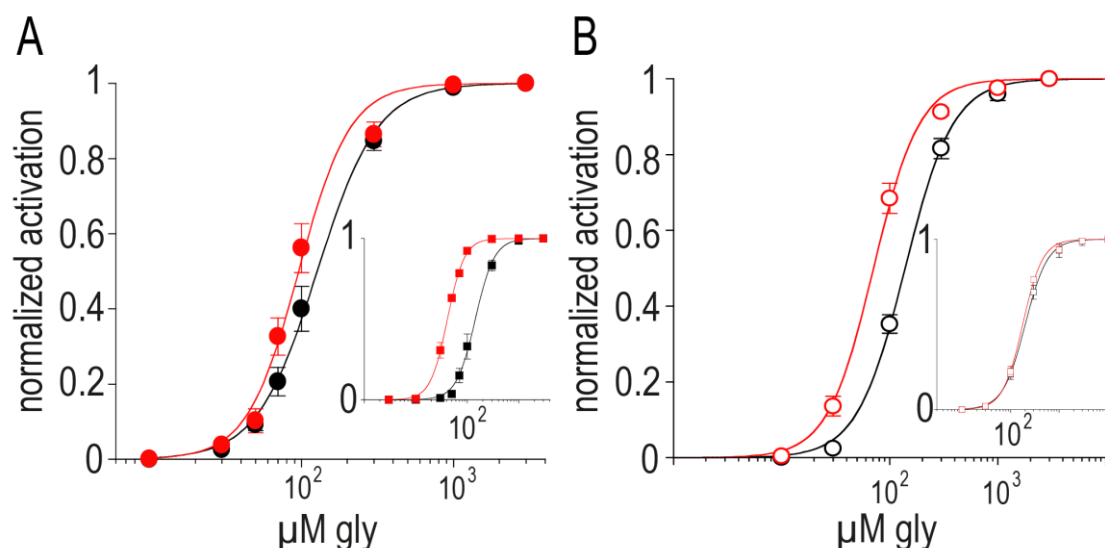


Figure 5: HA and LA modulation of pro increases the apparent affinity towards Gly and depends on the used agonist concentration. A. Concentration depend activation of $\alpha 1$ GlyRs by Gly alone (black symbols) and in the presence of 10 μM and 500 μM (inset) pro (red symbols). Pro increases the affinity of $\alpha 1$ GlyRs towards Gly without affecting the slope of the activation. Values are mentioned in the result section. Here and in **B.** each data point represents mean \pm S.E.M. of 5 to 6 oocytes. Inset shows the Gly activation in the absence (black squares) and after a 30 s long pre application of 500 μM pro (red squares). **B.** Activation of $\alpha 1$ Phe293Ala GlyRs by Gly in the absence (open black symbols) and presence of 500 μM (inset) and 1000 μM pro (open red circles) indicating a weak increase of the apparent affinity towards Gly (values are mentioned in the result section). Inset shows the Gly activation in the absence (open black squares) and presence of 500 μM pro (open red squares).

To clarify if the pro HA potentiation only enhances the cooperativity of the Gly activation, we analyzed the effects of pro on the Gly activation of $\alpha 1$ Phe293Ala GlyRs. As shown above, pro HA modulation is abolished at these $\alpha 1$ GlyRs (Fig. 1B). If the enhancement of the cooperativity indeed base on the pro HA potentiation, no comparable effect on the Gly activation should be observable at this pro HA modulation insensitive mutation.

We first analyzed the effects of 10 and 500 μM pro on the Gly activation of $\alpha 1$ Phe293Ala GlyRs and observed no changes in the parameters of the Gly activation (Fig. 5B inset). We increased the pro concentration up to 1 mM for analyzing the effects of a LA site potentiation characteristic concentration. In the presence of 1 mM pro the apparent affinity of $\alpha 1$ Phe293Ala GlyRs towards Gly increased from $188 \pm 10 \mu\text{M}$ up to $72 \pm 5 \mu\text{M}$, significantly ($n = 5$; $P < 0.001$, paired t-test; Fig. 5B). No change to the cooperativity is observable. All values are summarized in table 2.

Table 2: Pro HA and LA effects on the EC50 Gly. EC50 and nH values were calculated for each of n oocytes with the monophasic Hill equation, and mean \pm S.E.M. are given.

GlyR type	EC50 Gly (μ M)	nHill	IMAX gly (μ A)	n
wt	148 \pm 19	2.0 \pm 0.1	5.6 \pm 0.5	6
+10 μ M pro	131 \pm 16	2.4 \pm 0.1***	5.4 \pm 0.6	6
+500 μ M pro	39 \pm 2***	2.4 \pm 0.1***	5.7 \pm 0.5	6
Phe293Ala	188 \pm 10	2.1 \pm 0.1	4.9 \pm 0.5	5
+10 μ M pro	182 \pm 8	2.1 \pm 0.1	4.9 \pm 0.4	5
+500 μ M pro	178 \pm 2	2.1 \pm 0.1	4.7 \pm 0.6	5
+1000 μ M pro	72 \pm 5***	2.1 \pm 0.1	4.6 \pm 0.4	5

Gly activation in the presence of 10, 500 and 1000 μ M pro at wt and α 1 GlyRs carrying the M3 Phe293Ala substitution. Data are means \pm S.E.M.; * P < 0.05, ** P < 0.01, *** P < 0.001 compared to the respective Gly activation in the absence of pro, paired t-test.

In summary, the pro HA and LA potentiation affect distinct parameters of the Gly activation. Whereas the pro LA potentiation, increases the apparent affinity HA potentiation enhances the cooperativity. This assumption is underlined by pro's effects on the Gly activation of α 1Phe293Ala GlyRs. At these HA site modulation absent α 1 GlyRs no change in the cooperativity was observable whereas pro concentrations inducing a LA site potentiation increase the apparent affinity of these GlyRs towards Gly. These results suggest the presence of distinct mechanisms by which pro potentiated the function of GlyRs.

The formation of a HA potentiation depends on the used Gly concentration

As reported above, pro HA site potentiation increases the cooperativity of the α 1 GlyR activation by Gly. Interestingly, visual inspection of the dose response curves in figure 5A indicates that the pro HA potentiation is only in the presence of Gly concentrations above the EC10.

This would suggest that the formation of a HA potentiation is also linked to the amount of occupied Gly binding sites in the ECD. If so, this could explain why several other investigations did not observed a biphasic potentiation of α 1 GlyRs by pro because of the low Gly concentrations used in these studies (Ahrens et al., 2004; Ahrens et al., 2008b; Pistis et al., 1997). That the strength of the agonist activation

determines the formation and type of an allosteric modulation is known at GlyRs for endocannabinoids (Xiong et al., 2011). As reported by us, the endocannabinoid and HA binding site for pro and 4-cpro overlap which makes it in our eyes conceivable that these drugs also share specific effects and features at GlyRs (chapter 2). To proof this assumption, we investigated pro modulation of EC₁₀ Gly-evoked currents (Fig. 6A, B).

Indeed, only a monophasic potentiation of the EC₁₀ Gly-evoked currents with an EC₅₀ value of $571 \pm 50 \mu\text{M}$ ($n\text{H} = 3.1 \pm 0.2$) was observable reflecting the corresponding LA EC₅₀ value ($685 \pm 34 \mu\text{M}$) of the EC₂₀ Gly potentiation by pro. The maximal fold change in current was significantly increased compared to the corresponding EC₂₀ Gly value and reached 8.1 ± 0.5 fold ($n = 4$; $P < 0.001$; Fig. 6B).

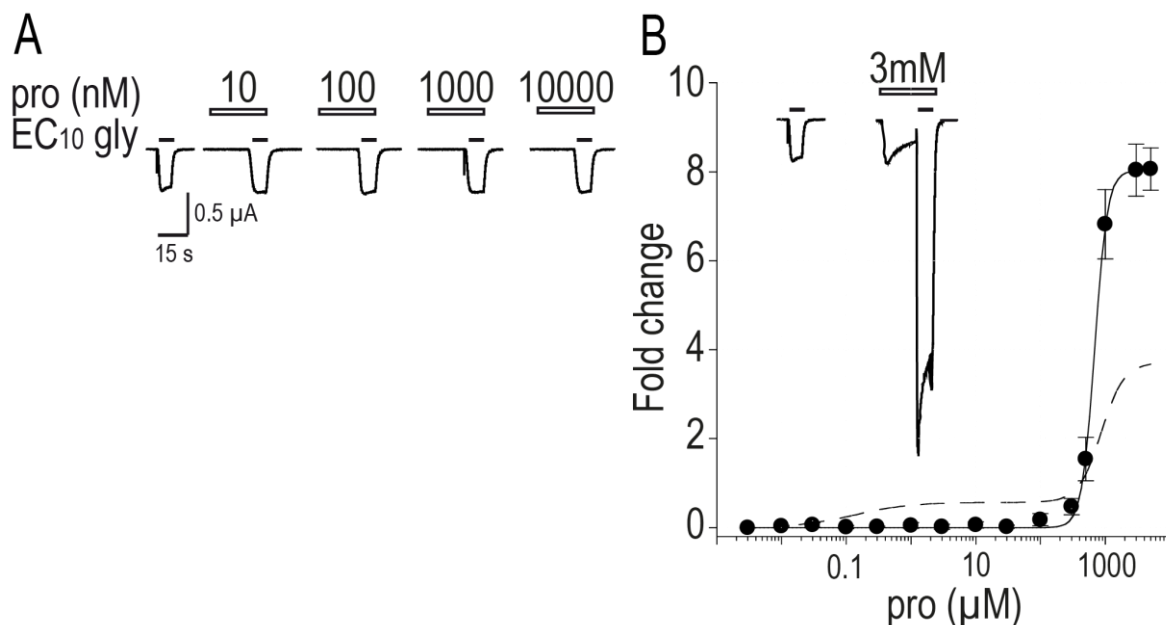


Figure 6: Pro HA and LA modulation depends on the used agonist concentration. **A.** Example traces showing the absent pro HA modulation of EC₁₀ Gly-evoked chloride currents. **B.** Monophasic EC₁₀ Gly-evoked current potentiation by pro (white filled circles). Inset shows the LA potentiation of the EC₁₀ Gly-evoked chloride current and direct activation by 3 mM pro.

In summary, EC₁₀ Gly-evoked currents were not potentiated by the HA site. The EC₅₀ value of the monophasic potentiation reflects perfectly the corresponding pro LA site value of the EC₂₀ Gly-evoked current potentiation. However, the EC₁₀ Gly-evoked current potentiation by pro is more efficient as the EC₂₀ Gly-evoked current potentiation. We therefore conclude that the strength of the Gly activation is important for the formation of a pro HA site potentiation and for the efficiency of the LA site potentiation

Conclusions

In this study, we investigated pro effects at wt and mutated $\alpha 1$ GlyRs. We observed that pro HA site modulation is affected at $\alpha 1$ GlyRs carrying amino acid substitutions in their 4-cpro HA binding site. In contrast, LA site potentiation was present at all investigated substitutions. Subsequent docking of pro into the 4-cpro HA site supported our results obtained by TEVC and unmasked hydrophobic contacts between pro and the investigated amino acids. Taken together the results proof that the pro and 4-cpro HA sites overlap but the molecules bind with distinct orientations in this site.

Concerning the pro LA site, we observed that the LA site potentiation suppresses the IVM potentiation indicating that the molecules share the same binding site. In line with this assumption are the results obtained by the computational docking of pro to the IVM site which is formed by amino acids of the M3 and M1 of adjacent subunits. TEVC characterization combined with site-directed mutagenesis of pro contacting residues, identified by computational docking revealed clear deteriorations in the parameters of the pro LA site modulation and partial agonism. In the case of $\alpha 1$ Ala288Ile GlyRs, no pro HA and LA modulation was observable but a partial agonism is evident.

We also observed that the endocannabinoid AEA, which binds to a distinct protein region, did not affect the function of $\alpha 1$ Ala288Ile GlyRs. In depth analysis reveal that the efficacy of the partial agonist GABA at these $\alpha 1$ GlyRs is massively increased compared to wt $\alpha 1$ GlyRs. This phenomenon is characteristically for a change in the gating behavior of an ion channel. These observations clearly show that the substitution affects massively the activation and transduction process in the GlyR.

Concerning the partial agonism by pro, we observed a competitive inhibition of pro's partial agonism by stry. By using the Schild-Gaddum equation we clarified that a linear dependency between the stry concentration and the change in the apparent affinity of pro exists which can be interpret as a classical competition between the molecules. Therefore direct evidence are given that the partial agonism by pro is mediated by a binding site localized in the LBD.

Moreover, we observed that the HA and LA site potentiation induces distinct effects on the Gly activation. Whereas the LA site potentiation increases the apparent affinity, pro HA site potentiation enhances the cooperativity. Finally, we unmasked that the formation of a HA site potentiation depends on the used Gly concentration.

These results suggest the presence of distinct mechanisms by which the pro HA and LA potentiation affect the function of $\alpha 1$ GlyRs and unravel for the first time the existence of functional multiple binding sites for pro at $\alpha 1$ GlyRs.

Discussion

HA and LA potentiation by pro is mediated via distinct binding sites in the TMDs

As shown in chapter 2, three distinct effects of 4-cpro and pro at homo- and heteromeric GlyRs were found: i) a HA modulation by nM to μ M, ii) a LA potentiation in by μ M to mM and iii) a direct activation by μ M to mM molecule concentrations. In this study, we unmasked that the general anesthetic pro binds to three distinct sites at homomeric α 1 GlyRs. We used detailed electrophysiological, computational and pharmacological analysis to determine the exact location of these sites and observed that the sites responsible for the allosteric HA and LA modulation are located in the GlyR TMDs whereas the site responsible for the partial agonistic activity is located in the LBD.

Our data also eliminates the possibility, that the HA and LA potentiation can be mediated by a single site. We observed several points speaking against this idea: Firstly, the increase of the IVM potentiation by the pro HA site. If distinct positive allosteric modulators (PAMs) behave in this way, the PAMs develop their efficacies via distinct sites. If the opposite effect exists, which is observable between the IVM and LA potentiation, their sites eventually overlap. Secondly, the potentiation by each site has distinct effects on the Gly activation. Whereas HA potentiation affects the cooperativity, LA potentiation increases the apparent affinity of the GlyR towards Gly. That a change in the cooperativity is a HA site related effect was validated by the use of the α 1Phe293Ala GlyRs. At this substitution HA potentiation by pro and related effects are abolished. Changes in the activation properties like an increase in the apparent affinity of the receptor towards full and partial agonists are typical for allosteric modulators (Kirson et al., 2012). An increase in the apparent affinity by an allosteric modulator, primary bases on an improvement of the signal transduction process within the receptor and not by an improved binding of the agonist in its site. Depending on the location of the modulator binding site, structural rearrangements in specific parts of the protein improved specific parameters of the transduction process (Colquhoun, 1998; Csermely et al., 2013; Del Sol et al., 2007; del Sol et al., 2009; Martin et al., 2000; Nussinov, 2012; Sauguet et al., 2014; Szilagyi et al., 2013; Tsai et al., 2009).

By the fact that we observed site specific effects on the Gly activation, we conclude that pro induces these effects by the occupation of distinct sites. Thirdly, we observed that the formation and efficacy of the HA and LA potentiation depend on the used Gly concentration. EC₁₀ Gly evoked currents were not HA potentiated but stronger enhanced by the LA site potentiation. We see in these phenomenons's site specific effects comparable to the Gly dependency of the endo- and cannabinoid modulation at GlyRs (Xiong et al., 2011; Xiong et al., 2012).

Moreover, this important fact for observing the pro HA modulation could explain why this dualistic modulation has been overlooked till yet. Regarding the literature, used agonist concentrations to describe pro effects at GlyRs were below the EC₂₀ (Ahrens et al., 2004; Ahrens et al., 2008a; Ahrens et al., 2008b; Pistis et al., 1997).

Based on these observations, we conclude that the HA and LA potentiation of α 1 GlyRs by pro is mediated via the action of two distinct binding sites. Such biphasic modulation is reminiscent of the action of zinc, which mediates a HA and LA modulation by distinct binding sites (Laube et al., 2000; Laube et al., 1995). Our assumption of distinct binding sites for pro within the TMDs of GlyRs is also consistent with recent findings reporting the existence of multiple binding pockets for anesthetic compounds at several pLGICs (Hamouda et al., 2011; Jayakar et al., 2013; Spurny et al., 2013). At nAChRs for example, three distinct sites in the TMDs were labeled by the photoreactive pro analogue azi-pm (Jayakar et al., 2013). One site is located in the channel pore, the second site in the TMD, between two adjacent subunits and the third site within the 4-helical bundle of one subunit.

Pro binds to the intrasubunit 4-cpro HA site between the M3 and M4

The physicochemical properties characterized pro as highly lipophilic and recently published investigations unmasked that allosteric effects by pro based on interactions with the lipid embedded TMDs of the GlyRs and other pLGICs (Chiara et al., 2014; Duret et al., 2011; Reiner et al., 2013a; Reiner et al., 2013b; Yip et al., 2013). We identified recently an deep buried intrasubunit HA binding site for 4-cpro build by non- and conserved TMD amino acids of the M3 and M4. The results obtained in this study, clearly support the assumption that pro binds to this 4-cpro HA binding site. Therefore speaks the results obtained by the TEVC analysis of pro effects at α 1 GlyRs carrying amino acid substitutions in their 4-cpro HA site.

Comparison of the pro and 4-cpro orientation in this site unmask clear differences. As shown in figure 1C, pro's OH group points towards the lipid protein interface equating to a 90° change in the orientation of this group compared to 4-cpro. Remarkably, this pro specific orientation prevents a hydrogen bonding with the Ser296 side chain which is an important polar interaction for the 4-cpro HA site modulation in $\alpha 1$ GlyRs (chapter 2).

We also characterized the M3 Phe293 residue as absolutely essential for the presence of a HA modulation by pro and 4-cpro. The residue is located in the middle of the HA site. Ala substitution of Phe293 abolishes pro and 4-cpro HA modulation at $\alpha 1$ GlyRs suggesting that an aromatic interaction between the residue and the molecules exist. Such aromatic interactions between proteins and bioactive molecules are common binding motifs (Dougherty, 2007; McGaughey et al., 1998; Pless et al., 2011; Pless et al., 2008).

Interestingly, HA modulation by pro depends on the presence of an additional, conserved aromatic residue named Phe402 which is located in the M4. Elimination of the aromatic side chain converts pro potentiation into an inhibition. The fact that the mutagenesis of aromatic residues of the M3 and M4 affects only the HA site modulation suggests that the aromatic network between the GlyR TMDs is involved in the HA modulation of $\alpha 1$ GlyRs by pro and 4-cpro. Further analysis including isofunctional substitutions at the M3 Phe293 and M4 Phe402 position and the remained aromatic residues should gain more information about the involvement of the aromatic network in the HA site modulation.

The pro LA site is located in the TMD interface of adjacent subunits

Concerning the pro LA site we can present data that clearly point out the involvement of the TMD interface. Moreover, we can assume that pro binds to IVM site. This is supported by the observations that the IVM potentiation is suppressed by the LA site potentiation. However, we want to note that we have measured only an apparent competition between IVM and LA site characteristic pro concentration. Sadly, the fluent transition between IVMs allosteric modulation and partial agonism is hard to control which makes the pharmacological verification of this theory extremely challenging (Lynagh and Lynch, 2010; Lynagh et al., 2011; Wang and Lynch, 2012). By using non activating derivatives of IVM, like selamectin it should be possible to clarify this thesis (Lynagh et al., 2011).

However, we speculate that the IVM and pro LA site overlap and that the M3 Ala288 residue is part of the pro LA site. As shown by Lynagh and colleagues, substitutions of Ala288 affect the pro and IVM mediated effects at $\alpha 1$ GlyRs (Lynagh and Lynch, 2010; Lynagh et al., 2011).

Based on the dockings of pro into the IVM site and following electrophysiological characterization of nearby residues (distance to pro ≤ 4 Å) we can present additional pro LA site determinants. All substitutions did not affect the pro HA potentiation but decreased the potency (Leu292Ala) and efficacy (Leu233Ala, Phe295Ala) of the pro LA site potentiation.

That the TMD interface is an important structure for the action of several allosteric modulators at GlyRs was shown by several investigations (Belelli et al., 1999; Li et al., 2010; Lobo et al., 2006; McCracken et al., 2010).

Due to the absent pro modulation at $\alpha 1$ GlyRs carrying the Ala288Ile substitution, we are convinced that residue is also central molecular determinant for the function of the GlyR. This idea is underlined by the fact that the substitution affects the gating of the channels which is clearly shown by the increase in the efficacy of the partial agonist GABA. We speculate that this effect eventually masked or eliminates the HA potentiation. Further analysis targeting this idea should clarify this assumption. However, in line with this suggestion that the residue is important for the general function of the GlyR are the observations by Mowrey and colleagues. They unravel the role of the Ala288 residue in the transduction process where it mediates the opening of the channel upon binding of Gly. Ala288 acts like a hinge for the movement of the above located M2-M3 linker that pulls the M2 and M3 simultaneously backward, securing the opening of the pore (Du et al., 2015; Mowrey et al., 2013). Interestingly, the amino acid substitution Met286Trp in the GABA_(A)R $\beta 2$ and 3 subtype which corresponds to the M3 Ala288 residue in α GlyRs results in pro insensitive GABA_(A)Rs (Krasowski et al., 2001). In the case of the nematode GluCl_s, the corresponding residue Gly329 is also important for the pro modulation (Lynagh et al., 2014). Taken together, these observations show that the M3 288 position is a direct determinant for the pro modulation in GlyRs and at other pLGICs.

Remarkably, increasing of the side chain hydrophobicity and especially the use of an Ile at the Ala288 position has dramatic effects on the action of several allosteric modulators at $\alpha 1$ GlyRs. As shown by Yamakura and colleagues, allosteric modulation by volatile anesthetics is lost at $\alpha 1$ Ala288Ile GlyRs (Yamakura et al.,

1999). Here, we can present with AEA another substance class which is ineffective at $\alpha 1$ GlyRs carrying the Ala288Ile substitution. As shown by Xiong and colleagues, the AEA binding site is in the vicinity of the M3 residue Ser296 (Xiong et al., 2012).

Pro induced chloride currents by binding to a site in the LBD

Allosteric modulators like pro are thought to act primarily on pLGICs at binding sites located in the TMDs. Thus modulation and partial agonism of pro at GlyRs may be explained by a common site similar to the action of IVM at GlyRs. IVM mediates potentiation of Gly evoked chloride currents as well as direct activation of the receptor upon binding to a site located in the TMD interface between adjacent subunits (Lynagh and Lynch, 2012a; Lynagh and Lynch, 2012b). However, based on the competitive effect of stry on the pro partial agonism, in stark contrast to the absence of competition between stry and IVM, our data are entirely consistent with an agonistic action of pro mediated by the extracellular Gly binding pocket of the GlyR (Grudzinska et al., 2005a; Shan et al., 2001).

This is also in line with previously published studies reporting that pro evoked currents at GlyRs can be blocked by stry (Dong and Xu, 2002; Pistis et al., 1997).

However, no information was given about the nature of this block. Therefore, we enlarged this observation by presenting data showing that increasing stry concentrations shift the DA EC₅₀ value of pro towards higher concentrations without affecting the efficacy of the partial agonism. These phenomena suggest the presence of a competitive inhibition by stry which is proof by the results from the Schild-analysis. By this method we unravel that the decrease in the DA EC₅₀ value behaves linear to the used stry concentrations underlining the presence of a pro binding site in the LBD. In silico docking of pro to the LBD highlighted the presence of multiple contacts between pro and residues responsible for the binding of stry and Gly (Grudzinska et al., 2005a). Taken together, we can present data unraveling for the first time the existence of functional multiple binding sites for pro at GlyRs.

References

- Ahrens J, Haeseler G, Leuwer M, Mohammadi B, Krampfl K, Dengler R and Bufler J (2004) 2,6 di-tert-butylphenol, a nonanesthetic propofol analog, modulates alpha1beta glycine receptor function in a manner distinct from propofol. *Anesth Analg* **99**(1): 91-96.
- Ahrens J, Leuwer M and Haeseler G (2008a) Strychnine-sensitive glycine receptors mediate the analgesic but not the hypnotic effects of emulsified volatile anaesthetics. *Pharmacology* **81**(3): 195.
- Ahrens J, Leuwer M, Stachura S, Krampfl K, Belelli D, Lambert JJ and Haeseler G (2008b) A transmembrane residue influences the interaction of propofol with the strychnine-sensitive glycine alpha1 and alpha1beta receptor. *Anesth Analg* **107**(6): 1875-1883.
- Bali M and Akabas MH (2004) Defining the propofol binding site location on the GABAA receptor. *Mol Pharmacol* **65**(1): 68-76.
- Belelli D, Pistis M, Peters JA and Lambert JJ (1999) The interaction of general anaesthetics and neurosteroids with GABA(A) and glycine receptors. *Neurochem Int* **34**(5): 447-452.
- Chiara DC, Gill JF, Chen Q, Tillman T, Dailey WP, Eckenhoff RG, Xu Y, Tang P and Cohen JB (2014) Photoaffinity labeling the propofol binding site in GLIC. *Biochemistry* **53**(1): 135-142.
- Chiara DC, Jayakar SS, Zhou X, Zhang X, Savechenkov PY, Bruzik KS, Miller KW and Cohen JB (2013) Specificity of intersubunit general anesthetic-binding sites in the transmembrane domain of the human alpha1beta3gamma2 gamma-aminobutyric acid type A (GABAA) receptor. *J Biol Chem* **288**(27): 19343-19357.
- Colquhoun D (1998) Binding, gating, affinity and efficacy: the interpretation of structure-activity relationships for agonists and of the effects of mutating receptors. *Br J Pharmacol* **125**(5): 924-947.
- Csermely P, Nussinov R and Szilagyi A (2013) From allosteric drugs to allo-network drugs: state of the art and trends of design, synthesis and computational methods. *Curr Top Med Chem* **13**(1): 2-4.
- Cui T, Mowrey D, Bondarenko V, Tillman T, Ma D, Landrum E, Perez-Aguilar JM, He J, Wang W, Saven JG, Eckenhoff RG, Tang P and Xu Y (2011) NMR structure and dynamics of a designed water-soluble transmembrane domain of nicotinic acetylcholine receptor. *Biochim Biophys Acta* **1818**(3): 617-626.
- de la Roche J, Leuwer M, Krampfl K, Haeseler G, Dengler R, Buchholz V and Ahrens J (2012) 4-Chloropropofol enhances chloride currents in human hyperekplexic and artificial mutated glycine receptors. *BMC Neurol* **12**: 104.

- Del Sol A, Arauzo-Bravo MJ, Amoros D and Nussinov R (2007) Modular architecture of protein structures and allosteric communications: potential implications for signaling proteins and regulatory linkages. *Genome Biol* **8**(5): R92.
- del Sol A, Tsai CJ, Ma B and Nussinov R (2009) The origin of allosteric functional modulation: multiple pre-existing pathways. *Structure* **17**(8): 1042-1050.
- Dong XP and Xu TL (2002) The actions of propofol on gamma-aminobutyric acid-A and glycine receptors in acutely dissociated spinal dorsal horn neurons of the rat. *Anesth Analg* **95**(4): 907-914, table of contents.
- Dougherty DA (2007) Cation-pi interactions involving aromatic amino acids. *J Nutr* **137**(6 Suppl 1): 1504S-1508S; discussion 1516S-1517S.
- Du J, Lu W, Wu S, Cheng Y and Gouaux E (2015) Glycine receptor mechanism elucidated by electron cryo-microscopy. *Nature* **526**(7572): 224-229.
- Duret G, Van Renterghem C, Weng Y, Prevost M, Moraga-Cid G, Huon C, Sonner JM and Corringer PJ (2011) Functional prokaryotic-eukaryotic chimera from the pentameric ligand-gated ion channel family. *Proc Natl Acad Sci U S A* **108**(29): 12143-12148.
- Franks NP and Lieb WR (1994) Molecular and cellular mechanisms of general anaesthesia. *Nature* **367**(6464): 607-614.
- Grudzinska J, Schemm R, Haeger S, Nicke A, Schmalzing G, Betz H and Laube B (2005a) The beta subunit determines the ligand binding properties of synaptic glycine receptors. *Neuron* **45**(5): 727-739.
- Grudzinska J, Schemm R, Haeger S, Nicke A, Schmalzing G, Betz H and Laube B (2005b) The beta subunit determines the ligand binding properties of synaptic glycine receptors. *Neuron* **45**(5): 727-739.
- Haeger S, Kuzmin D, Detro-Dassen S, Lang N, Kilb M, Tsetlin V, Betz H, Laube B and Schmalzing G (2010) An intramembrane aromatic network determines pentameric assembly of Cys-loop receptors. *Nature structural & molecular biology* **17**(1): 90-98.
- Hales TG and Lambert JJ (1991) The actions of propofol on inhibitory amino acid receptors of bovine adrenomedullary chromaffin cells and rodent central neurones. *Br J Pharmacol* **104**(3): 619-628.
- Hamouda AK, Stewart DS, Husain SS and Cohen JB (2011) Multiple transmembrane binding sites for p-trifluoromethyl-diaziriny-*etomidate*, a photoreactive Torpedo nicotinic acetylcholine receptor allosteric inhibitor. *J Biol Chem* **286**(23): 20466-20477.
- Hess B, Kutzner C, van der Spoel D and Lindahl E (2008) GROMACS 4: Algorithms for highly efficient, load-balanced, and scalable molecular simulation. *J Chem Theory Comput* **4**(3): 13.
- Hibbs RE and Gouaux E (2011) Principles of activation and permeation in an anion-selective Cys-loop receptor. *Nature* **474**(7349): 54-60.

- Hornak V, Abel R, Okur A, Strockbine B, Roitberg A and Simmerling C (2006) Comparison of multiple Amber force fields and development of improved protein backbone parameters. *Proteins* **65**(3): 712-725.
- Jayakar SS, Dailey WP, Eckenhoff RG and Cohen JB (2013) Identification of propofol binding sites in a nicotinic acetylcholine receptor with a photoreactive propofol analog. *J Biol Chem* **288**(9): 6178-6189.
- Jurd R, Arras M, Lambert S, Drexler B, Siegwart R, Crestani F, Zaugg M, Vogt KE, Ledermann B, Antkowiak B and Rudolph U (2003) General anesthetic actions in vivo strongly attenuated by a point mutation in the GABA(A) receptor beta3 subunit. *FASEB J* **17**(2): 250-252.
- Kirson D, Todorovic J and Mihic SJ (2012) Positive allosteric modulators differentially affect full versus partial agonist activation of the glycine receptor. *J Pharmacol Exp Ther* **342**(1): 61-70.
- Krasowski MD, Nishikawa K, Nikolaeva N, Lin A and Harrison NL (2001) Methionine 286 in transmembrane domain 3 of the GABAA receptor beta subunit controls a binding cavity for propofol and other alkylphenol general anesthetics. *Neuropharmacology* **41**(8): 952-964.
- Langosch D, Thomas L and Betz H (1988) Conserved quaternary structure of ligand-gated ion channels: the postsynaptic glycine receptor is a pentamer. *Proc Natl Acad Sci U S A* **85**(19): 7394-7398.
- Laube B, Kuhse J and Betz H (2000) Kinetic and mutational analysis of Zn²⁺ modulation of recombinant human inhibitory glycine receptors. *J Physiol* **522 Pt 2**: 215-230.
- Laube B, Kuhse J, Rundstrom N, Kirsch J, Schmieden V and Betz H (1995) Modulation by zinc ions of native rat and recombinant human inhibitory glycine receptors. *J Physiol* **483 (Pt 3)**: 613-619.
- Lazareno S and Birdsall NJ (1993) Estimation of competitive antagonist affinity from functional inhibition curves using the Gaddum, Schild and Cheng-Prusoff equations. *Br J Pharmacol* **109**(4): 1110-1119.
- Li GD, Chiara DC, Cohen JB and Olsen RW (2010) Numerous classes of general anesthetics inhibit etomidate binding to gamma-aminobutyric acid type A (GABAA) receptors. *J Biol Chem* **285**(12): 8615-8620.
- Lobo IA, Trudell JR and Harris RA (2006) Accessibility to residues in transmembrane segment four of the glycine receptor. *Neuropharmacology* **50**(2): 174-181.
- Lynagh T and Laube B (2014) Opposing effects of the anesthetic propofol at pentameric ligand-gated ion channels mediated by a common site. *J Neurosci* **34**(6): 2155-2159.
- Lynagh T and Lynch JW (2010) A glycine residue essential for high ivermectin sensitivity in Cys-loop ion channel receptors. *Int J Parasitol* **40**(13): 1477-1481.

- Lynagh T and Lynch JW (2012a) Ivermectin binding sites in human and invertebrate Cys-loop receptors. *Trends Pharmacol Sci* **33**(8): 432-441.
- Lynagh T and Lynch JW (2012b) Molecular mechanisms of Cys-loop ion channel receptor modulation by ivermectin. *Front Mol Neurosci* **5**: 60.
- Lynagh T, Webb TI, Dixon CL, Cromer BA and Lynch JW (2011) Molecular determinants of ivermectin sensitivity at the glycine receptor chloride channel. *J Biol Chem* **286**(51): 43913-43924.
- Maksay G, Laube B, Schemm R, Grudzinska J, Drwal M and Betz H (2009) Different binding modes of tropeines mediating inhibition and potentiation of alpha1 glycine receptors. *J Neurochem* **109**(6): 1725-1732.
- Martin C, Berridge G, Higgins CF, Mistry P, Charlton P and Callaghan R (2000) Communication between multiple drug binding sites on P-glycoprotein. *Mol Pharmacol* **58**(3): 624-632.
- McCracken ML, Borghese CM, Trudell JR and Harris RA (2010) A transmembrane amino acid in the GABAA receptor beta2 subunit critical for the actions of alcohols and anesthetics. *J Pharmacol Exp Ther* **335**(3): 600-606.
- McGaughey GB, Gagne M and Rappe AK (1998) pi-Stacking interactions. Alive and well in proteins. *J Biol Chem* **273**(25): 15458-15463.
- Moraga-Cid G, Sauguet L, Huon C, Malherbe L, Girard-Blanc C, Petres S, Murail S, Taly A, Baaden M, Delarue M and Corringer PJ (2015) Allosteric and hyperekplexic mutant phenotypes investigated on an alpha1 glycine receptor transmembrane structure. *Proc Natl Acad Sci U S A* **112**(9): 2865-2870.
- Moraga-Cid G, Yevenes GE, Schmalzing G, Peoples RW and Aguayo LG (2011) A Single phenylalanine residue in the main intracellular loop of alpha1 gamma-aminobutyric acid type A and glycine receptors influences their sensitivity to propofol. *Anesthesiology* **115**(3): 464-473.
- Mowrey DD, Cui T, Jia Y, Ma D, Makhov AM, Zhang P, Tang P and Xu Y (2013) Open-channel structures of the human glycine receptor alpha1 full-length transmembrane domain. *Structure* **21**(10): 1897-1904.
- Nury H, Van Renterghem C, Weng Y, Tran A, Baaden M, Dufresne V, Changeux JP, Sonner JM, Delarue M and Corringer PJ (2011) X-ray structures of general anaesthetics bound to a pentameric ligand-gated ion channel. *Nature* **469**(7330): 428-431.
- Nussinov R (2012) Allosteric modulators can restore function in an amino acid neurotransmitter receptor by slightly altering intra-molecular communication pathways. *Br J Pharmacol* **165**(7): 2110-2112.
- O'Shea SM, Becker L, Weiher H, Betz H and Laube B (2004) Propofol restores the function of "hyperekplexic" mutant glycine receptors in *Xenopus* oocytes and mice. *J Neurosci* **24**(9): 2322-2327.

- Orser BA, Wang LY, Pennefather PS and MacDonald JF (1994) Propofol modulates activation and desensitization of GABAA receptors in cultured murine hippocampal neurons. *J Neurosci* **14**(12): 7747-7760.
- Pistis M, Belelli D, Peters JA and Lambert JJ (1997) The interaction of general anaesthetics with recombinant GABAA and glycine receptors expressed in *Xenopus laevis* oocytes: a comparative study. *Br J Pharmacol* **122**(8): 1707-1719.
- Pless SA, Hanek AP, Price KL, Lynch JW, Lester HA, Dougherty DA and Lummis SC (2011) A cation- π interaction at a phenylalanine residue in the glycine receptor binding site is conserved for different agonists. *Mol Pharmacol* **79**(4): 742-748.
- Pless SA, Millen KS, Hanek AP, Lynch JW, Lester HA, Lummis SC and Dougherty DA (2008) A cation- π interaction in the binding site of the glycine receptor is mediated by a phenylalanine residue. *J Neurosci* **28**(43): 10937-10942.
- Reiner GN, Delgado-Marin L, Olguin N, Sanchez-Redondo S, Sanchez-Borzone M, Rodriguez-Farre E, Sunol C and Garcia DA (2013a) GABAergic pharmacological activity of propofol related compounds as possible enhancers of general anesthetics and interaction with membranes. *Cell Biochem Biophys* **67**(2): 515-525.
- Reiner GN, Perillo MA and Garcia DA (2013b) Effects of propofol and other GABAergic phenols on membrane molecular organization. *Colloids Surf B Biointerfaces* **101**: 61-67.
- Sali A and Blundell TL (1993) Comparative protein modelling by satisfaction of spatial restraints. *J Mol Biol* **234**(3): 779-815.
- Sauguet L, Shahsavari A and Delarue M (2014) Crystallographic studies of pharmacological sites in pentameric ligand-gated ion channels. *Biochim Biophys Acta*.
- Shan Q, Haddrill JL and Lynch JW (2001) Ivermectin, an unconventional agonist of the glycine receptor chloride channel. *J Biol Chem* **276**(16): 12556-12564.
- Sousa da Silva AW and Vranken WF (2012) ACPYPE - AnteChamber PYthon Parser interface. *BMC Res Notes* **5**: 367.
- Spurny R, Billen B, Howard RJ, Brams M, Debaveye S, Price KL, Weston DA, Strelkov SV, Tytgat J, Bertrand S, Bertrand D, Lummis SC and Ulens C (2013) Multisite binding of a general anesthetic to the prokaryotic pentameric *Erwinia chrysanthemi* ligand-gated ion channel (ELIC). *J Biol Chem* **288**(12): 8355-8364.
- Szilagyi A, Nussinov R and Csermely P (2013) Allo-network drugs: extension of the allosteric drug concept to protein-protein interaction and signaling networks. *Curr Top Med Chem* **13**(1): 64-77.
- Trapani G, Latrofa A, Franco M, Altomare C, Sanna E, Usala M, Biggio G and Liso G (1998) Propofol analogues. Synthesis, relationships between structure and affinity at GABAA receptor in rat brain, and differential electrophysiological

- profile at recombinant human GABAA receptors. *J Med Chem* **41**(11): 1846-1854.
- Tsai CJ, Del Sol A and Nussinov R (2009) Protein allostery, signal transmission and dynamics: a classification scheme of allosteric mechanisms. *Mol Biosyst* **5**(3): 207-216.
- Wang J, Wang W, Kollman PA and Case DA (2006) Automatic atom type and bond type perception in molecular mechanical calculations. *J Mol Graph Model* **25**(2): 247-260.
- Wang J, Wolf RM, Caldwell JW, Kollman PA and Case DA (2004) Development and testing of a general amber force field. *J Comput Chem* **25**(9): 1157-1174.
- Wang Q and Lynch JW (2012) A comparison of glycine- and ivermectin-mediated conformational changes in the glycine receptor ligand-binding domain. *Int J Biochem Cell Biol* **44**(2): 335-340.
- Wolf MG, Hoefling M, Aponte-Santamaria C, Grubmuller H and Groenhof G (2010) g_membed: Efficient insertion of a membrane protein into an equilibrated lipid bilayer with minimal perturbation. *J Comput Chem* **31**(11): 2169-2174.
- Wyllie DJ and Chen PE (2007) Taking the time to study competitive antagonism. *Br J Pharmacol* **150**(5): 541-551.
- Xiong W, Cheng K, Cui T, Godlewski G, Rice KC, Xu Y and Zhang L (2011) Cannabinoid potentiation of glycine receptors contributes to cannabis-induced analgesia. *Nat Chem Biol* **7**(5): 296-303.
- Xiong W, Cui T, Cheng K, Yang F, Chen SR, Willenbring D, Guan Y, Pan HL, Ren K, Xu Y and Zhang L (2012) Cannabinoids suppress inflammatory and neuropathic pain by targeting alpha3 glycine receptors. *J Exp Med* **209**(6): 1121-1134.
- Yamakura T, Mihic SJ and Harris RA (1999) Amino acid volume and hydrophobicity of a transmembrane site determine glycine and anesthetic sensitivity of glycine receptors. *J Biol Chem* **274**(33): 23006-23012.
- Yevenes GE and Zeilhofer HU (2011) Allosteric modulation of glycine receptors. *Br J Pharmacol* **164**(2): 224-236.
- Yip GM, Chen ZW, Edge CJ, Smith EH, Dickinson R, Hohenester E, Townsend RR, Fuchs K, Sieghart W, Evers AS and Franks NP (2013) A propofol binding site on mammalian GABAA receptors identified by photolabeling. *Nat Chem Biol* **9**(11): 715-720.
- Zhang L and Xiong W (2009) Modulation of the Cys-loop ligand-gated ion channels by fatty acid and cannabinoids. *Vitam Horm* **81**: 315-335.

Characterization of thymol and 4-chlorothymol effects on the function of human glycine receptors

Michael Kilb, Alexander Winschel, Tim Lynagh and Bodo Laube

Neurophysiology and Neurosensory Systems, Technische Universität Darmstadt, Germany

Abstract

We previously reported that the general anesthetic propofol (pro) and a chlorinated derivate named 4-chloropropofol (4-cpro) are potent biphasic allosteric modulators of native and recombinant human glycine receptors (GlyRs). Here, we examined by two-electrode-voltage-clamp (TEVC) electrophysiology the effects of the structural related phenols thymol (thy) and 4-chlorothymol (4-cthy) on the function of human homomeric GlyRs expressed in *Xenopus laevis* oocytes. In the nano- to low micromolar concentration range, thy caused an high-affinity (HA) potentiation of the glycine (Gly) evoked currents at $\alpha 1$ and $\alpha 2$ GlyRs up to 53 % with EC₅₀ values for potentiation of 173 ± 28 nM and 140 ± 13 nM, respectively. However, $\alpha 3$ GlyRs were not potentiated by equal thy concentrations. Surprisingly, 4-cthy showed no HA modulation of $\alpha 1$ - but a HA potentiation of $\alpha 2$ - with an EC₅₀ value of 223 ± 0.4 nM and HA inhibition of $\alpha 3$ GlyRs with an IC₅₀ value of 4.7 ± 0.4 μ M. Comparable to pro and 4-cpro, both compounds exert a subtype unspecific low-affinity (LA) potentiation of the Gly-evoked currents with EC₅₀ values between 0.4 and 1.7 mM. TEVC analysis combined with site-directed mutagenesis, co-application of pro and the substituted cysteine accessibility method (SCAM) provide evidence that the HA modulation of GlyRs by thy and 4-cthy is mediated by the pro and 4-cpro HA binding site and that non-conserved residues located in the M3 and M4 mediate the subtype specific 4-cthy HA modulation in α GlyR subtypes. Together these results underline that multiple functional subtype specific binding sites for monophenols exist at human GlyRs and that certain molecules of this substance class could act as GlyR subtype specific HA modulators.

Introduction

GlyRs are pentameric ligand-gated ion channels (pLGICs) that mediate rapid chemoelectric signaling in the spinal cord, brain stem and certain higher areas of the central nervous system (cns). Functional GlyRs are either homomers formed by $\alpha 1$, $\alpha 2$ or $\alpha 3$ GlyR subunits or heteromers formed by α and β GlyR subunits. Because β subunits possess a binding site for the anchoring protein gephyrin, synaptic GlyRs are largely $\alpha\beta$ heteromers, whereas extrasynaptic GlyRs are α homomers. There is immunohistochemical and/or mRNA evidence for tissue-specific expression of different subtype combinations, for example $\alpha 1\beta$ heteromers in the spinal cord and brain stem, synaptic $\alpha 3\beta$ heteromers in the hippocampus and nociceptive pathways of the spinal cord and extrasynaptic $\alpha 2$ homomers in the mature hippocampus (Betz and Laube, 2006; Lynch, 2009).

Although numerous classes of compounds modulate GlyR responses to glycine (Gly), only a few compounds show a clear specificity for different GlyR subtypes because several of these compounds also modulate γ -aminobutyric acid type A receptors (GABA(A)Rs) (Yevenes and Zeilhofer, 2011a).

The general anesthetic propofol (pro) is such a modulator of Gly- and GABA(A)Rs (Grasshoff and Gillissen, 2005). It enhances agonist responses of inhibitory GlyRs and type A γ -aminobutyric acid receptors (GABA(A)Rs) (Barann et al., 2008; Pistis et al., 1997).

Recently, it has been shown that a chlorinated derivative of pro, named 4-chloropropofol (4-cpro) shows profoundly increased modulatory potency at homomeric $\alpha 1$ GlyRs (de la Roche et al., 2012). Moreover, data obtained by Eckle and colleagues reveal that 4-bromopropofol (4-brpro) is also a GlyR specific modulator (Eckle et al., 2014). We obtained data showing that 4-cpro exhibits an increased modulatory potency at homomeric $\alpha 1$ GlyRs compared to pro (chapter 2). Moreover, we unmasked that pro and 4-cpro exert a complex biphasic allosteric modulation at homo- and heteromeric GlyRs in form of a subtype specific HA- and non specific LA allosteric modulation. By using the TEVC technique in combination with site-directed mutagenesis, in silico dockings and the use of compounds knowing to modulate the GlyR function we unravel the exact location of the pro and 4-cpro binding sites responsible for the biphasic allosteric modulation and partial agonistic effects (chapter 2 and 3). These observations raise the possibility that certain

monophenols might serve as GlyR-specific modulators, for which there is a considerable demand (Yevenes and Zeilhofer, 2011b).

In the present study, we considered the possibility that monophenols with similar structures compared to pro and 4-cpro modulate GlyRs equally compared to pro and 4-cpro. Thus, we analyzed the effects of thy and 4-cthy on the function of homomeric α GlyRs subtypes. Thy, is a substantial component of thyme essential oil and enhances agonist responses of GABA_(A)Rs (Garcia et al., 2006; Priestley et al., 2003). It may also modulate neuronal excitability by interacting with nAChRs (Boudry and Perrier, 2008). The chlorinated variant 4-cthy has not been tested for modulation of pLGICs, but experiments show that it interacts with components of the membranes in a similar manner to thy and pro (Reiner et al., 2009), giving it similar access to GlyR TMDs, where monophenols are likely to bind (Ahrens et al., 2008; Betz and Laube, 2006).

To proof our assumption, we analyzed in detail thy and 4-cthy effects on the agonist responses of recombinant homomeric α 1-, α 2- and α 3 GlyRs. Depending on the GlyR subtype combination, we observed a biphasic dose-dependent allosteric modulation of Gly responses by both compounds, which could be again divided into a HA and LA modulation. Concerning the HA modulation, thy and 4-cthy showed distinct effects at the function of homomeric GlyR subtypes. This subtype specific modulation is mediated by molecule binding to the pro and 4-cpro HA site. Moreover, we unmasked additional, non-conserved residues in the M3 and M4 which are responsible for the subtype specific HA modulation by 4-cthy. Based on these data we propose that monophenols, especially halogenated, are subtype-specific high-affinity modulators of GlyRs in defined neuronal circuits and during neuronal development.

Materials & Methods

Materials

All chemicals were purchased from Sigma-Aldrich (München, Germany) and from Applichem (Darmstadt, Germany). cRNAs were synthesized by in vitro transcription from linearised plasmid cDNAs using the Ambion SP6 mMESSAGE mMACHINE® SP6 Kit (Life-technologies, Carlsbad, USA).

Chemicals

Thy (2-isopropyl-5-methylphenol), 4-cthy (4-chloro-2-isopropyl-5-methylphenol), pro (2,6-diisopropylphenol), tricaine (ethyl 3-aminobenzoate methanesulfonate), gentamicin (sulfate salt), collagenase (type II A) and dimethyl sulfoxide (DMSO) were purchased from Sigma-Aldrich (Munich, Germany). Propyl methanethiosulfonate (PMTS) was purchased from Toronto Research Chemicals, Downsview, ON, Canada. 1M stock solutions of thy and 4-cthy were prepared with DMSO in glass vessels and stored at -20 °C before dissolving further in Ringer's solution on the day of experiment. All other chemicals were purchased from Applichem (Darmstadt, Germany).

cDNAs, cRNA synthesis and oocytes expression

For the isolation of stage V and VI oocytes, ovarian lobes were surgically removed from adult female *Xenopus laevis* clawfrogs anaesthetized by immersion in 0.3% (w/v) tricaine methane sulfonate (Sigma). All protocols were approved by the local animal care and use committee (II25.3-19c20/15; RP Darmstadt, Germany). Oocytes were carefully dissected, stored and prepared as described in chapter 2 and by Haeger and colleagues (Haeger et al., 2010).

Electrophysiological recordings and data analyzes

Two-electrode voltage clamp recordings of whole cell currents were performed in Ringer's solution at a holding potential of -70 mV as described previously (Laube et al., 2000). Modulation of EC20 Gly currents by thy and 4-cthy were measured and analyzed following previously described procedures in chapter 2.

PMTS accessibility and covalent modification

First the EC₂₀ Gly was determined for each α 1Gly394Cys expressing oocyte. PMTS (1 mM) was then applied in the absence of Gly for 5 min. Then the response to the initial EC₂₀ Gly was determined 5, 10, 15 and 20 min after application of PMTS and the fold change of the Gly currents over the initial current was calculated for each oocyte. Subsequent, the EC₂₀ Gly was redetermined to measure pro and 4-cthy effects. Experimental values are presented as means \pm S.E.M. of peak current responses. The statistical significance of differences between mean values was assessed by paired and unpaired student's t-test and considered to be significant at * $P < 0.05$. All experiments were performed at room temperature.

Results

Previous analysis by us (chapter 2 and 3) unmasked a subtype specific HA- and LA allosteric modulation of homo- and heteromeric GlyRs by pro and 4-cpro. The biphasic modulation is mediated by a HA and a LA binding site. Each site is located in transmembrane domains (TMDs) but in distinct areas. Based on these observations, we asked us if the structurally closely related phenols thy and 4-cthy are equal allosteric modulators of human GlyRs.

Thy and 4-cthy effects at homomeric $\alpha 1$ GlyRs

We first investigated thy and 4-cthy effects on the EC₂₀ Gly-evoked currents of homomeric $\alpha 1$ GlyRs. Pre-application of 1 nM to 100 μ M thy resulted in a dose-dependent HA potentiation of the current reaching a maximum of 0.53 ± 0.1 fold between 1 and 50 μ M thy at homomeric $\alpha 1$ GlyRs (Fig. 1A, upper panel). The current potentiation could be described by a monophasic Hill equation, yielding an EC₅₀ value for the HA potentiation by thy of 173 ± 28 nM (nH 1.2 ± 0.1 ; Fig. 1B). Surprisingly, equal 4-cthy concentrations had no obvious effect on the Gly-evoked currents (Fig. 1A lower panel, B).

Molecule concentrations above 100 μ M caused again a dose dependent increase in the currents resulting in an maximum percentage potentiation of the current up to 4.6 ± 0.5 fold for thy and 1.6 ± 0.2 fold for 4-cthy (Fig. 1C). Saturation of the LA potentiation developed between 3 and 5 mM for each molecule (Fig. 1D). Visual inspection of the Gly-evoked current modulation unmasked a biphasic potentiation for thy and a monophasic potentiation for 4-cthy (Fig. 1D). Monophasic fits of the LA potentiation yielded EC₅₀ values of 981 ± 62 μ M for thy and 1109 ± 41 μ M for 4-cthy. All values are reported in table 1.

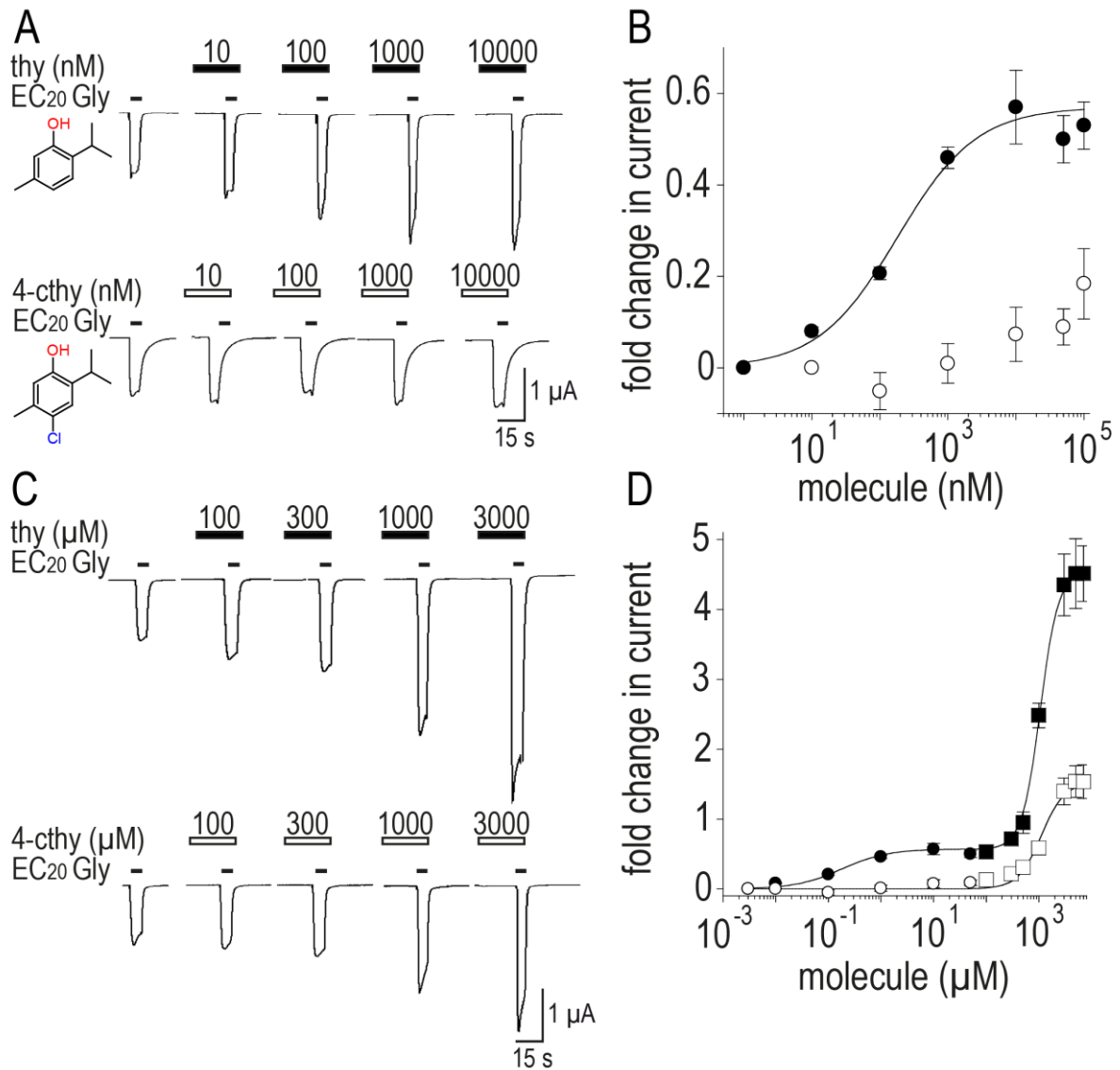


Figure 1: Modulation of homomeric α 1 GlyRs by thy and 4-cthy. **A.** Example recording from an oocyte injected with α 1 GlyR cRNA, showing EC₂₀ Gly responses in the presence of nM to μ M concentrations of thy (top panel) and 4-cthy (lower panel). **B.** Averaged fold change in current (mean \pm S.E.M. of 7 oocytes) caused by nM to μ M molecule concentrations of thy (black filled circles) and 4-cthy (white filled circles). Data were fit with a monophasic Hill equation. **C.** Example recording from an oocyte showing EC₂₀ Gly responses in the presence of μ M to mM concentrations thy (top panel) and 4-cthy (lower panel). **D.** Averaged Change in current (fold mean \pm S.E.M. of 7 oocytes) caused by nM to mM molecule concentrations of thy (black filled symbols) and 4-cthy (white filled symbols). Data for 4-cthy modulation were fit with a monophasic Hill equation and data for thy with a biphasic Hill equation ($R^2 = 0.99$), indicating a HA and LA component. In calculating LA potentiation, maximal HA potentiation is subtracted from the total increase in current.

In summary, thy potentiate homomeric α 1 GlyRs in a biphasic manner comparable to pro and 4-cpro. In contrary low concentrations of 4-cthy caused no obvious modulation of the Gly-evoked current. However, higher μ M to mM concentrations caused a monophasic dose-dependent LA potentiation of the Gly-evoked current.

Surprisingly, in the high micro- to low millimolar concentration ranges none of the molecules exert a partial agonistic activity at homomeric $\alpha 1$ GlyRs.

Thy and 4-cthy are GlyR subtype-specific HA site modulators

Next, we determine the sensitivity of homomeric $\alpha 2$ and $\alpha 3$ GlyRs towards thy and 4-cthy. At $\alpha 2$ GlyRs responses to Gly were increased in a dose-dependent manner by low concentrations of thy (1 nM to 100 μ M; Fig. 2A, B), reflecting the HA potentiation of $\alpha 1$ GlyRs by thy. Saturating concentrations (~ 10 μ M) increased the Gly evoked currents up to 0.27 ± 0.02 fold, which is significantly less than at $\alpha 1$ GlyRs ($P < 0.001$, unpaired t-test; $n = 7$). However, the EC₅₀ value was 140 ± 13 nM (nH 0.9 ± 0.1) and reflected homomeric $\alpha 1$ GlyR values. At $\alpha 3$ GlyRs, no dose-dependent HA modulation is present (Fig. 2A lower panel, B).

Like $\alpha 1$ GlyRs, both $\alpha 2$ and $\alpha 3$ GlyRs were dose-dependently potentiated by thy concentrations from 100 μ M up to 7 mM (Fig. 2C, D). The EC₅₀ values for this LA potentiation were for $\alpha 2$ 1029 ± 52 μ M and for $\alpha 3$ GlyRs 1035 ± 61 μ M. The maximum fold change in current was 2.95 ± 0.28 fold at $\alpha 2$ GlyRs and did not differ from $\alpha 1$ GlyRs values. $\alpha 3$ GlyRs were potentiated to a significantly lesser extent than $\alpha 1$ GlyRs (0.99 ± 0.11 fold, $P < 0.001$, unpaired t-test; $n = 7$). A partial agonism in the investigated concentration ranges is only evident at $\alpha 3$ GlyRs. All values are reported in table 1.

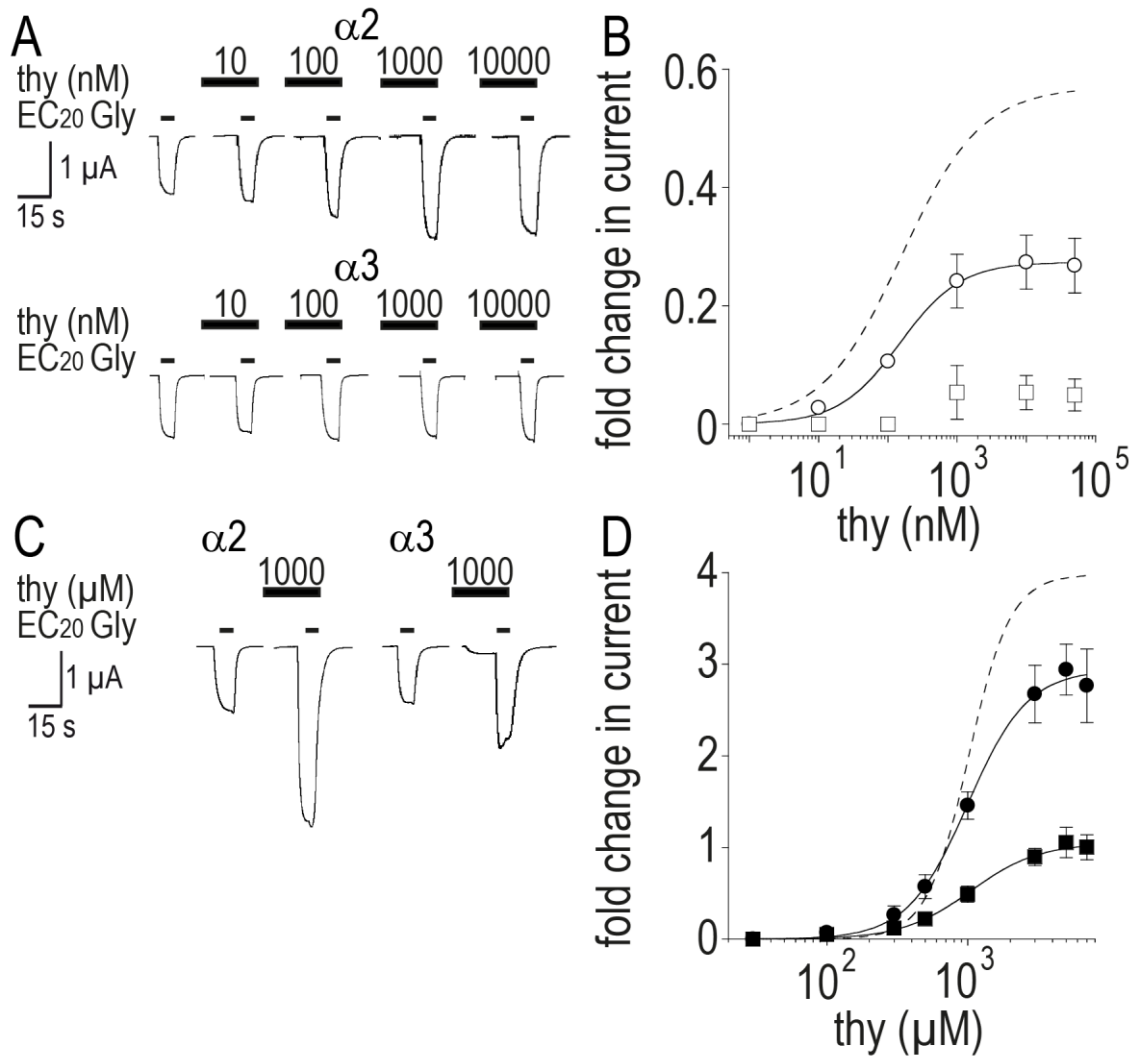


Figure 2: GlyR subtype modulation by thy. **A.** Example recordings from oocytes injected with $\alpha 2$ GlyR (top panel) and $\alpha 3$ GlyR (lower panel) cRNA. EC₂₀ Gly was applied to oocytes alone or in the presence of increasing concentrations of thy. The averaged changes in current are plotted in **B** (mean \pm S.E.M., of 7 cells, circles $\alpha 2$, squares $\alpha 3$, dashed line $\alpha 1$ from Fig. 1B). **C.** Responses of $\alpha 2$ and $\alpha 3$ GlyR-expressing oocytes to Gly in the presence of 1 mM thy. The averaged changes in current caused by high μ M and mM thy concentrations at $\alpha 2$ and $\alpha 3$ GlyRs are plotted in **D** (mean \pm S.E.M., of 7 cells, circles $\alpha 2$, squares $\alpha 3$, dashed line $\alpha 1$ from Fig. 1D).

Next, we determine the sensitivity of homomeric $\alpha 2$ and $\alpha 3$ GlyRs towards 4-cthy. In contrast to $\alpha 1$ GlyRs, 4-cthy induces a dose-dependent HA potentiation at $\alpha 2$ GlyRs (Fig. 3A, upper panel). The EC₅₀ value of the HA potentiation by 4-cthy was 223 ± 21 nM (Fig. 3B). Saturating concentrations ($\sim 10 \mu$ M) potentiate the current to a maximum of 0.37 ± 0.03 fold (Fig. 3B). The values are not significantly different compared to thy HA potentiation at $\alpha 2$ GlyRs, indicating that the C'4 chlorination does not improve the HA potentiation at $\alpha 2$ GlyRs.

In contrast, 4-cthy exert a HA inhibition of the EC₂₀ Gly evoked currents at $\alpha 3$ GlyRs. This dose dependent inhibition saturates around 10μ M (Fig. 3A lower panel) with an

IC₅₀ value of $4.7 \pm 0.4 \mu\text{M}$ and a maximum inhibition of the current of 0.25 ± 0.03 fold (Fig. 3B).

Regarding the LA modulation, $\alpha 2$ and $\alpha 3$ GlyRs were robustly potentiated by mM concentrations of 4-cthy (Fig. 3C). However, $\alpha 2$ GlyRs with an EC₅₀ of $351 \pm 23 \mu\text{M}$ were threefold more sensitive to LA modulation by 4-cthy than $\alpha 1$ GlyRs ($P < 0.001$, unpaired t-test; $n = 6$). In contrary the $\alpha 3$ GlyRs LA EC₅₀ was $1282 \pm 84 \mu\text{M}$, which reflects the $\alpha 1$ GlyR LA EC₅₀ value. As shown in figure 3D, neither at $\alpha 2$ nor $\alpha 3$ GlyRs the maximum strength of the LA current potentiation by 4-cthy differed (2.1 ± 0.17 fold for $\alpha 2$ - and 1.56 ± 0.1 fold for $\alpha 3$ GlyRs). With saturating concentrations of 4-cthy, a weak but dose-dependent partial agonism of $\alpha 2$ GlyRs was observable. All values are reported in table 1.

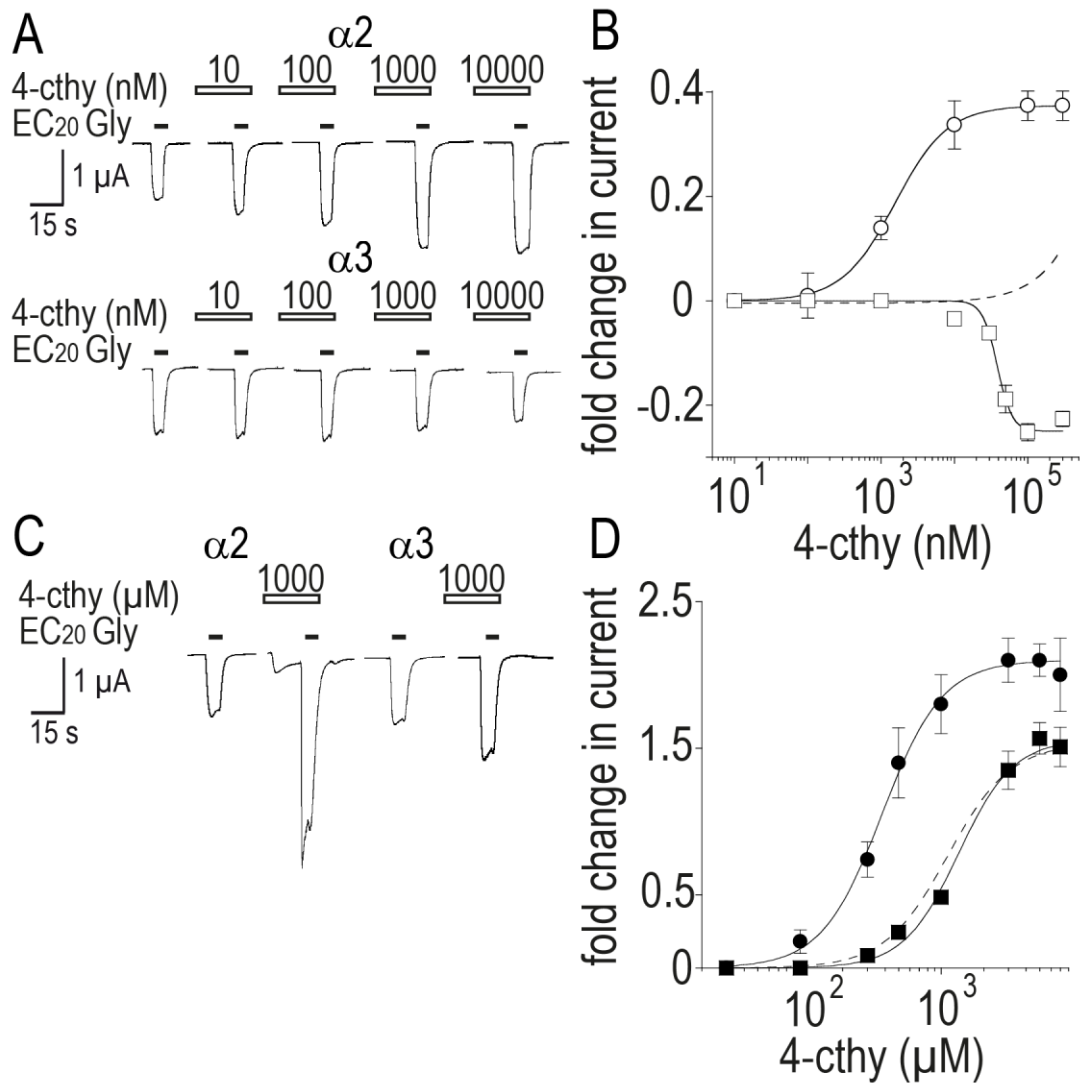


Figure 3: GlyR subtype modulation by 4-cthy. **A.** Example recordings from oocytes injected with wt $\alpha 2$ GlyR (upper panel) and $\alpha 3$ GlyR (lower panel) cRNA. EC₂₀ Gly was applied to oocytes alone or in the presence of increasing concentrations of 4-cthy. **B.** Averaged changes in current caused by nM to μ M concentration of 4-cthy (mean \pm S.E.M. of 7 cells, circles $\alpha 2$, squares $\alpha 3$). Dashed line is an approximation of data points for 4-cthy at $\alpha 1$ GlyRs). **C.** Example responses of $\alpha 2$ and $\alpha 3$ GlyR-expressing oocytes to Gly in the presence of 1 mM 4-cthy. The averaged changes in current caused by high μ M and mM 4-cthy concentrations at $\alpha 2$ and $\alpha 3$ GlyRs are shown in **D** (mean \pm S.E.M. of 7 cells, circles $\alpha 2$, squares $\alpha 3$, dashed line $\alpha 1$ from Fig. 1D).

Table 1: Parameters for HA site modulation, LA site modulation and direct activation (DA site) by thy and 4-cthy at homomeric GlyRs (subtype listed in left column). EC₅₀ and nH values were calculated for each of n cells with the monophasic Hill equation, and mean ± S.E.M. are given. Maximum fold change indicates the maximum change in current, respectively. For direct activation, maximum activation by lthy or l4-cthy is given under the *Maximum fold change* column, expressed as the percentage fraction of maximum activation by Gly (IMAX-Gly).

GlyR HA site	thy				4-cthy			
	EC ₅₀ (nM)	nH	Maximum fold change	n	EC ₅₀ (nM)	nH	Maximum fold change	n
α1	173 ± 28	1.2 ± 0.1	0.53 ± 0.1	7	<i>nm</i>	<i>nm</i>	0.09 ± 0.02 ^a	7
α2	140 ± 13	1.1 ± 0.05	0.27 ± 0.02*	7	223 ± 21	1.1 ± 0.1	0.37 ± 0.03***	8
α3	<i>nm</i>	<i>nm</i>	0.08 ± 0.02 ^{a***}	7	4700 ± 430 ^b	1.6 ± 0.1	0.25 ± 0.03 ^{b***}	7
LA site	EC ₅₀ (μM)	nH	Maximum fold change	n	EC ₅₀ (μM)	nH	Maximum fold change	n
α1	981 ± 62	2.2 ± 0.2	4.08 ± 0.55	7	1109 ± 41	2.1 ± 0.1	1.61 ± 0.24	7
α2	1029 ± 52	2.1 ± 0.1	2.95 ± 0.28	6	351 ± 23***	2.3 ± 0.2	2.11 ± 0.17	6
α3	1035 ± 61	2.1 ± 0.2	0.99 ± 0.11***	6	1282 ± 84	2.5 ± 0.4	1.56 ± 0.1	6
DA site	EC ₅₀ (mM)	nH	% lthy/IMAX-Gly	n	EC ₅₀ (mM)	nH	% l4-cthy/IMAX-Gly	n
α1	<i>na</i>	<i>na</i>	<i>na</i>	6	<i>na</i>	<i>na</i>	<i>na</i>	6
α2	<i>na</i>	<i>na</i>	<i>na</i>	6	1.3 ± 0.01	6.4 ± 0.04	13 ± 1	6
α3	1.6 ± 0.2	2.3 ± 0.2	12 ± 1	6	<i>na</i>	<i>na</i>	<i>na</i>	6

Data are means ± S.E.M. *na* no activation; *nm* no modulation; ^a not significantly different to the EC₂₀ Gly variation; ^b IC₅₀ and maximum % inhibition; **P* < 0.05, ***P* < 0.01, ****P* < 0.001 compared to EC₂₀ Gly concentrations, unpaired t-test.

In summary, thy and 4-cthy exerted a subtype specific HA modulation at GlyRs. The subtype specific HA modulation by 4-cthy mirrored the effects by 4-cpro. This is in strong contrast to the common LA potentiation by thy and 4-cthy. We also observed a GlyR subtype specific partial agonism. Whereas thy or 4-cthy had no partial agonistic activity at α1 GlyRs, we observed that thy directly activates α3 and 4-cthy α2 GlyRs.

Co-application of 4-cthy abolish pro and thy HA site potentiation at homomeric $\alpha 1$ GlyRs

Next, we asked us if the absent 4-cthy HA modulation at $\alpha 1$ GlyRs is the result of an absent binding of the molecule. To solve this question, we tested if 4-cthy affects the pro and thy HA potentiation. We co-applied a pro HA site saturating characteristic concentration of 4-cthy (10 μ M) together with equal concentrations of pro and thy and measured the molecules effects on the EC₂₀ Gly-evoked currents. We induced and measured pro and thy HA potentiation by 10 μ M, respectively and after recovery of the initial EC₂₀ Gly-evoked current strength, oocytes were incubated for 30s in a mixed solution of 4-cthy/thy and 4-cthy/pro with a final concentration of 10 μ M for each molecule (Fig. 4A). In each case, the presence of 4-cthy significantly reduced the current potentiation by thy and pro ($P < 0.001$, paired t-test; $n = 4$, respectively). Potentiation by thy, went down from 0.4 ± 0.05 to 0.1 ± 0.02 fold and for pro, current potentiation was reduced from 0.4 ± 0.1 down to 0.1 ± 0.02 fold (Fig. 4B).

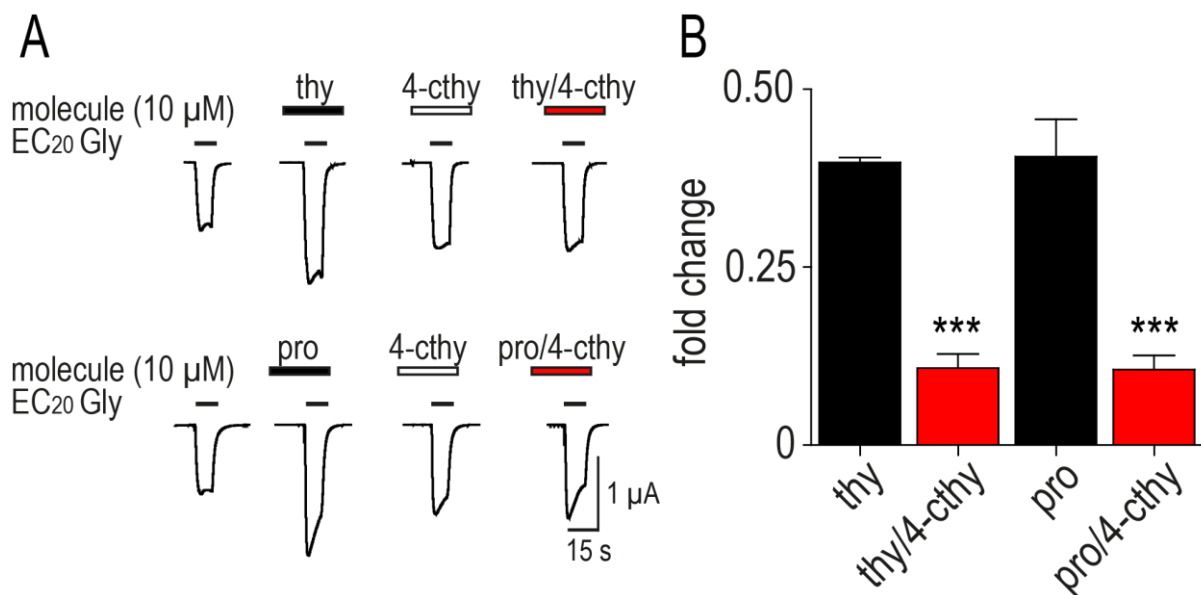


Figure 4: Co-application experiments indicating the presence of a common HA binding site in $\alpha 1$ GlyRs.

A. Example recordings showing current modulation by co-applications of 10 μ M concentrations of 4-c-thy, thy and pro (red filled bars). **B.** Column diagram representing the percentage change in current by thy and pro in the presence of 4-cthy (mean \pm S.E.M. of 4 oocytes). For the statistical analyses, the strength of the current modulation by 10 μ M thy or pro were compared with the currents strength in the presence of 4-cthy ($***P < 0.001$, paired t-test; mean \pm S.E.M. of 4 oocytes, respectively).

In summary, the presence of 4-cthy abolished thy and pro HA potentiation. Based on these findings, we assume that low μ M concentrations of 4-cthy bind to the pro and thy HA site in $\alpha 1$ GlyRs and abolishes the HA potentiation by the molecules.

Characterization of thy and 4-cthy effects at $\alpha 1$ GlyRs carrying amino acid substitutions in the pro and 4-cpro HA site

Based on the above shown results we speculate that the HA modulation of GlyRs by thy and 4-cthy is mediated by the pro and 4-cpro HA site (Fig. 5A). To proof this assumption, we investigated thy and 4-cthy effects on the function of $\alpha 1$ GlyRs carrying amino acid substitutions in the pro and 4-cpro HA site (chapter 2 and 3).

We first characterized the M3 $\alpha 1$ Phe293Ala substitution which abolishes pro and 4-cpro HA potentiation in $\alpha 1$ GlyRs. The presence of nM to μ M concentrations of thy evoked no HA potentiation of the Gly-evoked currents but μ M to mM concentrations induced a LA potentiation reaching a maximum fold potentiation of 2.1 ± 0.2 with an EC₅₀ value of $1107 \pm 112 \mu$ M (Fig. 5B). Comparison of the parameters with the respective wt $\alpha 1$ GlyR values, revealed a significant change in the EC₅₀ value of the LA potentiation ($P < 0.001$; unpaired t-test; $n = 4$).

Next, we investigated the M3 $\alpha 1$ Ser296Ala substitution which does not affect the pro but abolished 4-cpro HA modulation. Thy induces a HA potentiation of the EC₂₀ Gly-evoked currents with a maximum fold increase of 0.39 ± 0.03 and an EC₅₀ value of 130 ± 3 nM. Again, LA potentiation was present reaching a maximum increase of 3.1 ± 0.4 fold with an EC₅₀ value of $489 \pm 67 \mu$ M (Fig. 5B). Comparison of the values with the respective wt $\alpha 1$ GlyR LA values revealed a nearly 2-fold significant left shift of the LA EC₅₀ value ($P < 0.001$, unpaired t-test; $n = 4$) and a slight but significant reduction in the maximum fold change in current ($P < 0.05$, unpaired t-test; $n = 4$).

Finally, we investigated thy effects on the M4 $\alpha 1$ Phe402Ala substitution which converted the pro HA potentiation into an inhibition. Remarkably, thy also induces a HA inhibition of the EC₂₀ Gly-evoked currents. The IC₅₀ reached 670 ± 80 nM and the maximum current inhibition was 0.28 ± 0.1 fold. Comparison with the respective wt $\alpha 1$ GlyR values revealed significant changes for each value ($P < 0.001$; unpaired t-test; $n = 4$).

Again a LA potentiation is evident, but the EC₅₀ value is significantly increased reaching a concentration of $1400 \pm 61 \mu$ M ($P < 0.001$, unpaired t-test; $n = 4$). In contrast, the maximum increase in current was 4.0 ± 0.2 fold which reflects perfectly the corresponding wt $\alpha 1$ GlyR value. At all investigated GlyRs, we observed no partial agonism by thy.

Next, we investigated the 4-cthy effects on the mutated $\alpha 1$ GlyRs. Reflecting thy effects, no HA modulation but a LA potentiation by 4-cthy is observable at $\alpha 1$ Phe293Ala GlyRs (Fig. 5C). LA potentiation reached a maximum increase in current of 0.86 ± 0.1 fold and an EC₅₀ value of 1109 ± 41 μ M (Fig. 5C; Table 2). Comparison with the respective wt $\alpha 1$ GlyR values reveal a significant change concerning the LA EC₅₀ value ($P < 0.001$; unpaired t-test; $n = 4$).

At $\alpha 1$ Ser296Ala GlyRs, pre-applications of 4-cthy resulted in a dose-dependent biphasic potentiation of the EC₂₀ Gly-evoked currents (Fig. 5C). The maximum increase in current reached 0.32 ± 0.03 fold, reflecting perfectly the fold change in current of the $\alpha 2$ GlyR HA potentiation. Saturation developed around ~ 10 μ M and the EC₅₀ value reached 133 ± 32 nM (Fig. 5C). LA potentiation reached a maximum increase in current of 2.11 ± 0.2 fold with an EC₅₀ value of 351 ± 23 μ M and comparison with the respective wt $\alpha 1$ GlyR values revealed a significant change accordingly the LA EC₅₀ value ($P < 0.001$, unpaired t-test; $n = 4$).

Finally, we investigated the $\alpha 1$ Phe402Ala substitution. HA modulation by 4-cthy is not observable but concentrations above ≥ 100 μ M potentiated the EC₂₀ Gly-evoked currents up to 1.56 ± 0.1 fold with an EC₅₀ value of 1023 ± 40 μ M reflecting the LA site potentiation at wt $\alpha 1$ GlyRs (Fig. 5C). Again, no partial agonism at all tested GlyR mutants was observable. All values are reported in table 2.

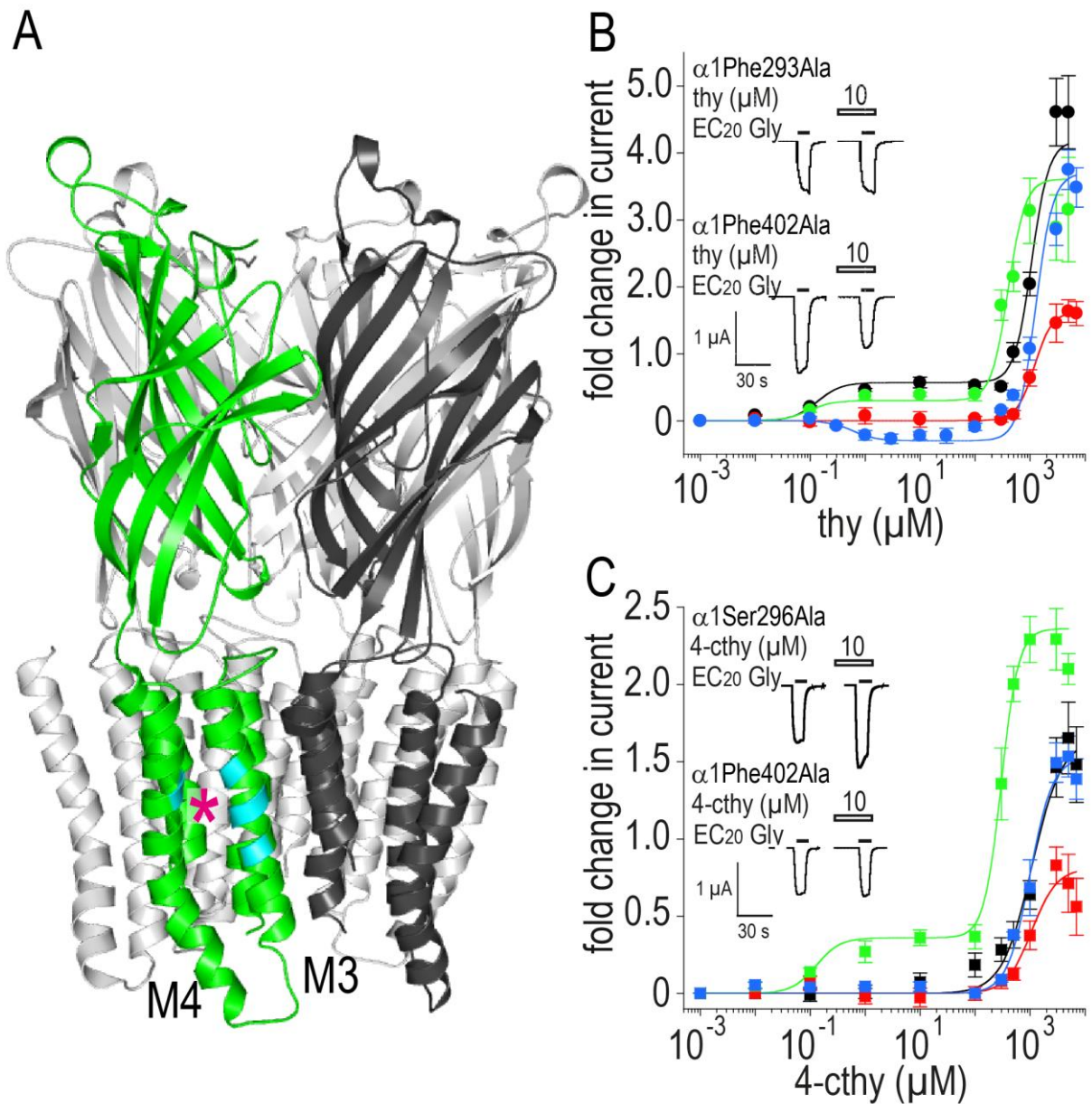


Figure 5: Model and mutational analyses of thy and 4-cthy effects at pro and 4-cpro HA site $\alpha 1$ GlyR mutants. **A.** Homology model of the $\alpha 1$ GlyR illustrating the pro and 4-cpro HA site (marked with a magenta star). Two subunits viewed from lateral (shown in green and black) are depicted with color coded regions indicating the pro and 4-cpro HA binding site in the M3 and M4. **B.** and **C.** Averaged change in currents (mean \pm S.E.M) by thy (**B.**) and 4-cthy (**D.**). **Insets** show recordings from oocytes injected with mutated $\alpha 1$ GlyR cRNAs and changes on the respective EC₂₀ Gly-evoked currents by 10 μ M thy and 4-cthy, respectively.

Table 2: Parameters for thy and 4-cthy effects at homomeric $\alpha 1$ GlyRs carrying amino acid substitutions in the pro and 4-cpro HA site (mutant listed in left column). EC₅₀ for each of n cells with the monophasic Hill equation, and mean \pm S.E.M. are given. Maximum fold change indicates the maximum change in current, respectively.

GlyR		thy			4-cthy		
HA site	EC ₅₀ (nM)	Maximum fold change	n	EC ₅₀ (nM)	Maximum fold change	n	
$\alpha 1$ wt	173 \pm 28	0.57 \pm 0.1	7	o	o	8	
$\alpha 1$ Phe293Ala	o	o	5	o	o	4	
$\alpha 1$ Ser296Ala	130 \pm 3	0.39 \pm 0.03	4	223 \pm 21	0.32 \pm 0.03***	4	
$\alpha 1$ Phe402Ala	670 \pm 80 ^{b***}	0.28 \pm 0.1 ^{a***}	4	o	o	4	
LA site	EC ₅₀ (μ M)	Maximum fold change	n	EC ₅₀ (μ M)	Maximum fold change	n	
$\alpha 1$ wt	981 \pm 62	4.08 \pm 0.55	7	1109 \pm 41	1.61 \pm 0.2	7	
$\alpha 1$ Phe293Ala	1107 \pm 112	2.1 \pm 0.2**	5	1109 \pm 41	0.86 \pm 0.1*	4	
$\alpha 1$ Ser296Ala	489 \pm 67***	3.1 \pm 0.4	4	351 \pm 23***	2.11 \pm 0.2	4	
$\alpha 1$ Phe402Ala	1400 \pm 61***	4.0 \pm 0.2	4	1023 \pm 40	1.56 \pm 0.1	4	

The respective Hill coefficients (nH) were between 0.7 and 1 for the HA site and between 1.3 and 2.2 for the LA site. o could not be detected; ^afold inhibition of the EC₂₀ Gly; ^bIC₅₀ and maximum % inhibition; * $P < 0.05$, *** $P < 0.001$ compared to $\alpha 1$ GlyRs, unpaired Student's t-test.

In summary, elimination of the aromatic side chains Phe293 and Phe402 has a dramatic effect on the thy HA modulation reflecting previously reported results by us (chapter 2 and 3). Thy HA potentiation was abolished (Phe293Ala) and converted (Phe402Ala). LA potentiation was present at these substitutions. In contrast, $\alpha 1$ GlyRs carrying the Ser296Ala substitution still show a template like biphasic potentiation. In the case of 4-cthy, we observed a biphasic potentiation at the Ser296Ala substitution which mirrors the $\alpha 2$ GlyR modulation. Remarkably, the substitution equates to the natural $\alpha 2$ GlyR amino acid at this position which supports the idea that this non conserved residue is an important determinant for the subtype specific HA modulation of GlyRs by 4-cthy and 4-cpro. Based on these results we assume that thy and 4-cthy HA modulation is mediated by the pro and 4-cpro HA site.

HA modulation determining residues in homomeric α GlyRs

Next, we were interested in the molecular background of the subtype specific HA modulation of $\alpha 2$ and $\alpha 3$ GlyRs. We speculate that the non-conserved M3 296 and especially the M4 394 ($\alpha 1$ numbering) residues are determinants for the subtype specificity and generated point mutations at this amino acids positions in the α GlyR

subtypes. We substituted the residues $\alpha 1$ Gly394 to Ala ($\alpha 2$) and Cys ($\alpha 3$), the $\alpha 2$ Ala303 to a Ser ($\alpha 1$) and the $\alpha 3$ Cys387 to a Gly ($\alpha 1$) and measured 4-cthy effects on the mutant GlyR function (Fig. 6A). Especially the $\alpha 1$ Gly394 residue is of high interest because this amino acid is variable in all GlyR subtypes and located in the vicinity of the HA binding site (Fig. 6B, inset).

We first measured if the substitutions affect the function of the GlyRs. Each substitution resulted in functional GlyRs with no obvious changes accordingly the Gly activation compared to the respective wt values (see appendix). Next, we analyzed 4-cthy effects on the Gly394Ala substitution which equates to the natural $\alpha 2$ GlyR residue. 4-cthy pre-applications resulted in a HA dose-dependent inhibition of the Gly-evoked current. The 4-cthy HA inhibition saturated around $\sim 10 \mu\text{M}$. The maximum inhibition of the currents reached -0.3 ± 0.1 fold with an IC_{50} value of $1300 \pm 400 \text{ nM}$. LA site modulation was again a dose-dependent potentiation of the currents up to 1.88 ± 0.18 fold yielding an EC_{50} value of $443 \pm 124 \mu\text{M}$. The calculated values reflected the $\alpha 2$ GlyR LA site values more than the template $\alpha 1$ GlyR values. Comparison of the values revealed a significant change accordingly the EC_{50} value of the LA site modulation ($P < 0.001$, unpaired t-test; $n = 4$; Fig. 6B).

Similar to $\alpha 1$ Gly394Ala GlyRs, 4-cthy also HA inhibited the function of the $\alpha 3$ GlyR reflecting Gly394Cys substitution. The maximum inhibition of the current was -0.50 ± 0.06 fold and the corresponding IC_{50} value reached $80 \pm 25 \text{ nM}$. 4-cthy LA site modulation of the Gly394Cys currents reached a maximum increase in current of 2.4 ± 0.24 fold and an EC_{50} value for potentiation of $530 \pm 76 \mu\text{M}$ (Fig. 6B). Comparison with the template GlyR LA site values revealed a significant change in the EC_{50} value of the LA site potentiation ($P < 0.001$; unpaired t-test; $n = 4$).

Accordingly the partial agonism, 4-cthy evoked no chloride currents at the investigated $\alpha 1$ GlyR mutants.

Next, we analyzed 4-cthy effects on the $\alpha 2$ Ala307Ser mutation. Pre-applications of 4-cthy in concentrations ranging from 100 pM to $10 \mu\text{M}$ had no obvious effect on the EC_{20} Gly-evoked current (Fig. 6C, inset). 4-cthy concentrations above $10 \mu\text{M}$ resulted in a dose dependent LA potentiation. The maximum increase in current was 1.86 ± 0.13 fold and the LA EC_{50} value was $331 \pm 13 \mu\text{M}$ (Fig 6C). Subsequent to the LA site potentiation, we observed a partial agonism by 4-cthy at $\alpha 2$ Ala303Ser GlyRs. The EC_{50} value and strength of the 4-cthy evoked currents were not significantly different compared to the calculated wt $\alpha 2$ GlyR values (data not shown).

Finally, we analyzed 4-cthy effects at the $\alpha 1$ GlyR corresponding $\alpha 3$ Cys387Gly substitution. Again, 4-cthy exerts no HA modulation (Fig. 6D inset). However, concentrations above 10 μ M induced a single LA potentiation with a maximum increase in current of 2.08 ± 0.21 fold and an LA EC₅₀ value of 454 ± 43 μ M. Compared to the respective wt GlyR values, the $\alpha 3$ Cys387Gly GlyRs showed a significant 1-fold left shift in the EC₅₀ value of the LA potentiation ($P < 0.001$, unpaired t-test; $n = 5$; Fig. 6D). All values are reported in table 3.

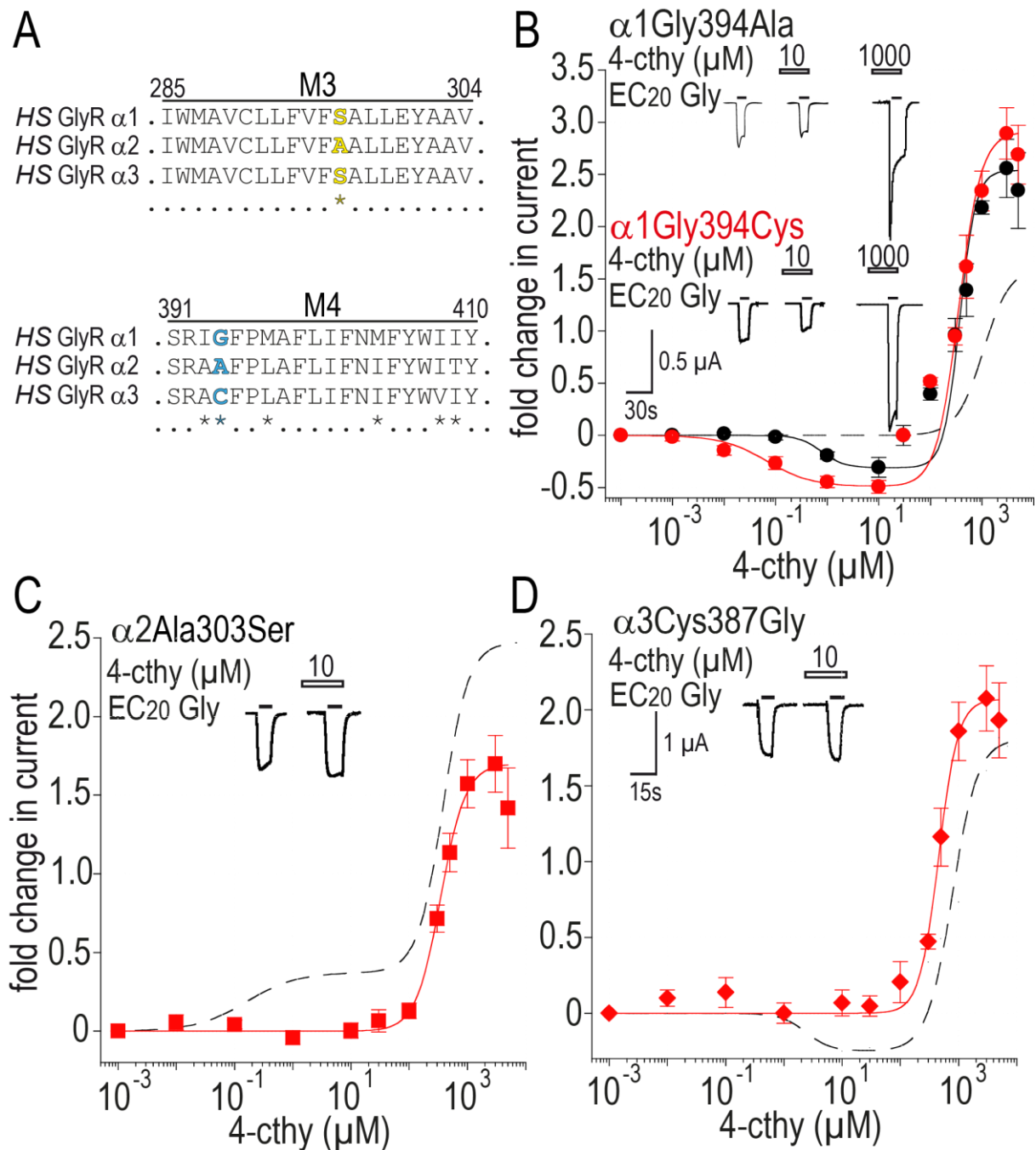


Figure 6: 4-cthy modulation of mutant α GlyRs. **A.** GlyR subtype amino acid alignment of the M3 and M4. Colored in blue the M4 Gly394 (α 1 numbering) non-conserved residue that was chosen for the investigation of 4-cthy effects. **B.** Averaged changes in currents of mutated α 1 GlyRs (mean \pm S.E.M. of 3 to 5 cells) caused by pM to μ M concentrations of 4-cthy (colored with the following code: in black α 1Gly394Ala and in red α 1Gly394Cys). Here and in the following cases, dashed lines represents 4-cthy effects of the respective α GlyRs. **Inset** shows recordings from oocytes injected with α 1Gly394Ala and α 1Gly394Cys GlyR cRNAs and 4-cthy effects on the EC₂₀ Gly-evoked currents. **C.** Averaged changes in currents by 4-cthy at α 2Ala303Ser GlyRs (red squares; mean \pm S.E.M. of 4 cells, respectively) caused by nM to mM concentrations of 4-cthy. **Inset** shows recordings from oocytes injected with α 2Ala303Ser GlyR cRNAs showing abolished 4-cthy effects on the EC₂₀ Gly-evoked currents. **D.** Averaged changes in currents of mutated α 3 GlyRs (red diamonds; mean \pm S.E.M. of 4 cells) caused by nM to mM molecule concentrations of 4-cthy. **Inset** shows recordings from oocytes injected with α 3Cys387Gly GlyR cRNAs showing abolished 4-cthy effects on the EC₂₀ Gly-evoked currents.

Table 3: Parameters for 4-cthy effects at mutated $\alpha 1$, $\alpha 2$ and $\alpha 3$ GlyRs (substitutions listed in left column). EC_{50} and n_H values were calculated for each of n cells with the monophasic Hill equation, and mean \pm S.E.M. are given. Maximum fold change indicates the maximum change in current. For direct activation, maximum activation by 4-cthy (I4-cthy) is given under the *maximum fold change* column, expressed as the percentage fraction of maximum activation by Gly (I_{MAX} Gly).

GlyR	4-cthy			
	HA site	EC_{50} (nM)	maximum fold change	n
$\alpha 1$ Gly394Ala		1300 ± 400^a	0.3 ± 0.1^a	4
$\alpha 1$ Gly394Cys		104 ± 20^a	0.5 ± 0.04^a	4
$\alpha 2$ Ala303Ser		<i>nm</i>	<i>nm</i>	5
$\alpha 3$ Cys387Gly		<i>nm</i>	<i>nm</i>	5
LA site	EC_{50} (μ M)	maximum fold change	n	
$\alpha 1$ Gly394Ala		$443 \pm 124^{***}$	1.9 ± 0.2	4
$\alpha 1$ Gly394Cys		$530 \pm 76^{***}$	2.4 ± 0.2	4
$\alpha 2$ Ala303Ser		331 ± 13	1.7 ± 0.1	5
$\alpha 3$ Cys387Gly		$454 \pm 43^{***}$	2.1 ± 0.2	5

The respective Hill coefficients (nH) were between 0.7 and 1 for the HA site and between 1.3 and 2.2 for the LA site. *nm* no modulation; ^aIC₅₀ and current inhibition * $P < 0.05$, *** $P < 0.001$ compared to the respective wt α GlyRs values reported in table 1, unpaired t-test.

In summary, $\alpha 1$ GlyRs carrying the $\alpha 2$ -, $\alpha 3$ - corresponding amino acid at the position Gly394, showed a dose-dependent HA inhibition by 4-cthy. Accordingly the LA site modulation, 4-cthy potentiated the $\alpha 1$ GlyR mutants but with significant changes in the potencies and efficacies compared to the respective wt GlyR parameters. Partial agonism by 4-cthy was not evident, reflecting the template behavior. At the $\alpha 2$ - and $\alpha 3$ GlyR mutants HA site modulation by 4-cthy was abolished by the $\alpha 1$ GlyR corresponding substitutions. The LA site potentiation and the $\alpha 2$ GlyR specific partial agonism by 4-cthy was still present.

PMTS modification of the M4 $\alpha 1$ Gly394Cys substitution abolishes 4-cthy HA inhibition

Finally, we asked us if $\alpha 1$ Gly394Cys GlyRs are accessible for the thiol reactive compound PMTS. PMTS can modify Cys side chains in proteins by the creation of a covalent disulfide bond between the thiol group of a Cys and PMTS. However, a successful modification depends on two aspects: the Cys must be accessible for PMTS and located in a hydrophilic environment that ionizes thiol groups. The ionization is the driving force of this non enzymatic coupling reaction (Karlín and

Akabas, 1998). A successful covalent modification can then be indicated by irreversible changes to the agonist activation of the protein.

We incubated oocytes expressing wt and $\alpha 1$ Gly394Cys GlyRs for 5 min in a 1 mM PMTS solution and compared the current strength of the EC20 Gly activation before and after. In the case of wt $\alpha 1$ GlyR expressing oocytes, incubation in PMTS caused only a single and significant increase in the current of 0.25 ± 0.04 fold (Fig. 7A; $P < 0.001$, paired t-test; $n = 5$ oocytes). Following EC20 Gly applications in 5 min steps over a total time of 20 min resulted in no additional current enhancements. In the case of the substitution, the EC20 Gly-evoked currents were increased up to 0.88 ± 0.07 fold and following Gly applications showed the presence of a stable increase in current over the observed total time span of 20 min which is characteristically for a PMTS modification of a Cys side chain (Fig. 7B, red symbols and line).

Next, we tested if the presence of 4-cthy affects the covalent modification of $\alpha 1$ Gly394Cys GlyRs. Therefore, we incubated the oocytes in a 10 μ M 4-cthy/ 1mM PMTS solution for 5 min and measured the EC20 Gly-evoked current strength over a total time of 15 min. In contrast to the incubation in PMTS alone, we detected a single significant 0.41 fold increase in the current directly after the incubation, but the current potentiation went down to the initial value following Gly applications (Fig. 7B $P < 0.001$, paired t-test; $n = 4$ oocytes).

Finally, we analyzed if the PMTS modification affects the 4-cthy modulation. Pre-application of nM to μ M 4-cthy concentrations to modified GlyRs (Fig. 7C; top vs. bottom panel) resulted in no detectable EC20 Gly-evoked current inhibition by 4-cthy (Fig. 7D). However, the presence of 5 mM 4-cthy potentiated the Gly-evoked currents of non- (-) and modified (+) GlyRs up to an equal value (Fig. 7D, inset).

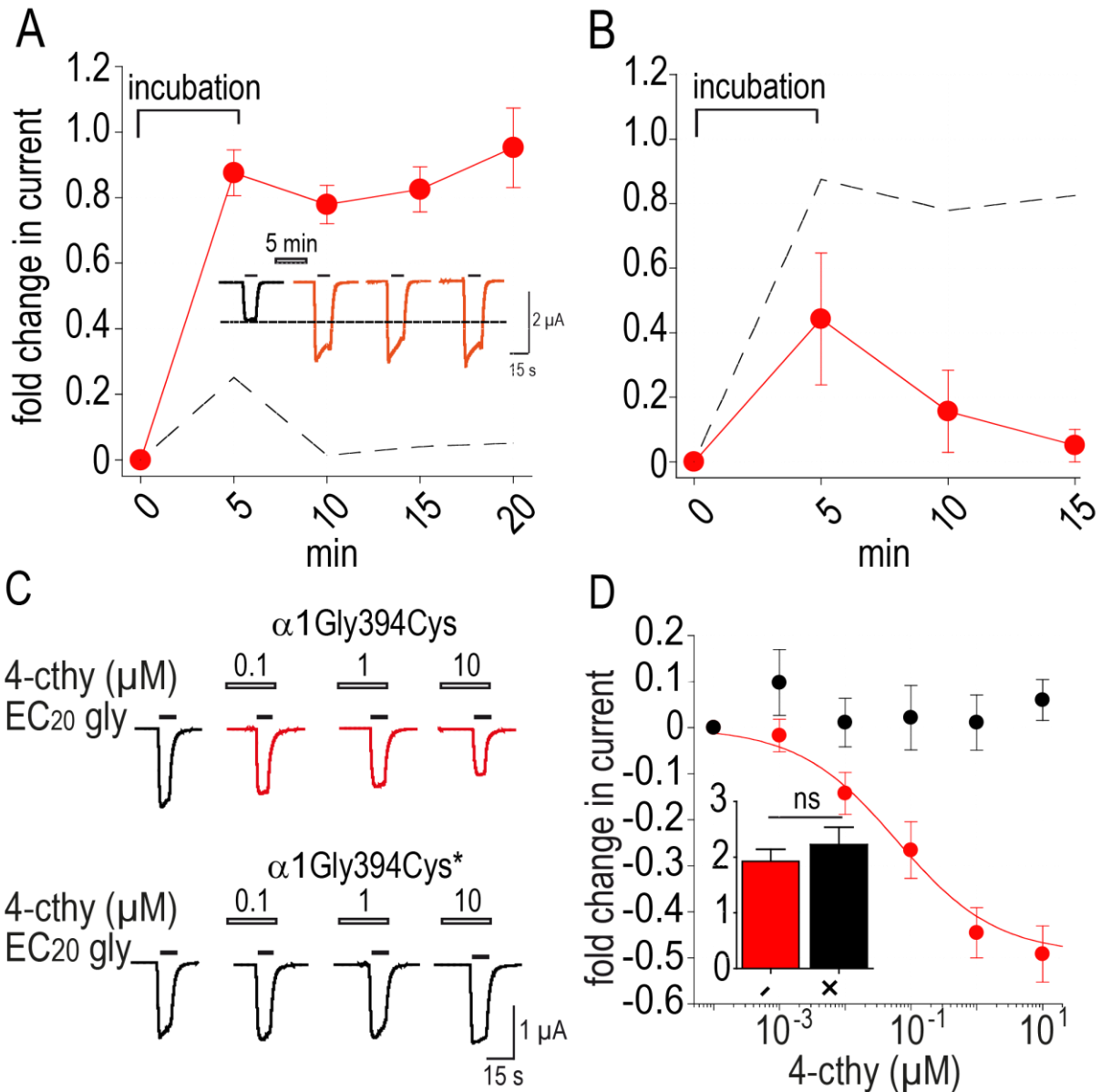


Figure 7: PMTS modifies $\alpha 1$ Gly394Cys GlyRs and abolishes 4-cthy HA inhibition **A.** Effects on wt (black circles) and $\alpha 1$ Gly394Cys GlyRs (red circles) EC₂₀ Gly-evoked currents after 5 min incubation in a 1 mM PMTS solution. Insets: recordings from oocytes expressing $\alpha 1$ Gly394Cys GlyR. Inset represents PMTS effects on EC₂₀ Gly-evoked currents of $\alpha 1$ Gly394Cys GlyRs before (black traces) and after incubation for 5 min in 1 mM PMTS (red traces). **B.** Absent EC₂₀ Gly-evoked current potentiation by PMTS after incubation of oocytes in a 10 μM 4-cthy / 1 mM PMTS solution (red circles and line). For a better comparison the effects on currents by 1 mM PMTS, are shown as a black dashed line (mean \pm S.E.M. of 4 cells respectively). **C.** Recordings from oocytes expressing $\alpha 1$ Gly394Cys GlyR showing 4-cthy HA inhibition (top panel) and absent modulation after incubation for 5 min in 1 mM PMTS (bottom panel). **D.** Absent 4-cthy HA inhibition of $\alpha 1$ Gly394Cys GlyRs (black circles) after covalent modification in a 1 mM PMTS solution. Red circles represent the 4-cthy HA inhibition of non modified $\alpha 1$ Gly394Cys GlyRs (mean \pm S.E.M. of 4 cells respectively). Inset represents a column diagram showing the fold change in current by 5 mM 4-cthy of non- (red bar) and modified (black bar) $\alpha 1$ Gly394Cys GlyRs (unpaired t-test; mean \pm S.E.M. of 4 oocytes, respectively).

In summary, PMTS covalently modifies α 1Gly394Cys GlyRs. The modification results in an irreversible potentiation of the chloride currents and can be blocked by co-incubation in HA site saturating concentrations of 4-cthy. Vice versa, PMTS blocks the HA inhibition of α 1Gly394Cys GlyRs by 4-cthy whereas LA potentiation is unaffected.

Conclusions

In the present study, we examined the effects of the monophenols thy and 4-cthy and characterized them as allosteric modulators of homomeric GlyRs. TEVC analysis also showed that the molecules are clear subtype-specific HA and LA modulators comparable to pro and 4-cpro (chapter 2 and 3). Co-application experiments with 4-cthy, indicated that 4-cthy and thy affect the GlyR function via binding to the pro and 4-cpro HA site. This assumption was proofed by the characterization of thy and 4-cthy effects at $\alpha 1$ GlyRs carrying amino acid substitutions in the pro and 4-cpro HA binding.

By amino acid substitutions of non-conserved residues in the M3 and M4 of $\alpha 1$ -, $\alpha 2$ - and $\alpha 3$ GlyRs, we were able to change the type of HA site modulation at each GlyR subtype. Especially the amino acid substitutions $\alpha 1$ Gly394Cys ($\alpha 1$ to $\alpha 3$), $\alpha 1$ Ser296Ala ($\alpha 1$ to $\alpha 2$) and $\alpha 2$ Ala304Ser ($\alpha 2$ to $\alpha 1$) converted the subtype specific type of HA modulation to the type HA modulation of the target wt type. Remarkably, the substitutions did not affect the common LA site potentiation and partial agonism. These data clearly underline that non conserved residues in the HA site are molecular determinants for the GlyR subtype specific HA modulation by 4-cthy.

In addition, we observed that the M4 Gly394Cys substitution can be covalently modified by PMTS. The modification blocked the substitutions HA inhibition by 4-cthy whereas LA site potentiation was unaffected. Vice versa, the presence of 10 μ M 4-cthy blocked the PMTS modification of these mutated $\alpha 1$ GlyRs underlining the idea that the HA site is located in this region of the GlyRs.

Discussion

HA and LA modulation by thy and 4-cthy is mediated by distinct binding sites

The HA and LA site modulation of the GlyR subtypes by thy and 4-cthy can be distinguished by several factors known to be characteristic for the action of a binding site (Laube et al., 2000). Obviously are the differences in the potency and efficacy between the HA and LA modulation, the presence of a plateau phase which divides the two distinct modulatory phases and the differential pharmacology in form of the subtype specific HA modulation. For example, HA EC₅₀ values for thy, are indistinguishable at $\alpha 1$ and $\alpha 2$ GlyRs, and no HA potentiation of $\alpha 3$ GlyRs was observed, whereas LA EC₅₀ values for thy are indistinguishable at all three subtypes. In the case of thy at $\alpha 3$ GlyRs, HA modulation is absent; LA modulation and direct activation are present. One might interpret this not as an example of the absence of the HA phase and the presence of the other two phases, but merely as an altered potency in $\alpha 3$ GlyRs of the same HA and LA modulation present in $\alpha 1$ GlyRs (which show HA and LA potentiation and no direct activation by thy). However, in the case of 4-cthy at $\alpha 2$ GlyRs, we observed multiple effects like HA-, LA modulation and direct activation. Furthermore, the similarity in thy EC₅₀ values for HA (140-173 nM) and LA effects (981-1035 μ M) across the subtypes reiterate the distinct potencies of each effect. Such differential sensitivities across the subtypes for at least one modulatory phase can be best explained by the presence of a common binding site with non conserved molecular determinants.

A new aspect is that binding can still occur, whereas modulation is absent. This is observable for 4-cthy at $\alpha 1$ GlyRs. The fact that the presence of HA site characteristic concentrations of 4-cthy abolishes pro and thy modulation can be counted as a direct evidence for two aspects. Firstly, the mentioned molecules bind to the same site and secondly, determinants of the HA site between the GlyR subtypes are different because 4-cthy exert a clear differential pharmacology at the GlyR subtypes.

Another aspect which is not fully confirmed but conceivable is that the addition of a methyl group is unfavorable for the HA site modulation of $\alpha 1$ GlyRs when simultaneously a chlorine atom is added to the C4-position. It can be speculated by recapitulation of the former presented results from chapter 2. Sadly, a final proof of

this hypothesis is at the moment not possible because this kind of structure is not available.

HA site modulation by thy and 4-cthy is mediated via the pro and 4-cpro site

Another mayor finding of this study is that the HA modulation of GlyRs by thy and 4-cthy is mediated via the pro and 4-cpro HA binding site. This is supported by several aspects: I.) The structural and physicochemical homologies between the molecules. Compared to pro and 4-cpro, only small changes in the grade of alkylation (5' and 6' position of the phenol scaffold) as well as in the lipophilic properties are given (Reiner et al., 2009). II.) Due to the similar pharmacological parameters by which the molecules modulate the GlyR function. This is for example clarified by the comparison of thy and pro HA and LA site values at homomeric α 1- and α 2 GlyRs. III.) By the loss of the pro and thy HA site potentiation in the presence of 4-cthy which indicates that 4-cthy reaches the site at wt α 1 GlyRs. IV.) The HA site specific changes at GlyRs carrying amino acid substitutions known to be crucial for the pro and 4-cpro HA site modulation. Noteworthy is the converted and absent thy HA modulation at α 1 GlyRs carrying the Phe402Ala (inhibition) and Phe293Ala (absent) substitution reflecting pro and 4-cpro effects at these mutant α 1 GlyRs (chapter 2 and 3). V.) The absent PMTS modification in the presence of 4-cthy and vice versa the absent 4-cthy HA site inhibition at PMTS modified α 1Gly394Cys GlyRs.

In summary, these indications clearly point out that HA modulation by thy and 4-cthy of GlyR subtypes function is mediated via the pro and 4-cpro HA binding site.

Non conserved amino acids in the M3 and M4 determine the type of HA site modulation at GlyRs

Another mayor finding of this study is that the subtype specific 4-cthy HA modulation is mediated by non conserved amino acids in the M3 and M4 in the α GlyR subtypes. The possibility to convert allosteric properties of a modulator by site-specific mutagenesis can be interpreted as an evidence for the involvement of the mutated elements in the allosteric action of a binding site. Similar observations were presented for ivermectin and cannabinoids at the GlyR (Lynagh et al., 2011; Xiong et al., 2011). As previously shown by Xiong and colleagues, substitution of the α 1Ser296 residue to the respective α 2 GlyR residue which is an Ala, reduced the sensitivity towards the cannabinoid THC from α 1 to α 2 GlyR levels indicating that the

position is involved in the GlyR subtype specific modulation by the mentioned cannabinoid (Xiong et al., 2011).

In our case, we can conclude that the opposite effect, the reduction of the Ser296 side chain is important for the creation of the 4-cthy HA site potentiation whereas the increase in the hydrophobicity and the length of the Gly394 side chain results in an inhibition.

These suggestions are in line with the 4-cthy effects at α 2Ala303Ser and α 3 Cys387Gly GlyRs. However, in the case of the α 3Cys387Gly GlyRs, we want to note that the modulatory important M3 serine (in α 1 GlyRs position 296) is still present which could explain why no HA site modulation is observable. It might be of great interest to analyze the 4-cthy HA site effects at α 3 GlyRs carrying the double substitutions Ser301Ala and Cys387Gly. If these α 3 GlyRs still show a 4-cthy HA site potentiation, our suggestion about the role of the side chain length at the M4 Gly394 (α 1 numbering) residue as a important determinant for the HA site potentiation would be secured.

That the M4 amino acid is a part of the HA binding site is supported by two additional points: The absent HA inhibition by 4-cthy after PMTS modification of α 1Gly394Cys GlyRs and vice versa the elimination of the PMTS modification in the presence of 4-cthy.

In summary, based on the above discussed points we can assume that the investigated M3 and M4 amino acids are direct molecular determinants of the subtype-specific HA site modulation of homomeric GlyRs by 4-cthy and with a high possibility also for pro, 4-cpro and thy.

References

- Ahrens J, Leuwer M, Stachura S, Krampfl K, Belelli D, Lambert JJ and Haeseler G (2008) A transmembrane residue influences the interaction of propofol with the strychnine-sensitive glycine $\alpha 1$ and $\alpha 1\beta$ receptor. *Anesth Analg* **107**(6): 1875-1883.
- Barann M, Linden I, Witten S and Urban BW (2008) Molecular actions of propofol on human 5-HT_{3A} receptors: enhancement as well as inhibition by closely related phenol derivatives. *Anesth Analg* **106**(3): 846-857, table of contents.
- Betz H and Laube B (2006) Glycine receptors: recent insights into their structural organization and functional diversity. *J Neurochem* **97**(6): 1600-1610.
- Boudry G and Perrier C (2008) Thyme and cinnamon extracts induce anion secretion in piglet small intestine via cholinergic pathways. *J Physiol Pharmacol* **59**(3): 543-552.
- de la Roche J, Leuwer M, Krampfl K, Haeseler G, Dengler R, Buchholz V and Ahrens J (2012) 4-Chloropropofol enhances chloride currents in human hyperekplexic and artificial mutated glycine receptors. *BMC Neurol* **12**(1): 104.
- Eckle VS, Grasshoff C, Mirakaj V, O'Neill PM, Berry NG, Leuwer M and Antkowiak B (2014) 4-bromopropofol decreases action potential generation in spinal neurons by inducing a glycine receptor-mediated tonic conductance. *Brit J Pharmacol*.
- Garcia DA, Bujons J, Vale C and Sunol C (2006) Allosteric positive interaction of thymol with the GABAA receptor in primary cultures of mouse cortical neurons. *Neuropharmacology* **50**(1): 25-35.
- Grasshoff C and Gillessen T (2005) Effects of propofol on N-methyl-D-aspartate receptor-mediated calcium increase in cultured rat cerebrocortical neurons. *Eur J Anaesthesiol* **22**(6): 467-470.
- Haeger S, Kuzmin D, Detro-Dassen S, Lang N, Kilb M, Tsetlin V, Betz H, Laube B and Schmalzing G (2010) An intramembrane aromatic network determines pentameric assembly of Cys-loop receptors. *Nature structural & molecular biology* **17**(1): 90-98.
- Karlin A and Akabas MH (1998) Substituted-cysteine accessibility method. *Methods Enzymol* **293**: 123-145.
- Laube B, Kuhse J and Betz H (2000) Kinetic and mutational analysis of Zn²⁺ modulation of recombinant human inhibitory glycine receptors. *J Physiol* **522 Pt 2**: 215-230.
- Lynagh T, Webb TI, Dixon CL, Cromer BA and Lynch JW (2011) Molecular determinants of ivermectin sensitivity at the glycine receptor chloride channel. *J Biol Chem* **286**(51): 43913-43924.

- Lynch JW (2009) Native glycine receptor subtypes and their physiological roles. *Neuropharmacology* **56**(1): 303-309.
- Pistis M, Belelli D, Peters JA and Lambert JJ (1997) The interaction of general anaesthetics with recombinant GABAA and glycine receptors expressed in *Xenopus laevis* oocytes: a comparative study. *Brit J Pharmacol* **122**(8): 1707-1719.
- Priestley CM, Williamson EM, Wafford KA and Sattelle DB (2003) Thymol, a constituent of thyme essential oil, is a positive allosteric modulator of human GABA(A) receptors and a homo-oligomeric GABA receptor from *Drosophila melanogaster*. *Br J Pharmacol* **140**(8): 1363-1372.
- Reiner GN, Labuckas DO and Garcia DA (2009) Lipophilicity of some GABAergic phenols and related compounds determined by HPLC and partition coefficients in different systems. *J Pharm Biomed Anal* **49**(3): 686-691.
- Xiong W, Cheng K, Cui T, Godlewski G, Rice KC, Xu Y and Zhang L (2011) Cannabinoid potentiation of glycine receptors contributes to cannabis-induced analgesia. *Nat Chem Biol* **7**(5): 296-303.
- Yevenes GE and Zeilhofer HU (2011a) Allosteric modulation of glycine receptors. *Brit J Pharmacol* **164**(2): 224-236.
- Yevenes GE and Zeilhofer HU (2011b) Molecular sites for the positive allosteric modulation of glycine receptors by endocannabinoids. *PLoS One* **6**(8): e23886.

6. General discussion

The glycine receptor (GlyR) transmembrane domains (TMDs); more than just anchors

TMDs are structures important for the function, assembly and allosteric modulation of pentameric ligand gated ion channels (pLGICs) (Baenziger and Corringer, 2011; Chen et al., 2009; Del Sol et al., 2007; Franks, 2006; Haeger et al., 2010; Hibbs and Gouaux, 2011; Mowrey et al., 2013; Sauguet et al., 2014; Yamakura et al., 1999). The results presented in this thesis show that especially the $\alpha 1$ Gly- and serotonin type 3A receptor (5-HT3AR) M3 and M4 are key determinants for these aspects. Visual inspection of the M4 amino acid side chain orientations in an $\alpha 1$ GlyR homology model based on the crystal structure of ELIC (see chapter 1) reveal the presence of multiple contacts to lipids and towards amino acids of the remained TMDs. The amino-amino acid contacts can be found within one subunit as well as to amino acids of the adjacent subunits, especially in a region named interface. The major type of relevant amino-amino acid contacts, mediating the assembly and function of $\alpha 1$ GlyRs, are aromatic interactions. This was validated by non- and isofunctional amino acid substitutions and subsequent electrophysiological investigations combined with biochemical assays targeting the expression, assembly and surface localization.

Based on these procedures, we observed that the elimination of specific aromatic interactions affects the function of the GlyR, negatively. Following the results obtained by the biochemical assays we can distinct between two situations responsible for the decreased or absent function: Firstly, a loss of surface located GlyRs and secondly that the impaired agonist activation based on alterations in the signal transduction process (Edelstein and Le Novere, 2013; Prinz, 2010). This is in line with previous findings, showing the importance of amino acid interactions within or between the pLGICs TMDs for the channel opening and closing. Moreover, with the characterization of the Ala288Ile mutation as a putative gating mutation, we obtained data showing the importance of a TMD amino acid for the signal transduction process. The Ala288Ile substitution increases the efficacy of $\alpha 1$ GlyRs towards the partial agonist GABA, massively (Bode and Lynch, 2013; Cadugan and Auerbach, 2007; Du et al., 2015; Mitra et al., 2004; Nemezc et al., 2016).

Remarkably, recently published investigations have supported our assumptions about the role of the TMDs as important determinant for the function of pLGICs (Carswell et al., 2015; Henault et al., 2015).

In addition, we estimated here for the first time the exact location of two functional binding sites for the general anesthetic propofol (pro) and structural derivatives within the TMDs. We unmasked the exact location of an intrasubunit high- (HA) site, and determined residues of the TMD interface between adjacent subunits as an important molecular determinant for the low affinity (LA) binding site. These observations are in line with the findings by Duret and colleagues which suggested that the GlyR TMDs mediate the pro modulation of the GlyR function (Duret et al., 2011).

Therefore, we can assume that the role of the pLGICs TMDs is more complex than initially thought. Increasing the knowledge about them could lead to a step forward in clinically relevant fields like the treatment of neurological channelopathies.

Indications that GlyRs are high affinity targets of pro in vivo

Another observation by this study, that GlyRs possess over three functional binding sites for pro and derivatives, was not observed before. Published investigations targeting the type of allosteric modulation of GlyRs by pro show in general a low potent, but high efficient monophasic current potentiation (Lynagh and Laube, 2014; Pistis et al., 1997). Based on our findings of a biphasic modulation mediated by distinct binding sites, the question came up which of our characterized types of modulation equates to the classical known pro modulation in GlyRs?

Reported EC₅₀ values for the Gly-evoked current potentiation by pro were in the low to mid μ M concentration range and the maximum fold change in current varies from 1- up to 5-fold (Ahrens et al., 2004; de la Roche et al., 2012; Duret et al., 2011; Ghosh et al., 2013; Jayakar et al., 2013; Krasowski et al., 2002; Krasowski et al., 2001a; Krasowski et al., 2001b; Nury et al., 2011; Pistis et al., 1997; Trapani et al., 1998; Yip et al., 2013). Subsequent to the known allosteric modulation by pro, the molecule converts to a partial agonist (Ahrens et al., 2004; Ahrens et al., 2008; Nguyen et al., 2009; O'Shea et al., 2004; Pistis et al., 1997).

The reported values by the above mentioned studies, are in a good accordance with the parameters of our observed LA site potentiation. Therefore we assume that this is the classical known modulation of GlyRs by pro. Moreover, we observed that subsequent to the LA site potentiation, pro converts into a low efficient and potent

partial agonist. Another finding which supports this assumption is the fact that low concentrations of Gly were stronger potentiated by the LA site, with values reflecting data reported by for example Pistis and Lynagh. We therefore assume that the classical known pro modulation is the LA site potentiation presented in this study.

If pro concentrations inducing a LA site potentiation exist in vivo, cannot be excluded. However, we want to note that clinical relevant concentrations of pro, inducing anesthesia are $\leq 10 \mu\text{M}$. In contrary, LA potentiation inducing pro concentrations induce neurotoxicity in long time sedated mice (Franks, 2006; Sebastiani et al., 2016). These facts shed doubts, if the LA site modulation and partial agonism by pro take part in the in vivo effects by pro.

Concerning the HA site modulation by nM to μM concentrations, O'Shea and colleagues restored GlyR malfunction directly by pro injections with a concentration $\leq 10 \mu\text{M}$ in transgenic hyperekplexia mice. These mice were not sedated. Moreover, Eckle and colleagues showed modulation of GlyR activity in the presence of HA site potentiation characteristic concentrations of 4-Bromopropofol in slice preparations of the spinal cord from mice (Eckle et al., 2014; O'Shea et al., 2004). The fact that low μM doses of pro and derivatives lead in vivo and in slice preparations to a reduction of hyperekplexia characteristic tremor episodes and affect the GlyR mediated tonic activity suggest, that the GlyR is indeed a high affinity target for pro and derivatives.

In line with this suggestion are the findings that the M3 Ser296 in $\alpha 1$ GlyRs is in vivo a target residue for another potent substance class of allosteric modulators. As shown by Xiong and colleagues, cannabinoids restore GlyR malfunction in transgenic hyperekplexia mice via interactions with the M3 Ser296, which is also a critical residue for the subtype specific 4-cpro and 4-cthy HA site modulation in $\alpha 1$ and $\alpha 2$ GlyRs (Xiong et al., 2014; Xiong et al., 2011). In addition, an apparent competition between 4-cpro and the endocannabinoid AEA was unmasked by us, showing that 4-cpro acts via this binding site formed by M3 and M4 residues.

Another mayor finding of this study is that the aromatic residues M3 Phe293 and M4 Phe402 are important for the HA site modulation. Elimination of the aromatic side chain abolished and converted HA modulation by pro and derivatives. As discussed above, the aromatic interactions between the GlyR TMDs are of great importance for the correct function of the protein. Based on the importance of these residues for the HA potentiation by pro and derivatives, it could be speculated if the mechanism by which this site affect the GlyR activation (increase of the cooperativity) based on a

strengthening of the aromatic network. However, in-depth analysis targeting this aspect has to be performed to solve this question.

The GlyR TMD interface; an important region for the common allosteric modulation of GlyRs

The fact that all molecules induced a LA potentiation complicated the search for molecular determinants of this site massively. However, by observing an decrease of the IVM potentiated Gly-evoked chloride currents by LA site potentiation characteristic pro concentrations and the subsequent TEVC characterizations of amino acids substitutions in the IVM binding site, we obtained data showing that the LA site is located in the TMD interface. Moreover, we collected basic data showing that the Ala288 residue plays an important role for the allosteric modulation and activation of the GlyR (Lynagh and Laube, 2014; Mowrey et al., 2013; Yamakura et al., 1999). The Ala288Ile substitution also abolishes the allosteric modulation of $\alpha 1$ GlyRs by the endocannabinoid AEA. As reported above AEA modulation based on a polar interaction between AEA and the M3 Ser296 which is an important determinant of the pro and derivatives HA binding site. Moreover, TEVC analysis concerning the GABA activation of these mutated $\alpha 1$ GlyRs unmasked a substitutions related effect on the gating. The efficacy by which the partial agonist GABA activated $\alpha 1$ Ala288Ile GlyRs is massively increased compared to wt values. Interestingly, pro also increases the partial agonist efficacy at wt GlyRs (Biro and Maksay, 2004). Therefore it can be speculate that the change in the gating behavior by the M3 Ala288Ile substitution is the key determinant for the absent AEA and pro modulation.

However, it could be also that the absent AEA and pro HA modulation base on substitutions related structural changes in the below located amino acid orientations (Nussinov, 2012). As shown in this study, the neighboring Val289 is a determinant of the HA site for pro and 4-cpro. Therefore, we cannot exclude that the Ile substitution induces a direct effect in form of an structural reorganization in the HA site. Further analysis including site-directed mutagenesis should proof this assumption. Interestingly, previously published studies unmasked in the M3 of the $\beta 1$ - and $\beta 3$ GABA(A)R subtype a methionine (Met) which is important for the monophasic pro modulation of the receptor function. This Met equates to the Ala288 in α GlyRs (see appendix). Substitution of the $\beta 1$ Met to a tryptophan (Trp) abolished pro potentiation in homo- and heteromeric GABA(A)Rs (Krasowski et al., 2001b). But, experiments

targeting a direct competition between pro and reactive etomidate derivate which binds to this residue, resulted only in a partial inhibition of the labeling reaction indicating a non competitive behavior between pro and the reactive etomidate at this position (Li et al., 2010). However, pro binding in the $\beta 3$ subtype of GABA(A)Rs can be blocked directly by an photo reactive derivate of pro (Yip et al., 2013). Remarkably, amino acid substitutions which increase the hydrophobicity of the 288 position abolished and converted the allosteric modulation of homomeric $\alpha 1$ GlyRs by volatile anesthetics (Yamakura et al., 1999). Taken together, these results indicate the importance of the GlyR TMD interface and especially Ala288, for the allosteric modulation by pro and other molecules as well as for the full and partial agonist activation.

4'Chlorination of pro and thy results is a key element for the creation of subtype-specific modulators at GlyRs

A major goal of medicinal chemistry is the generation of compounds that selectively target one subtype of a receptor family. For example, $\alpha 3$ -containing GlyRs are an attractive therapeutic target, because in contrast to the wide distribution of $\alpha 1$ -containing GlyRs in spinal cord motor circuitry, $\alpha 3$ -containing GlyRs appear restricted to nociceptive pathways (Harvey et al., 2004). Furthermore, establishing the tissue- or circuit-specific expression of the various subtypes would be greatly facilitated by compounds that show subtype specific modulations, allowing the functional dissection of subtype distribution. For the chlorinated pro and thy variants, we observed such effects. Therefore we speculate that monophenolic compounds appear uniquely promising basic modules for the creation of high affinity GlyR subtype specific modulators. This is shown perfectly with 4-cthy that exert no effect at $\alpha 1$ GlyRs; potentiation at $\alpha 2$ GlyRs; and inhibition of $\alpha 3$ GlyRs. Similarly, the pharmacological profile of 4-cpro can be also used to discriminate between homo- and heteromeric $\alpha 1$ and $\alpha 1\beta$ as well as between homomeric $\alpha 1$, $\alpha 2$ and $\alpha 3$ GlyRs. This is promising for in vivo experiments, since halogenated pro do not increase GABA-ergic activity that leads to anesthesia and 4-bromopropofol has been characterize as an GlyR specific pro derivate in spinal neurons (Eckle et al., 2014; Krasowski et al., 2001a; Trapani et al., 1998). Thus, our identification of residues determining the type of HA at GlyRs by using GlyR active halogenated pro derivatives may provide a lead in developing subtype-specific compounds and foster the design

of novel GlyR subtype-specific modulators which act in physiologically relevant concentrations.

References

- Ahrens J, Haeseler G, Leuwer M, Mohammadi B, Krampfl K, Dengler R and Bufler J (2004) 2,6 di-tert-butylphenol, a nonanesthetic propofol analog, modulates alpha1beta glycine receptor function in a manner distinct from propofol. *Anesth Analg* **99**(1): 91-96.
- Ahrens J, Leuwer M, Stachura S, Krampfl K, Belelli D, Lambert JJ and Haeseler G (2008) A transmembrane residue influences the interaction of propofol with the strychnine-sensitive glycine alpha1 and alpha1beta receptor. *Anesth Analg* **107**(6): 1875-1883.
- Baenziger JE and Corringer PJ (2011) 3D structure and allosteric modulation of the transmembrane domain of pentameric ligand-gated ion channels. *Neuropharmacology* **60**(1): 116-125.
- Biro T and Maksay G (2004) Allosteric modulation of glycine receptors is more efficacious for partial rather than full agonists. *Neurochem Int* **44**(7): 521-527.
- Bode A and Lynch JW (2013) Analysis of hyperekplexia mutations identifies transmembrane domain rearrangements that mediate glycine receptor activation. *J Biol Chem* **288**(47): 33760-33771.
- Cadugan DJ and Auerbach A (2007) Conformational dynamics of the alphaM3 transmembrane helix during acetylcholine receptor channel gating. *Biophys J* **93**(3): 859-865.
- Carswell CL, Sun J and Baenziger JE (2015) Intramembrane aromatic interactions influence the lipid sensitivities of pentameric ligand-gated ion channels. *J Biol Chem* **290**(4): 2496-2507.
- Chen X, Webb TI and Lynch JW (2009) The M4 transmembrane segment contributes to agonist efficacy differences between alpha1 and alpha3 glycine receptors. *Mol Membr Biol* **26**(5): 321-332.
- de la Roche J, Leuwer M, Krampfl K, Haeseler G, Dengler R, Buchholz V and Ahrens J (2012) 4-Chloropropofol enhances chloride currents in human hyperekplexic and artificial mutated glycine receptors. *BMC Neurol* **12**: 104.
- Del Sol A, Arauzo-Bravo MJ, Amoros D and Nussinov R (2007) Modular architecture of protein structures and allosteric communications: potential implications for signaling proteins and regulatory linkages. *Genome Biol* **8**(5): R92.
- Du J, Lu W, Wu S, Cheng Y and Gouaux E (2015) Glycine receptor mechanism elucidated by electron cryo-microscopy. *Nature* **526**(7572): 224-229.
- Duret G, Van Renterghem C, Weng Y, Prevost M, Moraga-Cid G, Huon C, Sonner JM and Corringer PJ (2011) Functional prokaryotic-eukaryotic chimera from the pentameric ligand-gated ion channel family. *Proc Natl Acad Sci U S A* **108**(29): 12143-12148.

- Eckle VS, Grasshoff C, Mirakaj V, O'Neill PM, Berry NG, Leuwer M and Antkowiak B (2014) 4-bromopropofol decreases action potential generation in spinal neurons by inducing a glycine receptor-mediated tonic conductance. *Br J Pharmacol* **171**(24): 5790-5801.
- Edelstein SJ and Le Novere N (2013) Cooperativity of allosteric receptors. *J Mol Biol* **425**(9): 1424-1432.
- Franks NP (2006) Molecular targets underlying general anaesthesia. *Brit J Pharmacol* **147 Suppl 1**: S72-81.
- Ghosh B, Satyshur KA and Czajkowski C (2013) Propofol binding to the resting state of the *gluobacter violaceus* ligand-gated ion channel (GLIC) induces structural changes in the inter- and intrasubunit transmembrane domain (TMD) cavities. *J Biol Chem* **288**(24): 17420-17431.
- Haeger S, Kuzmin D, Detro-Dassen S, Lang N, Kilb M, Tsetlin V, Betz H, Laube B and Schmalzing G (2010) An intramembrane aromatic network determines pentameric assembly of Cys-loop receptors. *Nat Struct Mol Biol* **17**(1): 90-98.
- Harvey RJ, Depner UB, Wassle H, Ahmadi S, Heindl C, Reinold H, Smart TG, Harvey K, Schutz B, Abo-Salem OM, Zimmer A, Poisbeau P, Welzl H, Wolfer DP, Betz H, Zeilhofer HU and Muller U (2004) GlyR alpha3: an essential target for spinal PGE2-mediated inflammatory pain sensitization. *Science* **304**(5672): 884-887.
- Henault CM, Juranka PF and Baenziger JE (2015) The M4 Transmembrane alpha-Helix Contributes Differently to Both the Maturation and Function of Two Prokaryotic Pentameric Ligand-gated Ion Channels. *J Biol Chem* **290**(41): 25118-25128.
- Hibbs RE and Gouaux E (2011) Principles of activation and permeation in an anion-selective Cys-loop receptor. *Nature* **474**(7349): 54-60.
- Jayakar SS, Dailey WP, Eckenhoff RG and Cohen JB (2013) Identification of propofol binding sites in a nicotinic acetylcholine receptor with a photoreactive propofol analog. *J Biol Chem* **288**(9): 6178-6189.
- Krasowski MD, Hong X, Hopfinger AJ and Harrison NL (2002) 4D-QSAR analysis of a set of propofol analogues: mapping binding sites for an anesthetic phenol on the GABA(A) receptor. *J Med Chem* **45**(15): 3210-3221.
- Krasowski MD, Jenkins A, Flood P, Kung AY, Hopfinger AJ and Harrison NL (2001a) General anesthetic potencies of a series of propofol analogs correlate with potency for potentiation of gamma-aminobutyric acid (GABA) current at the GABA(A) receptor but not with lipid solubility. *J Pharmacol Exp Ther* **297**(1): 338-351.
- Krasowski MD, Nishikawa K, Nikolaeva N, Lin A and Harrison NL (2001b) Methionine 286 in transmembrane domain 3 of the GABAA receptor beta subunit controls a binding cavity for propofol and other alkylphenol general anesthetics. *Neuropharmacology* **41**(8): 952-964.

- Li GD, Chiara DC, Cohen JB and Olsen RW (2010) Numerous classes of general anesthetics inhibit etomidate binding to gamma-aminobutyric acid type A (GABAA) receptors. *J Biol Chem* **285**(12): 8615-8620.
- Lynagh T and Laube B (2014) Opposing effects of the anesthetic propofol at pentameric ligand-gated ion channels mediated by a common site. *J Neurosci* **34**(6): 2155-2159.
- Mitra A, Bailey TD and Auerbach AL (2004) Structural dynamics of the M4 transmembrane segment during acetylcholine receptor gating. *Structure* **12**(10): 1909-1918.
- Mowrey DD, Cui T, Jia Y, Ma D, Makhov AM, Zhang P, Tang P and Xu Y (2013) Open-channel structures of the human glycine receptor alpha1 full-length transmembrane domain. *Structure* **21**(10): 1897-1904.
- Nemecz A, Prevost MS, Menny A and Corringer PJ (2016) Emerging Molecular Mechanisms of Signal Transduction in Pentameric Ligand-Gated Ion Channels. *Neuron* **90**(3): 452-470.
- Nguyen HT, Li KY, daGraca RL, Delphin E, Xiong M and Ye JH (2009) Behavior and cellular evidence for propofol-induced hypnosis involving brain glycine receptors. *Anesthesiology* **110**(2): 326-332.
- Nury H, Delarue M and Corringer PJ (2011) [X-ray structures of general anesthetics bound to their molecular targets]. *Med Sci (Paris)* **27**(12): 1056-1057.
- Nussinov R (2012) Allosteric modulators can restore function in an amino acid neurotransmitter receptor by slightly altering intra-molecular communication pathways. *Br J Pharmacol* **165**(7): 2110-2112.
- O'Shea SM, Becker L, Weiher H, Betz H and Laube B (2004) Propofol restores the function of "hyperekplexic" mutant glycine receptors in *Xenopus* oocytes and mice. *J Neurosci* **24**(9): 2322-2327.
- Pistis M, Belelli D, Peters JA and Lambert JJ (1997) The interaction of general anaesthetics with recombinant GABAA and glycine receptors expressed in *Xenopus laevis* oocytes: a comparative study. *Br J Pharmacol* **122**(8): 1707-1719.
- Prinz H (2010) Hill coefficients, dose-response curves and allosteric mechanisms. *J Chem Biol* **3**(1): 37-44.
- Sauguet L, Shahsavari A and Delarue M (2014) Crystallographic studies of pharmacological sites in pentameric ligand-gated ion channels. *Biochim Biophys Acta*.
- Sebastiani A, Granold M, Ditter A, Sebastiani P, Golz C, Pottker B, Luh C, Schaible EV, Radyushkin K, Timaru-Kast R, Werner C, Schafer MK, Engelhard K, Moosmann B and Thal SC (2016) Posttraumatic Propofol Neurotoxicity Is Mediated via the Pro-Brain-Derived Neurotrophic Factor-p75 Neurotrophin Receptor Pathway in Adult Mice. *Crit Care Med* **44**(2): e70-82.

- Trapani G, Latrofa A, Franco M, Altomare C, Sanna E, Usala M, Biggio G and Liso G (1998) Propofol analogues. Synthesis, relationships between structure and affinity at GABAA receptor in rat brain, and differential electrophysiological profile at recombinant human GABAA receptors. *J Med Chem* **41**(11): 1846-1854.
- Xiong W, Chen SR, He L, Cheng K, Zhao YL, Chen H, Li DP, Homanics GE, Peever J, Rice KC, Wu LG, Pan HL and Zhang L (2014) Presynaptic glycine receptors as a potential therapeutic target for hyperekplexia disease. *Nat Neurosci* **17**(2): 232-239.
- Xiong W, Cheng K, Cui T, Godlewski G, Rice KC, Xu Y and Zhang L (2011) Cannabinoid potentiation of glycine receptors contributes to cannabis-induced analgesia. *Nat Chem Biol* **7**(5): 296-303.
- Yamakura T, Mihic SJ and Harris RA (1999) Amino acid volume and hydrophobicity of a transmembrane site determine glycine and anesthetic sensitivity of glycine receptors. *J Biol Chem* **274**(33): 23006-23012.
- Yip GM, Chen ZW, Edge CJ, Smith EH, Dickinson R, Hohenester E, Townsend RR, Fuchs K, Sieghart W, Evers AS and Franks NP (2013) A propofol binding site on mammalian GABAA receptors identified by photolabeling. *Nat Chem Biol* **9**(11): 715-720.

7. Summary

Glycine receptors (GlyRs) are pentameric ligand-gated ion channels (pLGICs) that mediate fast synaptic transmission. A GlyR subunit comprised of a large N-terminal extracellular domain (ECD), four transmembranedomains (TMD1–4), a long intracellular loop (IL) connecting M3 and M4, and a short extracellular C-terminus. At the first glance, one would suppose that the primary task of the TMDs is to anchor the protein in the cell membrane. However, TMDs are more than just anchors: They build in their entirety the central located ion conducting channel and mutations of TMD amino acids can result in massive functional disorders. Moreover, previously published data indicate that structural rearrangements between the TMDs exist, which are key processes for the opening and closing of the channel.

Therefore, it is of great interest to increase the knowledge about the TMDs functions because a decreased GlyR activity is evident in chronic inflammatory and neuropathic pain as well as in the hyperekplexia disease.

In this study we characterized the role of the GlyR TMDs for the assembly, function and allosteric modulation by the general anesthetic propofol (pro) and derivatives.

In chapter 1, we found that the TMDs are important determinants for the assembly and function of both the $\alpha 1$ Gly- and the 5-HT_{3A} receptor. This was determined by using truncated and mutated receptors. Biochemical analysis unmasked that especially aromatic residues located in the M1, M3 and M4 within one subunit are key determinants for the GlyR assembly. Two-electrode-voltage clamping (TEVC) combined with homology modeling and molecular dynamics simulations revealed that aromatic TMD residues formed an interhelical aromatic network which secures the geometry and correct function of the GlyR.

In chapter 2, we characterized the role of the TMDs for the allosteric modulation of the GlyR function by the general anesthetic propofol (pro) and its chlorinated derivate 4-chloropropofol (4-cpro). We observed that pro and 4-cpro exhibit three distinct effects on GlyRs: a subtype specific high-affinity (HA) modulation of the Gly-induced activation by low nanomolar concentrations; a common low-affinity (LA) potentiation by high micromolar concentrations; and a subtype specific partial agonism by millimolar concentrations. Remarkably, whereas a pro HA and LA potentiation is evident at homo- and heteromeric GlyRs, the 4-cpro HA potentiation is (1) much more potent than pro at $\alpha 1$ GlyRs, (2) manifests as inhibition uniquely at $\alpha 3$

GlyRs and (3) is not present at $\alpha 1\beta$ heteromeric GlyRs. Based on homology modeling, site-directed mutagenesis and the use of the endocannabinoid anandamide (AEA) which forms a polar interaction with the M3 Ser296 in $\alpha 1$ GlyRs, we provide evidences for a so far unrecognized, functional intrasubunit transmembrane-domain (TMD) HA binding site for 4-cpro formed by amino acid residues of the M3 and M4 in GlyRs.

In chapter 3, we enlarged former analysis concerning the HA and LA potentiation by focusing on pro's effect at $\alpha 1$ GlyRs in a greater detail. We estimated the exact locations of three functional pro binding sites in $\alpha 1$ GlyRs. This was done by using the TEVC technique combined with site-directed mutagenesis, in silico dockings of pro to a $\alpha 1$ GlyR homology models and the use of the GlyR modulating reagents ivermectin (IVM), AEA and strychnine (stry). We obtained data suggesting that the pro HA potentiation is mediated by the binding of pro to the 4-cpro HA site, whereas the pro LA potentiation is controlled by a site located in the TMD interface which overlaps with the IVM site. Concerning the partial agonism by pro, we unmasked that pro-evoked chloride currents can be inhibited competitive by the antagonist stry underlining the presence of a pro binding site in the ligand binding domain (LBD).

By using a $\alpha 1$ GlyR mutant which shows no HA modulation (Phe293Ala), we were able to estimate site specific mechanisms on the agonist activation of $\alpha 1$ GlyRs. Whereas the pro HA site potentiation increases the cooperativity, the pro LA site potentiation increases the apparent affinity towards Gly at $\alpha 1$ GlyRs. Moreover, we observed that the formation of a HA potentiation by pro, depends on the strength of the $\alpha 1$ GlyR activation. Finally, we investigated the pro insensitive M3 amino acid substitution Ala288Ile in a greater detail and unmasked that the substitution is not modulated by AEA and affects the gating in $\alpha 1$ GlyRs.

Finally, we characterized by TEVC the effects of the phenols thymol (thy) and 4-chlorothymol (4-cthy) on the function of homomeric α GlyRs. Whereas thy caused a HA potentiation of the Gly-evoked currents at $\alpha 1$ - and $\alpha 2$ GlyRs, $\alpha 3$ GlyRs were not potentiated by equal thy concentrations. Surprisingly, 4-cthy showed no HA modulation at $\alpha 1$ -, a HA potentiation at $\alpha 2$ - and HA inhibition at $\alpha 3$ GlyRs. Both compounds exert the common subtype unspecific LA potentiation. By using site-directed mutagenesis, co-application of pro and the substituted cysteine accessibility method (SCAM), we unmasked that the HA site modulation by thy and 4-cthy of GlyRs is achieved by the occupation of the pro and 4-cpro HA binding site.

Moreover, we provide evidences that non-conserved residues located in the M3 and M4 mediate the subtype specific 4-cthy HA modulation in all α GlyR subtypes. Together these results increase the knowledge about the GlyR TMDs as key structures for the protein assembly and function. In addition, this study unmasked for the first time that multiple, functional binding sites for the clinical relevant drug pro exist and estimate their exact locations. These sites are located in the ECD and TMDs and are also occupied by derivates. Due to this fact, natural as well as artificial substances of this molecule class might be able to act with a high possibility as clinical relevant HA modulators at GlyRs which could be a real step forward in the treatment of GlyR subtype specific diseases like the chronification of pain.

Zusammenfassung

Glycinrezeptoren (GlyRs) sind pentamere ligandengesteuerte Ionenkanäle (pLGICs), die eine schnelle synaptische Übertragung vermitteln. Eine GlyR Untereinheit besteht aus einer großen N-terminalen extrazellulären Domäne (ECD), vier Transmembrandomänen (TMD1-4), einer langen intrazellulären Schleife (IL), welche die M3 mit der M4 verbindet, sowie einem kurzen extrazellulären C-Terminus. Auf den ersten Blick scheint es, als sei die primäre Aufgabe der TMDs die Verankerung des Proteins in der Zellmembran.

Allerdings verfügen die TMDs über mehr als nur ihre Ankerfunktion: Sie bilden in ihrer Gesamtheit den zentral gelegenen ionenleitenden Kanal und Mutationen von TMD-Aminosäuren können zu massiven Funktionsstörungen führen. Darüber hinaus konnte gezeigt werden, dass strukturelle Veränderungen der TMDs das Öffnen und Schließen des Kanals bewirken. Daher ist es von großem Interesse, das Wissen über die Funktionen der TMDs zu erweitern, weil eine verringerte Aktivität der GlyRs bei chronisch verlaufenden Entzündungen, neuropathischen Schmerzen sowie in der Hyperekplexie Erkrankung eine maßgebliche Rolle spielen.

Diese Studie charakterisiert die Rolle der GlyR TMDs für die Assemblierung, Funktion und allosterische Modulation des GlyRs durch das Anästhetikum Propofol (pro) und Derivate.

In Kapitel 1 stellten wir fest, dass die TMDs wichtige Determinanten für die Assemblierung und Funktion der $\alpha 1$ Gly- und den 5-HT_{3A} Rezeptor sind. Dies wurde durch die Verwendung trunkierter und mutierter Rezeptoren bestimmt. Die biochemische Analyse entlarvte, dass vor allem die aromatischen Aminosäuren der M1, M3 und M4 innerhalb einer Untereinheit, Schlüsselfaktoren für die Assemblierung der GlyR Untereinheiten sind. Mittels der Zwei-Elektroden-Spannungsklemme (eng. TEVC) in Kombination mit Homologie-Modellen und molekularen Dynamiksimulationen konnte gezeigt werden, dass die aromatischen Aminosäuren der TMDs ein aromatisches Netzwerk bilden, das sowohl die Geometrie als auch die korrekte Funktion des GlyR bewirkt.

In Kapitel 2 wurde die Rolle der TMDs für die allosterische Modulation der GlyR Funktion durch das Anästhetikum pro und sein chloriertes Derivat 4-chloropropofol (4-cpro) untersucht. Wir beobachteten, dass pro und 4-cpro drei verschiedene Effekte auf die Funktion der GlyRs hat: Eine Subtypen spezifische hochaffine (HA)

Modulation der Gly-induzierten Aktivierung durch nanomolare Konzentrationen; eine unspezifische niederaffine (LA) Potenzierung durch hohe mikromolare Konzentrationen; und einen Subtypen spezifischen partiellen Agonismus durch millimolare Konzentrationen. Als bemerkenswert stellte sich heraus, dass pro bei homo- und heteromeren GlyRs immer eine HA und LA Potenzierung der Funktion bewirkt, währenddessen 4-cpro eine sehr starke HA Potenzierung (1) bei $\alpha 1$ -, (2) eine HA Hemmung bei $\alpha 3$ - und (3) keine HA Modulation von $\alpha 1\beta$ heteromeren GlyRs bewirkt. Mittels Homologie-Modellierung, ortsgerichteter Mutagenese und unter der Verwendung des Endocannabinoids Anandamid (AEA), welches eine polare Wechselwirkung mit dem M3 Ser296 in $\alpha 1$ GlyRs bildet, konnten wir Beweise für die Existenz einer bisher unbekannt, funktionellen innerhalb einer GlyR Untereinheit lokalisierten HA Bindungsstelle für 4-cpro sicherstellen, die durch Aminosäuren der M3 und M4 gebildet wird.

Kapitel 3 vertieft die vorherigen Analysen und fokussiert sich auf die pro medierte HA und LA Potenzierung von $\alpha 1$ GlyRs. Wir lokalisierten die drei funktionellen pro Bindungsstellen in $\alpha 1$ GlyRs. Dies wurde unter Verwendung der TEVC Technik in Kombination mit der ortsgerichteten Mutagenese, in-silico dockings von pro in einem $\alpha 1$ GlyR Homologie-Modell und unter der Verwendung der GlyR modulierenden Reagenzien Ivermectin (IVM), AEA und Strychnin (stry) durchgeführt.

Wir erhielten Daten, die darauf hindeuteten, dass die HA Potenzierung durch pro mittels der Bindung von pro in der 4-cpro HA Bindetasche entsteht, während die LA Potenzierung von pro durch die TMD-Schnittstelle zweier benachbarter Untereinheiten gesteuert wird, welche mit der IVM Bindetasche überlappt. Was den partiellen Agonismus von pro betrifft, konnten wir zeigen, dass die pro-induzierten Chloridströme durch den Antagonisten stry kompetitiv gehemmt werden können, was mit dem Vorhandensein einer pro Bindungstasche in der Ligandenbindungsdomäne (LBD) gleichzusetzen ist.

Schließlich charakterisierten wir mittels TEVC die Wirkungen der Phenole Thymol (thy) und 4-Chlorothymol (4-cthy) auf die Funktion von homomeren α GlyRs. Während thy eine HA Potenzierung der Gly-induzierten Ströme an $\alpha 1$ - und $\alpha 2$ GlyRs verursacht, wurden $\alpha 3$ GlyRs unter der Verwendung gleicher Konzentrationen nicht potenziert. Überraschenderweise bewirkte 4-cthy keine HA Modulation bei $\alpha 1$ -, eine HA Potenzierung bei $\alpha 2$ - und eine HA Hemmung bei $\alpha 3$ GlyRs. Beide Verbindungen bewirkten jedoch eine Subtypen unspezifische LA Potenzierung. Durch die

Verwendung der ortsgerichteten Mutagenese, der Koapplikation von pro und der Ermittlung der Zugänglichkeit eines eingesetzten Cysteines (SCAM) konnte gezeigt werden, dass die HA Modulation durch thy und 4-cthy durch die Besetzung der pro und 4-cpro HA Bindetasche entsteht.

Darüber hinaus konnten wir zeigen, dass nicht konservierte Aminosäuren der M3 und M4, die Subtypen spezifische 4-cthy HA Modulation in alpha GlyR Untereinheiten mediiieren. Im gesamten, erweitern diese Ergebnisse das Wissen über die GlyR TMDs als Schlüsselstrukturen für die Assemblierung und Funktion der GlyRs. Zusätzlich zeigt diese Studie zum ersten Mal, dass mehrere funktionelle Bindungstaschen für das klinisch relevante Arzneimittel pro existieren und zeigt deren genaue Lage. Diese Taschen befinden sich in der ECD als auch in den TMDs und werden auch durch Derivate besetzt. Daher, sind natürliche als auch künstlich geschaffene Moleküle dieser Substanzklasse mit hoher Wahrscheinlichkeit klinisch relevante HA Modulatoren von GlyRs, was eine wichtige Erkenntnis für die Behandlung von GlyR assoziierter Krankheiten wie neurophatische Schmerzen oder der Hyperekplexia bedeuten kann.

8. Appendix

8.1 Authorship contributions

Chapter 1

Participated in research design: Betz, Laube, Schmalzing, Tsetlin

Conducted experiments: Kilb, Laube, Haeger, Kuzmin, Detro-Dassen, Lang

Performed data analysis: Betz, Laube, Tsetlin, Schmalzing, Kuzmin

Wrote the manuscript: Betz, Laube, Tsetlin, Schmalzing

Chapter 2

Participated in research design: Kilb, Laube, Berry, Leuwer, O'Neil

Conducted experiments: Kilb and Bibby

Performed data analysis: Kilb and Bibby

Wrote or contributed to the writing of the manuscript: Kilb, Lynagh, Berry, Leuwer, O'Neil and Laube

Chapter 3

Participated in research design: Kilb and Laube

Conducted experiments: Kilb, Berry, Schemm

Performed data analysis: Kilb, Berry, Schemm

Wrote or contributed to the writing of the manuscript: Kilb, Berry, Schemm and Laube

Chapter 4

Participated in research design: Kilb and Laube

Conducted experiments: Kilb and Winschel

Performed data analysis: Kilb and Winschel

Wrote or contributed to the writing of the manuscript: Kilb, Lynagh and Laube

All co-authors gave their permission for publishing.

Chapter 1 was published in 2010 under the title "An intramembrane aromatic network determines pentameric assembly of Cys-loop receptors" in *Nat Struct Mol Biol* **17**(1): 90-98.

8.2 Primer sequences

Table 1: GlyR mutagenesis and sequencing primers

GlyR	Mutagenesis primer 5'→3'
α1Gly394Cys	cgacaaaatatcccgcatt tgct ccccatggc
α2Ala303Ser	gccttctgtttgtgttt tct gccttactggaatcgc
α3Cys387Gly	atctcccagacc gg ttcccattagct

GlyR	Sequencing primer 5'→3'
α1TM1/2/3	gaaagccattgacattggatggc
α1TM4	aaactcttcatccagagggccaag
α2Ala303Ser	actgggcatcaccacagtcttaac
α3Cys387Gly	acacagagttcaggatcacgag

8.3 Glycine activation of wt and mutated glycine receptors

Table 2: Glycine activation of wt and mutated GlyRs

GlyR	EC ₅₀ gly (μM)	ηH	IMAX gly (μA)	n
α1	111 ± 4	2.5 ± 0.1	6.9 ± 0.5	26
α2	238 ± 31	1.8 ± 0.1	6.9 ± 0.5	24
α3	152 ± 15	1.8 ± 0.1	6.7 ± 0.4	27
α1β	207 ± 7	2.9 ± 0.1	5.4 ± 0.2	16
α1Ile229Ala	229 ± 30 ^{***}	2.1 ± 0.1	4.2 ± 0.3 ^{**}	6
α1Leu233Ala	102 ± 10	2.3 ± 0.2	7.4 ± 0.6	6
α1Ser267Ala	90 ± 4 [*]	2.1 ± 0.1	8.8 ± 1.1	7
α1Arg271Lys	13420 ± 1560 ^{***}	2.4 ± 0.4	0.2 ± 0.02 ^{***}	6
α1Ala288Ile	37 ± 16 ^{***}	1.3 ± 0.1 ^{***}	7.7 ± 0.3	6
α1Val289Ala	140 ± 3	1.9 ± 0.1	3.5 ± 0.3 ^{**}	6
α1Cys290Ala	190 ± 17 ^{**}	2.6 ± 0.2	7.5 ± 1.6	6
α1Leu292Ala	99 ± 6	2.1 ± 0.1	3.2 ± 0.5 ^{**}	6
α1Phe293Ala	212 ± 13 ^{***}	2.0 ± 0.1	6.2 ± 0.4	13
α1Val294Ala	113 ± 14	1.5 ± 0.1 ^{***}	3.3 ± 0.3 ^{***}	6
α1Phe295Ala	117 ± 14	1.6 ± 0.1 ^{**}	4.3 ± 0.5 [*]	6
α1Ser296Ala	104 ± 6	2.4 ± 0.2	5.7 ± 0.7	5
α1Ile393Ala	64 ± 8 ^{***}	2.5 ± 0.1	4.7 ± 0.1 ^{**}	9
α1Gly394Ala	78 ± 9 ^{**}	2.1 ± 0.1	5.9 ± 0.7	9
α1Gly394Cys	134 ± 17	1.7 ± 0.1 ^{**}	4.4 ± 0.2	10
α1Met397Ala	48 ± 3 ^{***}	2.1 ± 0.05	4.2 ± 0.2	9
α1Phe402Ala	199 ± 10 ^{**}	2.0 ± 0.1	3.4 ± 0.5 ^{**}	14
α1Phe405Ala	138 ± 7	2.0 ± 0.1	8.4 ± 0.8	10
α2Ala303Ser	237 ± 4	1.8 ± 0.1	7.2 ± 0.8	8
α3Cys387Gly	244 ± 30	2.1 ± 0.2	6.8 ± 0.4	9

* $P < 0.05$, *** $P < 0.001$ compared to respective wt GlyR values, unpaired t-test

8.4 Biochemical and pharmacological Characterization of heteromeric $\alpha 1\beta$ GlyR expression and formation

Due to the fact that $\alpha 1$ GlyRs subunits form homomers, the presence of heteromeric $\alpha 1\beta$ GlyRs must be determined. To secure heteromeric $\alpha 1\beta$ GlyR expression and formation we used pharmacological and biochemical methods. A higher amount of β GlyR protein was initiated by the injection of wt GlyR subtype cRNAs in a 1 ($\alpha 1 = 25$ ng) to 4 ($\beta = 100$ ng) ratio. The strength of the $\alpha 1\beta$ GlyR protein expression was then investigated over 2 days by radioactive ^{35}S methionine labeling. At day 1 a weak 58 kDa protein band (Fig. 1A, lane 4) was observable indicating the presence of β GlyR protein. The intensity of the protein band went down at day 2 indicating a reduced expression level (Fig. 1A, lane 7). Therefore, we used for TEVC investigations day 1 oocytes after cRNA injection.

Next, day 1 oocytes expressing $\alpha 1$ and β GlyR cRNA were pharmacological characterized for the presence of heteromeric $\alpha 1\beta$ GlyRs. For this approach we analyzed the effects of the α GlyR subtype inhibitor lindane (Li) on the Gly activation as described previously (Islam and Lynch, 2012).

After determination of the oocytes respective EC₅₀ Gly, effects of 10 and 30 μM Li on homomeric $\alpha 1$ GlyRs (control) and heteromeric $\alpha 1\beta$ GlyR EC₅₀ Gly-evoked current was investigated. Example recordings of Li effects on GlyR Gly-evoked currents are shown in the top panel in Fig 3B. Whereas Li had no effect on the heteromeric $\alpha 1\beta$ GlyR activation (black currents), Li inhibited homomeric $\alpha 1$ GlyR EC₅₀ Gly-evoked currents (red currents). The homomeric $\alpha 1$ GlyR current strength was significantly reduced down to 70 ± 5 % by 10 μM and 34 ± 3 % by 30 μM Li compared to the initial current strengths in the absence of Li (Fig. 1B; lower panel; paired t-tests, $P < 0.001$; $n = 6$ oocytes, respectively).

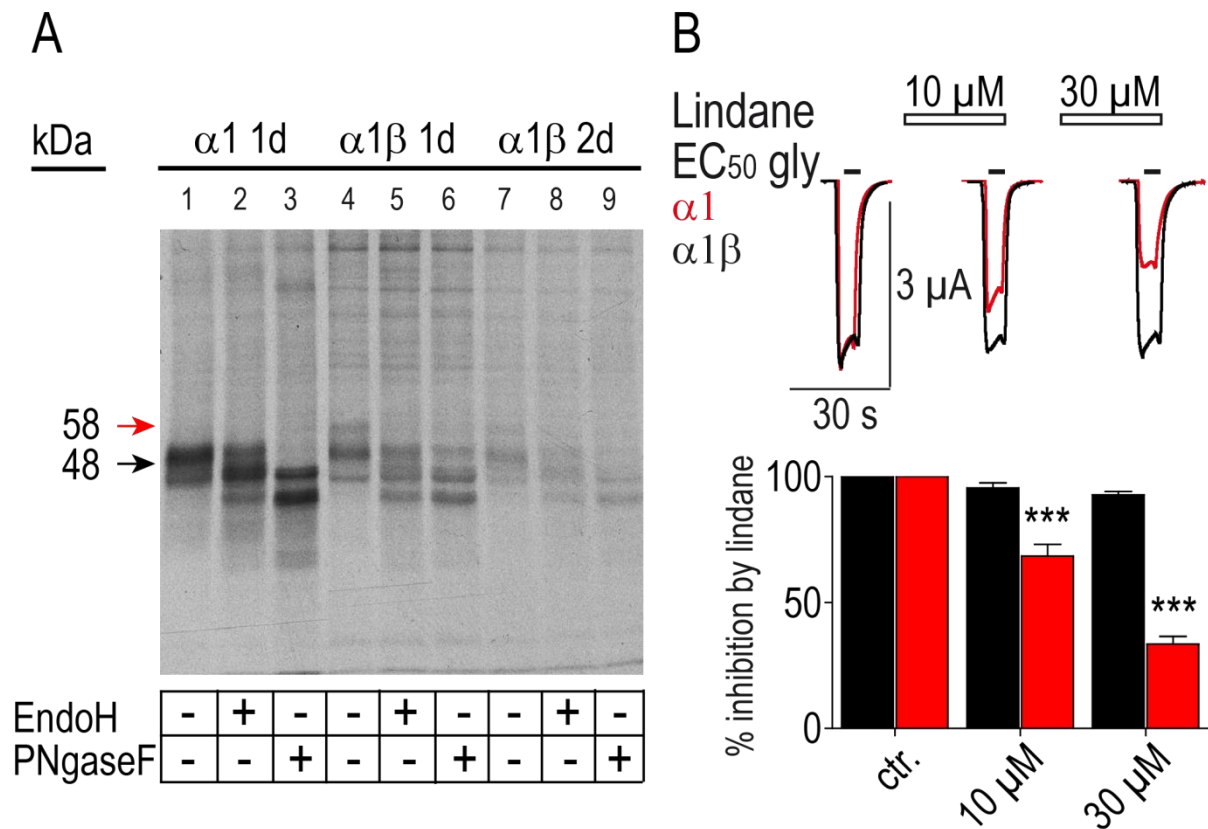


Figure 1: Biochemical and pharmacological characterization of the heteromeric $\alpha 1\beta$ GlyRs expression. **A.** Autoradiogram of [³⁵S] methionine-labeled $\alpha 1$ homo- (lane 1-3) and heteromeric (lane 4-9) $\alpha 1\beta$ GlyR cRNA expression over two days. The black arrow shows the presence of $\alpha 1$ - (48 kDa bond), the red arrow the presence of β GlyR subtype protein (58 kDa bond). **B.** Example traces representing the homo- and heteromeric GlyR EC₅₀ Gly-evoked current modulation by lindane. Homomeric $\alpha 1$ GlyR inhibition is shown in red. Lower panel presents the averaged effects of lindane on the homo- (red column) and heteromeric (black columns) $\alpha 1\beta$ GlyR EC₅₀ Gly-evoked currents. Each data point represents mean \pm S.E.M. of n = 6 oocytes, respectively; ****P* < 0.001, paired t-test.

8.5 Protein alignment

HS GlyR α 1	NFK-GPPVNV	SCNIFINSFG	SIAETTM DYR	VNIFLRQWN	DPRLAY-NEY	P-DDSLDLDP
HS GlyR α 2	NFK-GPPVNV	TCNIFINSFG	SVTETTM DYR	VNIFLRQWN	DSRLAY-SEY	P-DDSLDLDP
HS GlyR α 3	NFK-GPPVNV	TCNIFINSFG	SIAETTM DYR	VNIFLRQWN	DPRLAY-SEY	P-DDSLDLDP
HS GlyR β 1	NFK-GIPVDV	VVNIFINSFG	SIQETTM DYR	VNIFLRQWN	DPRLKLP SDF	RGSDALTVDP
HS GABAAR α 1	GLG-ERVTEV	KTDIFVTSFG	PVSDHDM EYT	IDVFFRQSWK	DERLKF---K	GPMTVLR LNN
HS GABAAR α 2	GLG-DSITEV	FTNIYVTSFG	PVSDTDM EYT	IDVFFRQSWK	DERLKF---K	GPMTVLR LNN
HS GABAAR α 3	GLG-DAVTEV	KTDIYVTSFG	PVSDTDM EYT	IDVFFRQSWK	DERLKF---D	GPMTVLR LNN
HS GABAAR β 1	DFG-GPPVDV	GMRIDVASID	MVSEVNMDYT	LTMYFQQSWK	DKRLSY---S	GIPLNLTLDN
HS GABAAR β 2	DFG-GPPVAV	GMNIDIASID	MVSEVNMDYT	LTMYFQQAWR	DKRLSY---N	VIPLNLTLDN
HS GABAAR β 3	DFG-GPPVCV	GMNIDIASID	MVSEVNMDYT	LTMYFQQYWR	DKRLAY---S	GIPLNLTLDN
HS GABAAR γ 1	DIG-VRPTVI	ETDVVNSIG	PVDFINMEYT	IDIIFAQTWF	DSRLKF---N	STMKVLMLNS
HS GABAAR γ 2	DIG-VKPTLI	HTDMYVNSIG	PVNAINMEYT	IDIFFAQTWF	DRRLKF---N	STIKVLR LNS
HS GABAAR γ 3	DIG-IKPTVI	DVDIYVNSIG	PVSSINMEYQ	IDIFFAQTWT	DSRLRF---N	STMKILTLNS
<hr/>						
HS GlyR α 1	SMLDSIWKPD	LFFANEKGAH	FHEITTDNKL	LRISRNGNVL	YSIRITLTLA	CPMDLKNFPM
HS GlyR α 2	SMLDSIWKPD	LFFANEKGAN	FHDVTTDNKL	LRISKNGKVL	YSIRLTLTLS	CPMDLKNFPM
HS GlyR α 3	SMLDSIWKPD	LFFANEKGAN	FHEVTTDNKL	LRIFKNGNVL	YSIRLTLTLS	CPMDLKNFPM
HS GlyR β 1	TMYKCLWKPD	LFFANEKSAN	FHDVTQENIL	LFIFRDGDVL	VSMRLSITLS	CPDLTLFPPM
HS GABAAR α 1	LMASKIWTTPD	TFHHNGKKS	AHNMTMPNKL	LRITDGTLL	YTMRLTVRAE	CPMHLEDFPM
HS GABAAR α 2	LMASKIWTTPD	TFHHNGKKS	AHNMTMPNKL	LRITDGTLL	YTMRLTVQAE	CPMHLEDFPM
HS GABAAR α 3	LLASKIWTTPD	TFHHNGKKS	AHNMTTPNKL	LRLVDNGTLL	YTMRLTIHAE	CPMHLEDFPM
HS GABAAR β 1	RVADQLWVPD	TYFLNDKKS	FVHGVTVKNRM	IRLHPDGTVL	YGLRITTTAA	CMMDLRRYPL
HS GABAAR β 2	RVADQLWVPD	TYFLNDKKS	FVHGVTVKNRM	IRLHPDGTVL	YGLRITTTAA	CMMDLRRYPL
HS GABAAR β 3	RVADQLWVPD	TYFLNDKKS	FVHGVTVKNRM	IRLHPDGTVL	YGLRITTTAA	CMMDLRRYPL
HS GABAAR γ 1	NMVGKIWIWIPD	TFFRNSRKS	AHWITTPNRL	LRIWNDGRVL	YTLRLTINAE	CYLQLHNFPM
HS GABAAR γ 2	NMVGKIWIWIPD	TFFRNSKKA	AHWITTPNRM	LRIWNDGRVL	YTLRLTIDAE	CYLQLHNFPM
HS GABAAR γ 3	NMVGKIWIWIPD	TIFRNSKTAE	AHWITTPNQL	LRIWNDGKIL	YTLRLTINAE	CYLQLHNFPM
<hr/>						
HS GlyR α 1	DVQTCIMQLE	SFGYTMNDLI	FEWQEQQ---	--AVQVADGL	TLPQFILK-E	EKDLRYCTKH
HS GlyR α 2	DVQTCIMQLE	SFGYTMNDLI	FEWLSDG---	--PVQVAEGL	TLPQFILK-E	EKELGYCTKH
HS GlyR α 3	DVQTCIMQLE	SFGYTMNDLI	FEWQDEA---	--PVQVAEGL	TLPQFLK-E	EKDLRYCTKH
HS GlyR β 1	DTQRCKMQLE	SFGYTTDDL	FIWQSGD---	--PVQLEK-I	ALPQFDIKKE	DIEYGNCTKY
HS GABAAR α 1	DAHACPLKFG	SYAYTRAEVV	YEWTRREP-AR	SVVVAE-DGS	RLNQYDLLGQ	TVDSGIVQ--
HS GABAAR α 2	DAHACPLKFG	SYAYTTSEVT	YIWTYNA-SD	SVQVAP-DGS	RLNQYDLLGQ	SIGKETIK--
HS GABAAR α 3	DVHACPLKFG	SYAYTTAEVV	YSWTLGK-NK	SVEVAQ-DGS	RLNQYDLLGH	VVGTEIIR--
HS GABAAR β 1	DEQNCTLEIE	SYGYTTDDIE	FYWNG----	EGAVTGVNKI	ELPQFSIVDY	KMVSKV--E
HS GABAAR β 2	DEQNCTLEIE	SYGYTTDDIE	FYWRG----	DNAVTVGVTKI	ELPQFSIVDY	KLITKKV--V
HS GABAAR β 3	DEQNCTLEIE	SYGYTTDDIE	FYWRG----	DKAVTGVVERI	ELPQFSIVEH	RLVSRNV--V
HS GABAAR γ 1	DEHSCPLEFS	SYGYPKNEIE	YKWKK----	P SVEVADPKYW	RLYQFAFVGL	RNSTEITH--
HS GABAAR γ 2	DEHSCPLEFS	SYGYPREEIV	YQWKR----	S SVEVGDTRSW	RLYQFSFVGL	RNTTEVVK--
HS GABAAR γ 3	DEHSCPLIFS	SYGYPKEEMI	YRWRK----	N SVEAADQKSW	RLYQFDFMGL	RNTTEIVT--
<hr/>						
		220		243		254
HS GlyR α 1	YN-TGKFTCI	EARFHLEKQ	GYLIQMYIP	SLIVILSWI	SFWINMDAAP	ARVGLGITT
HS GlyR α 2	YN-TGKFTCI	EVKFHLEKQ	GYLIQMYIP	SLIVILSWV	SFWINMDAAP	ARVALGITT
HS GlyR α 3	YN-TGKFTCI	EVRFHLEKQ	GYLIQMYIP	SLIVILSWV	SFWINMDAAP	ARVALGITT
HS GlyR β 1	YKGTGYTTCV	EVIFTLRRQV	GFYMMGVYAP	TLIVVLSWL	SFWINPDASA	ARVPLGIFSV
HS GABAAR α 1	-SSTGEYVVM	TTHFHLKRI	GYFVIQTYIP	CIMTVILSQV	SFWLNRESVP	ARTVFGVTTV
HS GABAAR α 2	-SSTGEYVVM	TAHFHLKRI	GYFVIQTYIP	CIMTVILSQV	SFWLNRESVP	ARTVFGVTTV
HS GABAAR α 3	-SSTGEYVVM	TTHFHLKRI	GYFVIQTYIP	CIMTVILSQV	SFWLNRESVP	ARTVFGVTTV
HS GABAAR β 1	FT-TGAYPRL	SLSFRLKRI	GYFILQTYMP	SILITILSWV	SFWINYDASA	ARVALGITT
HS GABAAR β 2	FS-TGSYPRL	SLSFRLKRI	GYFILQTYMP	SILITILSWV	SFWINYDASA	ARVALGITT
HS GABAAR β 3	FA-TGAYPRL	SLSFRLKRI	GYFILQTYMP	SILITILSWV	SFWINYDASA	ARVALGITT
HS GABAAR γ 1	-TISGDYVIM	TIFFDLSSRM	GYFTIQTYIP	CILTVVLSWV	SFWINKDAVP	ARTSLGITT
HS GABAAR γ 2	-TISGDYVVM	SVYFDLSSRM	GYFTIQTYIP	CTLIVVLSWV	SFWINKDAVP	ARTSLGITT
HS GABAAR γ 3	-TSAGDYVVM	TIYFELSRRM	GYFTIQTYIP	CILTVVLSWV	SFWIKKDATP	ARTALGITT
<hr/>						
		276	283	303		
HS GlyR α 1	LTMTTQSSGS	RASLP-KVSY	VKAIDIWMAV	CLFVFSALL	EYAAVNFVS-	---RQHKELL
HS GlyR α 2	LTMTTQSSGS	RASLP-KVSY	VKAIDIWMAV	CLFVFAALL	EYAAVNFVS-	---RQHKREFL
HS GlyR α 3	LTMTTQSSGS	RASLP-KVSY	VKAIDIWMAV	CLFVFSALL	EYAAVNFVS-	---RQHKELL
HS GlyR β 1	LSLASECTTL	AAELP-KVSY	VKALDVWLIA	CLFVGFASLV	EYAVVQVMLN	NPKRVEAEKA
HS GABAAR α 1	LTMTTLSISA	RNSLP-KVAY	ATAMDWFIIV	CYAFVFSALI	EFATVNYFT-	-----KRGY
HS GABAAR α 2	LTMTTLSISA	RNSLP-KVAY	ATAMDWFIIV	CYAFVFSALI	EFATVNYFT-	-----KRGW
HS GABAAR α 3	LTMTTLSISA	RNSLP-KVAY	ATAMDWFIIV	CYAFVFSALI	EFATVNYFT-	-----KRSW
HS GABAAR β 1	LTMTTISTHL	RETLP-KIPY	VKAIDIYLMG	CFVVFVFLALL	EYAFVNYIFF	GKGPQ--KKG
HS GABAAR β 2	LTMTTINTHL	RETLP-KIPY	VKAIDMYLMG	CFVVFVFLALL	EYALVNYIFF	GRGPQRQKKA
HS GABAAR β 3	LTMTTINTHL	RETLP-KIPY	VKAIDMYLMG	CFVVFVFLALL	EYAFVNYIFF	GRGPQRQKKL
HS GABAAR γ 1	LTMTTTLSTIA	RKSLP-KVSY	VTAMDLFVSV	CFVVFVFAALM	EYGLTHYFVS	NQKGTATKD
HS GABAAR γ 2	LTMTTTLSTIA	RKSLP-KVSY	VTAMDLFVSV	CFVVFVFSALV	EYGLTHYFVS	NRK-PSKDKD
HS GABAAR γ 3	LTMTTTLSTIA	RKSLP-RVSY	VTAMDLFVTV	CFVVFVFAALM	EYATLNYVSS	CRKPTTKKT

```

HS GlyR α1  KLFIQRAKKI  DKISRIGFPM  AFLIFNMFYW  IYKIVRRED  VHNQ---
HS GlyR α2  KKFVDRAKRI  DTISRAAFPL  AFLIFNIFYW  ITYKIIRHED  VHKK---
HS GlyR α3  KVFIDRAKKI  DTISRACFPL  AFLIFNIFYW  VIYKILRHED  IHQQQD-
HS GlyR β1  PVIPTAAKRI  DLYARALFPF  CFLFFNVIYW  SIYL-----
HS GABAAR α1  KKTFNSVSKI  DRLSRIAFPL  LFGIFNLVYW  ATYLNREPQL  KAPTPHQ
HS GABAAR α2  KKTFNSVSKI  DRMSRIVFFPV  LFGTFNLVYW  ATYLNREPVL  GVSP---
HS GABAAR α3  TKTYNSVSKV  DKISRITFPV  LFAIFNLVYW  ATYVNRESAI  KGMIRKQ
HS GABAAR β1  IPDLTDVNSI  DKWSRMFFPI  TFSLFNVVYW  LYYVH-----
HS GABAAR β2  IPDLTDVNAI  DRWSRIFFPV  VFSEFNIVYW  LYYVN-----
HS GABAAR β3  IPDLTDVNAI  DRWSRIVFPF  TFSLFNLVYW  LYYVN-----
HS GABAAR γ1  GRIHIRIAKI  DSYSRIFFPT  AFALFNLVYW  VGYLYL----
HS GABAAR γ2  GRIHIRIAKM  DSYARIFFPPT  AFCLFNLVYW  VSYLYL----
HS GABAAR γ3  GRIHIDILEL  DSYSRVFFPPT  SFLEFNLVYW  VGYLYL----

```

Amino acid alignment: Comparison of the human GABA(A)- and GlyR amino acids sequences by clustal multiple sequence alignment (Hibbs and Gouaux, 2011). Green filled arrows indicate the position of the Cys-loops. The TMDs were colored with the code: M1 (220-243) green, M2 (254-276) red, M3 (283-303) light blue and M4 (388-412) orange. Important residues for pro and derivatives effects at GlyRs were colored with the code: yellow residues for the HA site, purple residues for the LA site modulation. Numbers indicate the $\alpha 1$ GlyR amino acid position. The sequence of the intracellular is not considered.

8.6 Common used abbreviations

gamma aminobutyric receptor type A (GABA(A)R)

glycine receptor (GlyR)

nicotinic acetylcholine receptor (nAChR)

serotonin receptor (5-HT₃R)

alpha (α)

beta (β)

gamma (γ)

short (K)

complementary deoxyribonucleic acid (cDNA)

complementary ribonucleic acid (cRNA)

4-chloropropofol (4-cpro)

4-chlorothymol (4-cthy)

propofol (pro)

thymol (thy)

lindane (Li)

strychnine (stry)

propyl methanethiolsulfonate (PMTS)

γ -aminobutyric acid (GABA)

alanine (Ala)

glycine (Gly)

cysteine (Cys)

isoleucine (Ile)
serine (Ser)
phenylalanine (Phe)
extracellular domain (ECD)
intracellular domain (ICD)
transmembrane domain (TMD)
Erwinia crysanthemii (ELIC)
Gloeobacter violaceus (GLIC)
glutamate gated chloride channel (GluCl)
high affinity (HA)
low affinity (LA)
direct activation (DA)
nanomolar (nM)
micromolar (μ M)
millimolar (mM)
half maximal effective concentration (EC₅₀)
half maximal inhibitory concentration (IC₅₀)
maximal inducible current (I_{MAX})
micro ampere (μ A)
second (s)
minute (min)
wildtype (wt)
molecular dynamic simulation (MDS)
two-electrode-voltage clamp (TEVC)

References

- Hibbs RE and Gouaux E (2011) Principles of activation and permeation in an anion-selective Cys-loop receptor. *Nature* 474(7349): 54-60.
- Islam R and Lynch JW (2012) Mechanism of action of the insecticides, lindane and fipronil, on glycine receptor chloride channels. *Br J Pharmacol* 165(8): 2707-2720.

9. Danksagungen

Ich danke von ganzem Herzen

....Prof. Dr. Bodo Laube für diese Möglichkeit und alles was damit einherging!

....Prof. Dr. med. Ralf Galuske für die beiden Habitate und manch spektakuläres Beisitzen.

....Prof. Dr. med. Martin Leuwer für die gedanklichen und molekularen "Schubser".

....Dr. Timothy Peter Lynagh einfach für alles.

....meiner Verlobten für ihre unendliche Geduld mit mir!

....meiner alten und neuen Familie für ihre großartige Unterstützung in alle Lebenslagen.

....meinem Freundeskreis dafür das ihr immer erkannt habt wann es mal wieder „Zeit“ war.

....Sandy für die vielen Spaziergänge wenn es mal nicht mehr weiter ging.

....Dr. Rudolf Schemm, Kirsten Geider, Petra Ofer, Linda Wiesinger, Gabi Wenz, Theodora Volovei und Alexander Winschel für eure tatkräftigen Unterstützungen.

....alle ehemaligen und aktuellen Mitglieder der AG Laube.

10. Ehrenwörtliche Erklärung

Ich erkläre hiermit ehrenwörtlich, dass ich die vorliegende Arbeit entsprechend den Regeln guter wissenschaftlicher Praxis selbstständig und ohne unzulässige Hilfe Dritter angefertigt habe.

Sämtliche aus fremden Quellen direkt oder indirekt übernommenen Gedanken sowie sämtliche von Anderen direkt oder indirekt übernommenen Daten, Techniken und Materialien sind als solche kenntlich gemacht. Die Arbeit wurde bisher bei keiner anderen Hochschule zu Prüfungszwecken eingereicht.

Darmstadt, den

Michael Peter Kilb

Professional Experience

- 2013-2016 Design and implementation of experiments for an international scientific project founded by the medical research council, UK: "Positive Allosteric Modulators (PAMs) of Strychnine-Sensitive Glycine Receptors - A New Concept in Treating Chronic Pain" (M.Leuwer@liverpool.ac.uk)
- Head pharmacological analysis by electrophysiological techniques
 - Project management
 - Leadership (PhD-, diploma-, master- and bachelor students)
- 2008-2013 Scientific assistant at Technische Universität Darmstadt, Department Cellular and Molecular Neurophysiology in the laboratory of Prof. Dr. Bodo Laube
- Development and organization of an multiuser lab
 - Project management
 - Presentation of scientific data for experts and non-expert audience
 - Leadership (PhD-, diploma-, master- and bachelor students)
- 2007-2008 Scientific Assistant at Max-Planck institute for Brain Research, Frankfurt am Main / Technische Universität Darmstadt in the laboratory of Prof. Dr. Bodo Laube
- Scholarship Hertie-foundation
 - General laboratory activity (molecular biological, biochemical and electrophysiological techniques)
- 2002-2007 Student Assistant at N-zyme Biotec GmbH, Darmstadt, Germany
- Responsible for literature review and database management
 - General laboratory activity (molecular biological and biochemical techniques)
- 2000-2001 Civilian service at Sozialstation Pustebblume, Bensheim
- Support and care of patients suffering Alzheimer or Parkinson disease and multiple sclerosis

Academic Experience

- 2008-2016 Doctoral thesis at Technische Universität Darmstadt, Supervisor: Prof. Dr. Bodo Laube
- PhD-Thesis: “The role of the human glycine receptor transmembrane domains for the function, assembly and allosteric modulation by the general anesthetic propofol and closely related derivatives
 - Initial description of a high-affinity binding site for phenolic compounds at human glycine receptors
 - Design and implementation of theoretical and practical training courses for employees and students
 - Presentation of scientific data for experts and non-expert audience
 - Degree: 1.0
- 2007-2008 Diploma at Technische Universität Darmstadt, Supervisor: Prof. Dr. Bodo Laube
- Diploma-Thesis: „Struktur- und Funktionsanalyse der Transmembranbereiche 3 und 4 der rekombinanten $\alpha 1$ Untereinheit humaner Glyzinrezeptoren in *Xenopus laevis* Oozyten“
 - Degree: 1.0, with distinction
- 2001-2007 Studies in biology at Technische Universität Darmstadt
- Majoring Animal Physiology, Biochemistry, Cellular and Developmental Biology
 - Degree: 1.0
- 1991-2000 High-school diploma at the Gymnasium Gernsheim

Scientific Publications

- 2016 Nature Communication (in preparation)
- 2016 Molecular Pharmacology (in preparation)
- 2016 Doctoral thesis
- 2010 Nature Structural & Molecular Biology **17**, 90–98 (2010)

Scientific Lectures

- 2015 University Copenhagen, Department for Drug Design and Pharmacology
(contact@theplesslab.dk)
- 2013 Symposia of the department biology at Technische Universität Darmstadt

Student Internships

- 08-09/2006 Max-Planck Institute for Brain Research, Frankfurt am Main, Germany
- Project: "Surface detection of pentameric ligand gated ion channels"
- 08-09/2005 N-zyme Biotec GmbH, Darmstadt, Germany
- Project: "Biochemical characterization of transglutaminase2 activity"

Language Skills

German (native language)
English (fluent in spoken and written)
French (basic knowledge)

Computer Skills

Advance command in MS-Office (Word, Excel and PowerPoint)
Advance command in database software (Endnote, Reference Manager)
Advance command in scientific software (Clampfit, GraphPad Prism, Kaleidagraph)
Good command in Adobe (Photoshop, InDesign and Illustrator)
Good command in molecular visualization software (PyMOL)

Interests

Table tennis
Endurance sports
Global politics and economic development
Scientific findings and research

Groß-Rohrheim, 21.09.2016

